Neural mechanisms of value-based choices : intracerebral electrophysiological and stimulation studies in humans

Romane Cecchi

THÈSE

Pour obtenir le grade de

DOCTEUR DE L'UNIVERSITÉ GRENOBLE ALPES

Spécialité : PCN - Sciences cognitives, psychologie et neurocognition

Arrêté ministériel : 25 mai 2016

Présentée par

Romane CECCHI

Thèse dirigée par **Julien BASTIN**, Université Grenoble Alpes

préparée au sein du **Laboratoire Grenoble Institut des Neurosciences**
dans **l'École Doctorale Ingénierie pour la Santé la Cognition et l'Environnement**

Mécanismes neuronaux des choix fondés sur la valeur : études électrophysiologiques et de stimulation intracérébrale chez les humains

Neural mechanisms of value-based choices: intracerebral electrophysiological and stimulation studies in humans

Thèse soutenue publiquement le **10 novembre 2021**,
devant le jury composé de :

Monsieur JULIEN BASTIN
MAITRE DE CONFERENCE HDR, UNIVERSITE GRENOBLE ALPES, Directeur de thèse
Madame LESLEY FELLOWS
PROFESSEUR, McGill University, Rapporteure
Monsieur STEFANO PALMINTERI
CHARGE DE RECHERCHE HDR, INSERM ILE-DE-FRANCE (PARIS 12), Rapporteur
Monsieur EMMANUEL PROCYK
DIRECTEUR DE RECHERCHE, INSERM DELEGATION AUVERGNE-RHONE-ALPES, Président
Madame CATHERINE TALLON-BAUDRY
DIRECTEUR DE RECHERCHE, INSERM ILE-DE-FRANCE (PARIS 12), Examinatrice
Madame ALIZEE LOPEZ-PERSEM
CHARGE DE RECHERCHE, INSERM ILE-DE-FRANCE (PARIS 6), Examinatrice

Acknowledgements

Tout d'abord, je tiens à remercier chaleureusement les membres de mon jury, les rapporteur·e·s **Lesley Fellows** et **Stefano Palminteri**, les examinatrices **Alizée Lopez-Persem** et **Catherine Tallon-Baudry**, et le président du jury **Emmanuel Procyk** d'avoir accepté d'évaluer ce travail.

Je suis également profondément reconnaissante envers le Ministère de l'Enseignement supérieur et de la Recherche qui m'a financé pendant ces quatre années de thèse.

Je tiens ensuite à remercier mon encadrant de thèse **Julien Bastin**. Merci, évidemment, de m'avoir apporté une expérience scientifique inestimable, mais aussi (et surtout) pour ton encadrement profondément humain et à l'écoute. Merci de m'avoir fait confiance lors de mon arrivée à Grenoble et enfin, merci d'avoir cru en moi certainement plus que moi-même.

Je remercie également sincèrement **Olivier David** de m'avoir permis de rejoindre son équipe et de m'avoir offert des conditions idéales pour ma réorientation.

Ce travail n'aurait pu être réalisé sans la participation de **Mathias Pessiglione** et **Fabien Vinckier**. Merci à vous pour nos échanges enrichissants tout au long de la thèse qui m'ont permis d'avoir un regard critique sur mon travail et qui ont toujours fait avancer les choses.

Merci à **Antoine Depaulis** pour ses commentaires bienveillants lors de mes oraux, pas toujours évidents, au laboratoire, et pour avoir décelé en moi un potentiel clownesque.

Je tiens également à remercier l'ancienne équipe 11, nouvelle équipe 21, du GIN pour leur accueil au sein du laboratoire. Merci en particulier à **Maëva** et **Clarissa** d'être venues occuper un bureau presque vide et d'avoir agrandi notre " équipe " de 2. Même si je dois avouer que je n'étais pas très présente, c'était toujours un plaisir de discuter avec vous deux. Merci **Arnaud** pour les quelques discussions qu'on a pu avoir quand tu n'étais pas à l'hôpital (et que tu avais besoin d'aide sur Matlab ☺), c'était toujours un bon moment (ps : tu me dois toujours une bière). Enfin, merci **Inès** pour l'aide précieuse que tu m'as apportée, ta bonne humeur et les potins de l'hôpital.

Un grand merci à toutes les **gestionnaires du GIN** pour m'avoir aidé à voyager à travers la France (et même l'Europe) pour les enregistrements. Je vous ai donné du fil à retordre ("Euh, c'est possible d'aller à Prague demain matin ?"), mais ce manuscrit montre que ça en valait la peine.

Je remercie également tous les neurologues, chercheurs et équipes médicales qui m'ont accueilli dans leurs hôpitaux afin que je puisse réaliser des enregistrements. Sans cet esprit de collaboration, ce travail ne serait évidemment pas le même. In particular, I would like to thank **Jiri** for his kindness and help in adapting my task into Czech and recording patients. I loved coming to Prague and meeting you. Je tiens également à remercier l'équipe de l'unité d'épileptologie de Rennes, **Anca**, **Thierry**, **Amaury**, **Véronique**, pour m'avoir intégré si facilement dans votre routine. Merci également pour tous les chocolats et l'aide apportée lors de ma première aventure épique sans argent. Enfin, je ne remercierai jamais assez les membres du service d'épilepsie de Grenoble pour leur gentillesse et leur aide tout au long de cette thèse, mais aussi pour l'ambiance joyeuse qui règne dans le service grâce à vous tous, j'ai toujours eu plaisir à passer mes journées à l'hôpital. **Philippe**, **Lorella**, **Marie-Pierre**, **Patricia**, **Anne**, **Maryline**, merci pour tout.

Un grand merci bien sûr à tous les patients que je suis venu embêter pour jouer aux jeux des chercheurs et qui ont tous participé de bon cœur alors que des choses plus importantes étaient en jeu.

Merci au Labo (l'autre) d'avoir été ma seconde maison pendant cette aventure grenobloise. Merci à la super équipe et à toutes les personnes avec qui j'ai pu grimper, **Julien**, **Guillaume²**, **Cédric**, **Yo**, **Manon**, **Meije**, **Alex**, **Benoit**, merci pour toutes les séances passées ensemble. Je vous dis à très vite en salle ou à l'extérieur, en falaise ou en bloc, peu importe mais on grimpe vite ensemble!

Merci à **Brice** et **Alice** de nous avoir fait découvrir la vie grenobloise et ses nombreux bars. Sans vous, on n'aurait probablement jamais vu l'intérieur d'un restaurant. Merci à Brice de comprendre mes râleries et surtout de les partager. La vie aurait eu moins de saveur sans nos conversations endiablées. On se voit bientôt ! Merci également aux **copains niçois** NG/VDG d'être là depuis toutes ces années, **Antoine**, **Cédric**, **Charles**, **Hugo**, **Ilio**, **Kev**, **Léo**, **July**, **Mad**, **Matteo**, **Marie**, **Martin**, **Max**, **Meumeu**, **Roch**, **Thomas**, la vie serait beaucoup moins festive sans vous (et la soundbox).

Pour finir, je remercie toute ma famille sans qui rien n'aurait été possible. **Jackie**, **Christian**, **Christine**, merci pour tous ces moments passés autour d'un bon repas. **Dorian**, merci d'avoir ouvert la voie des docteurs et de donner des conseils que je suis incapable de suivre (comment on fait pour ne pas se relire ?). **Papa**, **Maman**, comment vous rendre la pareille pour tout ce que vous avez fait pour nous ? Merci de nous avoir donné la liberté de choisir ce que l'on voulait faire. J'espère que lorsque vous verrez ce travail, vous comprendrez pourquoi je n'étais pas toujours là. **Enzo**, merci d'être un si bon petit frère. **Savéria**, merci d'avoir toujours été mon modèle (malgré toi). Cette fois, je prends un peu d'avance, mais quelques mois, est-ce que ça compte vraiment ? Merci en général pour tout l'amour que vous m'apportez, c'est ce qui me permet de tenir dans les moments de doute.

Enfin, merci à **Guillaume** pour à peu près tout. Quelques lignes ne suffisent pas, mais merci d'être à mes côtés tous les jours, de me rassurer, de me soutenir et de m'encourager inlassablement. Merci de ne jamais perdre espoir et de prendre les choses avec légèreté. J'ai hâte de découvrir ce que l'avenir nous réserve.

List of studies

This dissertation is based on the following research articles:

Intracerebral mechanisms explaining the impact of incidental feedback on mood state and risky choice

Romane Cecchi, *Fabien Vinckier, Jiri Hammer, Petr Marusic, Anca Nica, Sylvain Rheims, Agnès Trebuchon, Emmanuel Barbeau, Marie Denuelle, Louis Maillard, Lorella Minotti, Philippe Kahane, Mathias Pessiglione*[*]*, Julien Bastin*[*]

Under review | Preprint available on bioRxiv

An intracranial study of gaze-dependent value signals predicting multi-attribute choices

Romane Cecchi[*]*, Clarissa Baratin*[*]*, Jiri Hammer, Petr Marusic, Nica Anca, Sylvain Rheims, Agnès Trebuchon, Louis Maillard, Lorella Minotti, Philippe Kahane, Mathias Pessiglione*[*]*, Julien Bastin*[*]

In preparation

Dissociable effects of intracranial electrical stimulation in the dorsal and ventral anterior insula on risky-decision making

Romane Cecchi, *Inès Rachidi, Lorella Minotti, Philippe Kahane, Mathias Pessiglione*[*]*, Julien Bastin*[*]

In preparation

[*]These authors contributed equally to this work

Contents


DO YOU THINK HUMANS ARE RATIONAL?
WELL *I* CERTAINLY AM.
EXCEPT WHEN HUNGRY, SLEEPY, FATIGUED, SICK, SAD, DRUNK, OVERWORKED, UNDERWORKED, ANXIOUS, STRESSED, BORED, WHEN I MISS MY COFFEE, WHEN I HAVE TOO MUCH COFFEE, WHEN I BROWSE THE INTERNET, WHEN I SEE THE OCEAN, WHEN MUSIC IS ON, WHEN SOMETHING BAD HAS HAPPENED, WHEN SOMETHING GOOD HAS HAPPENED, AND WHEN IT'S MORNING, NIGHT, EARLY AFTERNOON, OR ANY TIME DURING WINTER, FALL, OR LATE SPRING.
OUTSIDE OF THAT I'M A COLD-HEARTED CALCULATING *MACHINE*.
SO... WHEN EXACTLY DO YOU FEEL RATIONAL?
ANY TIME YOU ASK ME MY OPINION.

I

Theoretical background of value-based choices

Do you prefer brownie or tiramisù? One can probably answer this question quite easily[1], but how exactly? According to decision theories from various disciplines ranging from economics (Von Neumann & Morgenstern, 1944) to psychology (Kahneman & Tversky, 1979), the choice hinges on assigning a *subjective value* to each of the desserts (Glimcher, 2014). In doing so, a decision can be made by comparing these values and picking the highest one. This type of decision making, known as *value-based decision making*, is ubiquitous in nature. It occurs whenever an animal is faced with a choice between several alternatives that carry different intrinsic values for it – e.g., choosing between different consumer goods, getting into a relationship, or wondering whether something is beautiful or morally right. Value-based decisions are thus not driven by the immediate sensory characteristics of the options (such as how fast this car is going towards me), but rather by the individual's subjective experience and idiosyncratic preferences (the answer to a choice is not necessarily the same for everyone). Unlike sensory judgments (known as perceptual decision making), there are generally no unambiguous "correct" answers in value-based decisions; the choices made depend on invisible values internal to the decision maker. To infer these values, one can rely on a person's behavior, i.e., on his or her observable choices: if a

[1] I do, and it's definitely tiramisù

person chooses option A over option B, it can be inferred that option A has a higher value. In doing so, however, we quickly realize that, even for the same individual, values are not constant for a given object or a situation. Indeed, it is easy to see that although the choice or situation seems totally similar, we do not always make the same decisions. For example, how can I explain that in my favorite restaurant, I sometimes choose lasagna and sometimes a salad? Choices can in fact be influenced by independent factors such as the internal states of the decision maker (e.g., am I very hungry) or external factors (e.g., the outside temperature). Understanding the influence and occurrence of these factors therefore seems essential to explain part of the inconsistency observed in choices.

In this chapter, I will start by delineating the theoretical framework of my experimental work, which will inevitably involve a great deal of definition about the different types of values and how they are used to make a decision. I will then describe some models that have been proposed to formalize the properties associated with values, and finally, I will outline some internal and external factors that have been identified as value modulators.

1. How do we choose?

a. The five steps of value-based decision making

Value-based choice can be seen as broken down into several processes that are necessary and sufficient for its proper execution. In 2008, Rangel, Camerer, and Montague proposed a unified framework of value-based decision making drawing on existing theoretical models of choice in economics, psychology and computer science (Rangel et al., 2008). This framework divides the required computations into five major processes, which I will outline now (Fig. I.1).

Representation

The first process of this framework is to consider the current state of the world so as to build a representation of the decision problem. This entails depicting the set of potential courses of action (e.g., chasing a prey or fetching water) given the external states or variables (e.g., proximity to a herd or a water source) and the internal states of an individual (e.g., hunger or thirst).

Valuation

The second computation relates to the valuation of the options. Each of the considered alternatives is assigned a value, which strongly depends on the representations of the internal and external states.

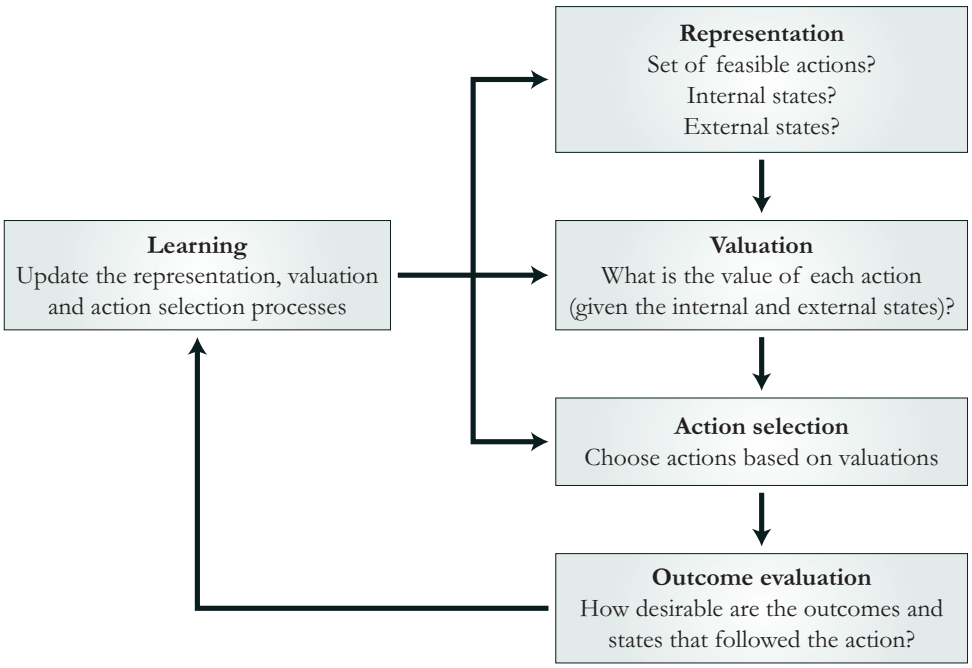

Figure I.1: The five processes involved in value-based choice. *(i)* representation of feasible actions; *(ii)* valuation of these actions; *(iii)* selection of the most appropriate action; *(iv)* evaluation of outcomes; and *(v)* learning based on the differences between the assessed outcomes and the initial assessment. From Rangel et al. (2008).

Action selection

Next, the different options are compared on the basis of their computed value (value comparison), enabling the best one to be selected (action selection) and executed. Therefore, values act as the driving force behind the choice revealed by the decision.

The valuation and action selection steps imply two fundamental properties of values:

1. *Common currency*

Assigning and comparing values seems fairly straightforward if one has to choose between options that differ only in one attribute. If, for example, we have to choose between buying an apple for 1€ or the exact same apple for 2€, we simply need to represent and compare prices. But what if we have to choose between an apple and an orange? Most of our choices involve options with countless attributes (such as size, taste, health benefits, etc.) to be combined into a coherent representation of value so that they can be compared with any other possible option. A central idea to the valuation step is therefore that options of many different kinds can be translated into some form of *common currency* to enable comparison and choice (Levy & Glimcher, 2012; Montague & Berns, 2002).

2. *Subjectivity*

Another noteworthy aspect is that, when faced with the same options, two individuals will not necessarily make the same choice. This suggests that they did not assign the same values to each possibility. Indeed, each of the options may be more or less desirable depending on one's idiosyncratic preferences (e.g., my preference for Brussels sprouts in the canteen is not necessarily shared by everyone). Thus, values are also *inherently subjective*.

Outcome evaluation

After the decision is made, a separate value signal measuring the desirability of the generated/experienced results is computed, this is the *outcome value*.

Learning

Finally, the predicted value and the outcome value are compared, resulting in a *prediction error* that is used to update the entire selection process (i.e., the first three steps of this framework). This makes it possible to learn from the choices made and thus improve the quality of future decisions. For example, this is the reason why one does not touch fire again after getting burned once. This computational process is the focus of a prolific area of research on decision-making called reinforcement learning.

*

This segregation of the decision system into five categories is not rigid, and many questions remain about the extent to which these processes are separable in the brain. For example, it is not clear whether stimulus valuation (step 2) takes place before action selection (step 3), or whether the two computations are performed in parallel (Cisek, 2012). Nevertheless, this framework is useful for establishing a common vocabulary and partitioning the study of value-based decision making into several testable processes.

b. The different types of valuation systems

In the same spirit of categorizing decision processes, the valuation stage (step 2) has been described as encompassing at least three different systems: the *Pavlovian system*, the *habitual system* and the *goal-directed system* (Fig. I.2; Daw and O'Doherty, 2014; Dolan and Dayan, 2013; Rangel et al., 2008). This partitioning stems from the widespread idea in decision psychology (and later in neuroscience and behavioral economics) that there is more than one category of possible strategies for acting.

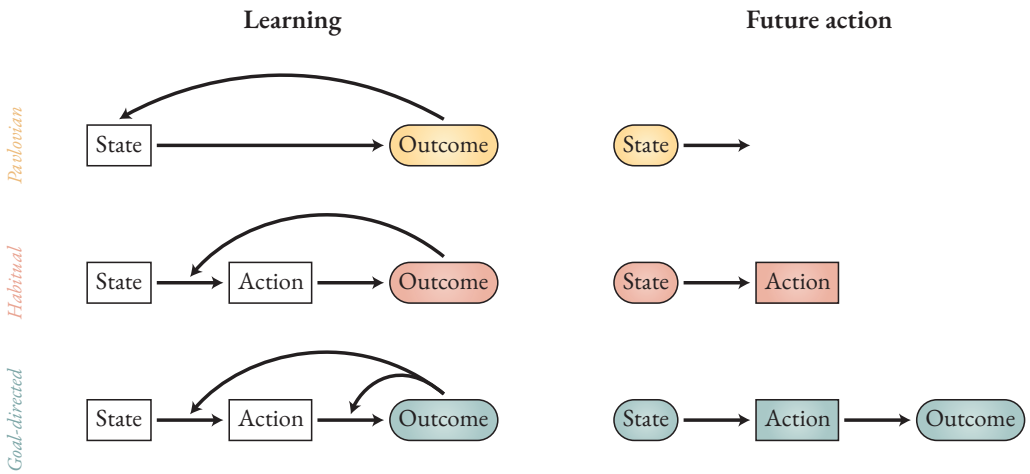

Figure I.2: The different types of valuation systems. (*top*) Pavlovian system: repeated predictive pairing of an arbitrary state or cue with a motivationally salient outcome (a reward or aversive event) causes a conditioned and typically innate response to be emitted when the state is encountered in the future, appropriately anticipating the outcome. (*middle*) Habitual system: if an action is executed while the animal is in a certain state, and the action leads to a reward, the action is reinforced such that encountering the state in the future makes executing that action more likely. If the value of the outcome was aversive, then the action is inhibited in the future. (*bottom*) Goal-directed system: if an action from a certain state leads to a reward, then an explicit representation of the sequence is remembered, which is available to guide actions when the state is encountered in future. From Seymour, Singer, et al. (2007).

The Pavlovian system

The Pavlovian system (Fig. I.2 top) takes its name from Ivan Pavlov's famous experiments on dogs, which formalized the concept of reflex or classical conditioning (see Box 1). It assigns values to a small set of behaviors that are either reflexive responses to classes of stimuli that were important in our evolutionary history (so-called "innate" behaviors, e.g., salivating at the sight of food), or learned responses to situations that predict the occurrence of those stimuli (classical conditioning, e.g., salivating at the sound of the food bag). Such Pavlovian behaviors differ according to the valence of the stimulus or environmental context, favoring approach behavior toward reward-predictive stimuli and avoidance behavior toward punishment-predictive stimuli (Huys et al., 2011). Although Pavlovian responses are generally advantageous, they are also rigid since they are automatically issued in the presence of associated stimuli, whether or not they are appropriate to the current situation. This rigidity is an important difference between the Pavlovian system and the other two systems, known as instrumental, which allow for flexible adaptation of behavior to a specific environment.

Box 1 | Pavlov's dogs and the discovery of classical conditioning

Ivan Petrovich Pavlov (1849-1936) was a Russian physiologist who won the Nobel Prize in 1904 for his work on digestive processes. In his research, he developed a protocol on the gastric function of dogs which consisted in measuring the quantity of saliva produced following the ingestion of food under different conditions. At the beginning of the protocol, the dogs only salivated when they ate food, but as his experiments progressed, Pavlov noticed that the dogs began to salivate abundantly even before they were fed, and even from the moment a feeding assistant entered the room. Based on these observations, he began to study what he called "psychic secretion", which would later be called Pavlovian or classical conditioning (Pavlov, 1927). He initiated a series of experiments in which he sought to elicit a conditioned response to a previously neutral stimulus. In one of them, he chose to use food as the unconditioned stimulus (i.e., the stimulus that elicits a response naturally and automatically), and the sound of a metronome as the neutral stimulus. The dogs were first exposed to the sound of the metronome and then the food was immediately presented. Initially, only the presentation of the food caused salivation (the unconditioned response). But after several conditioning trials, Pavlov found that *"the sounds from the metronome had acquired the property of stimulating salivary secretion"* (Pavlov, 1927, p. 26). In other words, the previously neutral stimulus (the metronome) had become what is known as a conditioned stimulus that caused a conditioned response (salivation).

The habitual system

The habitual system (Fig. I.2 middle) uses the repetition of stimulus-response associations to learn which action should be taken in a particular state of the world (i.e., it produces "habits"). In this system, values are assigned to actions through trial-and-error experience and are proportional to the expected reward that these actions generate. In contrast to the Pavlovian system, the habitual system learns associations between a stimulus and an action (rather than a stimulus and its associated outcome), and can assign values to a large number of actions (through repeated training). However, in such a mechanism, the action is not performed with the intention of obtaining or avoiding the outcome. This means that actions can be selected even if the outcome is no longer relevant or valued by the individual (e.g., driving to work when one wants to go to the grocery store).

The goal-directed system

Finally, the goal-directed system (Fig. I.2 bottom) assigns values to actions on the basis of desirable goals at the time of choice. This involves learning the association between a specific action (e.g., inserting a coin into a candy machine) and its valued outcome (e.g., the candy). Such a system relies on the ability to represent available states, actions, and goals at any time and involves flexible computation of action plans. Thus, unlike the habitual system, the goal-directed system can respond quickly to a change in the environment or internal state by updating the value of an action whenever the value of its outcome changes.

Interactions between valuation systems

Overall, three valuation systems producing different behaviors have been described. These systems were proposed as operating in parallel, which implies that they consistently assign different values to the same options. In the case where the assigned values lead to mutually exclusive actions, the three systems would compete to control the behavior (Daw et al., 2005). An example of this would be an individual considering taking an extra bite of food while feeling full: The Pavlovian system would assign a high value to the food, while the goal-directed system would give it a low value (Rangel et al., 2008). Such conflicts have been a major assumption to (partially) justify unexpected or inconsistent behaviors and choices (Dayan et al., 2006).

From a computational perspective, it has been proposed that habitual and goal-directed systems are captured by two distinct classes of reinforcement learning models, the model-free and model-based methods, respectively (Daw et al., 2005), whereas the Pavlovian system could use features of both models (Rigoli et al., 2012). Specifically, model-free models promote the execution of experienced behavior (learned by trial-and-error) with little effort, while model-based models make decisions through a flexible but computationally demanding process that uses an internal model of the world. Yet, while these proposals have provided insight into many aspects of cognition, tensions have emerged within the model-based/model-free computational dichotomy (Miller et al., 2018). Alternative proposals question, for instance, whether model-free mechanisms are part of the goal-directed system rather than the habit system, or even whether such mechanisms are necessary to explain human and animal behavior.

Ultimately, the exact nature of the computation or even the number of valuation systems is still a matter of debate. Nevertheless, it remains clear from a wealth of studies that the values underlying decision making are fractionated at the behavioral, computational and even neural levels, corroborating the existence of distinct valuation systems (Daw & O'Doherty, 2014; Dolan &

Dayan, 2013; Miller et al., 2018; Rangel et al., 2008). In my experimental work I was specifically concerned with the goal-directed system, which will therefore be the focus of the rest of this manuscript.

c. Focus on the goal-directed system valuation process

As just described, the goal-directed system assigns values to actions through the computation of action-outcome associations. Theoretically, this approach involves assessing the *benefits* associated with the pursued goal, but also incorporating the *costs* associated with the possible course of action. Indeed, the actions themselves can have an impact on the perception of a goal (e.g., consider the difference between climbing five floors or walking two meters to get a chocolate square). Consequently, the *decision* value used in the comparator process (step 3 of the previous framework) is thought to provide an integrated representation of two types of values: the *stimulus value* and the *action cost* (Fig. I.3; Pessiglione et al., 2018; Rangel and Hare, 2010).

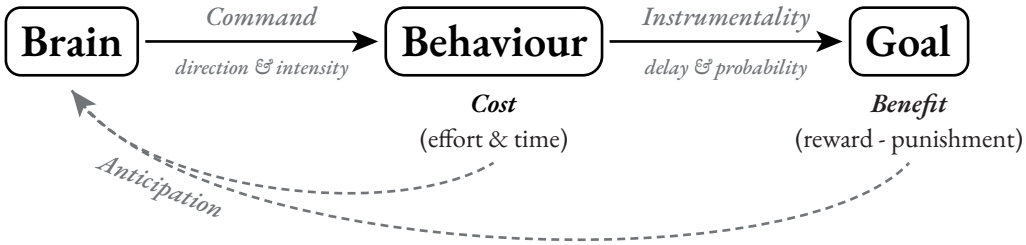

Figure I.3: A schematic view of the goal-directed system. The box-and-arrow schema illustrates goal-directed behavior. From Pessiglione et al. (2018).

Stimulus value

The **stimulus** (or goal) **value** is a measure of the *expected benefit* of undertaking an action to achieve a goal, regardless of the costs of this action. The action may be set as the goal itself (e.g., walking because I like it) or it may lead to a valuable outcome (e.g., walking to get somewhere). Importantly, goal value arises from the intrinsic meaning of two different types of predicted outcomes: *rewards* and *punishments*.

Rewards (or *gains*) have a positive value and refer to something that is sought after (Schultz et al., 1997). They are usually described in terms of the behavior they elicit, such as approach or consumption behaviors. Rewards can be primary (e.g., food), include external stimuli (e.g., objects or money), the performance of a certain act, or an internal state. In general, rewards are also associated with positive emotions and pleasure, although the hedonic satisfaction associ-

ated with a stimulus (liking) might be distinct from the work involved in obtaining it (wanting; Berridge & Kringelbach, 2015).

Punishments (or *losses*) have a negative value and refer to something that is sought to be escaped or avoided. In this sense, punishments relate to any aversive event or stimulus. In particular, we can mention sensory punishments (e.g., pain or foul tastes), and psychological punishments, which are primarily frustrations related to the occurrence of an unwanted event (e.g., losing money) or the failure to obtain a desired reward.

For instance, moving abroad may be set as a goal because it has high positive value on the dimensions of learning and personal growth, but it also carries negative values associated with being separated from family and friends. Understandably, a goal can be designated as such only if the values of rewards (positive) exceed the values of punishments (negative). Still, as mentioned earlier, these values reflect the decider's individual estimation of the attractiveness or unattractiveness of the available options and thus are by their very nature subjective. Moreover, as will be detailed later (see section I.3.), the goal value (and thus rewards and punishments) can be weighted differently within the same individual based on *modulators* such as uncertainty, risk, or the internal states of the decision maker.

Action costs

Action costs reflects the value of taking the action required to achieve a goal regardless of the expected benefits that the action might generate. They result in a devaluation of the stimulus value and are typically revealed by preferences for less costly alternatives. Action costs can be divided into two categories: time and effort (Pessiglione et al., 2018). Time spent on a given action is a cost because it becomes unavailable for other actions that might be profitable. Similarly, effort is a cost because it involves the consumption of resources that might be needed later to engage in another desired activity and that will require other costly processes to be restored. While the metabolic costs of physical effort are obvious, the extent to which cognitive effort also consumes biological resources remains debated (Kroemer et al., 2016; Pessiglione et al., 2018). Nevertheless, mental effort is generally experienced as aversive (Eisenberger, 1992) and humans tend to avoid engaging in cognitively demanding activities (Kool et al., 2010; Westbrook et al., 2013), suggesting that cognitive effort also entails a cost.

Punishments vs. action costs

Both punishments and action costs have the consequence of decreasing the value of benefits, and have therefore often been mixed up in the literature. Yet they can be clearly distinguished by

considering whether the devaluation is related to the action (action cost) or the outcome (punishment/loss; Rangel & Hare, 2010). This distinction is meaningful since, for example, one can reduce the effort costs associated with an action (e.g., reduce the physical distance needed to buy an item), but cannot change the associated losses (e.g., its price). Nonetheless, it remains that both can be considered as aversive stimuli.

Decision value

Finally, stimulus value and action cost are integrated into a decision value given by:

$$Decision\ Value = Stimulus\ Value - Action\ Cost$$

These decision values are the ones that are thought to be compared when making a choice (Pessiglione et al., 2018; Rangel & Hare, 2010). Basically, when a single course of action is involved, it is only initiated if the net value of this computation is positive (i.e., better than doing nothing). This means that the highest cost a person is willing to accept, in order to achieve a particular goal, is equal to the stimulus value. Therefore, action costs are typically viewed as a measure of the motivation intensity.

Summary

- **Value-based choice** can be seen as broken down into **five processes that are necessary and sufficient for its proper execution**: (*i*) representation, (*ii*) valuation, (*iii*) action selection, (*iv*) outcome evaluation and (*v*) learning.
- **Values** are implemented as a **common currency** and are **inherently subjective**.
- The belief that more than one strategy for acting is possible has led to the **distinction of three types of valuation systems**: the Pavlovian system, the habitual system and the goal-directed system.
- Within the **goal-directed system**, **different types of values** can be distinguished (see Box 2).
- The **goal or outcome** of a decision can be multidimensional, including **rewards** (or **gains**) and **punishments** (or **losses**).

Box 2 | Overview of the different types of value and terminology

Goal-directed decision making involves different types of valuation – and therefore different values – throughout its decision-making process. While the distinction between these values is ubiquitous in the literature, the same terms may have been used inconsistently in different fields or at different times. For the sake of clarity, the different types of values discussed in this manuscript, their interpretation, and the correspondence with different terms proposed in the literature are reviewed below.

- **Stimulus value**: Expected benefit (i.e., integration of rewards and punishments) from the outcome of a decision.
  This valuation has received many names in the literature: It is called *predicted value / utility* (Kahneman et al., 1997) or *anticipated value* (Loewenstein, 1987) by economists, while psychologists alternatively use the terms *goal* or *stimulus value* (Hare et al., 2008; Rangel & Hare, 2010), *subjective desirability* (Dorris & Glimcher, 2004) or *affective forecasting* (Wilson & Gilbert, 2005).

- **Action cost**: Value of the costs related to the action required to achieve a goal. It includes the time spent doing the action and the amount of effort required (physical and mental).

- **Decision value**: Driver of the choice embedded in the comparison process, it is revealed by the decision and integrates the representation of stimulus value and action costs.
  Synonyms: *Action value* (Rangel & Hare, 2010) or *decision utility* (Kahneman et al., 1997)

- **Outcome value**: Measure of the pleasantness of the experienced or generated decision outcome (Rangel & Clithero, 2012).
  Synonyms: *experienced value* (Ruff & Fehr, 2014), *instant utility* (Kahneman et al., 1997)

- **Prediction error**: Difference between obtained and expected outcomes (i.e., the difference between outcome and stimulus value). Two kinds can be distinguished: *reward prediction errors* (RPE) when the outcome is appetitive and *punishment prediction errors* (PPE) when the outcome is aversive.

2. Can we predict choices? – Computational models of value comparison and selection

A fundamental goal of research in decision-making is to explain behavior, that is, to answer the question of why humans (or animals) act as they do. To achieve this goal, a widespread practice consists in using computational modeling. The idea is to define specific hypotheses about the decision process in ways that narrow it to its essential components. As such, models provide a framework to summarize existing knowledge, can help translate observations into predictions of future events, facilitate the interpretation of complex data, and allow for the comparison of competing hypotheses about underlying mechanisms. In the next section, I will present different computational models that have been proposed to formalize how decision values are *compared* and *selected* when making a choice.

a. Static models of decision making

The argmax rule

The field of decision making has long been dominated by an economic perspective, seeking to specify the minimal internal representation that could, in theory, account for a given set of observed choices (Caplin & Glimcher, 2014). One of the earliest concepts in the field was that humans should be rational and their decisions should serve to maximize their well-being (the *homo economicus*). In other words, a decision maker would always choose the option with the highest value. More formally, this amounts to performing an "*argmax*" operation among the values (V) of the elements from the choice set (Glimcher, 2014):

$$Choice = argmax\{V_1, V_2, ..., V_n\}$$

This operation implies that selecting a sub-optimal option is impossible, even for the closest difference between options in the choice set, provided that the valuation of each option is correct.

The argmax rule gives choices a purely deterministic nature (i.e., choice is settled on the option with the highest desirability). However, it is often observed that individuals are very stochastic, in the sense that when asked to choose from the same set of options several times, they often make different choices (Tversky, 1969). To capture choice irregularities and imperfect behaviors, later theories have had to introduce some form of stochasticity in option selection or uncertainty in the representation of values.

The softmax rule

One approach, already used in the reinforcement learning field, has been to model the probability of choosing a particular option by a *softmax* or logistic transformation of the values (Luce, 1959). This model simply predicts that the *probability* of choosing an option increases with its desirability (Fig. I.4a). When there are only two options to choose from (say A and B), it reduces to the following equation:

$$p_A = \frac{1}{1 + e^{-(\alpha+\beta(V_B - V_A))}}$$

Where the probability of choosing option A (p_A), is determined by the difference in value (V) between the two options A and B. The free parameter α refers to the intercept indicating whether there is a bias in choice, while the free parameter β, called "inverse temperature", reflects the slope of the sigmoid function controlling the influence of values on choice. This latter ranges from $\beta = 0$ for a completely random response to $\beta = \infty$ for a deterministic choice of the highest value option (Fig. I.4a). Thus, instead of systematically picking the highest value option, the softmax function provides a probabilistic choice model that captures the fact that inconsistent choices increase when option values are close.

Signal detection theory

An alternative approach to accounting for choice variability has emerged from signal detection theory (SDT). The roots of this model lie in the design and analysis of radar signals (Peterson et al., 1954), from which it quickly spread to cognitive sciences, where it provided a theoretical framework to explain perceptual decision making in the face of sensory uncertainty (Tanner Jr. & Swets, 1954). In this context, SDT is applicable to any binary decision situation where the response of the decision maker can be assessed by the actual presence or absence of a stimulus (Fig. I.4b). The general premise is that decisions rely on evidence sampled from internal probabilistic representations of both signal and noise, which are compared on the basis of an internal criterion. If the internal signal is stronger than the criterion, the stimulus will be reported present, otherwise it will be reported absent. Four types of response are then distinguished: hit (signal is reported present when it is), false alarm (signal is reported present when absent), miss (signal is reported absent when present) and correct rejection (signal is reported absent when it is). The probability of each response type can be used to recover two parameters: bias and sensitivity. Bias represents the tendency to favor one answer over another (i.e., less evidence is needed for that answer to be selected), while sensitivity (or discriminability d') corresponds to the abil-

ity to distinguish between each stimulus. In other words, sensitivity reflects the "similarity" of the stimuli, so that d' is a measure of performance which is independent of bias.

In the case of value-based decision making, the internal probability distributions represent the values of two options to choose from. The closer the values are, the less distinguishable they will be (small d') and the greater the probability of observing inconsistent choices. The response types "miss" and "false alarm" then constitute a single error category corresponding to not choosing the option with the highest value.

The softmax rule and SDT thus yield quantitatively similar predictions. Nevertheless, these two approaches differ insofar as they suggest different sources of decision stochasticity. On the one hand, the softmax function assumes that option values are properly represented, but that noise is introduced in the mapping between the internal state and the response (i.e., during the comparison and selection processes). Whereas SDT assumes that values are inherently generated in a probabilistic way.

*

Both softmax and SDT models are easy-to-implement and robust procedures that are useful for analyzing performance in simple contexts. However, they share two significant limitations. First, they treat information in the environment as being static, leaving out the temporal aspect of decision making. Yet, a well-known decision phenomenon, called the speed-accuracy trade-off, states that decision time and performance are negatively related, so that the accuracy of a decision can be traded for its speed (Heitz, 2014). Second, they provide only limited mechanistic insight into how choices are made. To address these limitations, a second class of models, which can be called dynamic, instead treats information in the environment as continuous and offers a way to incorporate choice probabilities alongside reaction times.

b. Dynamic models of decision making

Most of our decisions are made under time pressure (e.g., thinking about which pair of socks to wear is not something that can be done for hours on end). Nevertheless, deciding when to stop deliberating is not simple, as it involves a balance between two opposing forces. On one hand, the quality of decision making improves when based on more information, on the other hand, the time spent deciding is costly. This balance is known as the speed-accuracy trade-off, a compromise that affects a large number of species, from acellular organisms to bumblebees to humans (Forstmann et al., 2016; Heitz, 2014). Several models have been developed to ac-

count for this phenomenon and explain how decisions are made under time pressure. The most popular class of models assumes that decisions are made by a process of accumulating noisy samples of information from the environment until a threshold of evidence is reached. These *accumulation-to-threshold* models are known as *sequential sampling models*.

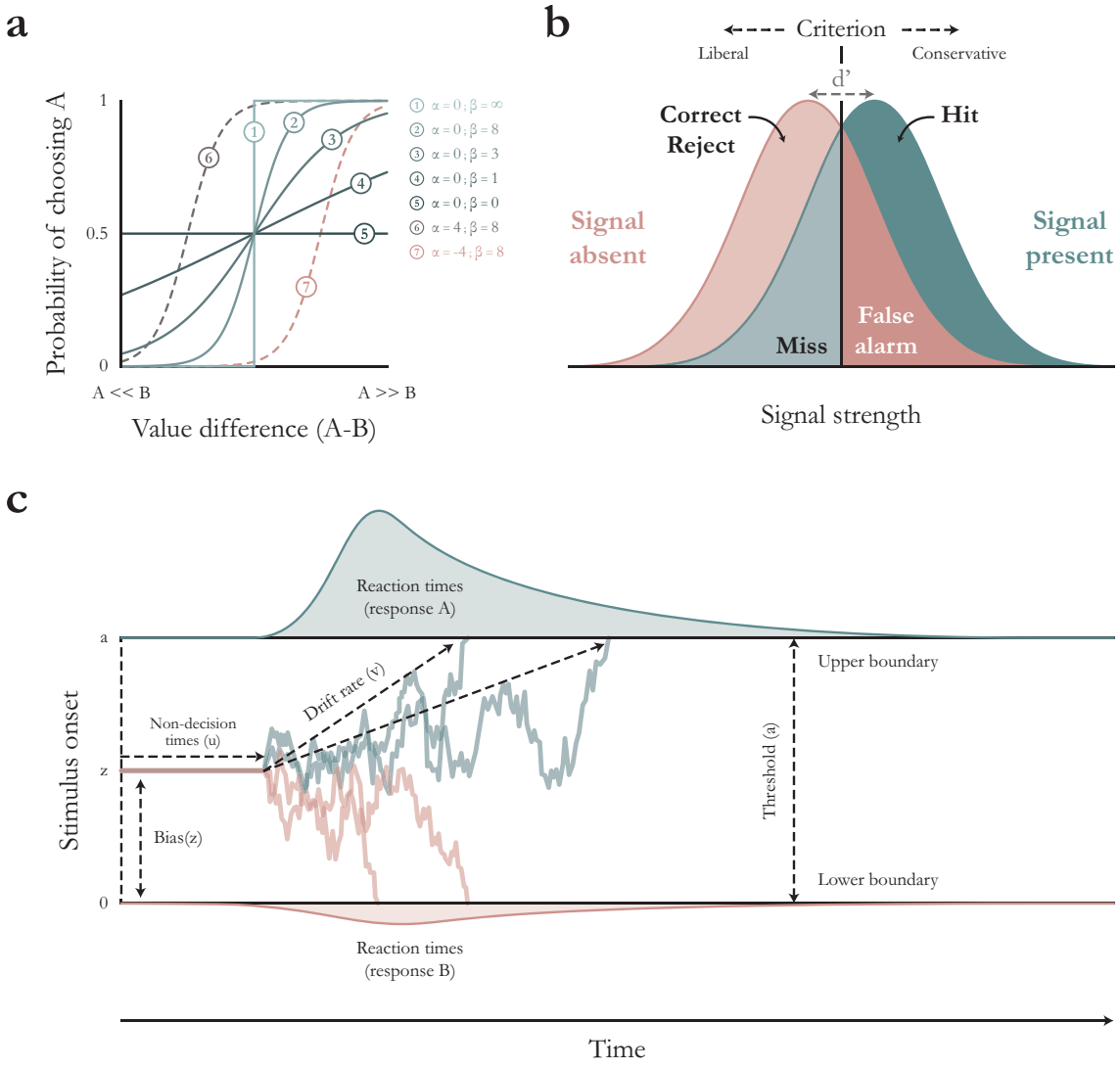

Figure I.4: Choice models for value comparison and selection. (a) Softmax rule. Probability of choosing option A as a function of the value difference between the two options A and B. Choice probabilities obtained for five different values of the inverse temperature parameter (β; curves 1-5) and three different values of the bias parameter (α; curves 2,6,7) of the softmax function are presented. (b) Signal detection theory model. The decision space consists of two normal distributions from which a sample is drawn and compared with a criterion to make a decision. The distance between the two distributions, called sensitivity (d'), determines the "similarity" of the stimuli. Adapted from Gardner (n.d.). (c) Schematic representation of the drift diffusion model (Ratcliff, 1978). A decision is made when the evidence, accumulated from a point z (here unbiased) and moving stochastically with a drift rate v, reaches one of the two symmetric thresholds. Noise in the accumulation of information means that processes do not always terminate at the same time or at the same boundary, producing reaction time distributions for both options. Adapted from Vinding et al. (2021).

Over the course of several decades, many versions of sequential sampling models have been developed (see Ratcliff & Smith, 2004 for a review). Among them, probably one of the most widespread is the drift diffusion model (DDM; Ratcliff, 1978), which has been able to account for a large amount of data in different domains, including perceptual discrimination and go-no-go tasks, before being extended to value-based decision making (M. M. Mormann et al., 2010; Tajima et al., 2016).

The drift diffusion model

The DDM has been widely used to explain observed patterns of choice and response time in simple binary decisions (e.g., choosing between an apple and an orange). This model assumes that each instant yields evidence about the stimulus, which is accumulated as a relative value signal from a starting point z to a decision threshold associated with a particular choice (Fig. I.4c). The amount of accumulated evidence evolves at every instant t as follows:

$$R_{t+1} = R_t + v + \epsilon_t$$

Where R_t denotes the relative value signal at instant t (measured from the beginning of the choice process), v is the drift rate, and ϵ_t represents a white Gaussian noise. The drift rate indexes the rate at which evidence is acquired (i.e., the higher the drift rate, the faster and more accurate the response). In value-based decision making, it is a function of the difference in value between the two options, such that it is biased towards the preferred option (M. M. Mormann et al., 2010). The zero point of the drift rate distinguishes between positive drift rates that tend toward the upper boundary and negative drift rates that tend toward the lower boundary. In this model, choice stochasticity is captured by the Gaussian noise ϵ_t which allows for variability in the accumulation of information over the course of a trial, giving rise to variability in reaction times and allowing the process to not always terminate at the same boundary (producing errors such as not choosing the option with the highest value).

*

Altogether, the computational models described in this section offer several levels of analysis of decision dynamics – from the simplest psychological descriptions of value comparisons to more detailed implementations. All of these models have been successfully applied in many domains, providing accurate quantitative accounts of how choice probabilities (and response times in the case of dynamic models) vary with the properties of choice options. However, a common feature of these models is that they introduce choice variability with stochastic functions, which

predict choices on average (choice probability), but cannot provide accurate predictions at the individual level. Yet, although it can be argued that decision-making mechanisms are inherently stochastic, it would also appear that the random components may in part reflect the influence of unobserved or unconsidered factors. Indeed, many factors such as risk or delay are widely recognized as having a predictable influence on option values during choice. Relatedly, a further limitation of such models is that they describe how values are compared, but leave unspecified how these values are constructed.

In order to better understand how decisions are made, many value modulators have been described and valuation models have been proposed, allowing, when combined with choice functions, to replace some of the randomness with bias. In the following section, I will introduce three of these modulators that have been the focus of my experimental work: risk, mood and visual attention.

Summary

- Over time, several computational models have been developed to capture **how decision values are compared and selected**.
- Early models from economics considered choices to be **deterministic** (**argmax** rule), while later models introduced **stochasticity** in option selection or value representation as a way to capture choice irregularities and imperfect behavior.
- **Static models** of choice, including the **softmax** function and **signal detection theory**, provide an effective description of choice behavior, but ignore the temporal aspect of the decision and lack a deeper mechanistic view of its process.
- **Dynamic choice models** such as **sequential sampling models**, and particularly the **drift diffusion model**, extend models from signal detection theory by providing a simple mechanistic explanation of the observed relationship between decision outcomes and reaction times.
- Overall, these models are limited by the fact that they do not describe how values are constructed, and that they account for the variability of choices with stochastic functions which only help to mimic behavior on average.

3. Modulators of the valuation system

As mentioned before, in a goal-directed choice, the stimulus value is built by weighing the intrinsic rewards and punishments of the expected outcome of the decision. Yet in our daily lives, many other factors can influence our perception of a goal. For example, the value attributed to an action may depend on the riskiness of its associated rewards, the time frame in which these rewards occur, or the social context (Rangel et al., 2008; Ruff & Fehr, 2014; Tobler & Weber, 2014). Such factors are referred to as value *modulators*. Their study contributes to explain part of the observed choice inconsistency and to build more accurate models of decision making. Three of them have been the focus of my experimental work: **risk**, **mood** and **visual attention**.

a. Uncertainty and risk

We make most of our decisions without knowing their consequences with certainty. Whether selecting a course of study, going to climb Mont Blanc, or even choosing a given road to avoid traffic, the expected outcome of each of these decisions depends on the occurrence of uncertain events. For all that, it is clear that not all decisions have the same degree of uncertainty. The economist Frank Knight was the first to draw a conceptual distinction between decisions under *risk* and under *uncertainty* (Knight, 1921, Ch.7). He defines *risk* as situations where the outcome is unknown, but the probability distribution governing that outcome is known. Whereas *uncertainty* is characterized by both an unknown outcome and an unknown probability distribution. The real world knowledge about the probability distribution of the potential outcomes of a choice can fall anywhere on a continuum, ranging from complete ignorance (i.e., the potential outcomes are not even known) at one extremity, through various degrees of partial ignorance (i.e., uncertainty), to risk (the full distribution of outcomes is precisely specified), to certainty (a single deterministic outcome is known).

Because of the persistence of uncertainty in our everyday lives, this topic has been one of the most prolific in the field of decision making. Consequently, as we will briefly mention, the evolution of theories governing uncertain choices has gone hand in hand with the observation of biases affecting stimulus value that go even beyond the scope of risk and uncertainty.

Expected Value Theory

The study of decision making under risk and uncertainty has a remarkably rich history that goes back to Blaise Pascal's early reflections on a standard problem present for several centuries in mathematical texts and known as the *division problem*: how to divide the total stake of a

game of chance in case of its premature interruption (Edwards, 2001)? Pascal posited that the *expected value* of such a situation could be computed by combining the amount of the objective outcomes and their probability level as follows:

$$EV(X) = \sum_x p(x) \cdot x$$

In this equation, the expected value (EV) of a gamble X is computed as the sum of all possible outcomes (x) weighted by their respective probability ($p(x)$; Tobler & Weber, 2014). From the middle of the 17th century, mathematical expectation and its maximization (i.e., choosing the option with the highest EV) thus became the central doctrine on how to choose rationally.

Expected Utility Theory

A little less than a century later, this approach was challenged on the basis of the so-called St. Petersburg paradox (see Box 3), which points out that people often fail to maximize expected value as they are only willing to pay a small price for the opportunity to play a game with a highly skewed payoff distribution and infinite expected value. To resolve this paradox, Daniel Bernoulli (Bernoulli, 1738/1954) suggested that the *utility* – the desirability or satisfaction – of an outcome should be distinguished from its monetary amount (i.e., its value), such that instead of maximizing expected value, choosers should maximize expected utility (EU):

$$EU(X) = \sum_x p(x) \cdot u(x)$$

Bernoulli postulates that "the utility resulting from any small increase in wealth will be inversely proportionate to the quantity of goods previously possessed" (Bernoulli, 1738/1954, p.25). In other words, each additional quantity is less satisfying than the previous one. In this formula-

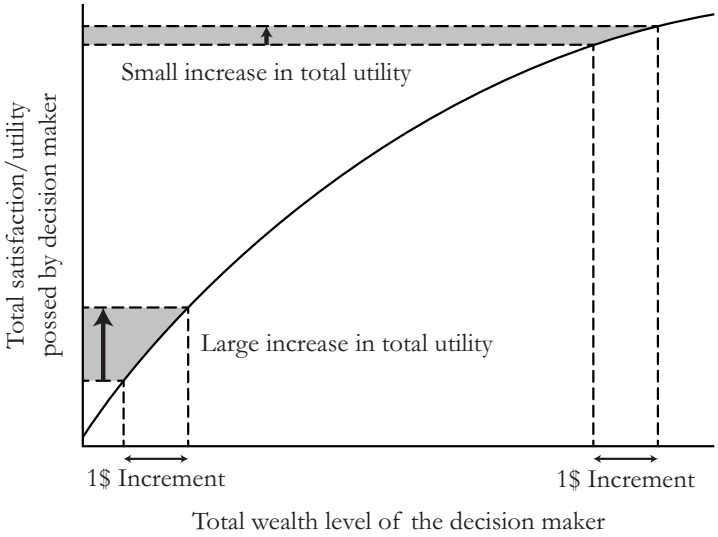

Figure I.5: Bernoulli's logarithmic utility function. The total satisfaction, or utility, conferred on the decision maker by an additional dollar decreases as a logarithmic function of total wealth. Adapted from Caplin and Glimcher (2014).

tion, the function that maps the real value (x) to the utility of that value ($u(x)$) is no longer linear but logarithmic (Fig. I.5). "Thus there is no doubt that a gain of one thousand ducats is more significant to a pauper than to a rich man though both gain the same amount" (Bernoulli, 1738/1954, p.24).

Box 3 | The St. Petersburg Paradox

The St. Petersburg paradox was originally introduced by Nicolaus Bernoulli (Daniel's cousin) in 1713 (de Montmort, 1713). Consider a game in which a fair coin is tossed until it lands on tails. The player pays a fixed amount of money up front, and then receives $\$2^n$ if the coin lands on tails on the n^{th} toss. Thus, if the coin lands on tails the first time, the prize is $2^1 = \$2$, and the game ends. However, if the coin lands on heads, it is put back into play. If it lands on tails the second time, the prize is $2^2 = \$4$, and the game ends. If the coin lands on tails again, it is put back into play. And so on. What would be a fair price to pay to enter the game? According to Pascal's theory, one needs to calculate the expected value of this gamble, which is the sum of the payoffs of all possible outcomes. The probability of the coin landing on tails on the first toss is $1/2$, and the player wins \$2. The probability of the coin landing on tails on the second toss is $1/4$, and the player wins \$4, and so on. Assuming that the game can continue as long as the toss gives a head, the expected value is as follows:

$$EV = 1/2 \times 2 + 1/4 \times 4 + 1/8 \times 8 + \cdots = 1 + 1 + 1 + \cdots = +\infty$$

Since the expected value is infinitely large, a rational gambler should be willing to bet his or her entire fortune to play this game. However, "few of us would pay even \$25 to enter such a game" (Hacking, 1983, p.563).

Years later, expected utility became the dominant normative theory (i.e. accounting for what should be chosen, as opposed to descriptive theories describing what is actually chosen) in economics following two main events. The first was the formulation by Von Neumann and Morgenstern (1944) of a set of axioms that are both necessary and sufficient to represent a decision maker's choices by maximizing expected utility (see Box 4), which made it a normatively attractive decision criterion. The second was when Savage (1954) introduced a more general formulation of this theory, called *subjective expected utility* (SEU), which extended it from risk to uncertainty. In this model, objective probabilities are replaced by subjective ones. The idea

being that an individual evaluates the probabilities of consequences a priori with his or her personal knowledge or beliefs. Thus, the model can be applied even when the true probabilities are not known to the decision maker.

Box 4 | Axioms of the (subjective) expected utility theory

- *Completeness*: For every A and B, either $A \geq B$ or $A \leq B$ or $A \sim B$, where $\geq$ and $\leq$ mean "is preferred to" and $\sim$ means "is equivalent to".
  This assumes that an individual has well-defined preferences and can always decide between two alternatives.
- *Transitivity*: For every A, B and C, if $A \geq B$ and $B \geq C$, then $A \geq C$
  This implies that when an individual decides according to the completeness axiom, he also decides consistently.
- *Continuity*: For every A, B and C, if $A \geq B \geq C$, then there exists a probability p ($\in [0, 1]$) such that B is equally good as $pA + (1 - p)C$
  This implies that if an individual prefers A to B and B to C, there should be a possible combination of A and C in which the individual is indifferent between that combination and B.
- *Independence*: For every A, B and C, if $A \geq B$, then for any C and p ($\in [0, 1]$), $pA + (1 - p)C \geq pB + (1 - p)C$
  This assumes that two gambles mixed with a third irrelevant one will maintain the same order of preference as when the two gambles are presented independently.

As early as the 1950s, the increasing discovery of choices that did not conform to this set of axioms, however, began to call into question the descriptive validity of subjective expected utility theory. Classic demonstrations of the failure of certain axioms include: the Allais paradox (also called the certainty effect; Allais, 1953; Kahneman & Tversky, 1979), *loss aversion* (Kahneman & Tversky, 1979), ambiguity aversion (as demonstrated in the Ellsberg effect; Ellsberg, 1961), *the framing effect* (Tversky & Kahneman, 1981) or the anchoring effect (Tversky & Kahneman, 1974)[2].

[2] This list is by no means exhaustive. Many other types of cognitive biases have been described as leading to behavior that deviates from expected utility theory, but it is beyond the scope of this manuscript to outline them all.

Prospect Theory

In order to accommodate these violations, the SEU theory was adapted and extended by Kahneman and Tversky (1979) into a descriptive model known as the *prospect theory*. This model proposes that distinct functions mediate the evaluation of probabilities and the translation of objective value into subjective utility. The value V of a simple option resulting in an outcome x with probability p (and nothing otherwise) is then given by:

$$V(x, p) = w(p)v(x)$$

Where w measures the impact of probability p on the attractiveness of the prospect and v measures the subjective value of the outcome x.

Prospect theory replaces the utility function u proposed by Bernoulli with a value function v over gains and losses relative to a dynamic *reference point*. This value function remains concave for gains, but is steeper and convex for losses (Fig. I.6a). These characteristics provide an account of two behavioral observations. First, the fact that human participants seem to have different rules of conduct towards gains and losses: they are risk averse for gains (as reported in the standard expected utility model), but risk seeking for losses (Kahneman & Tversky, 1979). That is, a certain option with a lower expected value than a risky gain will be preferred, while the risk of a large loss will be chosen to avoid a certain loss. Second, the steeper slope for losses than for gains provides an explanation for a property known as *loss aversion*, in which people generally require more compensation for giving up a good than they would have been willing to pay

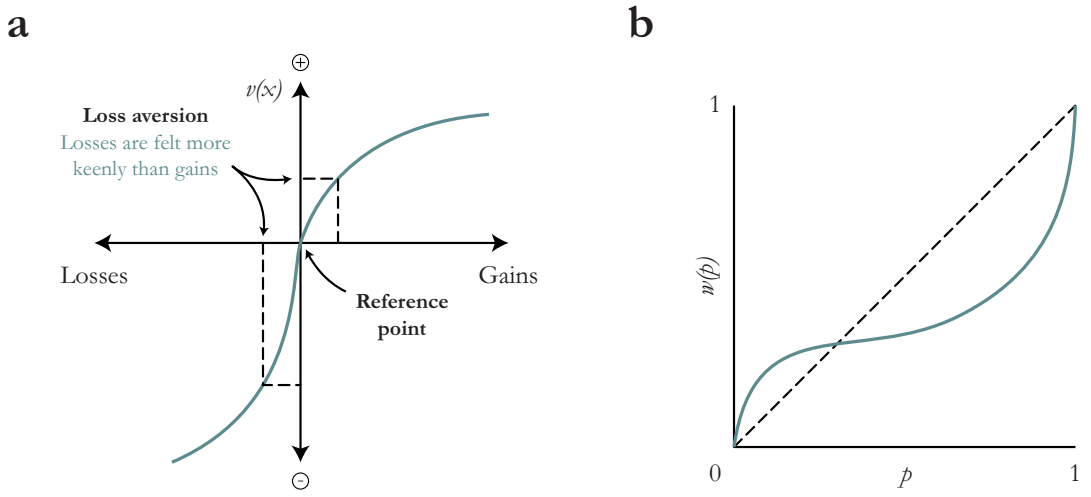

Figure I.6: Representative value and weighting functions from prospect theory. (a) Value function, showing concave curvature for gains, convex curvature for losses, and steeper gradient for losses than gains. (b) Inverse S-shaped probability weighting function. Adapted from C. R. Fox and Poldrack (2009).

to obtain it in the first place. Thus, loss aversion gives rise to risk aversion for mixed (gain-loss) prospects (e.g., most people reject a 50-50 chance of winning $100 or losing $100).

Prospect theory also proposes that probability is not linearly related to the true probability, but rather is integrated by a non-linear weighting function w (Fig. I.6b) that captures decreasing sensitivity to changes in probability. The inverted S-shape of this function captures notably the observed tendency to overweight low probabilities and underweight moderate to high probabilities (Kahneman & Tversky, 1979).

Thus, prospect theory provides a descriptive account of many of the so-called biases in risky decisions that cannot be explained by expected utility theory. Yet the expected utility model is still used in many applications today. One possible explanation for this is that utility theory has more degrees of freedom. So, although it can take more information into account, it gives much weaker testable predictions. Moreover, expected utility has been shown to be very strong in giving correct predictions in many areas of its applications (see Lewandowski, 2017 for a comparative view of the two approaches).

Summary

- Most of our decisions rely on the occurrence of **uncertain events**.
- Blaise Pascal postulated that the **expected value** of a risky choice could be calculated by combining the quantity of objective outcomes and their probability level.
- Daniel Bernoulli refined this theory by stating that decision-makers rather maximize the **expected utility** of a decision, that is, its desirability or satisfaction, given that each additional quantity of a good is less satisfying than the previous one.
- The identification of a number of paradoxes in this theory led Kahneman and Tversky (1979) to adapt and extend it into a descriptive model known as **prospect theory**.
- In particular, the latter theory takes into account the observation that human participants appear to have **different rules of conduct with respect to gains and losses**, a phenomenon known as **loss aversion**.

b. Mood

Intuitively, affects play an important role in our daily choices. Don't we say that some behaviors are made by following our heart, or because it *feels right*? Yet, the impact of emotional states on decision making has been ignored across disciplines for many years (Lerner et al., 2015). Decision-making was seen as a cognitive process, which was therefore necessarily opposed to emotions. This view goes back to Plato, who suggested that the soul had a tripartite structure, consisting of cognition, emotion and motivation. He argued that these components were distinct, that they were in competition and that cognition was superior to the others (Scherer, 2000). Thus, in order to make rational choices, one had to override emotional impulses. In recent decades, however, this trichotomy has been refuted and there has been growing interest in understanding the role of affective states in decision making as a result of several observations. First, that even affects that are not directly related to the decision at hand (i.e. *incidental* affects) can have an impact on choices (Clore, 1992; Lerner & Keltner, 2000). Second, that emotional deficits, whether related to psychiatric illness (Cáceda et al., 2014), injury (Damasio et al., 1994), or experimentally induced (e.g., Chou et al., 2007), can degrade the quality of decision making. And finally, that introducing affect into decision models can significantly increase their explanatory power (e.g., Mellers et al., 1997). In this section I will focus specifically on the effects of *mood* on decision making by first providing a brief definition of mood and its causes, and then describing some computational models that have been used in laboratory experiments to accurately quantify the effects of mood on behavior.

What is mood?

Mood can be defined as an affective state distinct from emotions (Eldar et al., 2016), which is typically measured along the valence dimension[3] (i.e., placed along a pleasure-displeasure continuum). According to Bennett et al. (2020), mood is characterized by four main properties: an integrative nature, a slow timescale, a non-intentional quality, and contextual modulation[4].

The *integrative property* states that the valence of mood reflects the cumulative impact of the valence of an individual's recent experiences, as opposed to emotions, which would rather be

[3] In the sense of the circumplex model of affect proposed by Russell (1980), which proposes that affects emerge from two basic systems, one of which is valence and the other arousal (i.e., intensity). Arousal, however, is rarely considered in this context, as affective states associated with mood are thought to be of low intensity and diffuse.

[4] These properties are largely shared by the theories and models outlined below. Nevertheless, it should be noted that this definition is one of many, as no consensus criteria currently prevail among typologies to strictly delineate the concept of mood from other related affective phenomena such as emotions.

the product of a single event. This property is widely held in theories of mood from various fields, including philosophy, psychology or ethology (Edgeworth, 1881; Kahneman et al., 1999; Mendl et al., 2010; Nettle & Bateson, 2012; Parducci, 1995; Ruckmick, 1936; Webb et al., 2019). It entails that an individual whose recent experiences have been generally pleasant is likely to have a positive mood, as opposed to a negative mood if the recent experiences have been primarily unpleasant (Isen et al., 1978; Morris, 1989). Specifically, mood can be viewed as a leaky integrator of the valence of transient experiences, such that recent events influence mood more strongly than events distant in time (Rutledge et al., 2014; Vinckier et al., 2018).

As opposed to emotions that occur in the short term, mood is generally said to incorporate the valence of momentary events on a time scale of hours to days (Larsen, 2000; Morris, 1989). However, this does not exclude the possibility that older events may influence mood, since remembering more or less pleasant events may itself be associated with valence. Thus, emotion and mood can be seen as parallel processes that interact and occur on different timescales (Eldar et al., 2016).

The *non-intentional property* reflects the idea that, unlike other affective states such as emotions, mood is not about anything specific (Rossi, 2019). In other words, a good or bad mood is not related to a particular event, as enjoyment may be tied to eating a favorite dessert or fear to the sight of a snake. Instead, mood is generally considered to be an unfocused and diffuse background affective state (Beedie et al., 2005; Larsen, 2000).

Finally, *contextual modulation* refers to the fact that events do not affect mood in the same way depending on the context in which they occur. In other words, the same event can have completely different effects on the valence of mood. Many contextual effects have been reported in the literature, such as the expectation or counterfactual effect (Bennett et al., 2020). The *expectation effect* is one of the most documented. It proposes that an event does not influence mood according to its utility (or value), but rather according to the degree of difference between its actual and expected utility (Eldar & Niv, 2015; Medvec & Savitsky, 1997; Mellers, 2000; Mellers et al., 1997; Otto & Eichstaedt, 2018; Rutledge et al., 2014; Villano et al., 2020). For example, the effect of test scores on university students' mood has been shown to depend on whether the scores exceed their expectations or not (Villano et al., 2020).

Mood induction and measurement

A key factor in studying the relationship between mood and decision making is being able to induce and measure mood in a reliable and consistent manner. A vast literature in psychology

suggests that mood can be manipulated by a wide range of techniques. Some of the most commonly used include presenting a movie or story with emotional content, listening to music, engaging in social interactions, displaying facial expressions, and receiving feedback or monetary outcomes (Westermann et al., 1996). Outside of the laboratory, various factors have also been shown to correlate with mood fluctuations, the most famous being the results of sporting events (Edmans et al., 2007) or sunlight levels (Bassi et al., 2013).

To measure the dynamics of emotional states, researchers have developed a technique known as *experience-sampling*, which involves asking participants about their subjective state at the moment. This technique, which requires repeatedly asking participants about their current mood, is considered "the gold standard" for studying momentary feelings in the real world. Yet, despite the strengths of this method, one of its limitations is that repeated reporting of mood may itself influence feelings, especially in a laboratory setting where sampling is more frequent. As a result, subjects' ratings may not be congruent with their actual state (Napa Scollon et al., 2009).

Rutledge: A computational model of momentary happiness

To address this issue, Rutledge et al. (2014) developed a computational model by examining momentary mood fluctuations during a laboratory-based probabilistic reward task. Specifically, subjects had to repeatedly choose between certain outcomes and gambles whose potential gains and losses varied from trial to trial. The main conclusion of this study was that mood fluctuations depend primarily on the difference between expected and actual outcomes, a finding that was previously reported as the expectation effect (see above). Still, the novelty of this study was that, by using computational modeling, it was possible for the authors to estimate the theoretical value of mood on a trial-by-trial basis, for each subject, even in the absence of actual mood ratings. In particular, subjective well-being was modeled as follows:

$$Happiness_t = \omega_0 + \omega_1 \sum_{j=1}^{t} \gamma^{t-j} CR_j + \omega_2 \sum_{j=1}^{t} \gamma^{t-j} EV_j + \omega_3 \sum_{j=1}^{t} \gamma^{t-j} RPE_j$$

Where, for each trial j (from the first trial to the current trial t), if the certain reward was chosen it was entered into the equation as CR_j. Conversely, if the gamble was chosen two terms were entered into the equation: EV_j, the expected value of the gamble, and RPE_j, the difference between the actual outcome and the EV. The weights ω (including a constant term ω_0) capture the influence of the different types of event. Finally, these influences decay exponentially over time with a forgetting factor $0 \leq \gamma \leq 1$ that makes recent events more influential than earlier ones. This work marks a turning point in the investigation of the precise mechanisms

through which mood influences behavior by providing a computational account of how mood fluctuations can arise from the feedback an individual receives.

Types of affective influences

When discussing the impact of emotional states on choice, it is useful to identify the distinct types of possible influence. Indeed, affects can come into play at different stages of the decision-making process. Loewenstein and Lerner (2003) distinguished between expected and immediate affects, the latter being further classified into anticipatory and incidental affects. *Expected affect* is defined as possible future emotions considered when determining the expected utility of different courses of action. They argue that this is actually the only type of affect that has been accounted for in classical models of decision making. Among the immediate affects, *anticipatory affects* arise from the choice at hand. They are a direct part of the decision process and are experienced when a decision maker anticipates the outcomes of choice options, such as the anticipatory fear of flying. Anticipatory affects differ from expected affects in that they are not "cognitive" but actually felt. *Incidental affects*, on the other hand, are by definition unrelated to the outcomes currently being considered, but may nevertheless cause alterations in the choice processes. Mood can fall into any of these three categories (e.g., as an expected affect when an action is chosen because it is expected to set a good mood), although it is most often incidental. In my experimental work, I was only interested in the *incidental influence* of mood.

Consequences of incidental mood on choices

There are a number of psychological theories that seek to explain how mood influences decision making (see Shevchenko, 2018 for a review). The *mood-as-information* theory, also known as the feeling-as-information model, is perhaps one of the most influential of these. In an initial study, Schwarz and Clore (1983) asked healthy individuals to indicate their degree of satisfaction with their lives while in a positive or negative mood, induced either by an episodic recall procedure (Experiment 1) or simply by the weather (Experiment 2). The results showed that recalling sad events or unfavorable weather conditions dampened participants' mood, resulting in a decrease in their life satisfaction ratings. Interestingly, mood did not affect the judgment of participants who were first asked about the weather, indicating that the incidental influence of mood (also known as misattribution) could be tempered by a greater awareness of the (unrelated) source of this affective state. These findings eventually gave rise to the mood-as-information theory, which posits that preexisting mood levels provide valuable information about a person's current situation, and thereby influence the processing strategies they adopt (Schwarz & Clore, 1983; 2003). That is, when faced with a task requiring a judgment, individ-

uals will typically frame their decision based on their current mood, such as asking themselves "How do I feel about it?". The judgment may then be misattributed in response to the current mood. As a result, evaluative *mood-congruent* judgments occur (Schwarz & Clore, 2007). Such a model assumes, for example, that people in good moods tend to view the world as more friendly and thus make more positive subjective judgments, while people in bad moods tend to evaluate the events around them as negative (Loewenstein & Lerner, 2003; Schwarz, 2012). This view has been supported by numerous studies, most notably in the context of uncertain or risky decisions where good mood has been consistently associated with risk-seeking choices, while bad mood has been associated with more risk-averse decision-making (e.g., Arkes et al., 1988; Bassi et al., 2013; Chou et al., 2007; Otto et al., 2016; Saunders, 1993).

Recently, researchers have begun to use computational methods in laboratory experiments to precisely quantify the effects of mood on decision making. In one study, mood was manipulated using a wheel-of-fortune game in which subjects won or lost a relatively large sum of money (Eldar & Niv, 2015). Among participants independently identified as less emotionally stable, winning the draw not only increased self-reported happiness (as predicted by Rutledge's model presented above) but also increased perceived subjective reward value in subsequent choices. Conversely, losing the draw reduced mood, as well as the effect of rewards on subsequent choices. These results suggest that mood influences decision making by biasing the perception of outcomes, with positive (negative) mood leading to higher (lower) valuation. Another study confirmed these findings in healthy subjects and with a similar computational model, showing that the integration over time of positive and negative feedback from a quiz task induced mood fluctuations which in turn modulated the relative weights assigned to gains and losses in a choice task (Vinckier et al., 2018). Specifically, good mood promoted risk-taking by overweighting potential gains, while bad mood tempered risk-taking by overweighting potential losses.

Overall, the foregoing results suggest that there is a *bi-directional influence* between mood and outcome processing during decision making. While mood fluctuations have been accurately modeled by an integrative process of feedback history and subjects' expectation (Rutledge et al., 2014), later models have included a reciprocal influence of mood on the perception of feedback to capture the fact that mood also distorts how subjects perceive outcomes in decision contexts (Eldar & Niv, 2015; Vinckier et al., 2018), taking events as more positive than they objectively are when in a good mood and conversely when in a bad mood. Crucially, specific dysfunctions of this feedback loop have been argued to contribute to the emergence of mood disorders such as depression or mood instability (Fig. I.7; Eldar et al., 2016).

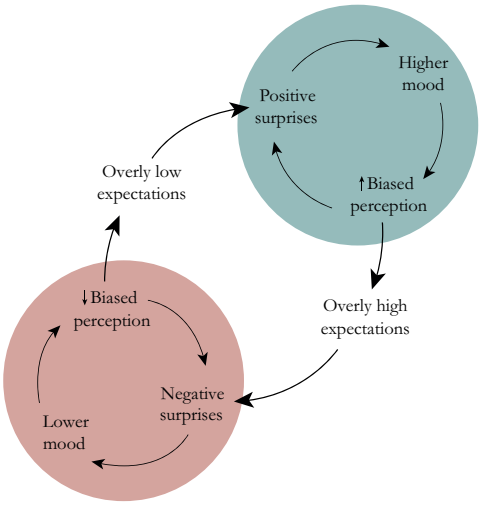

Figure I.7: Schematic of possible mood dysfunctions. Positive feedback loops reinforcing good and bad moods, and possible transition between them. From Eldar et al. (2016).

Summary

- **Mood is an affective state distinct from emotions**, which is typically set along a pleasure-displeasure continuum. It can be described by 4 main properties: an integrative nature, slow timescale, non-intentional quality and contextual modulation.
- In the laboratory, mood can be induced by **mood induction procedures** that typically expose participants to emotionally valenced stimuli.
- Recently, Rutledge et al. (2014) developed a **computational model of mood** that captures how mood fluctuations can result from the **feedback** an individual receives. One of the key features of this model is that mood depends primarily on the **difference between expected and actual outcomes**.
- Mood can have different types of influence on decision making, including an **incidental effect** (i.e., unrelated to the outcome of the current decision), which was the focus of the present work.
- Behavioral experiments using computational models have refined the model proposed by Rutledge et al. (2014) in suggesting that **mood and outcome processing influence each other** during decision making, such that feedback from a decision influences mood, and in turn, mood influences the perception of feedback.

In my first experimental study, I used the mood model of Vinckier et al. (2018) that accounts for this bi-directional interaction to retrieve participants' mood levels on each trial of a risky choice task (see section III.5. for a detailed description of this model).

c. Visual attention

Another potential underlying source of choice stochasticity highlighted in the literature is attention. Attention is a broad concept, generally defined as a mechanism that prioritizes relevant input and determines the quality of target information processing (Chun et al., 2011). This mechanism is believed to have evolved out of necessity to account for the computational limits of the brain's ability to process information and ensure that behavior is controlled by relevant material (Pashler et al., 2001). Part of the challenge in studying the impact of attention on choice lies in the inherent difficulty of measuring it. In early studies, researchers have used verbal protocols in which participants were prompted to verbalize every thought they had, either concurrently with the decision process or retroactively (Payne et al., 1978). However, these protocols can interfere with the task at hand and provide only approximate information about the timing of different stages of the decision process. A more direct approach, which has since become the dominant method, has been to track eye movements during the decision process. This stems from the fact that, under normal conditions, eye movements and visual attention are thought to move synchronously and select common targets in the visual field (Deubel & Schneider, 1996; Hoffman & Subramaniam, 1995; Shepherd et al., 1986). Thus, visual fixations would reflect what is actually being considered/processed.

Visual attention and value interactions

When making a decision involving visible options (e.g., in front of a market stall or on the shelves of a supermarket), people typically shift their gaze between these options until one is selected. In this context, two methodological approaches have been used to investigate the role of visual attention during value-based choice (Fig. I.8). The first, called *free attention* or "participant-controlled viewing", involves observing how participants freely move their gaze during decision making through the use of an eye-tracking device. The second is *forced attention* or "experimenter-controlled viewing", in which researchers exert at least partial control over the location and duration of fixations by, for instance, displaying the choice alternatives or their individual components sequentially. The latter allows direct control of attention during decision making, but is less ecological than free viewing.

To our knowledge, the first study that linked value to visual attention used forced attention (Shimojo et al., 2003). In this one, participants were asked to choose the most attractive of two faces whose exposure time was manipulated by the experimenters on each trial. Their results indicated that over time, gaze tended to shift toward the option that was ultimately chosen and

that manipulating gaze duration biased observers' preference decisions. The authors referred to this phenomenon as the *gaze cascade effect*. That is, they argue that a causal relationship exists between gaze and preference, such that participants looked longer at valued faces (preference determines gaze) and their valuation increased for the items they looked at more (gaze determines preference).

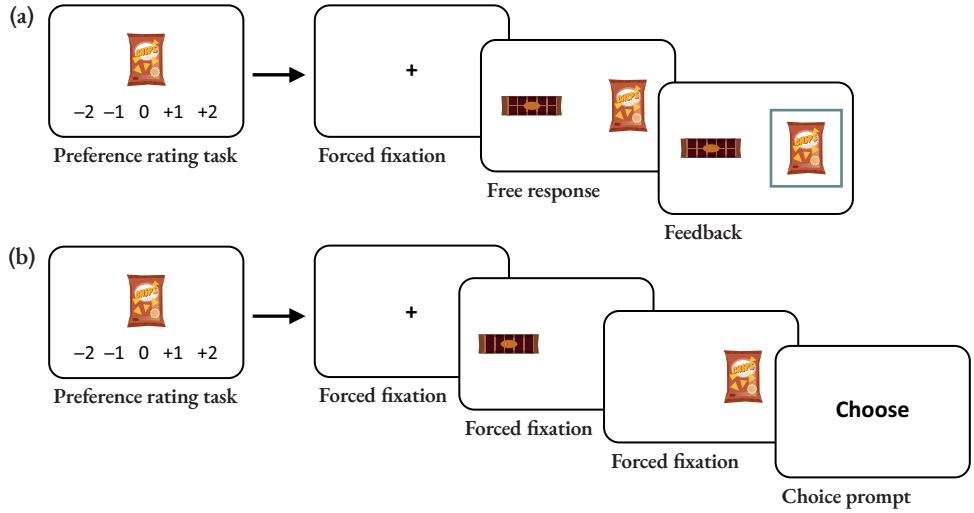

Figure I.8: **Experimental procedures for investigating visual attention during value-based choice**. In both procedures, participants typically begin by rating on a scale how much they like the items presented. In a free attention task (a), participants see two of the previously rated alternatives and must choose one. In the forced attention task (b), the experimenter controls exposure in several ways. Sometimes the visibility of the choice options is alternated, as shown here, or the experimenter may require a fixation time for each of the alternatives using exogenous cues (not shown). Finally, in some studies, the food chosen in a randomly selected trial is given to consume, while others are only hypothetical choices. Adapted from M. M. Mormann and Russo (2021).

Ever since, strong empirical evidence has replicated these results, showing that people tend to look longer or be distracted by higher value options (a phenomenon called "value-based attentional capture"; Anderson et al., 2011; Gluth et al., 2020; Gluth et al., 2018), and that the option they look at the most tends to be chosen (Cavanagh et al., 2014; Krajbich & Rangel, 2011; Krajbich et al., 2010; Thomas et al., 2019). One interpretation of such results is that visual attention is directed toward items based on their value, and that looking at an option increases its value, either by amplifying it (Krajbich & Rangel, 2011; Krajbich et al., 2010; Smith & Krajbich, 2019) or by moving it up by a constant amount (Cavanagh et al., 2014). However, these studies are largely correlational, and the direction of causality between visual attention and choice is still debated (M. M. Mormann & Russo, 2021). While the gaze cascade effect suggests a bidirectional relationship between visual attention and choice (Shimojo et al., 2003), another stream of evidence holds that only one direction applies, namely that visual attention

has a causal effect on value during choice (Krajbich & Rangel, 2011; Krajbich, 2019; Krajbich et al., 2010).

Evidence for the causal role of visual attention on choice

The claim that visual attention amplifies value is based on a substantial amount of experimentation employing various exogenous manipulations. For example, in one experiment, Armel et al. (2008) manipulated relative *exposure times* using a forced attention paradigm in which options were displayed one at a time. They found that the item that appeared on the screen for a longer period of time was more likely to be chosen if it was positive, but less likely if it was negative. Along similar lines, Lim et al. (2011) used a paradigm in which both choice items were kept on the screen but gaze was directed by an exogenous cue. Again, items that received more attention were more likely to be chosen. Another set of studies attempted to alter the physical properties of the stimuli by changing their *visual salience* to more subtly influence attention. In one of them, the researchers increased the brightness of one of the elements so that it would be looked at more than the other (M. M. Mormann et al., 2012). This manipulation effectively increased choices for the more salient element, a result that has been replicated in subsequent studies (Kunar et al., 2017; Towal et al., 2013). In addition, still other studies have shown that exogenously influencing attention by manipulating the *timing of the decision prompt* (Pärnamets et al., 2015; Tavares et al., 2017), the *location of systematically better items* (Colas & Lu, 2017), or *spatial cues* (Mrkva & Van Boven, 2017) resulted in a corresponding choice bias.

Although these studies have made significant progress in establishing the causal link between visual attention and choice, they use techniques that directly interfere with the natural choice process, alter the properties of choice alternatives, or manipulate participants' expectations. Thus, it cannot be ruled out that some other explanation may account for these results. Interestingly, however, a recent study specifically aimed at overcoming these limitations, by using a separate attentional learning task to induce a spatial bias in attention, reached the same conclusion of a causal effect of visual attention on choice (Gwinn et al., 2019).

Some literature argues that this hypothesis is also strengthened by evidence against the reverse relationship (i.e., that value would have a causal role on eye fixations). In particular, the fact that, during binary decisions, initial fixations were equally likely to go to higher or lower value options, and that the duration of a given fixation was not correlated with the value of the option being looked at (Krajbich & Rangel, 2011; Krajbich et al., 2010; Krajbich et al., 2012). However, these claims can be qualified by the extensive evidence that reward cues direct attention even

when that cue is not salient, irrelevant to the task, or results in negative outcomes (Anderson et al., 2011; Gluth et al., 2018; M. M. Mormann & Russo, 2021).

A computational model of the relationship between visual attention and value

To model the relationship between attention and choice, Krajbich et al. (2010) have proposed a simple variant of the drift-diffusion model in which the evolution of the relative decision value signal depends on the pattern of attention (Fig. I.9). This model, called the attentional drift-diffusion model (aDDM), is identical to the basic drift-diffusion configuration (see section I.2.b.), except that the drift rate is no longer constant within the decision, but now depends on the option to which visual attention is directed. In other words, gaze has an amplifying effect on the attended option. For instance, when a given option is being attended, the relative decision value signal evolves according as follows:

$$R_{t+1} = R_t + \theta \times (\beta v_{attended} - v_{unattended}) + \epsilon_t$$

Where β measures the attentional bias towards the value of the attended option ($v_{attended}$). If $\beta = 1$, the model is identical to the basic model and choice is independent of attention, but if $\beta > 1$, choices are biased towards the option that is attended longer.

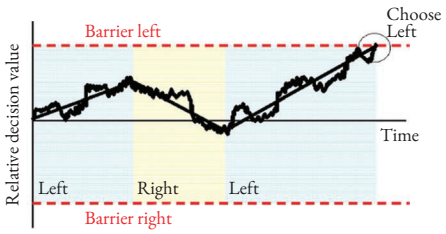

Figure I.9: Attentional drift-diffusion model. A relative decision value (RDV) evolves over time with a slope that depends on what the subject is looking at. In addition to the average drift, there is also Gaussian noise. When the RDV reaches one of the two barriers the subject makes the corresponding choice. The colored regions indicate what the subject is currently looking at, blue for the left item on the screen and yellow for the right. From Krajbich et al. (2010).

Two features of this model are worth mentioning. First, it predicts that exogenous changes in attention should bias choices toward the most attended option when its value is positive, but should have the opposite effect when the value is negative. Consistent with this prediction and as mentioned above, several studies have shown that choices can be biased by exogenous manipulations of visual attention, including a positive bias toward appetitive stimuli and negative bias toward aversive stimuli. Second, the model makes strong quantitative predictions about the correlation between visual attention, choices, and reaction times that have been supported by several studies (e.g., Krajbich et al., 2010; Pärnamets et al., 2015; Smith & Krajbich, 2019). In particular, using a free attention task in which participants were asked to choose between

two food items, the original study demonstrated that the model could account for the fact that more fixated options were more likely to be chosen (Krajbich et al., 2010). Thus, although mere computational fits are insufficient to provide direct evidence of causality, these results certainly point toward an attentional bias on choices that is not simply mediated by subjective value.

*

Overall, the use of eye-tracking and modeling of choice behavior provides substantial evidence supporting a causal and amplifying effect of visual attention on subjective value during binary choices. These results have been further extended to consumer choices (Krajbich et al., 2012) and choices with multiple alternatives (Krajbich & Rangel, 2011).

Summary

- Attention is a broad concept, generally defined as a mechanism that prioritizes relevant input and determines the quality of target information processing. Studies investigating the effects of attention have focused primarily on **visual attention**, as it is thought to move synchronously with eye movements and is therefore easily quantifiable.
- Behavioral studies in humans suggest that a **bi-directional relationship occurs between visual attention and choice**, such that visual attention is directed toward items based on their value, and, conversely, **looking at an item increases its value**.
- To account for the effect of visual attention on choices, Krajbich et al. (2010) proposed a simple variant of the DDM, called the **attentional drift-diffusion model**, in which the evolution of the relative decision value signal depends on the eye fixation pattern.

In my second experimental study, I investigated the effects of visual attention on decision making by focusing on multi-attribute choices that were given less attention than single-attribute binary choices (see subsection II.3.c.).

II

The neural underpinnings of value-based decisions

Having outlined the theoretical tenets of value-based decision making, we now turn to how value is processed in the brain to inform choices. In this chapter, I will first introduce the measures that can be performed to study neural activity. Next, I will review the literature on the encoding of expected value and prediction error signal in the brain, distinguishing between reward and punishment processing. Finally, I will present the neural correlates underlying the value modulators that I focused on in my experimental work, namely spontaneous brain activity, mood, and visual attention.

1. Brain activity measurements

Brain activity can be measured using different techniques that operate at different levels: that of neurons (single-unit recordings), populations of neurons (local field potentials) or brain regions (functional magnetic resonance imaging). It is important to note, however, that the different methods address different aspects of neuronal function. Indeed, the interpretation of a given result may depend strongly on what is being measured: neuronal firing, brain metabolism, neurotransmitter levels or any other brain property.

Cognitive neuroscience techniques can be divided into two broad categories that provide distinct and complementary information about brain function: measurement techniques and manipulation techniques. As the name implies, measurement techniques measure changes in brain function while a research participant (human or animal) is engaged in a cognitive activity. These techniques can be called *correlational* because they show that signals from a brain region coincide with a function of interest, but do not demonstrate that a region is necessary for that function. Manipulative techniques, on the other hand, examine how disruptions in brain function alter cognitive function or behavior through a transient change in neural firing frequency/neurotransmitter levels, or through permanent tissue damage. For this reason, manipulative techniques are called *causal* approaches.

Each method has its strengths and limitations. In general, three factors are distinguished of primary importance: temporal resolution, spatial resolution and invasiveness (Fig. II.1). Temporal resolution refers to the frequency in time with which measurements or manipulations can be performed. It is important because some processes require good temporal resolution to be distinguished from one another. Spatial resolution refers to the ability to distinguish adjacent brain regions that differ in function. Finally, invasiveness refers to the ability to make measurements without damaging or disturbing the brain. Non-invasive techniques record endogenous brain signals and thus can be performed repeatedly on human volunteers, whereas invasive techniques are only used on non-human animals and/or human patients (e.g., prior to neurosurgery).

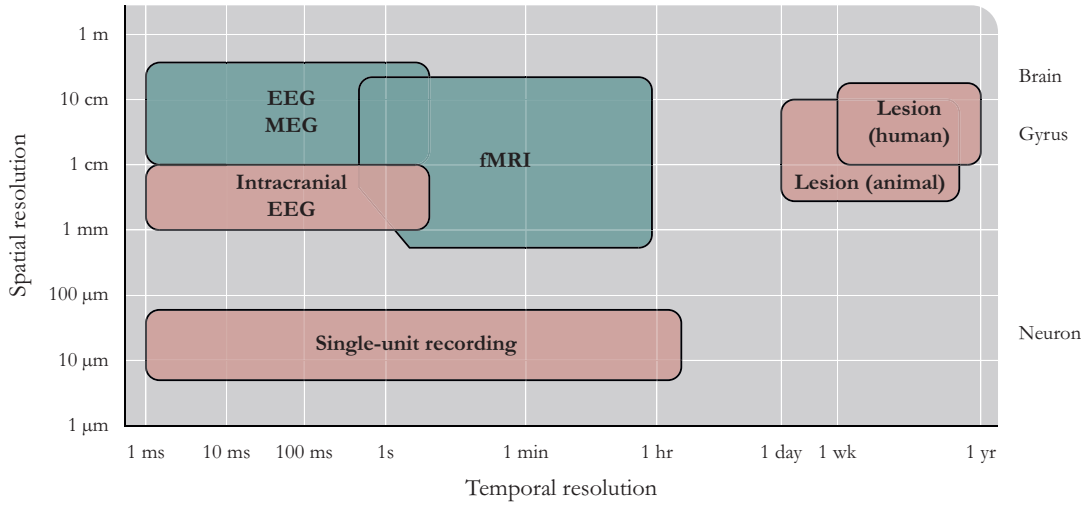

Figure II.1: Schematic overview of the spatial and temporal resolution scale of brain measurement methods. Non-invasive methods are shown in green and invasive methods in red. EEG: electroencephalography; MEG: magnetoencephalography; fMRI: functional magnetic resonance imaging. Adapted from Ruff and Huettel (2014).

a. Measurement techniques

Single unit recordings: the firing rate

Neurons are cells that communicate through electrical impulses called action potentials. These action potentials have a stereotyped amplitude and waveform for a given neuron and the rate at which they are emitted can vary in response to stimuli. Thus, variations in the firing rate of neurons are used to determine whether a stimulus (or any type of behavior) alters the ongoing information processing with which these neurons are associated. The measurement of action potentials requires the insertion of very thin electrodes into the neural tissue immediately adjacent to the neurons of interest. The electrode itself does not cause appreciable damage to the brain, but opening the skull to access the brain is an invasive surgical procedure that carries significant risks. The fundamental advantage of single-neuron recording is that it provides direct information about the timing and synchronization of action potentials in a region with extraordinary temporal resolution. Analysis of single neurons can also reveal the diversity of processes within a brain region. However, this technique also has important limitations. The invasive nature of single neuron recording limits its use to non-human animals (but see section VI.1.a. about microelectrode recordings in humans). In addition, most published papers focus on neurons in a single brain region, thereby limiting the insights that can be gained into complex cognitive processes, most of which involve interactions between multiple brain regions. Data from single-unit recordings are therefore often highly complementary to data from techniques with broader spatial coverage but more limited spatial and temporal resolution.

Local Field Potentials

While action potentials only relate to the activity of a single neuron, local field potentials (LFP; also known as intracranial EEG) reflect the aggregated activity of small populations of neurons represented by their extracellular potentials. LFPs are recorded within cortical tissue (or other deep brain structures), usually using extracellular micro-electrodes, which distinguishes them from electroencephalography (EEG), recorded on the surface of the scalp with macro-electrodes, and electrocorticography (EcoG), recorded on the surface of the brain using large subdural electrodes (Fig. II.2a). LFPs are characterized by oscillatory activity that is thought to play a role in neuronal communication (Fries, 2005) and can be broken down into several frequency ranges. In particular, in addition to the standard frequency ranges investigated in surface EEG, namely delta (1-3 Hz), theta (4-8 Hz), alpha (8-12 Hz), beta (13-30 Hz), and gamma (30-50 Hz), LFPs allow measurement of the high gamma band (50-150 Hz), which is highly attenuated by skull

and scalp in EEG recordings. This is significant since it has been shown that high gamma band activity is strongly correlated with the ensemble spiking of cells in the immediate vicinity of the electrode contact (Fig. II.2b-c; Ray et al., 2008). A benefit of LFP recordings is therefore that, through the high gamma oscillations, they can be a useful indicator of the firing dynamics of the recorded neuron population. In addition, LFPs recordings provide anatomically precise information about the selective involvement of neuronal populations at the millimeter scale and the temporal dynamics of their engagement at the millisecond scale. Also, compared to single-cell recordings, multiple electrodes are typically implanted simultaneously, providing information about functional interactions within and between networks at different stages of neuronal computation (Parvizi & Kastner, 2018). A major limitation of this method is that it is highly invasive and is therefore usually only performed in rodents or non-human primates. However, a few rare clinical cases allow the recording of LFP in humans. Most of them are epileptic patients who undergo stereo-electroencephalography (sEEG) recordings to identify the locus of the seizure (Fig. II.2a; see Nuwer et al., 2019 for a review). The others, even rarer, are patients undergoing deep brain stimulation surgery used for the treatment of refractory psychiatric and neurological disorders (e.g., major depressive disorder, obsessive compulsive disorder, Parkinson disease; Lozano et al., 2019). In all cases, these recordings are subject to clinical and hospital constraints and the location of the electrodes is not under the control of the researchers.

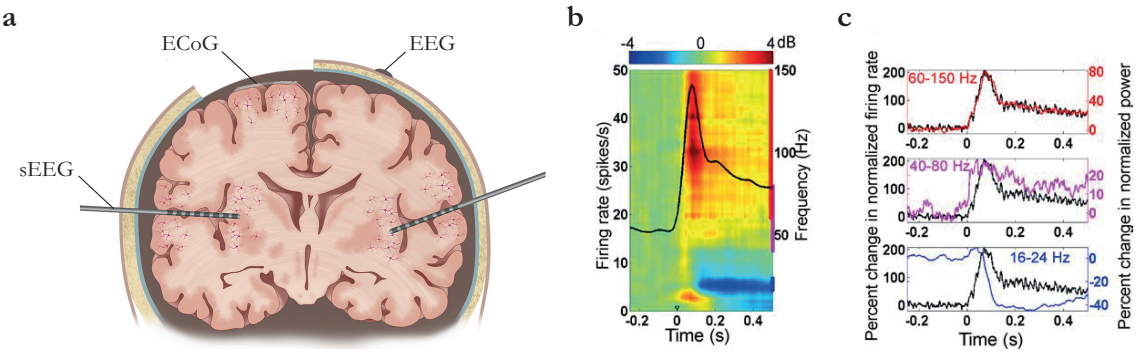

Figure II.2: Local field potentials recordings and relation to firing rate. (a) Illustration of different electrodes used to record cerebral activity. The stereo-electroencephalography (sEEG) electrodes are inserted directly into the cortical tissue and can record local field potentials, while the electroencephalography (EEG) electrodes are placed non-invasively directly on the scalp and the electrocorticography (EcoG) electrodes are placed on the cortical surface. Adapted from Grande et al. (2020). (b) Time-frequency plot of the change of LFP power relative to baseline. The firing rate of the neuronal population is plotted in black. (c) Change in normalized firing rates (black traces) plotted along with the change in normalized power in the high-gamma (red, top), low-gamma (magenta, middle), and beta (blue, bottom) frequency ranges. The overlap between firing rate and high gamma power has been advanced as an argument for considering high gamma power as an indicator of local activity in a neuronal population. (c-d) are from Ray et al. (2008).

Functional magnetic resonance imaging (fMRI)

Since its development in the early 1990s, fMRI has become the dominant measurement technique in cognitive neuroscience. In contrast to the techniques seen so far, fMRI does not exactly measure electrical activity, but rather the indirect consequences of neuronal activity (the hemodynamic response). More precisely, it records the variation in blood oxygen level through the BOLD (blood-oxygen-level-dependent) signal, based on the premise that neurons consume more oxygen when they become active (see Huettel et al., 2014 for a detailed description). BOLD activity was found to be more related to LFPs than to single-unit recordings (Logothetis et al., 2001). Nevertheless, high gamma activity was shown to be reflected in the BOLD signal, thus establishing a link between spiking activity and BOLD signal (Mukamel, 2005; Nir et al., 2007). One of the main advantages of fMRI lies in its accessibility, as it can be performed with human volunteers and on standard clinical MRI scanners. In addition, fMRI has excellent spatial resolution allowing sampling of the entire brain. However, its temporal resolution is well below that of electrophysiological techniques, which may make it difficult to study highly dynamic mental processes.

b. Manipulative techniques

The techniques presented so far reveal correlations between behavioral variables and measures of brain activity. In other words, they make it possible to identify whether, where and when the variables relevant to the decision are represented in the brain. However, these techniques do not provide information on whether these neural representations are *actually* involved in behavior. This knowledge is fundamental to establish truly mechanistic models of decision making, which would allow, for example, to identify the neural mechanisms underlying the pathological perturbations of decision making in brain disorders.

Lesion studies

Lesion studies are a powerful means of studying the impact of neural processes on behavior. In humans, these studies are closely related to the clinical fields of neurology and neurosurgery, as brain lesions leading to behavioral deficits occur as a result of accident or disease. Understanding these deficits is obviously very important for diagnosis, treatment and rehabilitation. Nevertheless, these patients also provide valuable data on the conditions under which a given anatomical substrate is necessary for a given process (Dunn & Kirsner, 2003; Fellows, 2012; Fellows et al., 2005). In humans, the main drawback of this approach is that, unlike animal studies,

natural brain lesions are often spatially diffuse and rarely selective to specific brain areas. It can therefore be difficult to attribute a deficit to a specific brain area.

Intracranial electrical stimulation

In animal research, direct electrical stimulation of neurons by intracranial electrodes is a routine practice. These stimulations are performed from electrodes inserted in the brain to perform the single unit or LFP recordings described above. This technique consists of applying weak electrical currents to the cortex that affect the activity of neurons in close proximity to the electrode. Because it is highly invasive, this method is not often used in humans, but as mentioned above, in rare cases, electrodes can also be implanted in patients to treat chronic and severe brain disorders such as Parkinson's disease or depression. In particular, a distinction can be made between intracranial electrical stimulation (iES; Desmurget et al., 2013) selectively applied during intraoperative procedures in patients with tumors or epilepsy and deep brain stimulation (DBS; Lozano et al., 2019), which is a neurosurgical procedure involving the implantation of electrodes into specific targets in the brain and the delivery of constant or intermittent electricity from an implanted battery. Under these conditions, it is possible to perform electrical stimulation while patients perform a cognitive task, thereby providing insight into the causal role of the stimulated brain region.

2. Coding of prediction error and predicted value signals in the brain

As previously discussed, value-based decision making can be divided into several distinct steps that require different value signals (see section I.1.a. and Box 2), including evaluating the outcomes of different options, and learning from those outcomes. Although many questions remain to be answered, empirical studies of decision making and reinforcement learning have indeed identified different types of neural representations of value that correspond to these stages and are associated with changes in activity in different neural structures. Among these different types of value, my experimental work notably related to the stimulus value, that is, the expected value of the outcome of a decision. In the next section, I will therefore attempt to describe the valuation system in the brain by focusing on two specific signals: the *prediction error* (as it is considered to play a central role in learning the value of stimuli) and *stimulus value*. Early studies that looked at the neural representation of the value network focused almost exclusively on reward valuation. I will therefore begin by outlining the neural basis of reward processing, and then present the various hypotheses regarding the existence of a separate system for punishment

processing. This brief review is not intended to be exhaustive, but simply to outline the results that inform my experimental work. Thus, although the valuation system has been studied in a wide range of species, I will focus here primarily on *electrophysiological* and *neuroimaging* work done in humans, as well as in non-human primates given the many biological and behavioral homologies they share.

a. Neural basis of rewards

Studies of the brain's valuation circuits have emerged from two largely separate fields. On the one hand, the study in the late 1990s of *dopaminergic* neurons in the midbrain led to the discovery of how we learn the value of goods and actions from experience. In parallel, a second field of investigation focused on finding signals that correlate with the *subjective values* of goods. This approach has made it possible to delineate a neural circuit involved in reward processing. At the core of this circuit is the role of the *ventral striatum* and the *orbital and ventromedial* parts of the *prefrontal cortex* (all of which are primary targets of the dopaminergic system) in representing and adjusting the stimulus value to inform decision-making (Haber & Knutson, 2010). Activity in these areas has been shown to consistently predict preferences of all kinds in humans and non-human primates. In order to give a general view of the structural and functional organization of this reward circuit, I will start by describing the anatomy of its main components before presenting the various evidences of their involvement in the so-called brain valuation system.

i. Neuroanatomy

The Dopaminergic system

Dopamine is a neurotransmitter (Carlsson, 1959) whose majority of neurons are found in the center of the midbrain and form three groups of cells, the retrorubral nucleus (RRN), the substantia nigra pars compacta (SNc) and the ventral tegmental area (VTA; (Fig. II.3). These groups of cells are contiguous, so there are no clear boundaries between them. From these small nuclei, dopaminergic neurons project to various brain regions where their axonal terminals release the neurotransmitter dopamine. The neurons of the SNc innervate mainly the basal ganglia, in particular the caudate and putamen nuclei (i.e., dorsal striatum), through the so-called nigrostriatal pathway. The VTA neurons send projections mainly to the *ventral striatum* (i.e., the nucleus accumbens and olfactory tubercle), the amygdala and the hippocampus via the mesolimbic pathway and to the *prefrontal* and cingulate cortices via the mesocortical pathway (Arias-Carrión et al., 2010).

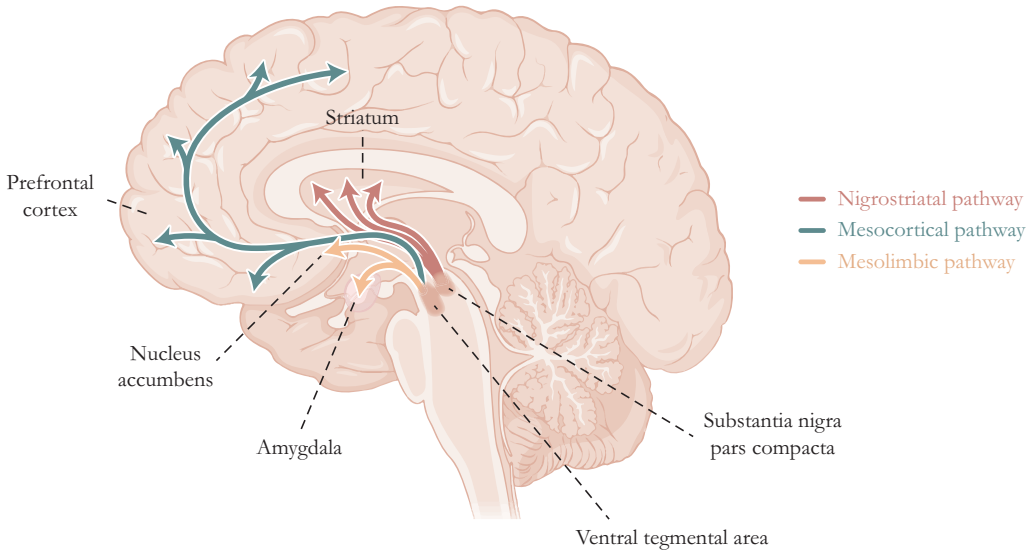

Figure II.3: The dopaminergic system of the midbrain and its projection pathways. Adapted from Arias-Carrión et al. (2010).

Dopamine release was initially closely associated with reward and motivation, so much so that an early and influential article (the "anhedonia hypothesis") argued that it alone constituted the brain's reward system (Wise, 1982). As we will see below, contemporary accounts tend to refine this hypothesis by distinguishing different aspects of reward (Schultz, 2007). In particular, rather than being involved in the subjective feelings of pleasure associated with reward, dopamine is now thought to be involved in effects like reinforcement by encoding a signal that can guide reward learning.

The basal ganglia

Dopamine acts on the reward circuit through the cortico-basal ganglia network. The basal ganglia are a group of interconnected subcortical nuclei located at the base of the forebrain and the top of the midbrain (Fig. II.4). The main components of the basal ganglia – as functionally defined – are the striatum, composed of both the dorsal striatum (caudate nucleus and putamen) and the *ventral striatum* (nucleus accumbens and olfactory tubercle), the globus pallidus (its internal GPi and external GPe segments), the substantia nigra (its pars compacta SNc and pars reticulata SNr), the subthalamic nucleus (STN), the ventral pallidum, and the ventral tegmental area (VTA; Redgrave et al., 2010).

Different levels of complexity exist in the organization of the basal ganglia. Since the late 1980s, the classical model in both humans and animals has been based on the presence of direct and indirect intrinsic pathways, both comprising a consecutive set of glutamatergic excitatory and GABAergic inhibitory projections (Fig. II.5a). This model includes descending cortical projec-

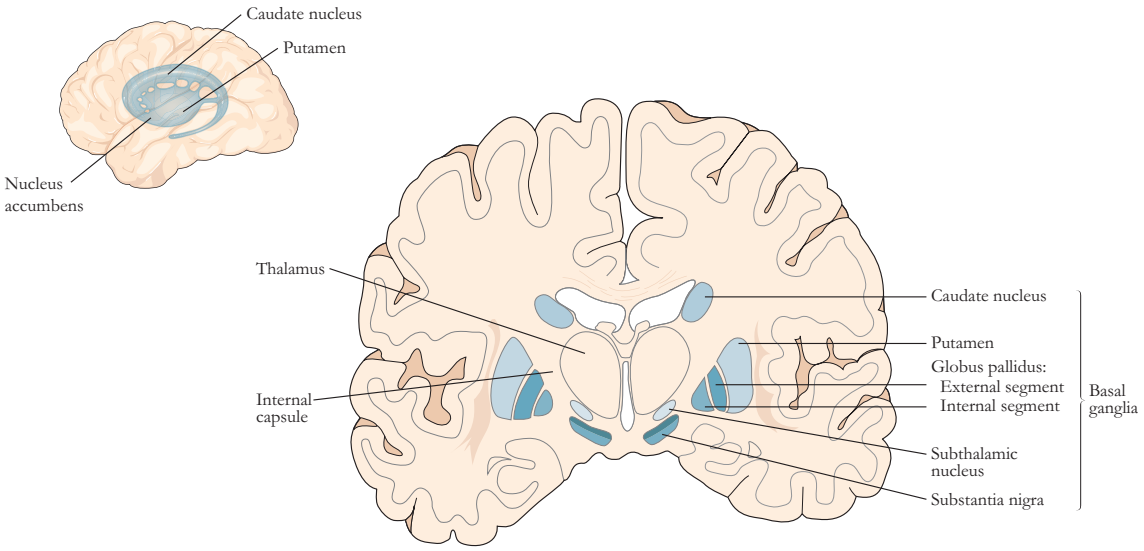

Figure II.4: Overview of the main components of the basal ganglia in lateral and coronal view. Adapted from Kandel et al. (2013).

tions to the dorsal striatum, which then converge to GPi and SNr, either directly or indirectly via GPe and STN. The output of GPi and SNr is then directed to the thalamus, which projects back to the cortex, forming a complete cortico-basal ganglia-thalamocortical loop. The direct and indirect pathways in the basal ganglia are modulated by endogenous dopamine release from the SNc, which acts on D1 dopamine receptors expressed primarily in the direct excitatory pathway, and on D2 receptors expressed primarily in the indirect inhibitory pathway, thereby balancing excitation and inhibition in the thalamo-cortical circuit. Besides this classical model, recent studies have highlighted a much denser intrinsic connectivity of the basal ganglia, leading to a

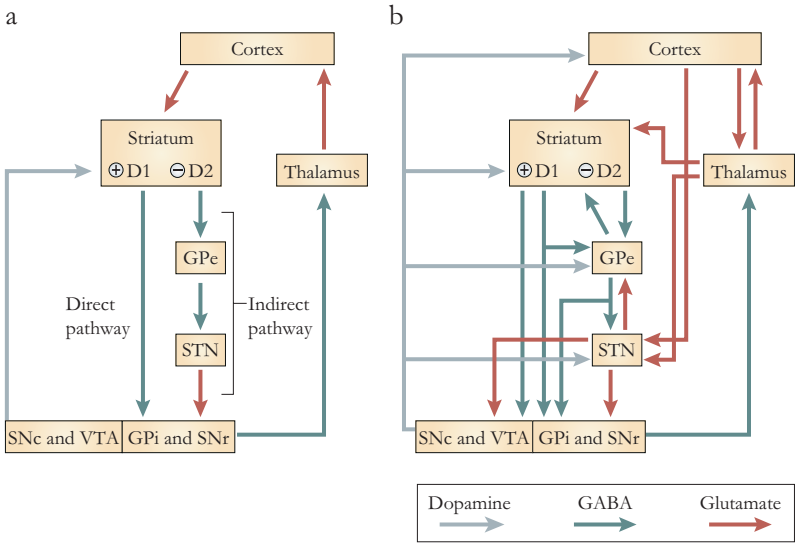

Figure II.5: Organization of intrinsic connections within the basal ganglia according to (a) the classical model and (b) the contemporary model. From Redgrave et al. (2010).

more complex circuit in which the transformations performed on inputs to generate outputs are less easy to forecast (Fig. II.5b).

Historically, the basal ganglia were best known for their importance in motor function, due to both the neuropathology of movement disorders and the idea that basal ganglia pathways return primarily to the motor cortex (Nauta & Mehler, 1993). This view of basal ganglia function, however, changed dramatically with the identification of other distinct functional loops, such as limbic (affective) or associative loops, allowing a shift from purely motor function to a more complex set of functions that mediate the full range of goal-directed behaviors (Fig. II.6; Haber and Knutson, 2010). In particular, the limbic circuit links the orbital and medial prefrontal cortices to the ventral striatum (the main input structure of the ventral basal ganglia), regions that, as we shall see, have proven important in the integration of reward-related information. The concept of parallel and distinct functional pathways has dominated the field for about 20 years. However, recent thinking has emphasized that a key element for learning and adapting goal-directed behaviors is the ability not only to evaluate different aspects of reward,

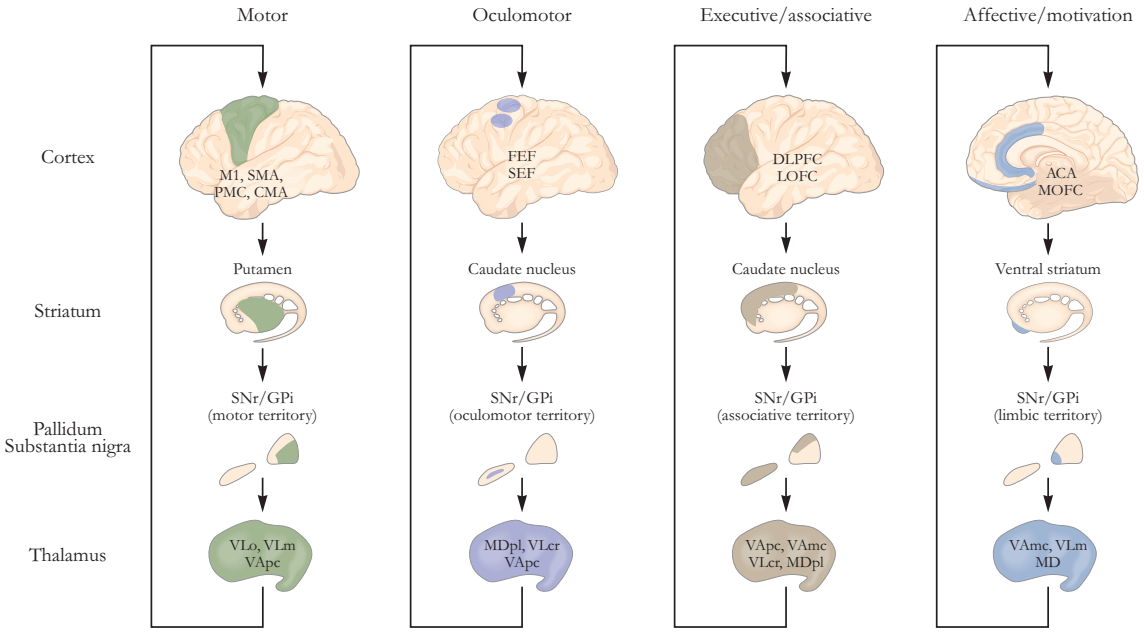

Figure II.6: Global anatomy of cortico-basal ganglia-thalamocortical circuits. The connections between the cerebral cortex and the basal ganglia can be viewed as a series of parallel, widely separated projection loops carrying sensorimotor, associative and limbic (affective) information. The functional territories represented in the cerebral cortex are maintained by the basal ganglia nuclei and thalamic relays. However, it should be noted that each level provides opportunities for activity within the loop to be modified or modulated by signals from outside the loop. ACA, anterior cingulate area; CMA, cingulate motor area; DLPFC, dorsolateral prefrontal cortex; FEF, frontal eye field; GPi, internal segment of the globus pallidus; LOFC, lateral orbitofrontal cortex; M1, primary motor cortex; MDpl, mediodorsal nucleus of thalamus, lateral part; MOFC, medial orbitofrontal cortex; PMC, premotor cortex; SEF, supplementary eye field; SMA, supplementary motor area; SNr, substantia nigra pars reticulata; VAmc, ventral anterior nucleus of thalamus, magnocellular part; VApc, ventral anterior nucleus of thalamus, parvocellular part; VLcr, ventrolateral nucleus of thalamus, caudal part, rostral division; VLm, ventrolateral nucleus of thalamus, medial part; VLo, ventrolateral nucleus of thalamus, pars oralis. From Kandel et al. (2013).

but also to develop appropriate courses of action and to inhibit maladaptive choices based on prior experience. This requires integration between different aspects of reward processing as well as interaction between reward circuits and brain regions involved in cognition. Indeed, it has been shown that communication pathways do exist between different parts of these circuits, demonstrating that while the ventral basal ganglia network is central to reward processing, it does not function in isolation.

The prefrontal cortex

The prefrontal cortex (PFC) represents the anterior part of the neocortex on the frontal lobe of the brain. This area is not uniform, but rather consists of distinct regions in terms of cytoarchitecture, connectivity and function. Of these, two regions have been identified as particularly important in reward processing: the orbitofrontal cortex (OFC) and the ventromedial prefrontal cortex (vmPFC).

The OFC constitutes the ventral surface of the frontal lobes. It is classically divided into the medial orbitofrontal cortex (mOFC, areas 13 and 11 in Fig. II.7) and lateral orbitofrontal cortex (lOFC, area 12 in Fig. II.7; Rolls et al., 2020). As shown in Fig. II.7 and supported by lesion studies in macaque (Mackey & Petrides, 2010), the orbitofrontal cortex in humans and macaques largely corresponds. The OFC receives inputs from the thalamus, as part of the

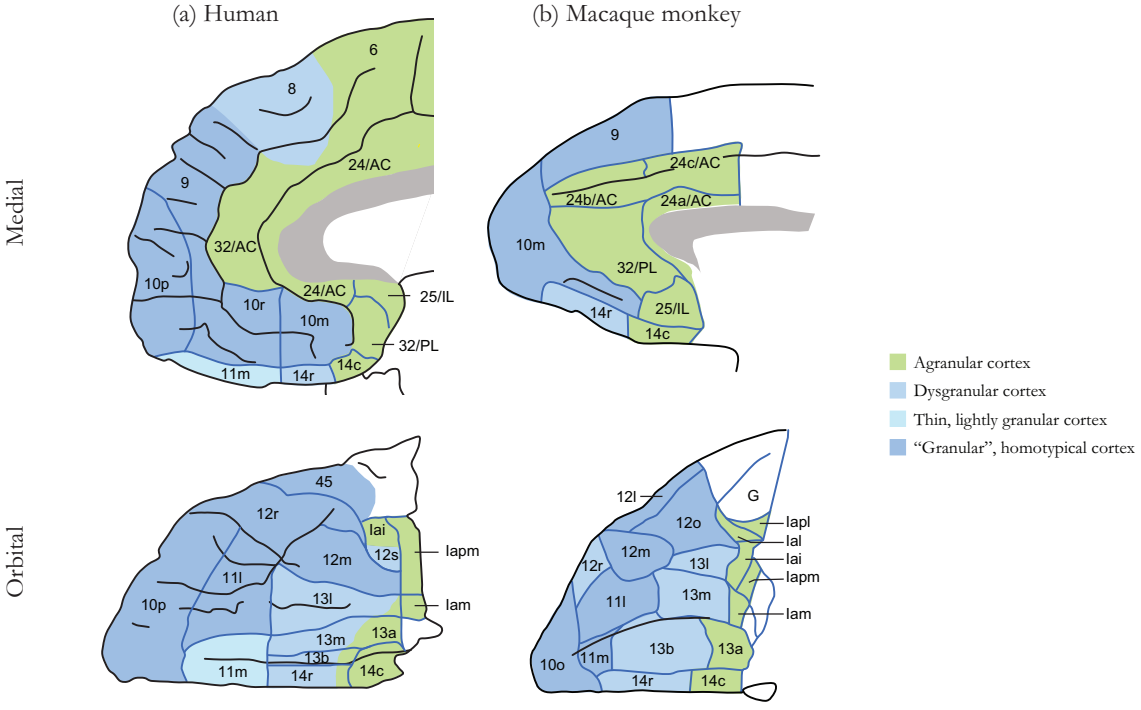

Figure II.7: Architectonic maps of the medial (top) and orbital (bottom) surfaces of the frontal lobe in (A) humans and (B) macaque monkeys. From Wallis and Rushworth (2014).

fronto-striatal limbic and associative loops (Fig. II.6), but it is also highly interconnected with all sensory modalities (including gustatory, visual, auditory, and sensorimotor). In addition, the OFC exhibits substantial connections with the limbic system, including the amygdala, entorhinal cortex, hippocampus, and parahippocampal gyrus (Price, 2006; 2007).

The vmPFC is located on the medial wall of the ventral surface of the PFC. It is identified by cytoarchitectonic areas 14 (gyrus rectus), 10m and 10r (Rolls et al., 2020), and sometimes areas 25 and 32 (Fig. II.7; Lopez-Persem et al., 2019). As for the OFC, the vmPFC of humans and macaques is largely comparable (Mackey & Petrides, 2010), and it is included in the fronto-striatal limbic loop receiving inputs from the thalamus (Fig. II.6). Nevertheless, their functional connectivity differs (Price, 2007). In particular, the vmPFC is strongly interconnected with limbic and autonomic structures such as the lateral hypothalamus and the periaqueductal gray region (Öngür & Price, 2000).

ii. Reward prediction error encoding

The dopaminergic system for value learning in non-human primates

The idea of a reward circuit probably originated in the mid-1950s, when Olds and Milner observed that rats could repeatedly press levers to receive tiny pulses of current injected through electrodes implanted deep into their brains (Milner, 1989; Olds & Milner, 1954). In particular, when the electrode was located in the region of the septum or nucleus accumbens, the rats preferentially self-stimulated to any other activity (even eating and drinking). These stimulation sites were soon dubbed "pleasure centers" since their neural activity strongly reinforced the behavior. Research over the next two decades identified dopamine as one of the key chemicals contributing to neural signaling in these regions, suggesting that one way to understand the reward circuit was to study dopamine.

Early studies of dopamine led to the idea that it carried "hedonic signals" in the brain and that, in humans, it was directly responsible for subjective pleasure. Since the major drugs of abuse act directly or indirectly through the dopamine system (Wise, 1996), this idea could, for example, easily explain addictive behavior by the habitual choice of short-term pleasure despite a host of long-term life problems, but had difficulty explaining the persistence of drug use when negative consequences accumulate. And indeed, later studies revealed that the effects of dopamine were much more complex than originally thought.

In a famous experiment, Schultz et al. (1997) trained monkeys to expect juice at a fixed interval after a visual or auditory cue while recording the activity of dopaminergic neurons. Before the

monkeys learned the predictive cues, the onset of juice was unexpected and produced a transient increase in the firing rate of dopaminergic neurons above basal levels (Fig. II.8 top). As the monkeys learned that certain cues predicted the arrival of the juice, the neurons no longer fired in response to the juice presentation - the reward - but earlier, in response to the predictive visual or auditory cue (Fig. II.8 middle). If a cue was presented but not followed by the usual reward, the firing stopped at the time the reward would have been presented (Fig. II.8 bottom). In contrast, if a reward exceeded expectations or was unexpected, because it appeared without a prior cue, firing was increased in proportion to the size of the positive surprise associated with the reward (Bayer & Glimcher, 2005). These observations suggest that dopamine release in the forebrain does not serve as a signal of pleasure but rather as a *reward prediction errors* (RPE) signal. An increase in the firing rate of dopaminergic neurons would signify a reward or stimulus related to a reward that was not predicted, while a decrease would signify that the predicted reward was less than expected or absent. Thus, alterations in dopamine release are thought to modify future responses to stimuli to maximize the likelihood of obtaining rewards and minimize unsuccessful pursuits. If a reward is completely consistent with what has been predicted based on environmental cues, dopamine neurons maintain their tonic (baseline) level of arousal. According to Schultz, this phenomenon means that as long as nothing changes in the environment, there is nothing more to learn and therefore there is no need to modify behavioral responses. Subsequent studies extended these results by showing that dopaminergic neurons incorporated the *subjective value* of reward into their prediction error signal since they integrated different modulators of value such as risk (Stauffer et al., 2014) or delay (Kobayashi & Schultz, 2008).

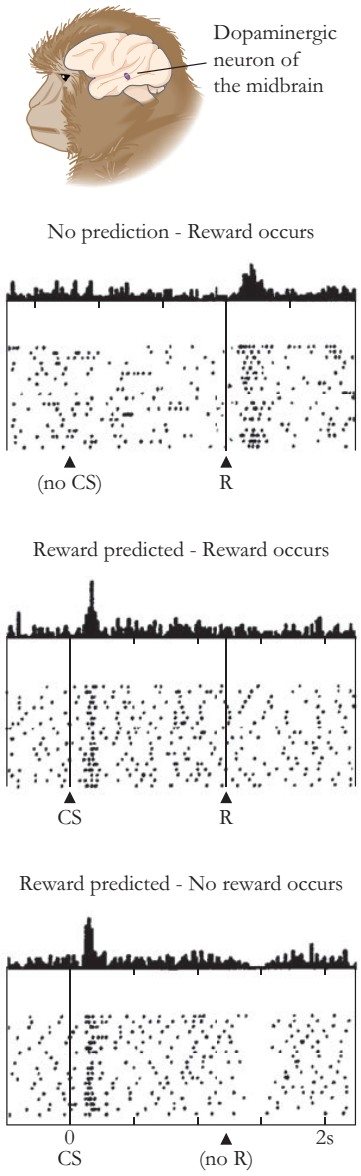

Figure II.8: Reward Prediction Error in dopaminergic neurons. Graphs show firing rates recorded from midbrain dopaminergic neurons in awake, active monkeys. CS: conditioned stimulus; R: reward. From Kandel et al. (2013).

Dopamine reward prediction errors in human

Dopamine reward prediction error signals are not limited to monkeys, but have also been found in electrophysiological studies in humans, not only in substantia nigra neurons (Zaghloul et al., 2009), but also in large cortical territories such as the vmPFC and lOFC (Gueguen et al., 2021). In addition, hundreds of human neuroimaging studies, using both classical (i.e., Pavlovian) and instrumental conditioning (see Box 5 for a definition), demonstrate reward prediction error signals in key target structures of dopaminergic neurons (Garrison et al., 2013), including the ventral striatum (e.g., McClure et al., 2003; J. P. O'Doherty et al., 2003; Pessiglione et al., 2006; Yacubian et al., 2006) and the mOFC (J. O'Doherty et al., 2001). The signal has been observed to reflect the dopamine response and to occur in striatal and frontal dopaminergic terminal areas rather than in midbrain cell body regions, a phenomenon which could be explained by the fact that it captures the sum of postsynaptic potentials (Schultz, 2016).

iii. Stimulus value encoding

Now that we have seen how values are learned, we can ask how these values are represented in the brain at the time of choice. Indeed, as stated earlier, decision theories posit that relevant features of choice options are embedded in a set of unitary subjective value signals, one for each option, at the time of decision making. These predicted stimulus values would indicate the value that the decision maker expects to derive from consuming or obtaining each proposed option in a given choice situation, regardless of the cost associated with the actions taken to obtain it. The location of the brain systems that compute and represent these subjective valuation signals during decision making has been the subject of extensive research in neuroeconomics. Numerous studies suggests that the targets of dopaminergic neurons, specifically the *ventral striatum* and the *orbital* and *ventromedial* portions of the *prefrontal cortex*, play a key role in encoding stimulus value in the brains of both human and non-human primates (Kable & Glimcher, 2009; Platt & Plassmann, 2014).

How are stimulus value signals measured?

Several procedures are widely used to obtain subject- and stimulus-specific measures of stimulus value. In non-human primates, *conditioning paradigms* have proven to be an effective tool for studying predicted value (Fig. II.9 left and Box 5). Indeed, the conditioned stimulus has no value to the animal at the beginning of conditioning, but gradually predicts the upcoming reward, without itself being a reward. Thus, by examining the activity at the time the conditioned stimulus appears, it is possible to dissociate the predicted value of the reward from

Box 5 | Paradigms commonly used to investigate subjective values

- *Classical (or Pavlovian) conditioning*: First described by Ivan Pavlov (see Box 1), the classical conditioning process involves associating a previously neutral stimulus (the conditioned stimulus) with an unconditioned stimulus (e.g. food).
- *Instrumental (or operant) conditioning*: This type of conditioning involves using reinforcement (or punishment) to increase (or decrease) a behavior. Through this process, an association is formed between the behavior and the consequences of that behavior.
- *Subjective rating*: This method simply involves asking participants to rate certain items based on "how much they like them". Subjective ratings were used for different modalities (visual, acoustic, gustatory and odorous; Kühn and Gallinat, 2012) and domains of pleasantness (e.g., faces, paintings, or houses; Lebreton et al., 2009).
- *Willingness-to-pay*: The Becker-DeGroot-Marschak (BDM; Becker et al., 1964) auction task, derived from behavioral economics, provides an alternative solution that encourages participants to accurately report subjective values. In this auction, participants are asked to indicate how much they are willing to pay for each item presented. Once all bids have been placed, one of them is randomly selected. The item is then sold according to the following rules. Let b be the bid made by the subject for the drawn item. After the auction, a random number n is drawn from a known distribution. If $b \geq n$, the subject has obtained the object and paid a price equal to n. On the other hand, if $b < n$, the subject did not get the item but also did not have to pay anything.
- *Preference task*: This paradigm typically asks participants to choose between two options. It assumes that if an individual chooses one item over another, it means that the value he or she assigns to that item is higher than the other. This operational definition of value is based on the fundamental idea in economics that individuals choose the option with the highest value.

All these tasks are illustrated in Fig. II.9.

other features of the outcome. In humans, stimulus value is classically determined using *rating* or *willingness-to-pay* tasks (Fig. II.9 right and Box 5). As with the conditioning paradigms, the logic behind the tasks is to induce subjects to activate the stimulus value circuit without necessarily activating the rest of the choice circuit. These tasks, performed in a non-economic context, have the advantage of isolating the stimulus value, but they are based on the assumption that the same brain regions would be involved in a choice situation.

For both species, another popular option is therefore to estimate the subjective value from choices themselves using *preference tasks* (Fig. II.9 and Box 5). This can be done under the assumption that individual choice probabilities are generated by something like a logistic choice model on the stimulus values (see section I.2.a. about the softmax rule). If the number of stimuli remains small, or if the stimulus values can be described using a simple function with a small number of parameters (e.g., expected utility theory or prospect theory), this is sufficient to estimate the stimulus value of each choice option (Rangel & Clithero, 2014).

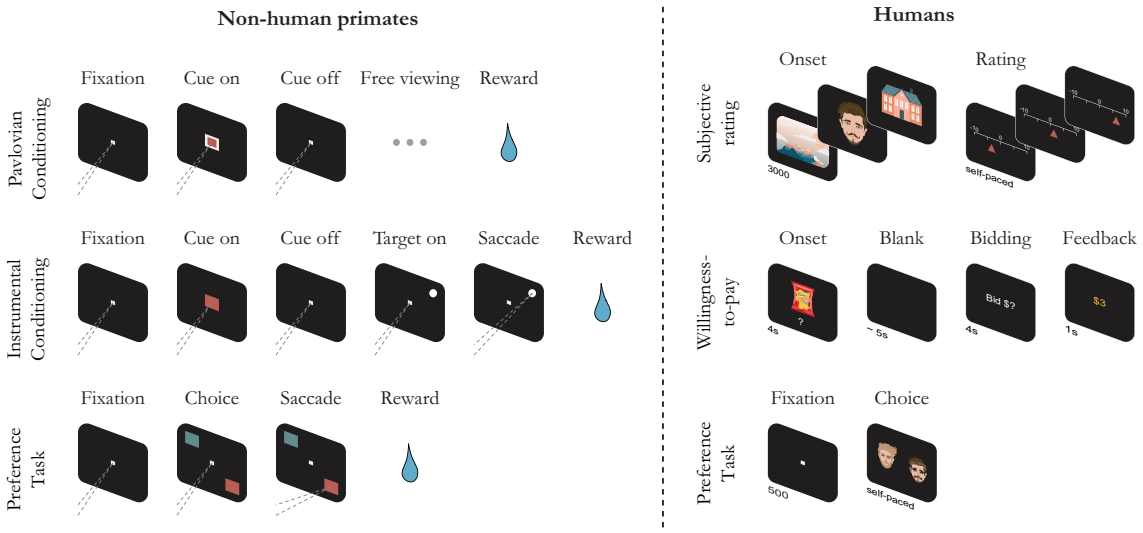

Figure II.9: Example of paradigms commonly used to investigate subjective values in non-human primates (left; adapted from S. W. C. Chang et al., 2011) and humans (right; adapted from Lebreton et al., 2009 and Plassmann et al., 2007).

Predicted valuation signals in the striatum

Single-unit recordings. Several single-cell studies in non-human primates have reported a relationship between reward expectancy and neuronal activity in the ventral striatum (Hassani et al., 2001; Hollerman et al., 1998; Schultz et al., 1992), with the latter being proportional to the reward magnitude (Cromwell & Schultz, 2003; Hassani et al., 2001). However, the dynamics of responses were found to vary greatly between striatal neurons. For example, in one study,

Schultz et al. (1992) studied the neurons of macaque monkeys while they performed a delayed go-no-go task. Lights of different colors instructed the animal to perform an arm extension or refrain from movement, respectively, when a trigger light was turned on a few seconds later. They found that neurons in the striatum exhibited a considerable variety of relationships to the task. These consisted of responses to instructions, sustained activations preceding the triggering stimulus, responses to the triggering stimulus, sustained activations immediately preceding the reward, and responses following the reward (Fig. II.10).

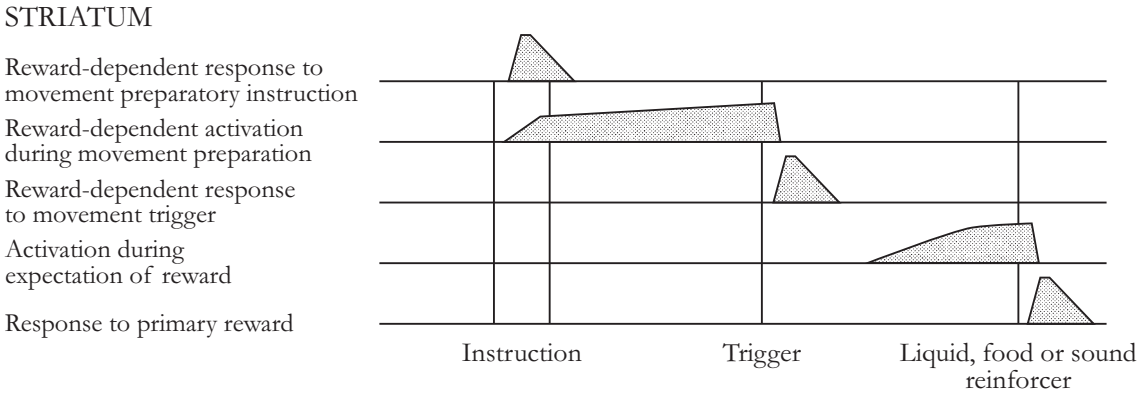

Figure II.10: Schematic overview of the forms or reward processing found in the ventral striatum. Reproduced from Schultz et al. (2000).

Local field potential recordings. Because of its deep position in the brain, the local field potentials of the ventral striatum are rarely explored in humans. Nevertheless, a few rare patients who underwent deep brain stimulation surgery for the treatment of refractory psychiatric disorders (obsessive-compulsive disorder, addiction or depression) are implanted in this region (C. Zhang et al., 2017). In this context, one study suggests that the ventral striatum reflects the expected reward value at cue onset and the experienced reward value at feedback in event-related potentials (M. X. Cohen et al., 2009b). In a follow-up study, the same team found the involvement of the gamma band (40-80Hz) during a similar task (M. X. Cohen et al., 2009a).

fMRI recordings. Finally, numerous fMRI studies in humans have reported a relationship between the value of the reward stimulus and neural activity in the ventral striatum. Early studies on this topic all showed that activity in the ventral striatum correlated with anticipation of monetary gains, and later studies have confirmed these initial findings (Breiter et al., 2001; Elliott et al., 2003; Kable & Glimcher, 2007; Knutson & Cooper, 2005; Knutson et al., 2005). Outside the monetary domain, studies have shown that activity in the striatum correlates with absolute product desirability (Erk et al., 2002; Knutson et al., 2007). A qualitative meta-analysis,

synthesizing the results of published fMRI experiments using ratings or choices to elicit value, supports this evidence by showing that BOLD signal in the ventral striatum is positively correlated with subjective expected values in a linear fashion (Fig. II.11; Bartra et al., 2013).

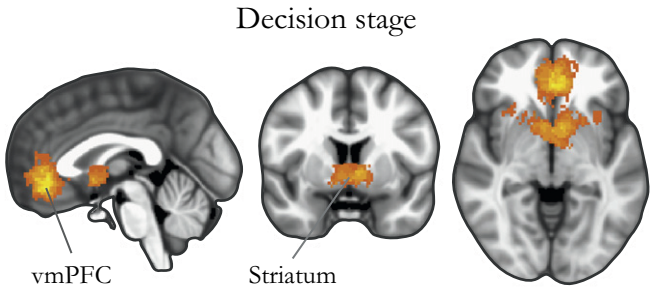

Figure II.11: Whole-brain meta-analysis of the positive effects of subjective value when a decision is evaluated. Adapted from Bartra et al. (2013).

Predicted valuation signals in the vmPFC/OFC

Lesion studies. A clear link between predicted valuation signals and the vmPFC/OFC has historically been established by anatomical and lesion studies. In non-human primates, multiple studies have shown that lesions in the OFC impair performance in goal-directed behaviors. Specifically, monkeys with OFC lesions were unable to make adaptive responses to objects after changes in the value of the underlying rewards for those objects (Izquierdo et al., 2004; West et al., 2011). These results indicate that in the absence of the OFC, animals fail to calculate subjective values on the fly. In human patients, a large literature stemming from the classic case of Phineas Gage (Damasio et al., 1994) has shown that OFC dysfunction is associated with choice deficits in a variety of areas (Cavedini et al., 2006; Hodges, 2001; Rahman et al., 1999; Strauss et al., 2014; Volkow & Li, 2004). Notably, lesions in the ventromedial frontal region result in less consistent preference judgments compared to healthy controls (Camille et al., 2011; Fellows & Farah, 2007; Henri-Bhargava et al., 2012). Finally, patients with OFC lesions also show abnormal behavior in gambling tasks, suggesting difficulty in coping with risk (Bechara et al., 1996; Clark et al., 2008; Rahman et al., 1999).

Single-unit recordings. Results from single-cell recordings in non-human primates also suggest that OFC neurons serve as a substrate for the computation and representation of predicted value. In an early study, Thorpe et al. (1983) observed that OFC neurons responded to the presentation of visual stimuli in ways that could not be explained in terms of simple sensory features. Indeed, the response of these neurons to the visual presentation of a liquid-filled syringe depended on whether, on previous trials, the liquid was appetitive (apple juice) or aversive (salt

water), even though the appearance of the syringe was visually indistinguishable between the two conditions. These observations thus led to the idea that these neurons possessed information about the "consequences of the animal's own responses". Subsequent studies confirmed these findings by showing that primate lOFC neurons responded to the administration of particular foods or juices in ways that depended on the motivational state or behavioral context of the animal (Fig. II.12; Rolls et al., 1989; Schultz et al., 2000; Tremblay and Schultz, 1999). In addition, single-cell recordings in monkeys also identified neurons reflecting expected values in the vmPFC (Abitbol et al., 2015; Bouret & Richmond, 2010; Strait et al., 2014).

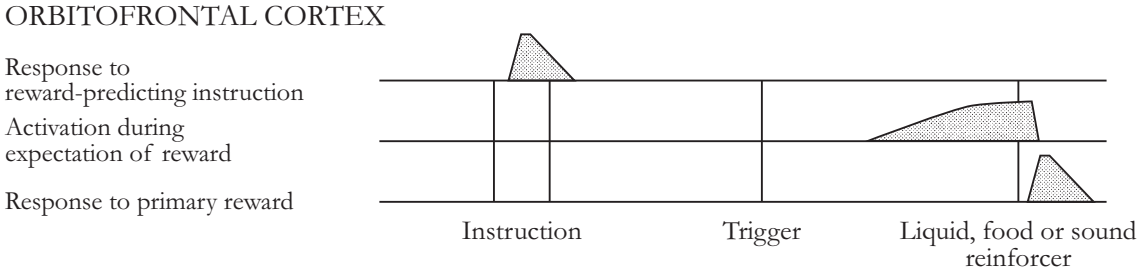

Figure II.12: Schematic overview of the forms or reward processing found in the orbitofrontal cortex. Reproduced from Schultz et al. (2000).

Building on this work, Padoa-Schioppa and Assad (2006) designed an experiment in which they estimated subjective value based on choices made in a preference task (Fig. II.9). In this experiment, the authors recorded OFC neurons while thirsty monkeys chose between two different fruit juices offered in different quantities, which were visually signaled to them. The choice patterns showed a quality/quantity trade-off, that is, the monkeys preferred one of the two juices when offered in equal quantities, but chose a less preferred juice if offered in sufficient amounts. The relative values of the two juices, inferred from the indifference point (i.e., the amount at which monkeys chose each juice with equal frequency), were then correlated with neural activity. The study identified three groups of neurons in the OFC: "offer value" cells that encode the value of one of the two juices (Fig. II.13A and B), "chosen juice" cells that encode the outcome of the binary choice (Fig. II.13C and D), and "chosen value" cells that encode the value of the chosen offer (Fig. II.13E). This study, replicated in follow-up studies (Padoa-Schioppa, 2009; Padoa-Schioppa & Assad, 2008), is critical in that it suggests that decisions would indeed be based on an evaluation step, as proposed in the model presented at the beginning of this manuscript (see section I.1.a.).

Local field potential recordings. Recording of local field potentials provides additional evidence for the link between both vmPFC and OFC with reward prediction. In monkeys, reward anticipation was found to be encoded in the high gamma band (50-100 Hz) of the prefrontal cortex, as well as in the beta band (15-29 Hz), but with reverse encoding: power in the beta band was higher for low rewards than for high rewards (Y. Zhang et al., 2016). In humans, the results appear to be similar. LFP recordings in the human medial and lateral OFC show an increase in the amplitude of local field potentials with the probability of reward (Y. Li et al., 2016), whereas the subjective value of food and non-food items is positively reflected in the high-frequency activity (35-150 Hz) of the vmPFC and the lOFC (Lopez-Persem et al., 2020). Likewise, high-frequency activity in the human OFC reflected multiple valuation components, such as the offer value and expected chosen value, in a choice task between a safe price and a risky gamble (Saez et al., 2018). Thus, a convergent pattern emerges in the involvement of high frequencies such as high gamma in outcome evaluation.

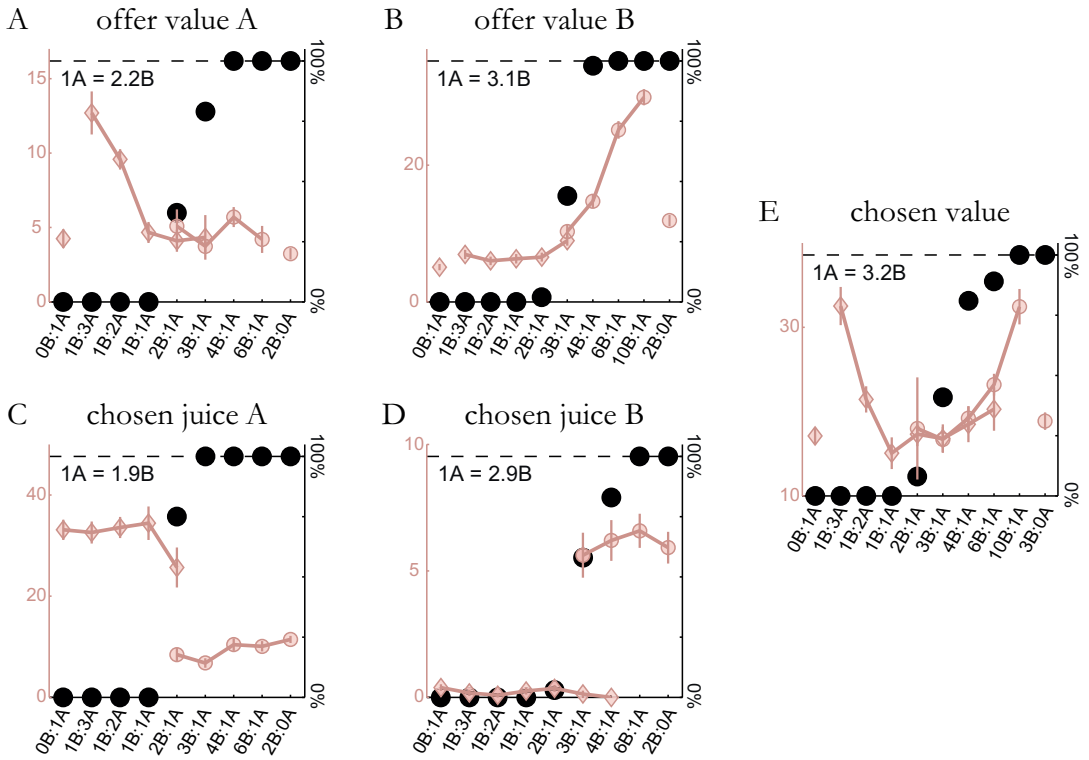

Figure II.13: Cell Groups in Orbitofrontal Cortex. The five panels represent the activity of five neurons (recorded in different sessions). In each panel, different offer types are ranked on the x axis by the ratio #B / #A, where #X is the quantity of juice X offered to the animal. Black dots represent the percent of trials in which the animal chose juice B (the choice pattern). Colored symbols represent the neuronal activity, with diamonds and circles indicating trials in which the animal chose juice A and juice B, respectively. From Padoa-Schioppa and Assad (2006).

fMRI recordings. Finally, a large number of studies performing fMRI recordings in humans have shown that the BOLD signal in the vmPFC correlates with the subjective values of choice alternatives, items to be evaluated or bid on (Lebreton et al., 2009; Plassmann et al., 2007). This finding is further supported by the same meta-analysis as mentioned above for the striatum (Bartra et al., 2013), showing a positive correlation between vmPFC and subjective expected value (Fig. II.11). Furthermore, the BOLD activity of the vmPFC was also found to correlate with the value of objects irrespective of their category, be it trinkets, snacks, and money (Chib et al., 2009; Levy & Glimcher, 2011) or faces, paintings and houses (Lebreton et al., 2009), but also irrespective of the modality, be it olfactory (J. D. Howard et al., 2015) or auditory (Abitbol et al., 2015). Overall, these results strongly support the idea that the vmPFC encodes the subjective value of expected gains, but also that a *common neural currency* is used by the brain to allow comparison between goods in the same unit.

The debate around vmPFC and OFC

A striking observation that may follow from the previous section is that, although involvement of the vmPFC and OFC in reward prediction is reported in both species, activations of the vmPFC are more frequent in humans, whereas neurophysiological studies in monkeys typically record from the OFC. This discrepancy is particularly salient because the vmPFC and OFC are part of distinct brain networks, with different patterns of anatomical connectivity and few direct interconnections (see section i.; Öngür et al., 2003; Wallis, 2011). Furthermore, as mentioned earlier, these two regions are homologous between monkeys (macaque) and humans (Fig. II.7). A first potential explanation for this difference could be that the vmPFC is less recorded at the single-cell level. Indeed, the OFC is more accessible for electrophysiological studies due to its position close to the brain surface and lateral enough to avoid accidental contact with the central sinus. A second possible explanation may be that tasks engaging the vmPFC in humans do not quite cognitively match the tasks used to examine the OFC in monkeys. In fact, the results may be very similar when efforts are made to precisely match behavioral tasks across species (Baxter et al., 2000; Gottfried et al., 2003). This observation raises the possibility that vmPFC and OFC may serve related but distinct functions that are solicited differently by behavioral tasks used in different species. An earlier theory based on neuroimaging studies indeed suggested functional differences between lateral OFC and mOFC/vmPFC based on outcome valence (Kringelbach, 2005). Although this theory has since been discarded, more recent findings still suggest a medial-lateral organization (Noonan et al., 2010; Rudebeck & Murray, 2011), in which notably neurons in the lateral OFC encode the value of external stimuli while those in more medial parts (mOFC/vmPFC) encode the value of outcomes associated with internal

states (Bouret & Richmond, 2010). A final consideration could be that it is differences in the methodologies used to study decision making in monkeys and humans that would account for the differential focus on OFC and vmPFC, including susceptibility artifacts in fMRI, or the heterogeneous nature of neural responses in OFC (Wallis, 2011). One way to reconcile these results could be to analyze the local field potentials of these regions, as it seems to link single-cell recordings with fMRI. In fact, a recent study in epileptic patients implanted with intracranial electrodes showed that the encoding of subjective values occurred both in the vmPFC and in the lateral OFC, although with different dynamics (Lopez-Persem et al., 2020). This study therefore favors the hypothesis that the discrepancies observed between the vmPFC and the OFC depend on the recorded signal rather than on specific tasks, but leaves open the question of the precise mechanisms and the role of each of these two brain regions.

Other predicted value areas

In addition to the striatum and vmPFC/OFC, other brain regions are commonly involved in reward valuation. Their description is beyond the scope of this manuscript, but we can nevertheless mention the *posterior cingulate cortex*, which is the brain area that responds most commonly alongside the vmPFC and ventral striatum, and has strong functional connectivity with the vmPFC (Bartra et al., 2013; Buckner & DiNicola, 2019; Lebreton et al., 2009), as well as the *hippocampus*, which is thought to be particularly recruited when choices are memory-based (Gluth et al., 2015; Lebreton et al., 2009; Lopez-Persem et al., 2020).

b. Neural basis of punishments: an opponent brain system?

So far, we have focused on the neural coding of rewards. However, our daily choices often require us to weigh the pros and cons of a series of actions before making a decision (see section I.1.c.). Early experiments in behavioral economics suggested that choices involving gains (appetitive domain) and losses (aversive domain) follow different policy rules (see section I.3.a. about Prospect theory). For example, the endowment effect shows that people are willing to pay more to keep something they own than to acquire the same thing when they don't (Kahneman et al., 1990). In addition, rewards and punishments trigger different types of subjective feelings (such as pleasure or pain, desire or fear) and elicit different types of behavior (approach or avoidance, stimulation or inhibition). These different observations have given rise to the idea that rewards and punishments may be processed by different parts of the brain, which may exert distinct influences on behavioral biases and clinical symptoms. Yet, while the neural correlates underlying reward processing are fairly well characterized, the neural basis of aversive processing

is subject to greater debate. The purpose of this section is to present current hypotheses on the possible implementation of reward and punishment systems in the brain.

i. How are value signals related to rewards or punishments distinguished?

In order to differentiate value signals specifically related to the valence of the outcome, dedicated tasks should be used. In particular, it is important to implement the comparison within the same behavioral task to avoid various confounding factors such as framing effects. Indeed, in the absence of either valence, subjects may change their reference point and, for example, consider an absence of reward as punishment or an absence of punishment as reward (Palminteri et al., 2015; Rangel & Clithero, 2012; Seymour & McClure, 2008; Vlaev et al., 2011). Nevertheless, opposing reward and punishment in the same protocol poses the delicate problem of comparing stimuli that do not necessarily have the same properties and whose values are not always in the same range. To circumvent this problem, studies that have addressed this issue used secondary stimuli such as money or abstract "points". This has the advantage of placing rewards and punishments in the same sensory range and allowing the value of stimuli to be inferred directly from their numerical nature. However, the generalizability of the results obtained with this type of task to other types of more "natural" stimuli is not guaranteed.

The clear separation of appetitive and aversive processing has most often been implemented in instrumental learning paradigms. In these paradigms, participants are repeatedly presented with a choice between two abstract stimuli (often fractal images or letters from exotic alphabets) representing the two possible actions. They are then asked to learn, through trial and error, to choose the most rewarding option or to avoid the most punishing one. In humans, two famous designs of this type are the Hiragana task (Frank et al., 2007; Frank et al., 2004) and the Agathodaimon tasks (Fig. II.14 top and middle; Palminteri, Justo, et al., 2012; Pessiglione et al., 2006).

- *The Hiragana task* consists of two sessions: a training session and a test session. In the training session, subjects are presented with fixed pairs of options (usually three pairs), represented by Hiragana symbols and associated with different probabilities of winning or losing. Probabilistic feedback follows the choice to indicate whether it is correct or incorrect. To assess whether participants learned more about the positive or negative outcomes of their decisions, they are then tested with new combinations of stimulus pairs (involving symbols from the training phase), this time in the absence of feedback. The ability to select the best possible stimulus is considered a measure of reward learning and the ability to avoid the worst stimulus is considered a measure of punishment learning.

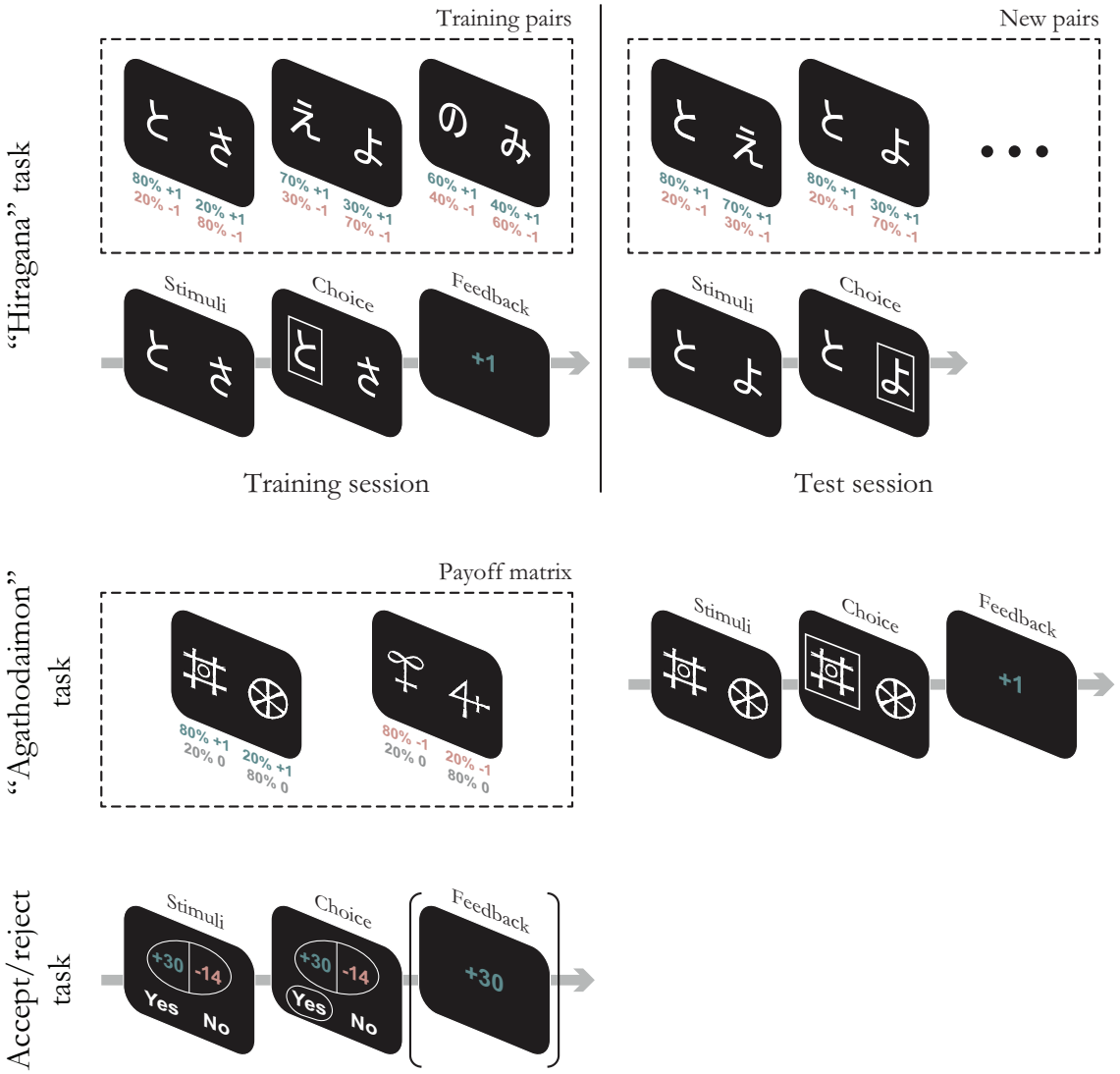

Figure II.14: Example of classical tasks used to compare reward and punishment processing. The Hiragana task (top; adapted from Shiner et al., 2012) and the Agathodaimon task (middle; adapted from Pessiglione et al., 2006) are instrumental learning paradigms. In these tasks, the objective of the participants is to find by trial and error the action with the highest expected value. In the accept/reject task (bottom; adapted from Tom et al., 2007), participants are asked to indicate their willingness to take the gamble (or challenge) given the potential gains and losses displayed on the screen. After their choice, a feedback may or may not be displayed.

- *The Agathodaimon task* distinguishes between reward-seeking and punishment-avoidance performance directly within a session. As in the Hiragana task, subjects are shown fixed pairs of symbols (usually two pairs), now materialized by Agathodaimon symbols. This time, however, rewards and punishments are never mixed within a pair. Some pairs of options have probabilities of winning or not winning, and others have probabilities of losing or not losing. The rates of correct responses in the two conditions are thus respectively considered measures of reward and punishment learning. Crucially, this task disentangles two concepts that were confounded in the previous task: outcome valence

(reward or punishment) and positive or negative prediction errors (both present in both conditions).

Another approach, inspired by effort discounting tasks in animals, is that of *accept/reject paradigms* (Fig. II.14 bottom). In such tasks, participants are presented with a unique combination of potential gains and losses on individual trials and are asked to decide whether to accept or reject each of the proposed combinations. The outcome is determined either by chance (50% chance of winning the gains at stake or losing the losses at stake; Martino et al., 2010; Tom et al., 2007) or by means of an additional task (Vinckier et al., 2018). Since the participants' goal is to win as much money (real or virtual) as possible, if they feel that the particular combination of potential gains and losses is "not worth it", they choose the "No" response to move on to the next trial, otherwise they choose the "Yes" response. A significant advantage of this paradigm is that it allows for the dissociation of behavioral sensitivity to gains and losses. In addition, the amounts of potential gains and losses can be directly correlated with brain activity so as to isolate the brain regions that are sensitive to them.

ii. The neural candidates for appetitive and aversive processes

As discussed above, it has been shown that the firing rate of dopaminergic neurons evolves positively and parametrically with reward prediction errors (RPE). One might then assume that the same system is used to encode punishment prediction errors (PPE), and that dopamine levels decrease with aversive events. This possibility seems unlikely, however, because the baseline firing rate of dopaminergic neurons is quite low and would not have sufficient range to accurately encode negative events (Bayer & Glimcher, 2005). This physiological constraint leads to the hypothesis that an adverse system could respond positively to aversive events. To date, the idea of an opponent system is still widely debated. Palminteri and Pessiglione (2017) have identified and discussed four hypotheses, which I will introduce here, that have been put forward regarding the neural implementation of this potential system (Fig. II.15).

Hypothesis 1: No opponent system

A first hypothesis is that dopaminergic activity in the basal ganglia circuits is sufficient for reward and punishment learning and that there is therefore no opponent system. According to this hypothesis, negative prediction errors are simply encoded in the duration of pauses in dopaminergic activity (Maia & Frank, 2011). Studies conducted in patients with Parkinson's disease, characterized by dopaminergic neuronal loss and treated with dopaminergic stimulators, support this idea (Bódi et al., 2009; Frank et al., 2004; Kéri et al., 2010). It has been no-

tably shown that patients under dopaminergic treatment were better at reward learning than patients without treatment, and conversely for punishment learning (Frank et al., 2004). An analogous study in patients with Tourette's syndrome obtained comparable results (Palminteri et al., 2009), increasing evidence suggesting the involvement of dopaminergic activity drops in punishment learning. In this context, it is proposed that an important role is played by an epithalamic nucleus called habenula, whose activity has been shown to provide an inhibitory input to midbrain dopaminergic neurons after omission of a reward in monkeys (Matsumoto & Hikosaka, 2007). In humans, habenula has also been shown to encode aversive events such as electric shocks and to impact striatal activity (Lawson et al., 2014). Nevertheless, although increased dopamine levels have been almost consistently associated with improved reward learning, the results regarding punishment learning are less consistent, with several studies showing no effect of dopaminergic drugs on avoidance behavior (Eisenegger et al., 2014; Pessiglione et al., 2006; Rutledge et al., 2009).

Hypothesis 2: Dopaminergic opponent system

A second hypothesis also assumes that dopaminergic activity underlies avoidance learning, but that this occurs through a different subset of midbrain neurons that positively encode punishment (Brooks & Berns, 2013). This hypothesis is based on electrophysiological observations in non-human primates that an anatomically distinct population of midbrain dopaminergic neurons responds positively to aversive stimuli (Matsumoto & Hikosaka, 2009). Consistently, punishment expectation and punishment prediction error were shown to be positively encoded in the ventral tegmental area and striatum during aversive conditioning tasks in human fMRI (Delgado et al., 2008; Pauli et al., 2015; Seymour, Daw, et al., 2007). A related implication of this second hypothesis is the idea that a functional gradient exists in the striatum, such that the dorsal striatum would be preferentially involved in punishment processing, while the ventral striatum would be more involved in reward processing. The fMRI data are generally consistent with this idea (Pessiglione et al., 2006; Seymour, Daw, et al., 2007). However, a study conducted in patients with Huntington's disease suggests instead that the dorsal striatum system would not be involved in learning as such, but rather in the selection between actions that result in negative outcomes (Palminteri, Justo, et al., 2012).

Hypothesis 3: Serotoninergic opponent system

A third hypothesis asserts that another neuromodulator, serotonin (5-HT), assumes the role of opponent signaling by encoding punishment prediction errors (Daw et al., 2002). The origin of this hypothesis lies in a large literature in rodents linking the serotonergic system (in par-

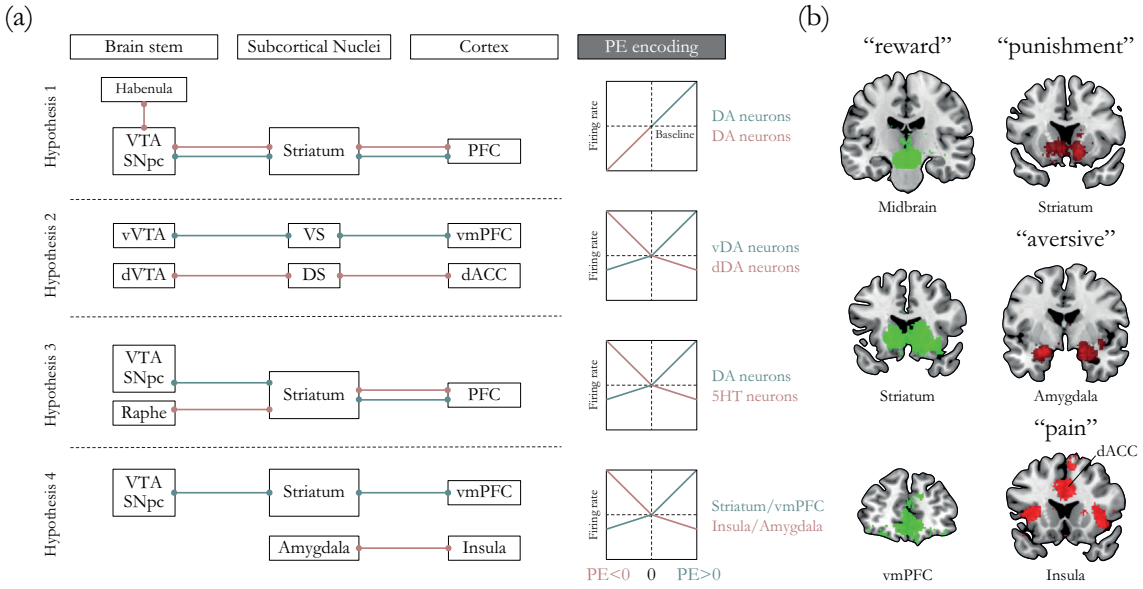

Figure II.15: Neural implementation of reward versus punishment processing. (a) Different hypotheses regarding the neural implementation of punishment avoidance (red) versus reward seeking (green). For each hypothesis, the key regions and connections of each oppositional system are shown on the left, with their theoretical pattern of activity as a function of prediction error (PE) plotted on the right. (b) Maps resulting from large-scale automated meta-analyses as implemented in Neurosynth. 5HT: serotonin; DA: dopamine; dACC: dorsal anterior cingulate cortex; dDA: dorsal dopamine; DS: dorsal striatum; dVTA: dorsal VTA; PFC: prefrontal cortex; SNpc: substantia nigra pars compacta; vDA: ventral dopamine; vmPFC: ventromedial PFC; VS: ventral striatum; VTA: ventral tegmental area; vVTA: ventral VTA. From Palminteri and Pessiglione (2017).

ticular the dorsal raphe) to behavioral inhibition (Soubrié, 1986). However, evidence for this proposition is scarce. Although serotonin has been shown to antagonize dopamine function in the VTA and striatum (Kapur & Remington, 1996; Lorrain et al., 1999), electrophysiological recording and pharmacological manipulation studies have implicated serotonin in both reward and punishment processing (J. Y. Cohen et al., 2015; Palminteri, Clair, et al., 2012). Furthermore, because the serotonergic system is much more anatomically widespread and genetically complex than the dopaminergic system, it may be impossible to delineate a single functional domain for this neuromodulator (Spies et al., 2015). Indeed, serotonin has been implicated in other types of aversive events such as the cost of information sampling (Crockett et al., 2012) or the opportunity cost induced by waiting for a reward (Fonseca et al., 2015; Schweighofer et al., 2008).

Hypothesis 4: Other opponent systems

Finally, the fourth hypothesis proposes that punishment processing is mediated by aversive signals encoded in other cortical and subcortical areas, most notably the anterior insula (see Box 6) and amygdala (Fig. II.16; Pessiglione and Delgado, 2015). This hypothesis is consistent with a body of electrophysiological, pharmacological, and lesion studies in animals (Hayes et al., 2014;

Namburi et al., 2016), as well as fMRI studies and meta-analyses in humans (Bartra et al., 2013; Garrison et al., 2013; Yacubian et al., 2006). For example, bilateral lesions of the amygdala were shown to impair implicit punishment learning, which was spared by bilateral lesions of the hippocampus (Bechara et al., 1995). Similarly, insular lesions were shown to specifically impair punishment learning (Palminteri, Justo, et al., 2012). Subsequent computational analyses indicated that the deficit was best rendered by decreasing the punishment parameter, consistent with fMRI (Pessiglione et al., 2006; Seymour et al., 2004) and electrophysiology (Gueguen et al., 2021) studies reporting encoding of punishment prediction errors in the anterior insula. In addition, the insula has been shown to respond to aversive outcomes that elicit intense feelings of arousal, such as disgusting images (Calder et al., 2007), but also to monetary losses, particularly loss anticipation (Knutson et al., 2003), which has been linked to risk predictions (Preuschoff et al., 2008) and risk-averse decisions (Kuhnen & Knutson, 2005). In such a model, one might expect that regions that encode positive events, such as the ventral striatum and vmPFC, would not be involved in aversive events. However, fMRI studies also provide several examples of overlapping appetitive and aversive processes in the human brain. For example, one study reported that the same area of the vmPFC was positively correlated with potential monetary gains and negatively correlated with potential losses (Tom et al., 2007), while activity in targeted regions, including the amygdala and insula, showed no increase in activity with potential losses. Similarly, mOFC activity has been positively correlated with monetary gains and food appetitiveness and negatively correlated with losses and food aversiveness (Plassmann et al., 2010).

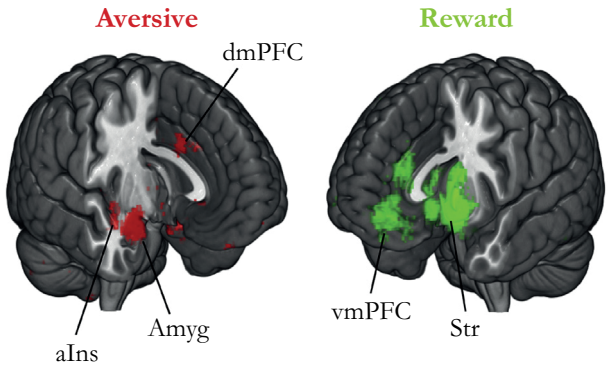

Figure II.16: Brain regions involved in reward and aversive processes. Results from a large-scale meta-analysis (Yarkoni et al., 2011) reveal that reward processing involves the striatum (Str) and ventromedial prefrontal cortex (vmPFC), whereas aversion processing involves the dorsomedial prefrontal cortex (dmPFC), anterior insula (aIns), and amygdala (Amyg). From Pessiglione and Delgado (2015).

Overall, the delineation of the neural systems responsible for reward and punishment valuation is still a matter of debate. In my experimental work, I addressed this issue by performing in-

tracerebral recordings in epileptic patients while they performed an accept/reject task allowing to isolate signals related to either potential monetary gains or losses. Intracerebral electroencephalographic (iEEG) activity was recorded by deep electrodes sampling regions potentially involved in this process, namely the prefrontal and insular cortex, with the aim to identify the neural dynamics of selective brain regions featured by appetitive or aversive events.

Box 6 | Anatomy of the insular cortex

The insular cortex is a complex and richly connected cytoarchitectonic structure. Originally considered as a simple visceral sensory region, the insula has gradually been recognized as a cortical hub involved in interoception, multimodal sensory processing and perceptual self-awareness. Recently, its role in attention, executive functions and decision making has also been highlighted, making it an important field of exploration (Benarroch, 2019; Craig & Craig, 2009; Droutman et al., 2015; Klein et al., 2013; Nieuwenhuys, 2012; Uddin et al., 2017).

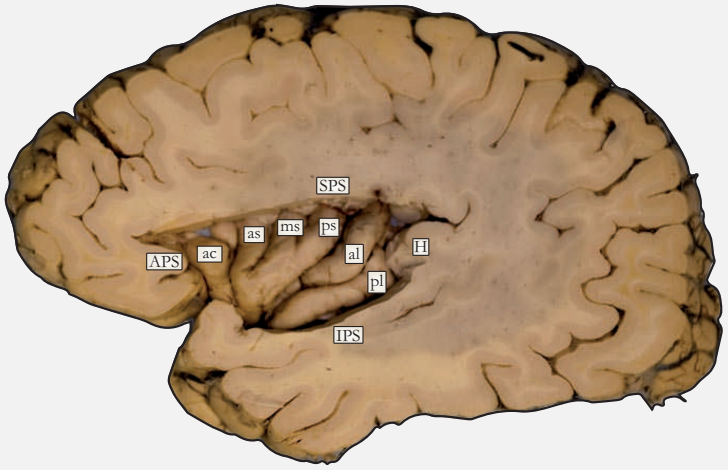

Figure II.17: Anatomy of the insula. Photograph of the left insular cortex of a human patient. as: anterior short insular gyrus; al: anterior long insular gyrus; ac: accessory gyrus; APS: anterior peri-insular sulcus; H: Heschl's gyrus; IPs: inferior peri-insular sulcus; ms: middle short insular gyrus; ps: posterior short insular gyrus; pl: posterior long insular gyrus; SPS, superior peri-insular sulcus. From Craig and Craig (2009).

The human insular cortex is delimited from the frontal, parietal, and temporal opercula by the peri-insular sulcus and is partitioned into posterior and anterior lobules by the central insular sulcus (Fig. II.17; Uddin et al., 2017; Wysiadecki et al., 2018). Though the direction and size of the gyri, as well as the exact number of short gyri, may vary between individuals and hemispheres (Wysiadecki et al., 2018), there are gen-

erally two long gyri in the posterior lobule and three short gyri in the anterior lobule, as well as an accessory gyrus that corresponds approximately to the location of the fronto-insular cortex.

On the basis of cytoarchitectonic analyses of the presence and density of cortical granular cell layer, the insula has been subdivided into posterior "granular", intermediate "dysgranular" and anterior "agranular" areas (Fig. II.18 left; Klein et al., 2013; Nieuwenhuys, 2012).

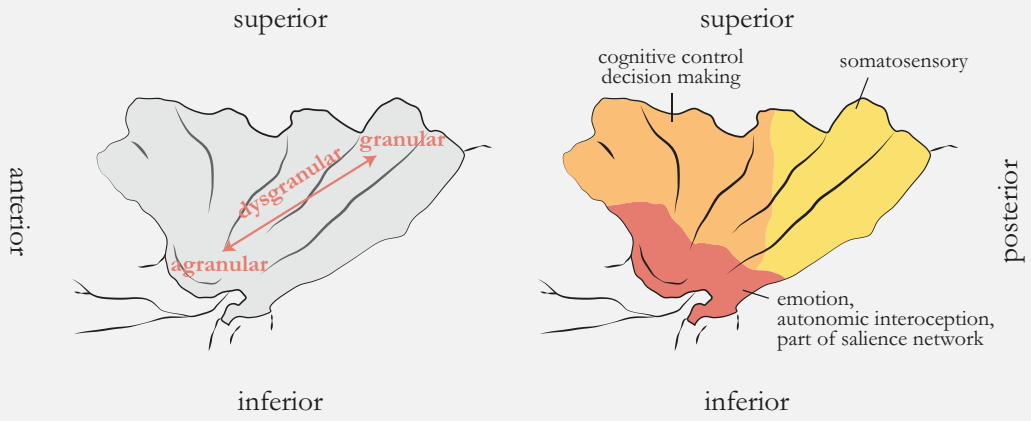

Figure II.18: Cytoarchitectonic and functional maps of the human insula. (left) Cytoarchitectonic gradient from agranular cortex in the anterior inferior insula via dysgranular cortex to granular cortex in the posterior part of the insula. (right) Tripartite model of the functional areas of the insula. Adapted from Klein et al. (2013).

The connectivity and functions of the insula in humans have been studied using several techniques, including tractography, fMRI, cortical microsimulation during evaluation for epilepsy surgery, and analysis of the clinical consequences of insular injury (Afif et al., 2010; Mazzola et al., 2017; Ryvlin & Picard, 2017; Stephani et al., 2011; Uddin et al., 2017). These studies indicate that the posterior insula has connections to the temporal, parietal, and posterior sensorimotor areas, the anterior insula connects to the frontal, orbitofrontal, anterior cingulate, and anterior temporal areas, whereas the medial insula shares connections to the anterior and posterior insular cortices (Ghaziri et al., 2017).

The human insula is generally divided into (at least) three functional regions: a posterior region functionally connected to areas involved in sensorimotor processing, a dorsal anterior region functionally connected to areas involved in cognitive control, and a ventral anterior subdivision functionally connected to limbic areas involved in

affective processes (Fig. II.18 right; L. J. Chang et al., 2013; Deen et al., 2011). Another view, however, suggests that this traditional perspective of cognitive-affective-interoceptive segregation may be oversimplified. In particular, dynamic analyses of functional network connectivity have shown that different subdivisions of the insula can also work in concert to integrate information within and across cognitive, affective, visual, and sensorimotor tasks (Uddin et al., 2014). Notably, the dorsal anterior insula has been shown to exhibit strong functional connectivity across multiple task domains (R. Li et al., 2020; Uddin et al., 2014).

3. The neural mechanisms underlying choice variability

At the behavioral level, we have detailed several modulators that could account for some of the choice stochasticity (see section I.3.). In this section, we will focus on describing the neural mechanisms underlying the behavioral variability generated by these modulators. Insight into these mechanisms is a valuable approach to better understand the origin of choice variability and further constrain theories of how values are constructed and used in decisions.

a. Baseline effects

Although accounting for some factors may substitute for the observed stochasticity in choices through bias, it appears that part of the behavioral variability may also be attributable to the biological properties of the brain system that we use to compute subjective value. Indeed, since the earliest neurophysiological recordings, scientists have observed the presence of ongoing activity in the brain that has a characteristic temporal and spatial structure (Gloor, 1969; Raichle, 2015). This so-called *spontaneous* activity is distinguished by remarkably large temporal modulations that are not attributable to any specific stimuli. The concern that such fluctuations were merely the result of technical and physiological noise was refuted by simultaneous recordings using different techniques (Laufs et al., 2003; Shmuel & Leopold, 2008), showing in particular that the same fluctuations in ongoing activity could be observed in both electrophysiology and fMRI.

Trial-to-trial variability in brain signals

The first clues to the implication of this spontaneous activity on cognitive functions emerged from the long-standing observation from electrophysiological recordings that the neuronal re-

sponses evoked by identical stimuli fluctuate over time (Dean, 1981; Shadlen & Newsome, 1998; Softky & Koch, 1993). This variability has also been replicated in fMRI studies, where it has been found that the BOLD signal from the same region and in the same subject exhibited significant variability from one trial to the next (Duann et al., 2002). In addition, a series of results showed that perception of visual contrast (Ress & Heeger, 2003), identification of fearful expressions (Pessoa & Padmala, 2005) or working memory performance (Pessoa et al., 2002) could each be predicted by unexplained variations in the BOLD response across trials for identical stimuli.

This effect was most explicitly linked to ongoing activity fluctuations in an influential study examining ongoing and stimulus-evoked activity using simultaneous optical and electrophysiological methods in the visual cortex of anesthetized cats (Arieli et al., 1996). In this study, the authors found that spontaneous fluctuations in brain activity could account for trial-to-trial variations in neuronal response elicited by identical stimuli. In particular, their data showed a linear relationship between ongoing activity immediately before stimulus onset and evoked activity levels, so that simply adding the average increase in stimulus-related activity to ongoing activity provided an excellent prediction of the activity level actually measured during the evoked response. Evidence for the persistence of task-independent ongoing activity in the evoked neuronal response to a stimulus has also been provided in functional imaging studies. For example, in one study, the authors found that the inter-trial variability of finger movement-related activity in motor cortex could be significantly explained by fluctuations in ongoing activity measured in the contralateral motor cortex (M. D. Fox et al., 2006). Through a clever analysis of the activity level recorded simultaneously in a region that belongs to the same intrinsic functional connectivity networks, but was not engaged by the task, it was thus possible to dissociate the ongoing and evoked components of the signal in the task-relevant region.

Functional relevance of spontaneous fluctuations

By addressing whether these ongoing activity fluctuations are functionally relevant, subsequent studies have provided clear links between neuronal and behavioral variability. In particular, extensive fMRI evidence has shown that, when using ambiguous or near-threshold items, pre-stimulus activity may serve as a predictor of perceptual decisions in various modalities. For example, in the auditory domain, higher pre-stimulus activity in bilateral auditory cortex was associated with better performance when attempting to detect near-threshold auditory stimuli (Fig. II.19a; Sadaghiani et al., 2009). In the visual domain, participants' categorization of Rubin's bistable vase-face image was biased toward faces when pre-stimulus activity levels in

the right fusiform facial area (a region known to be involved in face processing) were higher (Fig. II.19b; Hesselmann, Kell, Eger, et al., 2008). Similarly, participants' responses during a random-dot movement task with near-threshold levels of coherence were biased toward coherent movement by levels of pre-stimulus activity in the right middle temporal cortex (a region involved in motion perception; Fig. II.19c; Hesselmann, Kell, and Kleinschmidt, 2008). Finally, the classification of a stimulus as painful was predicted by the anterior insula (aIns) pre-stimulus signal level in a near-threshold pain detection paradigm (Wiech et al., 2010). Similar results were also obtained in perceptual decision tasks with electrophysiological recordings in monkeys (Shadlen & Newsome, 2001; Williams et al., 2003) and magnetoencephalography in humans, showing notably that pre-stimulus alpha and gamma band fluctuations in visual areas can influence the conscious detection of an upcoming stimulus (Wyart & Tallon-Baudry, 2009).

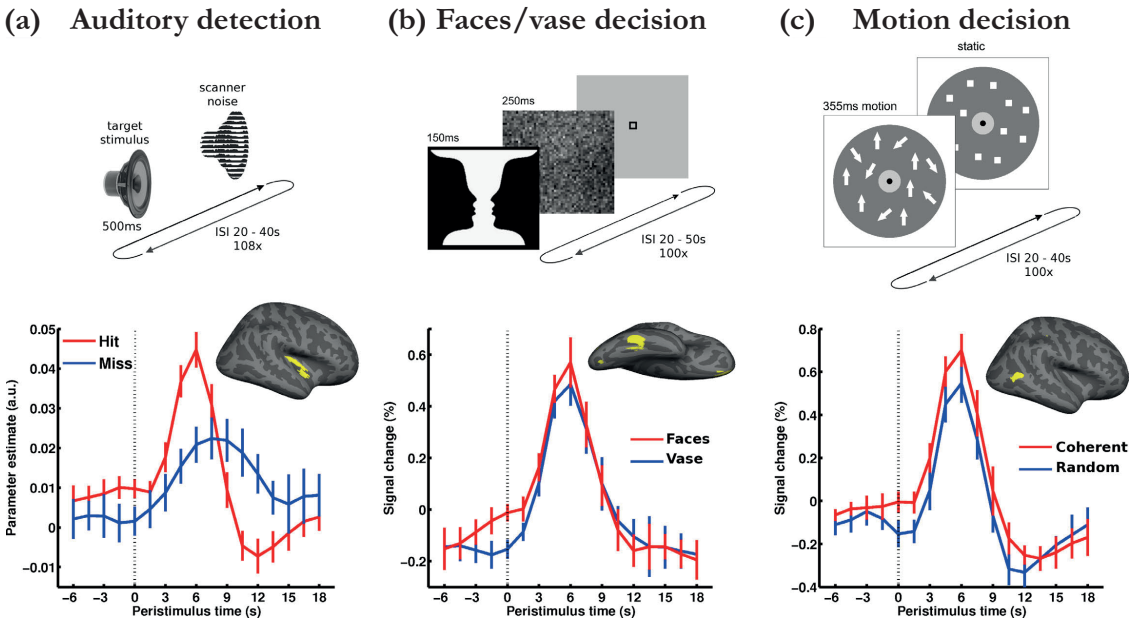

Figure II.19: Impact of spontaneous variations in brain activity on perceptual decisions. The upper part illustrates the paradigms. In each experiment, the pre-stimulus BOLD signal (dotted vertical line marking stimulus onset) was examined as a function of perceptual outcome and sampled from accordingly specialized sensory areas. The corresponding regions of interest are presented on a canonical inflated cortical surface of the right hemisphere. In all experiments, higher pre-stimulus time course in the respective sensory region biased towards perceiving stimulus properties for which these regions are particularly sensitive. From Sadaghiani et al. (2010).

Baseline activity and value-based decision making

In the field of value-based decision making, Maoz et al. (2013) examined activity in the dorsolateral prefrontal cortex and striatum (regions whose activity has been previously linked to the subjective value of delayed reward) of monkeys deciding between smaller, immediate rewards and

larger, delayed rewards. In doing so, they found neurons whose spiking activity was predictive of the spatial location of the selected target or the magnitude of the chosen reward even before the choice options were presented. Moreover, the predictive power of these neurons increased as the values associated by the animals with the two decision alternatives became closer. In a similar study investigating neuron activity in the orbitofrontal cortex when monkeys choose between different types of juice in different quantities, Padoa-Schioppa (2013) surprisingly found that trial-to-trial fluctuations in the activity of *offer-value* cells (Fig. II.13A and B) did not explain the variability of choice in near-indifference decisions. In contrast, quasi-indifference decisions were correlated with fluctuations in the activity of the *chosen juice* cells (Fig. II.13C and D) before the offer. However, predictive activity was largely related to the outcome of the previous trial.

In human neuroimaging studies, several findings indicate that brain activity preceding the presentation of choice options may influence the final decision, particularly when the alternatives are safe versus risky (Chew et al., 2019; Huang et al., 2014; Kuhnen & Knutson, 2005; Lopez-Persem et al., 2016; Vinckier et al., 2018). Specifically, baseline activity in typical brain valuation regions has been shown to be involved in biasing subsequent choice selection. For example, activity in the nucleus accumbens and medial frontal gyrus may bias subsequent risky decision making (Huang et al., 2014). Similarly, baseline activity in the ventromedial prefrontal cortex reflected the strength of prior preferences (Lopez-Persem et al., 2016). In addition, these results are also consistent with the idea of distinct neural circuits for reward and punishment valuation presented earlier (Fig. II.15 hypothesis 4), as baseline activity in distinct regions was found to be involved in either risk-taking or risk-aversion. In particular, high baseline activity in the vmPFC or nucleus accumbens promoted risk-taking, whereas high baseline activity in anterior insula tempered risk-taking (Kuhnen & Knutson, 2005; Vinckier et al., 2018), suggesting that different brain regions are related to different aspects of decision-making.

While it is relatively well established that pre-stimulus activity influences choice, some studies have also shown that baseline activity can be tied to mental constructs such as pleasure, satiety, or mood (as we will see in more detail next), which are themselves influenced by external events (Abitbol et al., 2015; Vinckier et al., 2018). For example, in one fMRI study, baseline vmPFC activity in humans was manipulated with music, which created a systematic bias in the subjective assessment. The same experiment was performed in monkeys where, this time, baseline activity was affected by the number of trials (satiety or fatigue effect) and induced the same type of bias. This study thus shows that across species, baseline activity is affected by context,

both internal (e.g., satiety) and external (e.g., music), and that in turn it has an influence on the expressed subjective value (Abitbol et al., 2015).

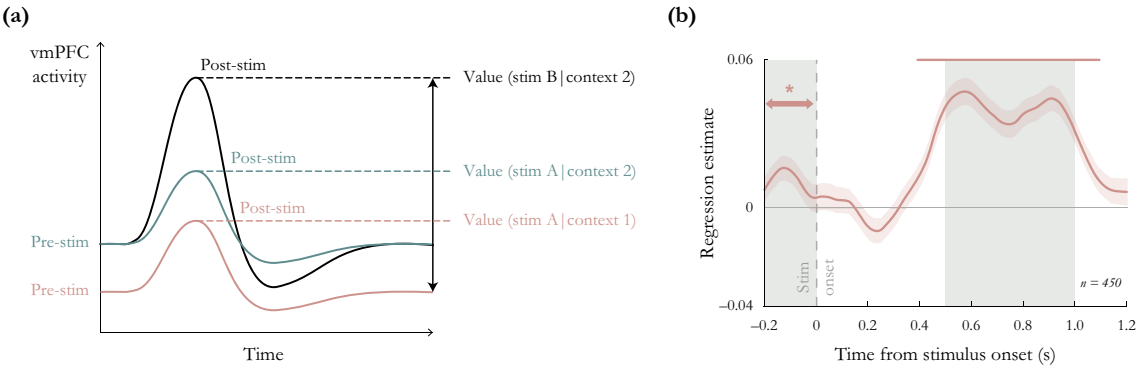

Figure II.20: Potential explanation of how contextual factor impacts subjective value. (a) The initial hypothesis is that a difference in context (context 2 in green vs. context 1 in pink) induces a shift in the baseline activity of the vmPFC (Pre-stim), which would persist in the post-stimulus activity. If the subjective value is encoded in the absolute peak of the evoked response, and not in the differential with respect to the baseline, this would have an impact on the subjective value given to the same stimulus A. From Abitbol et al. (2015). (b) However, a recent study observed that the correlation between pre-stimulus activity and subjective value was lost at the onset of the stimulus before reappearing later. From Lopez-Persem et al. (2020).

An initial hypothesis regarding the mechanism by which the baseline influences the evoked response to a stimulus was that an increase in baseline activity would persist in the evoked activity, resulting in a higher signal and thus a higher value, presuming that the value is encoded in the absolute level of activity, not in the difference from the baseline (Fig. II.20a; Abitbol et al., 2015). According to such a mechanism, the link to the upcoming value should persist between the baseline and the evoked response. However, a recent intracerebral electroencephalography (iEEG) study in humans observed that the correlation with value was momentarily lost in this period (Fig. II.20b; Lopez-Persem et al., 2020).

Overall, these results lead to the view that trial-to-trial variations in pre-stimulus activity influence the valuation process at the time of choice, thereby influencing the behavioral response and partially explaining choice stochasticity. However, the precise mechanism by which spontaneous activity influences value-based decision making is far from being resolved. Although neuroimaging studies provide fairly consistent insights, the temporal resolution of fMRI meets its limitations in isolating successive stages of information processing (e.g., how baseline activity is reflected in value-related brain responses). Indeed, choices occur rapidly, reflect the fast dynamic structure of neural networks, and are exactly the type of phenomenon that requires greater temporal precision than fMRI can provide. Still, the brain areas that are critical to the

valuation of reward and punishment in value-based decision making (e.g., the vmPFC and anterior insula) are too deep to be studied by conventional non-invasive electrophysiological methods such as EEG or MEG. Single-cell or iEEG studies therefore seem to be the most appropriate. Yet, electrophysiological investigations in animals do not allow clear conclusions on the impact of ongoing fluctuations on choice and, to my knowledge, only one study has investigated this phenomenon in humans (Lopez-Persem et al., 2020). Moreover, this study showed anticipatory value signaling only in a reward rating task with no choice and reports discrepancies in the mechanisms compared to fMRI studies. Therefore, the precise dynamics of how spontaneous fluctuations affect decisions under multidimensional choices remain to be elucidated.

Summary

- **Ongoing brain activity** has been witnessed since the earliest neurophysiological recordings and occurs at a wide range of temporal and spatial scales.
- This activity is called **spontaneous** as it is characterized by remarkably large temporal modulations that are not attributable to any specific stimulus.
- The observation that spontaneous fluctuations in brain activity could explain trial-to-trial variations in neuronal response elicited by identical stimuli led to the idea that these fluctuations might be functionally relevant.
- Later studies subsequently showed that pre-stimulus activity could serve as a predictor for perceptual decisions in various modalities.
- **In the field of value-based decision making**, electrophysiology and neuroimaging studies in humans and non-human primates suggest that trial-to-trial variations in pre-stimulus activity of typical brain valuation regions (i.e., vmPFC, aIns) influence the valuation process at the time of choice, thus impacting the behavioral response and partially explaining choice stochasticity.
- Some studies have also shown that baseline activity can be influenced by mental constructs such as pleasure, satiety or mood, which are themselves influenced by external events.
- Despite these advances, several issues and discrepancies can be pointed out:

- Temporal resolution of fMRI is limited to be able to isolate the successive stages of information processing.
- Brain areas critical to valuation are too deep to be studied by conventional non-invasive electrophysiological methods.
- Single-cell studies in animals do not allow clear conclusions on the impact of ongoing fluctuations on choice.
- The only iEEG study in humans (i) focuses only on reward valuation, (ii) was not conducted in a choice context, and (iii) reports differences with the mechanisms hypothesized in fMRI.

In my first experimental study these concerns were addressed by taking advantage of the excellent spatiotemporal resolution and signal-to-noise ratio inherent to iEEG signals recorded with deep electrodes in the cortex of epileptic patients while they performed a multidimensional choice task involving potential gains and losses.

b. Mood in the brain

As detailed earlier, research in cognitive and affective sciences has provided ample evidence of the interactions between mood and decision making (see section I.3.b.). At the neural level, however, the mechanisms underlying this phenomenon have long been overlooked. This is because mood is a psychological construct that is difficult to define and measure, making the study of its neural correlates particularly challenging. As a result, early studies did not directly address this issue, but rather looked for neural responses to stimuli that trigger short-lived emotional responses, showing in particular that human emotions were most often associated with activity in brain regions of the limbic system, including the amygdala and anterior cingulate cortex, but also the ventral striatum, anterior insula and medial prefrontal regions (Murphy et al., 2003).

Using a computational model, the study by Rutledge et al. (2014) was one of the first to establish a link between mood and brain activity. In this one, subjects were asked to perform a probabilistic reward task designed to elicit fairly rapid changes in affective state, while being asked at regular intervals to answer the question "How happy are you right now?" Correlating BOLD activity at the time of option and outcome onset with mood assessed by the model resulted in a significant correlation in the ventral striatum, consistent with the striatal representation of reward prediction errors contributing to mood changes (expectation effect). In addition, repeating this correlation at the time of the question presentation revealed a significant link with

happiness ratings in the anterior insula. A follow-up study reinforced these findings by showing that boosting dopamine levels pharmacologically increased happiness resulting from certain rewards (Rutledge et al., 2015). These observations thus seem to suggest some overlap between regions involved in decision-making processes and mood. Hence, if mood can influence the constituent processes of decision making, it stands to reason that affective states would have an impact on choices.

Impact of mood on value-based decision making

Subsequent fMRI studies indeed provided evidence that mood exerts a specific impact on the neural mechanisms underlying reward and loss processing. In one study, Eldar and Niv (2015) showed that for participants who tend to be less stable in mood, a large, unexpected outcome affected emotional state and biased reward perception in the same direction. Specifically, for these participants, BOLD responses to reward in the striatum and vmPFC were stronger after a positive mood induction and weaker after a negative mood induction. Another study, conducted in healthy subjects, refined the relationship between mood and valuation circuitry by showing that mood had a specific impact on activity during expectation of reward (Young & Nusslock, 2016). In particular, participants underwent a positive or neutral mood induction procedure combining the use of music and sentences, and then performed a delayed monetary incentive task that assessed reward and loss processing. Results indicated that positive mood (compared to neutral) increased activity specifically during reward anticipation in neural regions that have previously been implicated in reward processing and goal-directed behavior, including the nucleus accumbens, lateral orbitofrontal cortex, anterior insula, and vmPFC. Nevertheless, this study did not include negative mood induction, which precluded accounting for the observed differential effects of positive and negative mood on decision making.

The flexible effects of positive and negative affective state on value representation were first demonstrated in an fMRI study of a related topic. Namely, this study investigated the effects of incidental anxiety on neural circuits involved in risky decision making. Their results indicated that under safe conditions, subjective expected values of gambling were positively coded in the vmPFC and ventral striatum, whereas in a threatening context, these processes ceased and were replaced by negative value coding in the anterior insula (i.e., increased activity for increasingly worse outcomes), as well as a general negative baseline shift in the vmPFC (Engelmann et al., 2015). Consistent with these findings, a recent study established that fluctuations in positive and negative mood were represented in the baseline activity of critical brain valuation regions (Vinckier et al., 2018). Specifically, mood correlated positively with baseline activity in

the vmPFC and negatively with baseline activity in the anterior insula (Fig. II.21). Ongoing mood-related activity would then be able to modulate the relative weights assigned to key dimensions of choice options (see Fig. II.20). Notably, using a computational model, they determined that high baseline activity in the vmPFC favored risk-taking by overweighting potential gains, whereas high baseline activity in the anterior insula tempered risk-taking by overweighting potential losses.

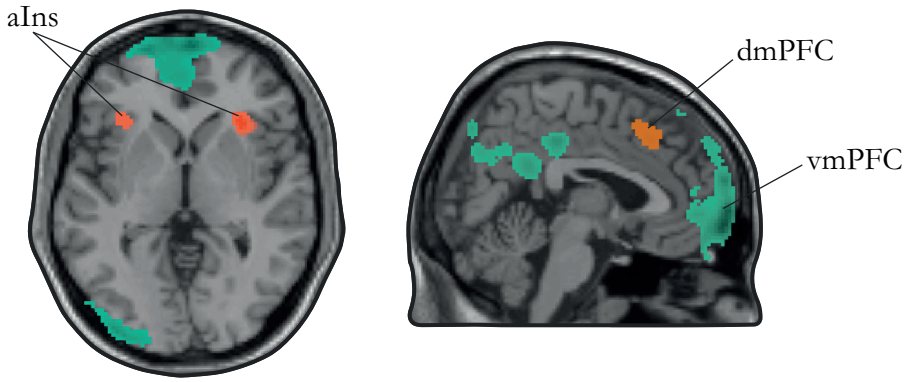

Figure II.21: Brain activity underpinning mood fluctuations. Statistical parametric map of regions reflecting mood (positive correlation in green, negative correlation in red). Four regions of interest were identified: ventromedial prefrontal cortex (vmPFC), anterior insula (aIns), dorsomedial prefrontal cortex (dmPFC) and ventral striatum (not shown). Adapted from Vinckier et al. (2018).

Overall, these fMRI investigations appear to converge on a similar model relating mood fluctuations to the relative activity of opponent brain systems associated with reward or punishment processing. Yet, a second strand of research using intracerebral electroencephalography recordings appears to challenge these findings by suggesting that mood fluctuations may instead correspond to changes in the frequency of oscillatory activity. In particular, two recent studies, combining mood estimates performed over several days with direct recording of intracerebral electroencephalographic signals, revealed a negative correlation between mood level and low frequency activity (< 10 Hz) and a positive correlation between mood and high gamma activity (> 50 Hz), most notably in the OFC and the hippocampus (Rao et al., 2018; Sani et al., 2018). Similarly, investigations of neural modulations across distinct frequency bands in the mesolimbic network (including the insula and OFC) revealed that higher frequencies (30-100 Hz) were associated with positive emotional displays, whereas lower frequency bands were selective of the neutral state (Bijanzadeh et al., 2019). Finally, stimulation of the lateral OFC has been associated with a marked improvement in mood, and subsequent spectral analysis revealed that this stimulation largely suppressed low-frequency power, with the strongest effects observed in the theta frequency band of the OFC, insula, and dorsal cingulate (Rao et al., 2018).

Summary

- Regions underlying mood encoding appear to overlap with regions involved in decision processes.
- The fMRI studies suggest that mood fluctuations are related to the relative activity of opponent brain systems associated with reward or punishment processing, which would ultimately allow them to influence choices.
- Electrophysiological studies in humans suggest instead that mood fluctuations correspond to changes in the frequency of oscillatory activity.

One aim of my first experimental work was to disentangle these findings by recording the intracerebral activity of implanted epileptic patients while they performed a choice task involving potential gains and losses interleaved with a mood induction procedure.

c. Neural correlates of visual attention

The brain mechanisms through which value and attention interact have been primarily investigated in the visual system, where the effects of value have been documented in the primary visual cortex, the lateral intraparietal area, and more broadly in the ventral visual stream (Peck et al., 2009; Serences, 2008; Stănişor et al., 2013). From this perspective, the origin of value influence remains unclear, but the ventromedial frontal area has been identified as a plausible candidate region (Hartikainen et al., 2012; Vaidya & Fellows, 2015b), especially arguing for its many direct and indirect connections to the ventral visual stream (Price, 2007).

In contrast, relatively few studies have addressed the influence of attention on value-based choices at the neural level. In a pioneering human fMRI study, Lim et al. (2011) investigated this issue using a binary choice task in which fixations of two appetitive stimuli were exogenously manipulated. In doing so, they found that the vmPFC and ventral striatum encoded a relative value signals corresponding to the difference in value between the fixated and unfixated items. This result thus suggests that attention influences values by shaping the activity of brain regions crucial to the valuation process. Critically though, the authors demonstrated that these fixation-dependent value signals were unrelated to the identity of the chosen item, leaving open the underlying mechanisms by which visual attention ultimately influences choices. A major limitation of this study is that, using fMRI, the authors had to considerably slow down the

choice process by asking participants to fixate on a particular item for a specified amount of time. As a result, the attention manipulation had a significant but small impact on choices.

To overcome these limitations, subsequent studies have taken advantage of the excellent temporal resolution of single-cell recordings in non-human primates to probe brain activity during natural free viewing (Hunt et al., 2018; McGinty, 2019; McGinty et al., 2016). Their results are consistent with those observed in humans as they show that value representations in the OFC can be influenced by the way attention is allocated between visual objects of different value. For example, in two studies conducted by the same team (McGinty, 2019; McGinty et al., 2016), macaque monkeys performed a Pavlovian appetitive conditioning task in which they learned to associate visual cues with rewards of different value (amount of juice; Fig. II.22a-b). Drawing on natural gaze patterns, the authors found that a large proportion of cells in the OFC encoded gaze position and that, in some cells, value encoding was amplified when subjects fixed their gaze near the cue (Fig. II.22c).

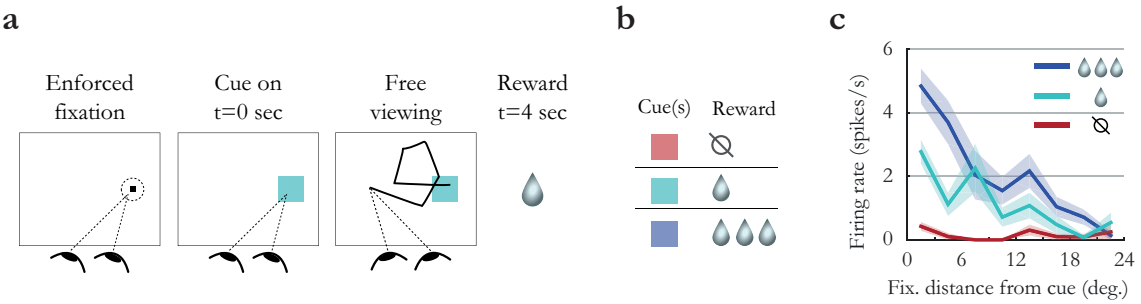

Figure II.22: Modulation of value signals in OFC neurons by gaze shifts. (a) Monkeys were trained to associate visual cues with a certain juice reward. (b) Each cue was associated with different amounts of juice. (c) Single-example cell in the OFC. Firing increased as a function of cue value (colors) and decreased as a function distance of fixation from the cue (x-axis). In addition, the effect of value was maximal for fixations on or near the cue, constituting an interaction between the value and distance effects. Adapted from McGinty (2019).

With the idea of disentangling possible interference between eye movement, reward, and decision, these results were further confirmed by a study exploring the associations between covert attentional shifts and single-cell activity in the primate OFC (Xie et al., 2018). In this study, the authors employed a passive-viewing task in which a pair of visual cues were presented to monkeys while they simply stared at them. After a period of time, the monkeys received the reward associated with one of the two randomly selected cues. By inducing a transient change in attention through a brief visual perturbation of one of the cues, it was possible to show that the neural activity of the OFC reflected the value of the currently attended cue, regardless of whether it was the cue with the highest value.

Altogether, these results in the non-human primate support the initial findings of Lim et al. (2011) whereby attention influences value-based behaviors through the modulation of neural value activity. Even so, some discrepancies can be noticed between these studies. For example, in the study by Xie et al. (2018), OFC activity in monkeys reflected only the highest value between alternatives, instead of the value difference between attended and unattended stimuli, as found by Lim et al. (2011) Whether these discrepancies are due to species difference or to the difference between neural signals recorded by fMRI and electrophysiology remains to be determined. Furthermore, none of the studies reported so far have established a direct link between neural activity modulated by visual attention and choice behavior. To address this concern, a recent study examined the influence of overt attention on behavior by asking how gaze shifts correlated with reward anticipation responses in a Pavlovian conditioning task and whether OFC activity mediated this correlation (McGinty, 2019). Although gaze allocation positively predicted the conditioned response, OFC activity was almost completely uncorrelated with it, meaning that no evidence was found that OFC mediates the predictive relationships between gaze and conditioned responses. In parallel, another study examined the causal contributions of the vmPFC and other prefrontal subregions to this fixation bias phenomenon by tracking the eye movements of lesioned patients and healthy controls as they chose between pairs of artworks (Vaidya & Fellows, 2015a). Contrary to the hypothesis suggested by previous work, lesions of the vmPFC and lateral PFC had no effect on this fixation bias, whereas lesions of the dmPFC increased the influence of fixations on choice. Thus, although visual attention may increase the subjective value of cues associated with a reward, the underlying mechanism remains largely unknown, as does the functional importance of gaze modulation of vmPFC/OFC value signals. Finally, all the studies cited so far entail simple choices involving one-dimensional options (rewarding or punishing), yet humans are regularly confronted with complex decisions involving the integration of multiple attributes with sometimes uncertain outcome. At the behavioral level, work addressing this issue has suggested that the attentional bias relates to attributes rather than options (Fisher, 2017). Specifically, the probability of choosing an option increased with the relative attention paid to the appetitive attribute, and decreased with additional time spent on the aversive attribute. These results are supported by a recent study showing that the gaze bias towards loss leads to loss aversion decisions (Sheng et al., 2020). Nevertheless, no study, to our knowledge, has addressed this issue at the neural level.

Summary

- Early studies suggest that vmPFC (in humans) and OFC (in non-human primates) activity underpin the effect of visual attention on choice by encoding a **fixation-dependent value signal**.
- Nevertheless, recent studies have **failed to establish a direct relationship** between fixation-dependent activity in these regions and choice behavior.
- In addition, some discrepancies have emerged between human fMRI studies and single-cell studies in non-human primates, which may be due to species or technical differences.
- Finally, recent behavioral studies suggest that the attentional bias is on the attribute rather than the options, but nothing is known at the neural level.

Answering these questions was the goal of my second experimental work. To do so, we recorded intracerebral EEG activity as well as eye-tracking data while human subjects performed a multi-attribute accept/reject decision-making task involving potential gains and losses. This combination of techniques is ideal for examining with good temporal precision how eye fixations interact with differential value coding in the human brain, and how choices may be affected by this interaction.

III

Intracerebral mechanisms explaining the impact of incidental feedback on mood state and risky choice

Romane Cecchi[1], Fabien Vinckier[2,3,4], Jiri Hammer[5], Petr Marusic[5], Anca Nica[6], Sylvain Rheims[7], Agnès Trebuchon[8], Emmanuel Barbeau[9], Marie Denuelle[9,10], Louis Maillard[11], Lorella Minotti[1,12], Philippe Kahane[1,12], Mathias Pessiglione[2,3,†], Julien Bastin[1,†]

[1] Univ. Grenoble Alpes, Inserm, U1216, CHU Grenoble Alpes, Grenoble Institut Neurosciences, 38000 Grenoble, France
[2] Motivation, Brain and Behavior (MBB) team, Paris Brain Institute, Pitié-Salpêtrière Hospital, Paris, France
[3] Université de Paris, Paris, France
[4] Department of Psychiatry, Service Hospitalo-Universitaire, GHU Paris Psychiatrie & Neurosciences, Paris, France
[5] Neurology Department, 2nd Faculty of Medicine, Charles University, Motol University Hospital, Prague, Czech Republic
[6] Neurology Department, University Hospital of Rennes, Rennes, France
[7] Functional Neurology and Epileptology Department, Hospices Civils de Lyon and Université de Lyon, Lyon, France
[8] Epileptology Department, Timone Hospital, Public Assistance Hospitals of Marseille, Marseille, France
[9] Centre de recherche Cerveau et Cognition (CerCo), CNRS-UPS, UMR 5549, Toulouse
[10] Neurology department, CHU Toulouse, Toulouse, France
[11] Neurology Department, University Hospital of Nancy, Nancy, France
[12] Neurology Department, University Hospital of Grenoble, Grenoble, France
[†] These authors contributed equally to this work

Under review

Preprint available on bioRxiv

1. Abstract

Identifying factors whose fluctuations are associated with choice inconsistency is a major issue for rational decision theory. Here, we investigated the neuro-computational mechanisms through which mood fluctuations may bias human choice behavior. Intracerebral EEG data were collected in a large group of participants (n = 30), while they were performing interleaved quiz and choice tasks. Neural baseline activity preceding choice onset was confronted first to mood level, estimated by a computational model integrating the feedbacks received in the quiz task, and then to the weighting of option attributes, in a computational model predicting risk attitude in the choice task. Results showed that 1) elevated broadband gamma activity (BGA) in the ventromedial prefrontal cortex (vmPFC) and dorsal anterior insula (daIns) was respectively signaling periods of high and low mood, 2) increased vmPFC and daIns BGA respectively promoted and tempered risk taking by overweighting gain versus loss prospects. Thus, incidental feedbacks induce brain states that correspond to different moods and bias the comparison of safe and risky options. More generally, these findings might explain why people experiencing positive (or negative) outcome in some part of their life tend to expect success (or failure) in any other.

Keywords

Mood, decision, reward, risk, electrophysiology, oscillatory activity, broadband gamma, computational model, ventromedial prefrontal cortex, anterior insula

2. Introduction

Humans often makes inconsistent decisions, even when facing seemingly identical choices. This surprising variability is a major difficulty for rational decision theory and a reason for introducing stochastic functions in choice models. However, even if stochastic functions help mimicking behavior on average, they cannot help predicting individual choice. For this, one need to identify factors whose fluctuations are systematically associated with changes in preference, in order to replace randomness with bias. Influent factors can be related to the internal state of the decision maker and/or the external context of the choice situation. In neuroscience, many studies have shown that brain activity preceding the presentation of choice options might provide a bias on the eventual choice, particularly when alternatives are safe versus risky options (Chew et al., 2019; Huang et al., 2014; Kuhnen & Knutson, 2005; Lopez-Persem et al., 2016; Padoa-Schioppa, 2013; Vinckier et al., 2018).

In some cases, baseline brain activity could be related to mental constructs such as pleasantness, satiety or mood, which were themselves under the influence of external events (Abitbol et al., 2015; Vinckier et al., 2018). These findings therefore provide a putative mechanism explaining why mood is predictive of risky choice: positive/negative events that increase/decrease mood at the mental level also modulate baseline activity at the neural level, changing the way dedicated brain regions valuate risky options. More precisely, good mood would lead to overweighting gain prospects, and bad mood to overweighting loss prospects, making the overall expected value of a risky option positive or negative, depending on circumstances. Such a mechanism could account for the well-documented impact of mood on buying lottery tickets or investing in financial markets (Bassi et al., 2013; Otto et al., 2016; Saunders, 1993), an effect that has been reproduced in the lab (Arkes et al., 1988; Chou et al., 2007; Eldar & Niv, 2015). It could also account for why depressed and manic patients have opposite attitudes toward risk, respectively focusing on negative and positive outcomes of potential actions (Leahy, 1999; Yuen & Lee, 2003).

Despite the importance of this phenomenon, producing disastrous decisions at both the individual scale in psychiatric conditions and the societal scale in real-life economics, the underlying mechanism at the neural level is still poorly understood. This is due to the limitations of functional magnetic resonance imaging (fMRI), which has been mostly used because mood fluctuations are difficult to track in animals, while invasive techniques are forbidden in humans, for obvious ethical reasons. There is nonetheless a particular clinical situation that offers the opportunity to record intra-electroencephalographic (iEEG) activity from deep electrodes, when

patients with refractory epilepsy are prior to surgery. These iEEG recordings have already been used to successfully decode mood from resting-state activity, a technical achievement that may open the route to closed-loop stimulation procedures (Bijanzadeh et al., 2019; Sani et al., 2018). They have also been used to specify the impact of lateral orbitofrontal cortex stimulation aiming at improving mood in moderately depressed patients (Rao et al., 2018). There is however a discrepancy between these pioneering iEEG studies, which reported that changes in mood states might correspond to changes in the frequency of oscillatory activity (Bijanzadeh et al., 2019; Kirkby et al., 2018; Rao et al., 2018; Sani et al., 2018), and fMRI studies that have related mood fluctuations to the relative activity of opponent brain systems associated to either reward or punishment processing.

To examine whether good and bad mood are associated to activity in different brain regions or different frequency bands, we recorded iEEG activity while patients were performing a task similar to that used in a previous fMRI study to induce mood fluctuations and test their impact on risky choices (Vinckier et al., 2018). Mood fluctuations were induced by feedbacks provided to participants on their responses to general knowledge questions. Choices were about whether to accept a challenge rewarded with monetary gains in case of success but punished with monetary losses in case of failure. To avoid repeating self-report too frequently, a computational model was developed, building on previous suggestion (Eldar & Niv, 2015), to generate mood level as an integration of past feedbacks, the perception of which was itself modulated by mood level. This theoretical mood level was positively correlated with activity in brain regions classically associated with reward, such as the ventromedial prefrontal cortex (vmPFC), and negatively correlated with regions associated with punishment, such as the anterior insula (aIns). In turn, baseline activity in these regions (prior to the presentation of choice options) was predicting a bias on choice, relative to an expected utility model. Indeed, high vmPFC activity favored the risky option (accepting the challenge) by increasing the weight on potential gain, whereas high aIns activity favored the safe option (declining the challenge) by increasing the weight on potential loss. Yet, due to the poor temporal resolution of fMRI, there was a remaining gap in the explanation, regarding the contribution of activity in mood-related regions during decision making. Here, leveraging the excellent temporal resolution of iEEG, we intended to separate brain activity related to feedback events, to overall mood level and to the choice process.

Thus, in an attempt to clarify the neuro-computational mechanism through which mood fluctuations might arise and bias decisions under risk, we collected iEEG data in a large group of participants ($n = 30$), while they were performing interleaved quiz and choice tasks. The objectives of our analytical approach were 1) to identify brain regions in which activity was related

to both mood state (good or bad) and choice (safe or risky), and 2) to examine whether mood fluctuations and related decisions were associated to a shift in frequency bands or in anatomical location of oscillatory iEEG activity.

3. Results

The aim of this study was to elucidate how intracerebral activity may underpin the impact of mood fluctuations on risky choices. Intracerebral electroencephalographic (iEEG) data were collected in thirty patients suffering from refractory epilepsy (39.5 ± 1.9 years old, 14 females, see demographical details in Supplementary Table III.S1), while they performed three unrelated but interleaved tasks. The first was a quiz task designed as a mood induction procedure; the second was a rating task used to quantify mood level; the third was a choice task used to unravel the effects of mood fluctuations on economic choices (Fig. III.1a). In the quiz task, subjects were asked to answer general knowledge questions and received feedback on their response (correct, incorrect or too late). In order to predictably modulate mood, the difficulty of questions and the validity of feedbacks were manipulated, unbeknownst to the subjects, so as to create episodes of high and low correct feedback rate (see Methods). In 25% of the trials, the effect of feedback history was assessed by asking subjects to rate their mood on a visual analog scale. Otherwise (in 75% of trials), the quiz and choice task were separated by a four-seconds rest period (black screen). In the choice task, subjects had to decide whether to accept or reject a given offer before performing a challenge consisting in stopping a moving ball inside a target. The offer comprised a gain prospect (i.e., the amount of money they would win in case of success), a loss prospect (i.e., the amount of loss in case of failure) and the difficulty of the upcoming challenge (target size). When accepting the offer, subjects played for the proposed amounts of money, otherwise, when declining, they played for minimal stakes (winning or losing 10 cents). All three choice dimensions (gain, loss and difficulty) were varied on a trial-by-trial basis. In order to avoid learning, and additional effects on mood, no feedback was provided regarding performance in the challenge (actual success rate was around 30% on average but significantly varied with difficulty). Subjects were explicitly informed that the three interleaved tasks were independent, such that responses to the quiz or mood ratings had no influence on choice options and hence on their monetary earnings.

Choice behavior

We first tested whether subjects performed the choice task correctly by checking that the three dimensions of the offer (gain prospect, loss prospect and challenge difficulty) were properly

integrated into their choices (Fig. III.1b). Choice acceptance was fitted at the individual level using a logistic regression model that included the three dimensions and significance of regression estimates was assessed at the group level (across $n = 30$ subjects) using two-sided, one-sample, Student's t-tests. Results show that acceptance rate significantly increased with gain ($\beta_{\text{gain}} = 0.12 \pm 0.02, t_{29} = 6.85, p = 2.10^{-7}$), but significantly decreased with loss ($\beta_{\text{loss}} = -0.10 \pm 0.02, t_{29} = -5.51, p = 6.10^{-6}$) and difficulty ($\beta_{\text{diff}} = -0.03 \pm 0.01, t_{29} = -2.97, p = 6.10^{-3}$). These results were expected given previous behavioral evidence with a similar choice task that subjects with epilepsy can integrate these three dimensions when making a decision (Vinckier et al., 2018).

We next assessed whether mood fluctuations impacted choices above and beyond the influence of these three dimensions. We thus tested the link between mood ratings and choice residuals, once the three dimensions had been regressed out (Fig. III.1c). To account for interactions and non-linearities in a principled way, we fitted a model based on expected utility theory, which was previously shown to best capture choices in this task (see Vinckier et al., 2018). In brief (see Methods for details), acceptance likelihood was estimated as a softmax function of expected utility, calculated as potential gain multiplied by probability of success (p_s, inferred from target size) minus potential loss multiplied by probability of failure ($1 - p_s$), with gain and loss terms weighted by distinct parameters (k_g and k_l respectively). Residuals of this choice model were then regressed against mood ratings at the individual level, and significance of regression estimates was assessed at the group level, using two-sided, one-sample, Student's t-test. Results indicate a significantly positive association between mood ratings and choice residuals ($\beta = 0.05 \pm 0.02, t_{29} = 2.32, p = 0.027$), meaning that variability in choices, beyond that induced by the three dimensions of the offer, was indeed partially explained by mood fluctuations.

Modeling mood fluctuations

Because frequent assessment of subjective emotional states can lead to inconsistent ratings (Napa Scollon et al., 2009), mood ratings were collected in a minority of the trials (25%). To retrieve mood levels in trials where no rating was provided, we used computational modeling. To ensure the model was based on solid grounds, we checked beforehand that mood ratings were influenced by the expected factors related to the quiz task.

We first verified that our manipulation of feedbacks was effective (Fig. III.1d): indeed the proportion of correct feedbacks was higher in episodes with intended high versus low correct feedback rate (0.60 ± 0.01 vs. 0.21 ± 0.01; $t_{29} = 22.99, p = 4.10^{-20}$; two-sided, paired Student's

t-test) and so was mood rating (0.22 ± 0.04 vs. -0.12 ± 0.06; $t_{29} = 3.76$, $p = 8.10^{-4}$, two-sided, paired, Student's t-test).

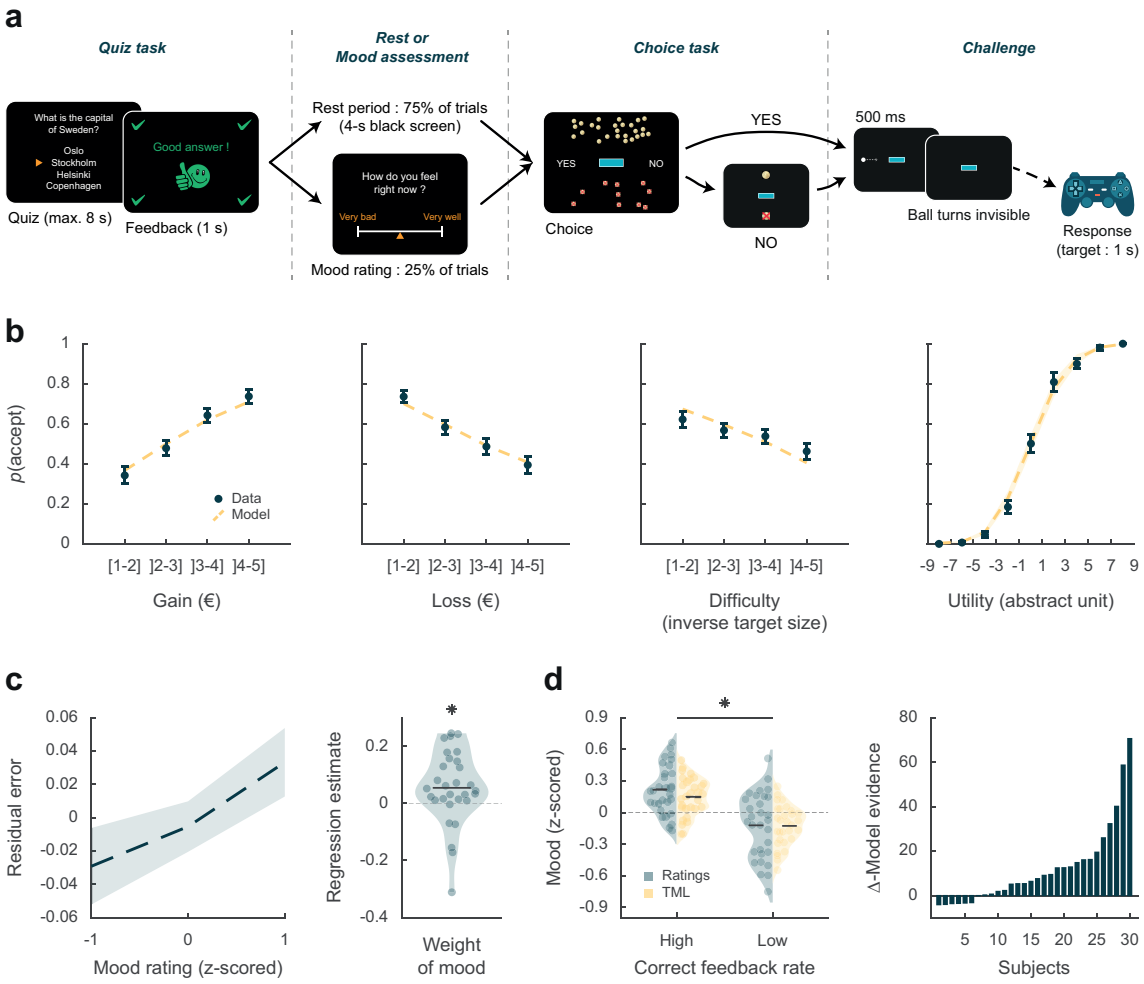

Figure III.1: Behavioral task and results. (a) Trial structure. Each trial included a quiz task, a rest or mood assessment period and a choice task followed by a challenge. In the quiz task, subjects answered a general knowledge question and received a feedback. The quiz task was followed by a rest period (75% of trials) or a mood rating task (25% of trials) on a visual analog scale. In the choice task, subjects had to decide whether to accept or reject a given challenge by taking into account gain prospects (represented by a bunch of regular 10-cent coins), loss prospects (crossed out 10-cent coins) and difficulty (inversely proportional to the size of the blue bar in the middle of the screen). The challenge consisted in stopping a moving ball, invisible when inside the blue target. (b) Choice behavior. Acceptance probability is plotted as a function of the three objective dimensions (gain, loss, difficulty) and modeled subjective utility of the proposed challenge. Circles are binned data averaged across subjects. Yellow dotted lines represent acceptance probability as computed by the choice model. Error bars represent inter-subject S.E.M. (c) Impact of mood on the choice model residual error (actual choice – modeled acceptance probability). Left panel: residual error is plotted as a function of mood rating. Right panel: the weight of mood on residual error is shown as individual regression estimates. Circles represent individual data and horizontal line represents mean across subjects (as in d, left panel). (d) Mood fluctuations. Left panel: Effect of correct feedback rate on mood rating and theoretical mood level (TML). Right panel: difference in model evidence between TML and a null model in which feedback had no impact on mood. Bars show subjects ranked in ascending order. Stars indicate significance ($p < 0.05$).

We then fitted individual mood ratings with a previously established computational model (Vinckier et al., 2018) that formalizes a reciprocal influence between mood and feedback (see Methods). This means that mood level increases with positive feedback (reciprocally, decreases with negative feedback) and in turn that feedbacks are perceived as more positive when mood is higher (reciprocally, more negative when mood is lower). Posterior estimates of free parameters indicated that indeed, the weight of feedback on mood (parameter ω_f), was significantly positive across subjects ($t_{29} = 4.72$, $p = 6.10^{-5}$; two-sided, one-sample, Student's t-test). Conversely, the weight of mood on feedback (parameter δ) was also significantly positive ($t_{29} = 3.30$, $p = 0.003$). The forgetting factor was 0.69 ± 0.04, meaning that feedback received five trials earlier still had an impact corresponding to 23% of the most recent feedback. In addition, the model included a linear effect of time, weighted by parameter ω_t, which was not significantly different from zero, meaning that task duration had no significant influence on mood. Using fitted parameters for every patient, a theoretical mood level (TML) was then estimated on a trial-by-trial basis. As seen with mood rating (Fig. III.1d), TML was significantly higher during episodes with high vs. low correct feedback rate ($t_{29} = 4.19$, $p = 2.10^{-4}$; two-sided, paired, Student's t-test). At the group level, Bayesian comparison indicated that the mood model was far more plausible (exceedance probability $Xp = 1$) than the null model assuming no influence of feedback but only the effect of time. However, the results of model comparison were more variable at the individual level (see Fig. III.1d), with the null model doing better than the mood model in 6 subjects (out of 30).

Intracerebral activity underpinning mood fluctuations

The next step was to establish a link between mood level and intracerebral electroencephalographic signals (iEEG). The iEEG dataset included a total of 3494 recording sites (bipolar montage, (see Methods) acquired from 30 patients (Supplementary Fig. III.S1). For each patient, recording sites were localized within the native anatomical brain scan and labeled according to either MarsAtlas (Auzias et al., 2016), Destrieux (Destrieux et al., 2010) or Fischl (Fischl et al., 2002) parcellation schemes, with slight modifications (see Methods). Out of the 3494 recording sites, 3188 were free from artefacts and located within the grey matter of the 50 covered areas. Among these areas, 42 regions (n = 3154 sites) with at least 10 recording sites across at least four patients were retained in the electrophysiological analyses (see Methods). We initially focused on broadband gamma activity (50-150 Hz, BGA), as converging lines of evidence showed that BGA correlates positively with both fMRI and spiking activity (Lachaux et al., 2007; Manning et al., 2009; Mukamel, 2005; Niessing et al., 2005; Nir et al., 2007; Winawer et al., 2013), but subsequently took all frequency bands into consideration.

We extracted BGA time series from all retained recording sites and performed multiple linear regressions (one per time point) across trials between BGA and mood rating or TML. We time-locked this analysis to the [-4 to 0 s] time window before prospects onset, i.e. during the time period corresponding to the rest or mood assessment period. Significance was tested across all recording sites within each region of interest (ROI), using two-sided, one-sample Student's t-tests on regression estimates, with correction for multiple comparisons across time points using a non-parametric cluster-level statistic (see Methods). To identify brain regions that were reliably associated with mood fluctuations (Fig. III.2a), we focused our analyses on ROIs within which BGA was significantly associated with both mood rating and TML, with the additional constraint that the sign of the correlation had to be consistent.

The vmPFC was the only ROI for which we found a positive correlation (Fig. III.2b) between BGA and both mood rating (best cluster: -1.37 to -1.04 s, $sum(t_{90}) = 122.3$, $p_{corr} = 0.010$) and TML (best cluster: -0.57 to -0.13 s, $sum(t_{90}) = 132.4$, $p_{corr} = 8.10^{-3}$). Conversely, we found a negative correlation in a larger brain network encompassing the daIns (Fig. III.2b), in which BGA was negatively associated with both mood rating (best cluster: -3.36 to -2.51 s, $sum(t_{85}) = -325.8$, $p_{corr} < 1.7.10^{-5}$) and TML (best cluster: -3.13 to -2.72 s, $sum(t_{85}) = -136.4$, $p_{corr} = 9.10^{-3}$). The additional brain regions in which BGA was negatively associated with mood level involved the dorsolateral prefrontal cortex, the visual cortex, the motor cortex, the dorsomedial premotor cortex, the ventral somatosensory cortex and the ventral inferior parietal lobule. Note that in the ventral anterior insula, BGA was negatively associated with mood rating, but not with TML.

Thus, our two a priori ROIs signaled mood level with opposite signs, whether the correlation with BGA was tested during mood rating only or extended to all trials using TML to extrapolate mood ratings. We also verified that the association between TML and BGA (averaged within the best temporal cluster for each ROI) remained significant when only considering trials with no rating (vmPFC: $\beta = 0.031 \pm 9.10^{-3}$, $t_{90} = 3.59$, $p = 5.10^{-4}$; daIns: $\beta = -0.02 \pm 8.10^{-3}$, $t_{85} = -2.67$, $p = 9.10^{-3}$). To assess whether vmPFC and daIns regions would represent separate components of mood, we entered them into a single regression model meant to explain TML. In order to obtain the time course of mood expression in the two ROIs (Fig. III.2c), we performed multiple regression between TML and BGA from all possible pairs of vmPFC and daIns recording sites recorded in a same subject (n = 247 pairs of recording sites, (see Methods) and tested the regression estimates across pairs within each ROI for each time point. The regression estimates were significant predictors of TML in both regions, but with opposite signs

(best cluster for the vmPFC: -0.71 to 0 s, $sum(t_{246}) = 414.1$, $p_{corr} < 1.7.10^{-5}$; best cluster for daIns: -3.05 to -2.76 s, $sum(t_{246}) = -113.8$, $p_{corr} = 0.018$).

Thus, BGA in the two main ROIs carried non-redundant information about mood level. To further investigate which component of mood was signaled by each region (Fig. III.2d), we regressed BGA against TML separately for high- and low-mood trials (35% with highest vs. lowest TML). In the vmPFC, regression estimates were significantly positive for high-mood trials only

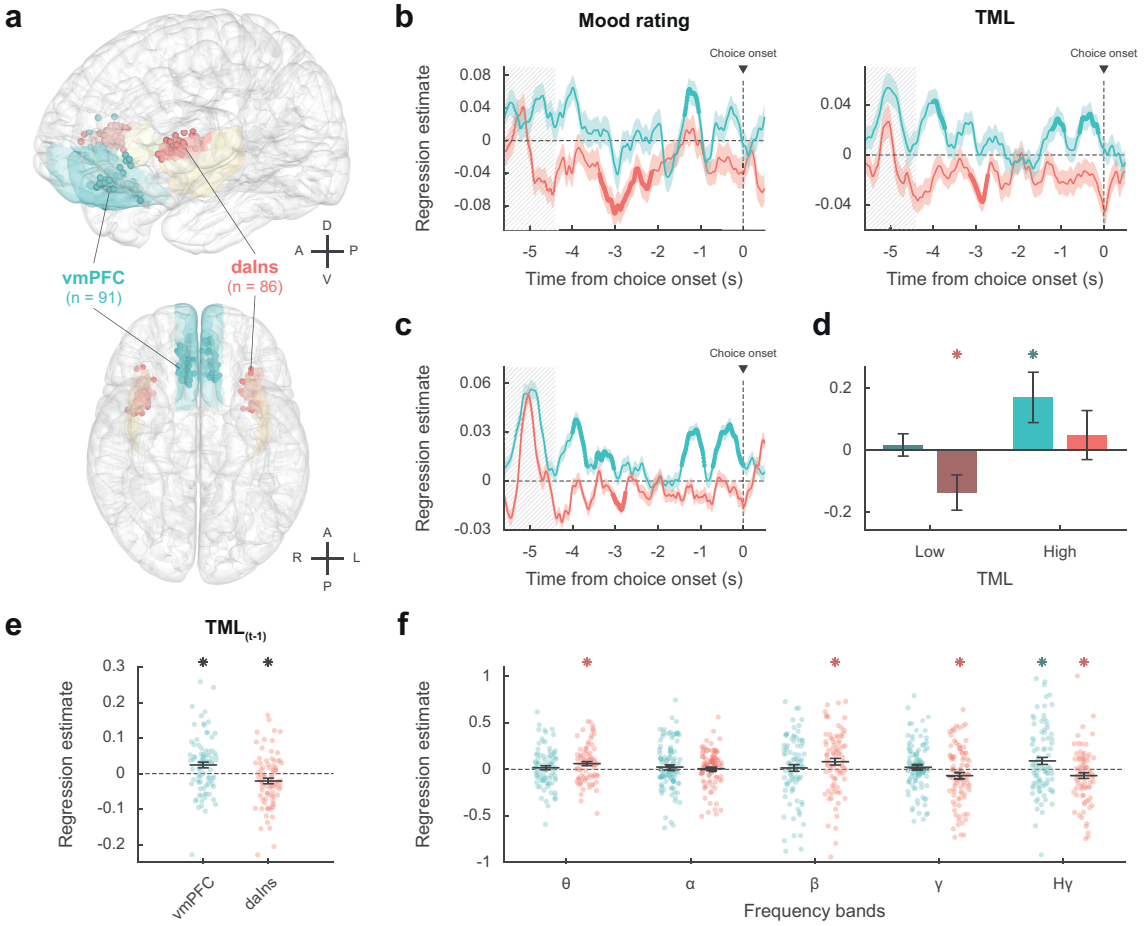

Figure III.2: Intracerebral activity underpinning mood fluctuations. (a) Anatomical location of the vmPFC (blue) and daIns (red) in the standard Montreal Neurological Institute template brain, along with all recording sites located in these areas (dots) and the entire insula (in yellow). Anterior (A), posterior (P), dorsal (D), ventral (V), left (L) and right (R) directions are indicated. (b) Time course of estimates obtained from the regression of BGA against mood rating (left) or TML (right). (c) Time course of estimates obtained from the regression of vmPFC and daIns BGA included in a same GLM fitted to TML. In panels b-c, lines indicate means and shaded areas ± SEM across recording sites. Bold lines indicate significant clusters ($p_{corr} < 0.05$). Grey hatched areas indicate the time window within which the quiz feedback was provided to subjects. (d) Average estimates (within the best temporal cluster for each ROI) obtained from the regression of BGA against the 35% lower or higher TML. Bars are means and error bars are SEM across recording sites. (e) Average estimates (over the baseline window: -4 to 0 s before choice onset) obtained from the regression of BGA against TML after excluding the last feedback. Dots represent individual regression estimates for each recording site, horizontal lines and error bars respectively represent mean and SEM across sites within each ROI. (f) Association between TML and activity in frequency bands. For each frequency band, power time series were averaged over the baseline window and entered in a regression model meant to explain TML. θ: 4-8 Hz; α: 8-13 Hz; β: 13-33 Hz; γ: 33-49 Hz; $H\gamma$: 50-150 Hz. In panels d-f, stars indicate significance ($p < 0.05$) of regression estimates (two-sided, one-sample, Student's t-test).

($\beta_{highTML} = 0.17 \pm 0.08$, $t_{90} = 2.10$, $p = 0.039$; two-sided, one-sample, Student's t-test), not for low-mood trials. Conversely, in the daIns, regression estimates only reached significance for low-mood trials ($\beta_{lowTML} = -0.14 \pm 0.06$, $t_{85} = -2.39$, $p = 0.019$), not high-mood trials. This double dissociation suggests that the vmPFC signals mood level when it gets better than average, and the daIns when it gets worse than average.

In order to check that TML was expressed above and beyond the component related to the last feedback (Fig. III.2e), we splitted TML into two regressors, one representing the last feedback only ($+1$ or -1) and one representing the integration of all preceding feedbacks, which is equivalent to TML estimated at the previous trial (see Methods). BGA in the best time clusters identified above were still significant predictors of TML (after removing the influence of the last feedback) in both the vmPFC ($\beta_{[-0.57-0.13]} = 0.024 \pm 8.10^{-3}$, $t_{90} = 2.99$, $p = 4.10^{-3}$) and daIns ($\beta_{[-3.13-2.72]} = -0.021 \pm 8.10^{-3}$, $t_{85} = -2.64$, $p = 0.010$; two-sided, one-sample, Student's t-test).

Finally, to ensure that our a priori focus on BGA was justified, we explored activity in other frequency bands (Fig. III.2f). For each frequency band and recording site, power time series were averaged over the pre-choice time window (-4 to 0 s) and regressed against TML. In the vmPFC, regression estimates were only significant in the high-gamma band ($\beta_{H\gamma} = 0.091 \pm 0.04$, $t_{90} = 2.41$, $p = 0.018$; two-sided, one-sample, Student's t-test). In the daIns however, regression estimates were not only significantly negative in the gamma and high-gamma bands ($\beta_{H\gamma} = -0.067 \pm 0.03$, $t_{85} = -2.18$, $p = 0.032$; $\beta_{\gamma} = -0.067 \pm 0.03$, $t_{85} = -2.0$, $p = 0.048$), but also significantly positive in the theta and beta bands ($\beta_{\beta} = 0.082 \pm 0.04$, $t_{85} = 2.31$, $p = 0.023$; $\beta_{\theta} = 0.062 \pm 0.02$, $t_{85} = 2.85$, $p = 6.10^{-3}$). To check whether low-frequency bands could provide additional information about mood level, we fitted TML with all possible General Linear Models (GLMs) containing BGA together with any combination of other frequency bands (see Methods). In both vmPFC and daIns, Bayesian model selection designated the BGA-only GLM as providing the best account of TML (vmPFC: expected frequency $Ef = 0.99$, exceedance probability $Xp = 1$; daIns: $Ef = 0.99$, $Xp = 1$). Thus, even if other frequency band activity was significantly related to TML in daIns, it carried redundant information relative to that extracted from BGA. Hence, BGA was the best neural proxy for mood level, at least in our two main ROIs.

Impact of baseline intracerebral activity on decision making

To identify which mood-related regions impacted choices, we regressed across trials the residuals of choice model fit against BGA (time-locked to choice onset), for every time point and record-

ing site. Among regions that encoded mood levels in their baseline, regression estimates were significant in five ROIs (Fig. III.3a and Supplementary Table III.S2), including positive correlation in vmPFC (best cluster: -1.64 to -1.31 s, $sum(t_{90}) = 91.2$, $p_{corr} = 0.020$) and negative correlation in daIns (best cluster: -0.95 to -0.67 s, $sum(t_{85}) = -85.2$, $p_{corr} = 0.029$). Taken together, these results mean that vmPFC and daIns baseline BGA not only express mood in opposite fashion, but also had opposite influence on upcoming choice.

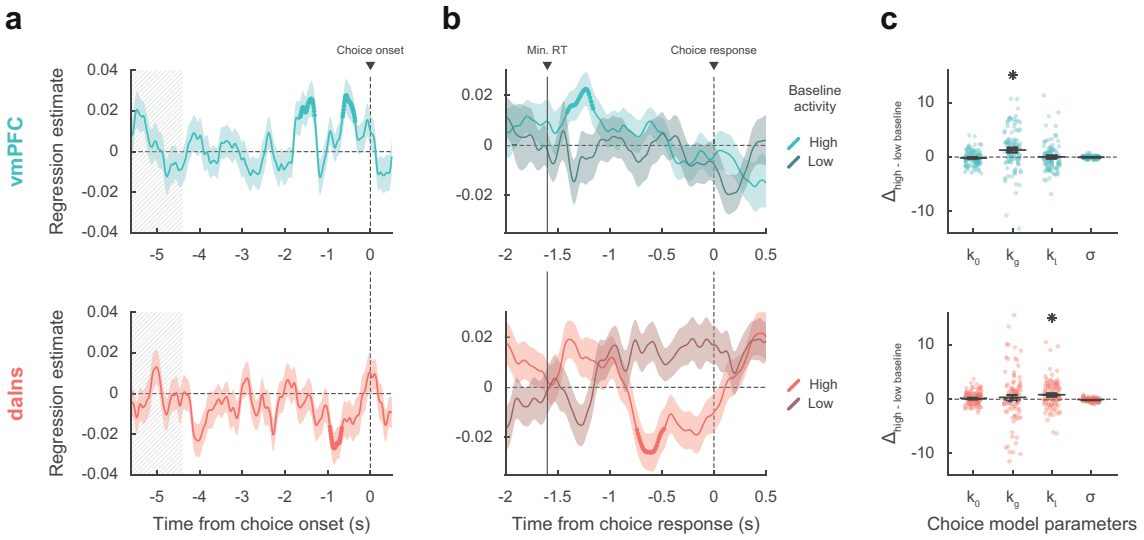

Figure III.3: Impact of intracerebral activity on decision making. (a) iEEG activity predicting choice. Plots show the time course of estimates obtained from the regression of choice residuals against BGA in vmPFC (top, blue) and daIns (bottom, red), averaged across recording sites ± SEM (shaded areas). Bold lines indicate significant clusters ($p_{corr} < 0.05$). Grey hatched areas highlight the time window within which quiz feedback was provided to subjects. (b) Time course of estimates from the regression of choices against BGA performed separately for high vs. low baseline BGA trials, in vmPFC (top, blue) and daIns (bottom, red). Vertical line indicates the minimum response time of trials used in the regression (1.6 sec). (c) Impact of baseline BGA on choice model parameters. Plots show the difference in model weights (posterior parameters) between fits to high- vs. low-BGA trials. Significant modulation was only found for k_g (weight on potential gain) with vmPFC BGA and for k_l (weight on potential loss) with daIns BGA. Dots represent individual data, horizontal lines and error bars respectively represent mean and SEM across recording sites. Stars indicate significance ($p < 0.05$).

Next, we tested whether baseline activity in our two ROIs was carried over choice-related activity so as to bias decision making (Fig. III.3b). For each contact of a given ROI, we regressed choices against BGA separately for trials with high and low baseline BGA (in the time window identified in the preceding analysis for each ROI). For the vmPFC, we found that when baseline BGA was high, choice-related BGA positively predicted choices (best cluster: -1.41 to -1.16 s, $sum(t_{90}) = 70.4$, $p_{corr} = 0.035$). In contrast, for the daIns, when baseline BGA was high, choice-related BGA negatively predicts choices (best cluster: -0.74 to -0.48 s, $sum(t_{85}) = -78.2$, $p_{corr} = 0.022$).

Finally, we investigated the computational mechanism through which baseline BGA (in the time window identified above for each ROI) could modulate decision making. For each contact of a given ROI, we fitted choices with a model in which the weights on the different terms of expected utility (k_0, k_g, k_l, and σ; (see Methods) were modulated by baseline BGA (Fig. III.3c). Comparing posterior parameters obtained with high versus low BGA trials (obtained by median split), we found that kg was significantly enhanced by vmPFC baseline ($t_{90} = 3.16$, $p = 2.10^{-3}$; two-sided, paired, Student's t-test) whereas kl was significantly enhanced by daIns baseline ($t_{85} = 2.90$, $p = 5.10^{-3}$). This suggests that iEEG baseline fluctuations in these two mood-related regions had opposite effects: increased vmPFC BGA would lead to overestimating gain prospects, while increased daIns BGA would lead to overestimating loss prospects.

4. Discussion

In the present study, we used a large dataset of iEEG signals recorded in 30 subjects to provide a neuro-computational account of how mood fluctuations arise and impact risky choice. We found that 1) baseline BGA in vmPFC and daIns was respectively signaling periods of high and low mood induced by incidental feedbacks, 2) beyond BGA, oscillatory activity in other frequency bands did not provide any additional information about mood level, 3) high vmPFC baseline BGA promoted risk taking by selectively increasing the weight of potential gains, whereas high daIns baseline BGA tempered risk taking by increasing the weight of potential losses, 4) baseline BGA in both regions was carried over BGA during decision making, which was predictive of the eventual choice. In the following, we successively discuss how BGA in these two regions relate to mood and choice.

BGA and mood

To avoid asking subjects to rate their mood on every trial, we used a computational model to interpolate mood level between mood ratings. The model was inspired from previous suggestions (Eldar & Niv, 2015; Rutledge et al., 2014) and already validated in a previous publication (Vinckier et al., 2018). The basic assumption is that mood is nothing but a weighted sum of positive and negative events (here, feedbacks received in the quiz task), the more recent having more weight than the more distant in the past. In addition, the model postulates that the way feedbacks are perceived are also affected by mood, in the sense that a same feedback is perceived as more positive when we are in a better mood. This makes reciprocal the influence between internal states (mood) and external events (feedback). The model was inverted on the basis of mood ratings and compared to a null model, where mood is just drifting with time, without any

influence of feedback. Even if the mood model was largely winning the Bayesian comparison at the group level, its evidence was surpassing the null model in about two thirds of participants, a proportion close to that reported is the previous publication (Vinckier et al., 2018). We nevertheless kept all patients in subsequent analyses to reach more robust conclusions that might be generalized to the entire population. Posterior estimates of free parameters confirmed the reciprocal influence between feedback and mood, the forgetting factor suggesting that mood was still impacted by the feedback received five trials in the past (about two minutes before), with a weight about four times lesser than the last feedback. Thus, the time scale of mood fluctuations was longer than acute emotional reactions to single stimuli, but much shorter than those observed in mood disorders.

When looking for neural correlates of mood fluctuations, we used both raw ratings and modeled mood levels as probes. The results were qualitatively similar but statistically more significant with theoretical mood level because it allowed including all trials in the analysis. To identify brain regions that could mediate the impact of mood on choice, we selected all regions that were significantly associated to both mood level (good or bad) and choice (safe or risky). We found the two main bilateral regions that were already identified with fMRI (Vinckier et al., 2018), plus unilateral visual or motor regions that were likely related to the side of the behavioral response. We note however that the anterior insula region defined anatomically corresponds to a dorsal part of the cluster identified with fMRI (hence the appellation of daIns) and that the vmPFC region included many recorded sites located in more ventral areas than the fMRI cluster. As with fMRI, we observed that correlation with mood level was positive in the vmPFC and negative in the daIns. This is consistent with many studies implicating the vmPFC in reward learning and the daIns in punishment learning (Fouragnan et al., 2018; Garrison et al., 2013; X. Liu et al., 2011; Palminteri & Pessiglione, 2017), including studies using iEEG (Gueguen et al., 2021). What we additionally show here is that the vmPFC and daIns are not just sensitive to the last reward or punishment outcome as in learning paradigms, but integrate feedbacks over a longer time scale. Indeed, the time course of regression estimates showed significant association with mood in time windows much later than the response to the last feedback, and the association remained significant when removing the impact of the last feedback from the computation of theoretical mood level used as regressor. We note that some expected regions are missing in our list, notably the ventral striatum, which has been shown to correlate positively with mood level (Eldar & Niv, 2015; Rutledge et al., 2014; Young & Nusslock, 2016). This region could not be investigated here because it was simply not sampled by the electrodes implanted for clinical purposes (i.e., for localization of epileptic foci). More generally, an inherent limitation to

iEEG is that parts of the brain are less sampled than others, so null results should be considered with caution, because of huge differences in statistical power across regions. Nevertheless, whole-brain analysis using fMRI showed that with this induction procedure, activity in other regions such as the ventral striatum or dorsal anterior cingulate cortex adds nothing to decoding of mood level (Vinckier et al., 2018).

Having identified the two main regions reflecting mood fluctuations, we tested whether mood fluctuations were associated to similar shifts in the frequency of oscillatory activity as was previously suggested (Bijanzadeh et al., 2019; Kirkby et al., 2018; Rao et al., 2018). On the contrary, we observed that higher mood had opposite effects on high-frequency oscillations in the two regions, with increased BGA in the vmPFC but decreased BGA in the daIns. Thus, mood fluctuations were better accounted for by relative high-frequency activity (BGA) in the two opponent regions. Indeed, when included in the same model, vmPFC and daIns BGA were both significant predictors of mood level. Conversely, including low-frequency activity in the model did not help predicting mood level. The information carried in low-frequency activity was therefore at best redundant with that of high-frequency activity, whereas the two regions carried at least partly independent information. When analyzing separately bad, neutral and good mood levels, we found that higher BGA signaled the two extreme tertiles: good mood in the vmPFC and bad mood in the daIns. This result suggests that the two regions were specifically concerned with good and bad mood, explaining why they were not just anti-correlated. Although we used a unidimensional rating going from bad to good mood, it could be that mood is in fact bidimensional, meaning that good and bad mood would be better conceived as independent components (Watson et al., 1988), relying on distinct brain systems. This is in keeping with clinical practice: absence of positive affect or excess of negative affect are considered as two independent criteria for depression.

The observation that mood is signaled by distinct brain systems and not different frequency bands all over the brain as in previous iEEG studies (Bijanzadeh et al., 2019; Kirkby et al., 2018; Rao et al., 2018) might be related to the use of positive and negative events to induce mood fluctuations and not direct stimulation of the cortical surface, which might put constraints on oscillatory activity. Besides, the good correspondence with previous fMRI results validates the shared view that BGA represents a time-resolved neural index of local neuronal activity, which typically correlates with both hemodynamic response and local spiking activity (Lachaux et al., 2007; Manning et al., 2009; Mukamel, 2005; Niessing et al., 2005; Nir et al., 2007; Winawer et al., 2013). We have confirmed this correspondence every time we compared iEEG and fMRI activity during the same behavioral paradigm (Gueguen et al., 2021; Lopez-Persem et al., 2020).

BGA and risky choice

Choice to accept or reject the challenge in our task was significantly modulated by the three attributes displayed on screen: gain prospect (in case of success), loss prospect (in case of failure) and difficulty of the challenge. We combined the three attributes using a standard expected utility model and examined the residuals after removing the variance explained by the model. Those residuals were significantly impacted by mood level, meaning that on top of the other factors, good / bad mood inclined subjects to accept / reject the challenge. The same was true for neural correlates of mood: higher baseline BGA in the vmPFC / daIns was associated to higher accept / reject rates, relative to predictions of the choice model. Thus, different mood levels might translate into different brain states that predispose subjects to make risky or safe decisions.

The remaining question is how baseline BGA in these regions can be mechanistically related to risky choice. To address this question, we examined BGA during decision making, which could be separated from baseline BGA thanks to the temporal resolution of iEEG recordings. We found some carry-over: higher BGA in the vmPFC / daIns again predicted the likelihood of accept / reject choices. This does not mean that the link between BGA and choice was maintained all along, it was actually lost at the offer onset and retrieved before the behavioral response. This pattern could not be observed with fMRI but was already reported regarding the subjective value signals (Lopez-Persem et al., 2020). This result suggests that the impact of baseline activity in mood-related regions was mediated by the contribution of the same regions (vmPFC and daIns) to the decision-making process. These regions have already been implicated in computing the subjective values that are compared to make a choice, with the vmPFC and daIns respectively providing positive and negative value signals (Bartra et al., 2013; Pessiglione & Delgado, 2015). Thus, the relative activity of two regions may provide an impulse to accept or reject an offer, depending on whether the differential is positive or negative.

An additional explanation would be that the two regions not only provide subjective values with opposite signs, but also that they provide values that differ in how the different attributes are weighted. To test this idea, we compared parameters of the choice model fitted separately onto trials with high versus low baseline BGA in the vmPFC and daIns. We found that high BGA in the vmPFC / daIns was respectively associated to overweighting of gain and loss prospects, and not just the constant that captures the global tendency to accept or reject. This result makes the link with the idea that we may see a glass half-full or half-empty when we are in a good or bad mood. It is also consistent with reports that pre-stimulus spiking or hemodynamic activity

in the vmPFC predicts how much rewards are liked (Abitbol et al., 2015; Lopez-Persem et al., 2020), whereas pre-stimulus activity in the daIns predicts how aversive punishments are perceived (Caria et al., 2010; Wiech et al., 2010). Overall, our findings suggest that mood-related neural fluctuations impact the valuation process in a valence-specific way, implemented by functionally opponent brain systems.

An obvious limitation of these findings is that although the dataset was collected in patients with epilepsy, we make interpretations as if it was collected in healthy subjects, assuming that pathological activity did not influence the neural or cognitive processes of interest. What was reassuring is that the behavior was remarkably comparable to that of young participants performing a similar task, while the iEEG results were fully compatible with fMRI results (Vinckier et al., 2018). Also, it does not seem very plausible that artifacts would by chance correlate, across task trials in patients with different forms of epilepsy, with the computational variables that were related to both neural and behavioral results. Indeed, in previous studies where we compared results with and without removing artifacted trials, results were unchanged. In fact, those trials can only degrade the correlation with computational variables, such that keeping them ensures that results would be more robust to replication.

In summary, we used intracerebral recordings in humans to specify the neuro-computational mechanisms through which mood fluctuations might arise from external events and impact risky choice. At longer time scales, these mechanisms could explain why people take more gambles (or less) after incidental events such as the victory (or defeat) of their favorite sport team, an effect that might be exacerbated in pathological conditions such as during manic (or depressive) episodes. The impact of mood on choice is a form of generalization, across different sources of reward and punishment, that may be catastrophic in pathological cases, leading people to believe that because they experienced positive (or negative) outcome in some part of their life, they are likely to succeed (or fail) in any other.

5. Material & Methods

Patients and electrode implantation

Intracerebral recordings were obtained from 30 patients suffering from drug-resistant focal epilepsy (39.5 ± 1.9 years old, 14 females, see demographical details in Supplementary Table III.S1) in 7 different epilepsy centers (Rennes University Hospital: n = 10; Grenoble University Hospital: n = 9; Lyon Neurological Hospital: n = 3; Prague Motol University Hospital: n = 3; Marseille La Timone Hospital: n = 2; Toulouse University Hospital: n = 2; Nancy University Hospital: n = 1). These patients underwent intracerebral recordings by means of stereotactically implanted multilead depth electrodes (sEEG) in order to locate epileptic foci that could not be identified by non-invasive methods. Electrode implantation was performed according to routine clinical procedures and all target structures for the pre-surgical evaluation were selected strictly according to clinical considerations with no reference to the current study. Nine to twenty semi-rigid electrodes were implanted per patient. Each electrode had a diameter of 0.8 mm and, depending on the target structure, contained 6-18 contact leads of 2 mm wide and 1.5-4.1 mm apart (Dixi Medical, Besançon, France). All patients gave written, informed consent before their inclusion in the present study, which received approval from the local ethics committees (CPP 09-CHUG-12, study 0907; CPP18-001b / 2017-A03248-45; IRB00003888; CER No. 47-0913).

Intracerebral EEG recordings

Neuronal recordings were performed using video-EEG monitoring systems that allowed for simultaneous recording of 128 to 256 depth-EEG channels sampled at 512, 1024 or 2048 Hz (depending on the epilepsy center). Acquisitions were made with Micromed (Treviso, Italy) system and online band-pass filtering from 0.1 to 200 Hz in all centers, except for Prague (Two Natus systems were used: either a NicoleteOne with a 0.16-134 Hz band-pass filtering or a Quantum NeuroWorks with a 0.01-682 Hz band-pass filtering) and Marseille (Deltamed system, 0.16 Hz high-pass filtering). Data were acquired using a referential montage with reference electrode chosen in the white matter. Before analysis, all signals were re-referenced to their nearest neighbor on the same electrode, yielding a bipolar montage.

Behavioral tasks

Presentation of visual stimuli and acquisition of behavioral data were performed on a PC using custom Matlab scripts implementing the PsychToolBox libraries (Brainard, 1997). All patient

responses were done with a gamepad (Logitech F310S) using both hands. Subjects performed a choice task combined with a mood induction procedure adapted from a previous study (Vinckier et al., 2018). Subjects completed two (n = 6) or three (n = 24) sessions of the experiment, consisting of 64 trials each, for a total of 128 or 192 trials. Each trial included 3 sub-parts: a quiz task, a rest or mood assessment period and a choice task.

Quiz task. In this task, a question and four possible answers were displayed on the screen. The question was randomly selected from a set of 256 possible questions that were adapted from the French version of the "trivial pursuit" game (e.g. Where is Park Güell located?) which were slightly adapted for Prague's epilepsy center. Subjects had to select the correct answer using the up and down keys and confirm their answer using the confirmation key within a maximum of 8 seconds. A feedback of 1 second was finally given (either a smiling face with a bell sound or a grimacing face with a buzzer sound) immediately after the answer or at the end of the available time if no answer had been made.

In order to predictably manipulate subjects' mood, episodes of high and low correct response rates were created unbeknownst to them by handling questions difficulty and feedbacks. Thus, questions were sorted by difficulty (assessed by mean accuracy estimated previously in a sample of healthy subjects; Vinckier et al., 2018) and grouped so as to create easy and hard episodes. Within a given session of 64 trials, we created one episode of 20 trials with easy questions followed by one episode of 20 trials with hard questions and three episodes of 8 trials with questions of medium difficulty. The episodes were organized so that easy and hard episodes were always preceded and followed by episodes of medium difficulty (e.g., medium – easy – medium – hard – medium). The order of easy and difficult episodes was counterbalanced across sessions and subjects. Furthermore, feedback was biased such that a wrong answer could lead to a positive feedback (whereas a correct answer always led to a positive feedback). The proportion of biased feedback depended on the difficulty of the episode: 50% in easy, 25% in medium and 0% in hard episode. Post-hoc debriefing showed that no patient was aware of this manipulation.

Mood rating – rest period. Mood assessment or rest period began with a 500 ± 100ms black screen used to ensure that a reasonable delay occurred after the last quiz feedback (which lasted 1 s). In 25% of the trials (i.e., in 16 out of 64 trials), the quiz task was followed by a mood rating task in which subjects were explicitly asked to rate their mood by answering the following question "How do you feel right now?". Subjects had to answer by moving a cursor from left (very bad) to right (very good) along a continuous visual analog scale (100 steps) with left and

right hand response buttons. Subjects were given at least 4 seconds to confirm their ratings with the confirmation button. Their response was then maintained on the screen until the end of the 4 seconds, so that they had no reason to speed-up their estimation. However, subjects were also discouraged from being too long to respond, as when they had not confirmed their rating within 4 seconds, a red message was displayed on the screen saying "Please validate your answer". The initial position of the cursor on the scale was randomized to avoid confounding mood level with movements' quantity. The position of mood ratings across trials within a session was evenly distributed and pseudo-randomized so that mood ratings were not predictable for the subjects, with the additional constraints that two mood ratings were spaced by a minimum of 2 trials and a maximum of 6 trials. In the remaining 75% of trials, the quiz task was followed by a rest period consisting of a 4-second black screen. Therefore, the delay between the end of the quiz feedback and the beginning of the choice task was kept to a minimum of 4.5 ± 0.1 seconds.

Choice task. The choice task began with the presentation of an offer consisting of three dimensions: a gain prospect (represented by a bunch of 10-cent coins, range: 1-5€), a loss prospect (represented by crossed out 10-cent coins, range: 1-5€) and the upcoming challenge difficulty (represented by the size of a target window located at screen center, range: 1-5 corresponding to 75-35% theoretical success; see training section for further details about how difficulty was adjusted to each participant). Subjects were asked to accept or reject this offer, by pressing a left or right button depending on where the choice option ("yes" or "no") was displayed. Subjects' choice determined the amount of money at stake: accepting meant that they would eventually win the gain prospect or lose the loss prospect based on their performance in the upcoming challenge, whereas declining the offer meant playing the challenge for minimal stakes (winning 10 cents or losing 10 cents).

The sequence of trials was pseudo-randomized such that all possible combinations of the three dimensions (gains, losses and challenge difficulty), continuously sampled along four intervals ([1-2],]2-3],]3-4],]4-5]), were displayed for one patient across sessions, with greater sampling of medium difficulty combinations ([2-3] and]3-4]) to maximize the occurrence of undetermined choices during which small ongoing fluctuations were previously shown to bias subsequent choices (Padoa-Schioppa, 2013). The positions of gain and loss prospects were randomly determined to be either displayed on top or bottom of the screen and similarly, the choice options ("yes" or "no") were randomly displayed on the left or right.

Subjects had a free time delay to accept or decline the offer. If they declined the offer, a 500 ms screen displayed the new offer (only gains and loss prospects changed so that subjects performed the challenge for a minimal stake of 10 cents). Thus, an important feature of the choice task was that the challenge was performed regardless of the choice answer to prevent subjects to eventually reject more offers to decrease experiment duration.

The challenge started 200ms after choice confirmation: a ball appeared on the left of the screen and moved, horizontally and at constant speed, towards screen center. Subjects were asked to press the confirmation button when they thought the ball was inside the basket displayed at screen center (i.e., the target window which size index the difficulty of the challenge). To facilitate the challenge, which was performed without any feedback, the ball always reached the center of the target after 1s. Thus, the size of the target window (i.e. the difficulty of the trial) represented the margin of error tolerated in patient response time (target: 1s after the movement onset of the ball). The larger the basket, the greater the tolerated spatiotemporal error was to consider a trial as successful, and therefore the easier was the trial. Importantly, the moving ball could only be seen during the first 500ms (half of the trajectory), and subjects had to extrapolate the last 500ms portion of the ball's trajectory to assess whether the ball was inside the target. No feedback was given to subjects about their performance or payoff after the challenge to prevent learning effects and also choice feedback effects on mood. However, to improve subjects' motivation to perform the task as accurately as possible, the total amount of money earned by the subjects during a session (calculated by adding gains and losses across all trials) was displayed at the end of a session.

Training. Before the main experiment, a training - divided into three steps - familiarized subjects with all sub-parts of the task. In the first step, subjects were familiarized with the challenge by performing 28 trials with a tolerated margin of error from $\pm$ 130 to $\pm$ 80 ms (56 trials if the accuracy of the first 28 trials was below 50%). Each training trial was followed by feedback informing whether the challenge was successful ("ok" in green) or missed ("too slow" or "too fast" in red). In the second step, subjects performed 64 trials of the full choice (i.e., the challenge was always preceded by an offer), and a feedback on the money won/lost in the trial was displayed at the end of each trial. The goal was to train subjects to properly integrate the three dimensions of the offer (gains, losses and difficulty) when making their choice. To help subjects learning the correspondence between the target size and challenge difficulty, trials were displayed by increasing difficulty level. Finally, the third and last part of the training (10 trials including 2 mood

ratings) was totally similar to the main task to allow subjects to familiarize with the quiz task and the mood ratings.

Another purpose of the training was also to tailor the difficulty of the challenge to each patient's ability. To do so, a tolerated margin of error was computed for each difficulty level, ranging from 75% (level 1) to 35% (level 5) of theoretical success which we estimated from each individual subjects by assuming that errors were normally distributed. Note that during training, the difficulty levels were updated after each trial (average and standard deviation of challenge performance were updated), while in the main task, the mean and standard deviation of patient performance (and therefore difficulty levels) were set based on every challenge performed during the training. The range of tolerated margins of error between subjects ranged from [$\pm$ 72 ms (level 1) to $\pm$ 22 ms (level 5)] in the most precise patient to [$\pm$ 198 ms to $\pm$ 123 ms] in less precise one.

Computational models

Mood ratings and choices were fitted using published computational framework (Vinckier et al., 2018).

Mood model. As mood was sampled in 25% of the trials, we linearly interpolated ratings in order to get one data point per trial. In all analyses, mood ratings were z-scored. A theoretical mood level (TML) was computed for each trial through the integration of quiz feedback as follows:

$$TML(t) = \omega_0 + \omega_f \sum_{j=1}^{t} \gamma^{t-j} F(j) + \omega_t t$$

where t is the trial index, γ and all ω are free parameters (ω_0 is a constant and all other ω are weights on the different components; γ, with $0 \leq \gamma \leq 1$, is a forgetting factor that adjusts the influence of recent events relative to older ones) and F is the subjective perception of feedback. This feedback was subjective as its perception was in return biased by TML:

$$F(t) = Feedback(t) + \delta \times TML(t-1)$$

where δ is a free parameter and $TML(t-1)$ is the TML carried from previous trial, before updating based on the feedback received in the current trial. The model assumes that mood effect is additive so that good mood leads events to be seen as more positive than they objectively are (a multiplicative effect would imply that a negative feedback is perceived as even worst when

one is in a good mood) and allowed an asymmetrical influence of positive and negative events on mood, using a free parameter R (with $R > 0$) for positive feedback instead of 1:

$$Feedback(t) = R \text{ or } -1$$

This model was compared to a control model in which only time was taken into account (linear function of trial index).

Choice model. Acceptance probability was calculated as a sigmoid function (softmax) of expected utility:

$$p(accept, t) = \frac{1}{1 + e^{-(utility + k_t \times t)}}$$

where k_t is a free parameter that accounts for a linear drift with time (trial index t) in order to capture fatigue effects. The utility function is based on expected utility theory where potential gains and losses are multiplied by probability of success (p_s) vs. failure ($1 - p_s$):

$$utility = k_0 + p_s \times k_g \times gain - (1 - p_s) \times k_l \times loss$$

However, distinct weights were used for the gain and loss components (k_g and k_l respectively), and a constant k_0 was added in order to capture a possible bias. The subjective probability of success (p_s) was inferred from the target size. The model assumes that subjects have a representation of their precision following a Gaussian assumption, meaning that the subjective distribution of their performance could be defined by its mean (the required 1 second to reach target center) and its width (i.e., standard deviation) captured by a free parameter σ. Thus, the probability of success was the integral of this Gaussian bounded by the target window:

$$p_s = \frac{1}{\sigma\sqrt{2\pi}} \int_{1-Size/2}^{1+Size/2} e^{\frac{-(x-1)^2}{2\sigma^2}} dx$$

*

Both models (mood and choice models) were inverted, for each patient separately with behavioral data, using the Matlab VBA toolbox (available at https://mbb-team.github.io/VBA-toolbox/), which implements Variational Bayesian analysis under the Laplace approximation (Daunizeau et al., 2014). This algorithm not only inverts nonlinear models, but also estimates the model evidence, which represents a trade-off between accuracy (goodness of fit) and complexity (degrees of freedom; Robert, 2007).

Behavioral analysis

Statistical analyses were performed with Matlab Statistical Toolbox (Matlab R2018a, The MathWorks, Inc., USA). All dependent variables (raw or z-scored behavioral measures, regression estimates and model outputs) were analyzed at the subject level and tested for significance at the group level using two-sided, one or paired-sample, Student's t-tests. All means are reported along with the standard error of the mean.

sEEG pre-processing

Before analysis, bad channels were removed based on a supervised machine-learning model trained on a learning database with channels already classified by experts and using a set of features quantifying the signal variance, spatiotemporal correlation and non-linear properties (Tuyisenge et al., 2018). All signals were then re-referenced with a local bipolar montage between adjacent contacts of the same electrode to increase the spatial specificity of the effects by canceling out effects of distant sources that spread equally to both adjacent contacts through volume conduction. The average number of recording sites (one site corresponding to a bipolar contact-pair) recorded per patient was 116 ± 7. Finally, all signals were down-sampled to 512 Hz.

Neuroanatomy

The electrode contacts were localized and anatomically labeled using the IntrAnat Electrodes software (Deman et al., 2018), developed as a BrainVisa (Rivière et al., 2009) toolbox. Briefly, the pre-operative anatomical MRI (3D T1 contrast) and the post-operative image with the sEEG electrodes (3D T1 MRI or CT scan), obtained for each patient, were co-registered using a rigid-body transformation computed by the Statistical Parametric Mapping 12 (SPM12; Ashburner, 2009) software. The gray and white matter volumes were segmented from the pre-implantation MRI using Morphologist as included in BrainVisa. The electrode contact positions were computed in the native and MNI referential using the spatial normalization of SPM12 software. Coordinates of recording sites were then computed as the mean of the MNI coordinates of the two contacts composing the bipole. For each patient, cortical parcels were obtained for the MarsAtlas (Auzias et al., 2016) and Destrieux (Destrieux et al., 2010) anatomical atlases, while subcortical structures were generated from Fischl et al. (2002), as included in Freesurfer. Each electrode contact was assigned to the gray or white matter and to specific anatomical parcels by taking the most frequent voxel label in a sphere of 3 mm radius around each contact center.

The MarsAtlas parcellation scheme was mainly used to label each recording site. This atlas relies on a surface-based method using the identification of sulci and a set of 41 regions of interest (ROIs) per hemisphere. These regions were completed with 7 subcortical regions, obtained from the procedure described by Fischl (as included in Freesurfer; Deman et al., 2018; Fischl et al., 2002). However, based on the literature, we applied slight modifications concerning our regions of interest. First, boundaries based on MNI coordinates were set to the ventromedial prefrontal cortex (vmPFC) region so that contacts more lateral than x = ±12 and more dorsal than z = 10 were excluded from the parcel (Lopez-Persem et al., 2019). Secondly, MarsAtlas parcellation scheme involved the insular cortex as a single region, making it impossible to distinguish sub-insular areas that appear to have distinct functional properties in decision-making (Droutman et al., 2015). We therefore used the Destrieux atlas (performed by Freesurfer; Deman et al., 2018) and MNI coordinates to segment the region corresponding to the insula into 3 sub-regions: (i) the ventral anterior insula (vaIns) corresponds to the anterior part (y > 5 in MNI space) of parcels 18 (*G_insular_short*), 47 (*S_circular_insula_ant*) and 48 (*S_circular_insula_inf*) of the Destrieux atlas, (ii) the dorsal anterior insula (daIns) corresponds to the anterior part (y > 5 in MNI space) of parcel 49 (*S_circular_insula_sup*) of the Destrieux atlas, and finally (iii) the posterior insula (pINS) corresponds to the posterior part (y < 5 in MNI space) of parcels 17 (*G_Ins_lg_and_S_cent_ins*), 48 and 49 of the Destrieux atlas, leading to a total of 50 ROIs.

For statistical analyses, only the 42 ROIs with at least 10 recording sites recorded across at least four subjects were retained. Among the 3494 initial recorded sites, 3154 recording sites were located within one of these 42 regions and were therefore kept for analysis. Note that data from both hemispheres were collapsed to improve statistical power.

Extraction of frequency envelopes

The time course of broadband gamma activity (BGA) was obtained by band-pass filtering of continuous sEEG signals in multiple successive 10 Hz-wide frequency bands (i.e., 10 bands, beginning from 50-60 Hz up to 140-150 Hz) using a zero-phase shift non-causal finite impulse filter with 0.5 Hz roll-off. The envelope of each band-pass filtered signal was next computed using the standard Hilbert transform. For each frequency band, this envelope signal (i.e., time varying amplitude) was divided by its mean across the entire recording session and multiplied by 100. This yields instantaneous envelope values expressed in percentage (%) of the mean. Finally, the envelope signals computed for each consecutive frequency band were averaged together to provide a single time series (the broadband gamma envelope) across the entire session. By con-

struction, the mean value of that time series across the recording session is equal to 100. Note that computing the Hilbert envelopes in 10Hz sub-bands and normalizing them individually before averaging over the broadband interval allows to counteract a bias toward the lower frequencies of the interval induced by the 1/f drop-off in amplitude. Finally, the obtained time series were smoothed using a sliding window of 250 ms, to get rid of potential artifacts, and down-sampled at 100 Hz (i.e., one-time sample every 10 ms).

The envelopes of theta, alpha, beta and gamma bands were extracted in a similar manner as the BGA except that steps were 1 Hz for theta and alpha, 5 Hz for beta and 4 Hz for gamma. BGA frequency range was defined as 50-150 Hz, gamma as 33-49 Hz, beta as 13-33 Hz, alpha as 8-13 Hz and theta as 4-8 Hz.

Electrophysiological analyses

The frequency envelopes of each recording site were epoched at each trial from 5600 ms prior choice onset to 500 ms after choice onset, encompassing the quiz feedback, the rest period (or mood assessment) between quiz and choice tasks and the choice onset (display of the offer). Electrophysiological data were analyzed using General Linear Model (GLM), providing a regression estimate for each time point and contact.

In a first GLM aimed at identifying areas underpinning mood fluctuations, power P (normalized envelope) was regressed across trials against mood M (real mood ratings or TML, normalized within subjects) at every time point:

$$P = \alpha + \beta M + \epsilon$$

With α corresponding to the intercept, β corresponding to the regression estimate on which statistical tests are conducted and ϵ corresponding to the error term.

To investigate whether vmPFC and daIns were sensitive to a specific mood state, the same GLM was performed except that BGA of each ROI was averaged over the best cluster identified in this first GLM (from -0.57 to -0.13 s before choice onset for the vmPFC and from -3.13 to -2.72 s for the daIns) and regressed across the 35% trials with the best or worst TML.

Next, to assess whether vmPFC and daIns regions would represent separate components of mood, TML was regressed across trials against BGA of these two regions at every time point as follows:

$$TML = \alpha + \beta_1 BGA_{vmPFC} + \beta_2 BGA_{daIns} + \epsilon$$

With α corresponding to the intercept, β_1 and β_2 corresponding to the regression estimates on which statistical tests are conducted and ϵ corresponding to the error term. For each of the 18 subjects with electrodes in both ROIs, regression was done for all possible pairs of vmPFC and daIns recording sites recorded within a given patient, leading to a total of n = 247 pairs of recording sites.

To check that TML was expressed above and beyond the variance induced by the last feedback, BGA was regressed across trials t against last feedback along with TML from the previous trial at every time point:

$$BGA(t) = \alpha + \beta_1 Feedback(t) + \beta_2 TML(t-1) + \epsilon$$

Where α corresponds to the intercept, β_1 and β_2 correspond to the regression estimates on which statistical tests are conducted and ϵ corresponds to the error term.

Next, to assess the effect of pre-choice brain activity on acceptance rate, the residual error of choice model fit C was regressed across trials against power P (normalized envelope) at every time point as follows:

$$C = \alpha + \beta P + \epsilon$$

With α corresponding to the intercept, β corresponding to the regression estimate on which statistical tests are conducted and ϵ corresponding to the error term.

Finally, to assess how baseline activity affects choice, the frequency envelopes of each recording site were epoched at each trial from 2000 ms prior choice response to 500 ms after choice response, and trials were split into "high" or "low" baseline activity based on the average pre-choice BGA in the best cluster identified in the GLM used to investigate effect of pre-choice brain activity on acceptance rate (from -1.64 to -1.31 s before choice onset for the vmPFC and from -0.95 to -0.67 s for the daIns). Choices were then regressed across the 40% highest or lowest baseline activity trials against BGA at every time point, as in the previous GLM. To ensure that baseline activity does not interfere with the reported effect, trials with a choice response time shorter than 1.5 up to 2 secs were eliminated from this analysis. Note that the RT threshold (from 1.5 to 2s) did not affect the result. We reported results from the analysis removing trials with a response time shorter than 1.6 seconds (longest response time removing less than 25% of trials).

For all GLMs, the statistical significance of each recording site was assessed through permutation tests. The pairing between responses and predictors across trials was shuffled randomly 300 times for each site. The maximal cluster-level statistics (the maximal sum of t-values across contiguous time points passing a significance threshold of 0.05) were extracted for each shuffle to compute a 'null' distribution of effect size across a time window of -4 to 0 s before choice onset (the baseline corresponding to the rest or mood assessment period). The p-value of each cluster in the original (non-shuffled) data was finally obtained by computing the proportion of clusters with higher statistics in the null distribution, and reported as the 'cluster-level corrected' p-value (p_{corr}).

For each ROI, a t-value was computed across all recording sites of the given ROI for each time point of the baseline (-4 to 0 s before choice onset), independently of patient identity, using two-sided, one-sample, Student's t-tests. The statistical significance of effects within each ROI was then assessed with permutation tests, as described above, except that the null distribution was computed from 60,000 random combinations of all contacts of a ROI, drawn from the 300 shuffles previously calculated for each site.

Contribution of frequency bands

To assess the contribution of the different frequency bands to mood representation, TML was regressed across trials against power P (normalized envelope) of each frequency band, averaged over time between -4 to 0 s before choice onset:

$$TML = \alpha + \beta P + \epsilon$$

With α corresponding to the intercept and ϵ to the error term. The significance of the regression estimates β was assessed across recording sites using two-sided, one-sample, Student's t-tests.

In order to determine whether other frequency bands provided additional information relative to the BGA, the following sixteen GLMs were compared:

$$TML = \beta_{BGA} \times BGA$$
$$TML = \beta_{BGA} \times BGA + \beta_{\gamma} \times P(\gamma)$$
$$TML = \beta_{BGA} \times BGA + \beta_{\beta} \times P(\beta)$$
$$TML = \beta_{BGA} \times BGA + \beta_{\alpha} \times P(\alpha)$$
$$TML = \beta_{BGA} \times BGA + \beta_{\theta} \times P(\theta)$$
$$TML = \beta_{BGA} \times BGA + \beta_{\gamma} \times P(\gamma) + \beta_{\beta} \times P(\beta)$$
$$TML = \beta_{BGA} \times BGA + \beta_{\gamma} \times P(\gamma) + \beta_{\alpha} \times P(\alpha)$$

$$TML = \beta_{BGA} \times BGA + \beta_{\gamma} \times P(\gamma) + \beta_{\theta} \times P(\theta)$$
$$TML = \beta_{BGA} \times BGA + \beta_{\beta} \times P(\beta) + \beta_{\alpha} \times P(\alpha)$$
$$TML = \beta_{BGA} \times BGA + \beta_{\beta} \times P(\beta) + \beta_{\theta} \times P(\theta)$$
$$TML = \beta_{BGA} \times BGA + \beta_{\alpha} \times P(\alpha) + \beta_{\theta} \times P(\theta)$$
$$TML = \beta_{BGA} \times BGA + \beta_{\gamma} \times P(\gamma) + \beta_{\beta} \times P(\beta) + \beta_{\alpha} \times P(\alpha)$$
$$TML = \beta_{BGA} \times BGA + \beta_{\gamma} \times P(\gamma) + \beta_{\beta} \times P(\beta) + \beta_{\theta} \times P(\theta)$$
$$TML = \beta_{BGA} \times BGA + \beta_{\gamma} \times P(\gamma) + \beta_{\alpha} \times P(\alpha) + \beta_{\theta} \times P(\theta)$$
$$TML = \beta_{BGA} \times BGA + \beta_{\beta} \times P(\beta) + \beta_{\alpha} \times P(\alpha) + \beta_{\theta} \times P(\theta)$$
$$TML = \beta_{BGA} \times BGA + \beta_{\gamma} \times P(\gamma) + \beta_{\beta} \times P(\beta) + \beta_{\alpha} \times P(\alpha) + \beta_{\theta} \times P(\theta)$$

With β corresponding to the regression estimates, and P each power time series averaged between -4 to 0 s before choice onset in the high-gamma (BGA), gamma (γ), beta (β), alpha (α) and theta (θ) frequency bands.

The model comparison was conducted using the VBA toolbox (Daunizeau et al., 2014). Log-model evidence obtained in each recording site was taken to a group-level, random-effect, Bayesian model selection (RFX-BMS) procedure (Rigoux et al., 2014). RFX-BMS provides an exceedance probability that measures how likely it is that a given model is more frequently implemented, relative to all the others considered in the model space, in the population from which samples were drawn.

Computational analysis of baseline activity effect on choices

For each electrode of a given ROI, BGA was averaged in each trial over the window corresponding to the best significant cluster obtained with our second GLM (regression of residual error of choice model fit against power). More specifically, activity was averaged from -1.64 to -1.31 s before choice onset for the vmPFC and from -0.95 to -0.67 s for the daIns. The choice model was then run separately with data from trials whose averaged activity was above or below the median baseline activity across trials. As we expected small effects, data were restricted to trials that were not overly determined by choice parameters (i.e., trials for which acceptance probability, as computed by the choice model with all trials, was between 2/7 and 5/7 of the patient's acceptance range). We also ensured that the mean and variance of choice dimensions (gain, loss and difficulty) were identical between our two trial subsets (high vs. low baseline BGA). All free parameters of the expected utility were free to fluctuate (the constant k_0, gain weight k_g, loss weight k_l and the weight associated with difficulty σ), while k_t was set with values obtained from the previously computed model (with all trials). Finally, significance of the difference be-

tween posterior parameters obtained with the two trial subsets (high versus low activity) was tested across all contacts of a given region using two-sided, paired, Student's t-tests.

Data and code availability

Raw data cannot be shared due to ethics committee restrictions. Intermediate as well as final processed data that support the findings of this study are available from the corresponding author (JB) upon reasonable request. The custom codes used to generate the figures and statistics are available from the lead contact (JB) upon request.

Acknowledgments

This work benefited from the program from University Grenoble Alpes, within the program "Investissements d'Avenir" (ANR-17-CE37-0018; ANR-18-CE28-0016; ANR-13-TECS-0013). JH and PM were funded GACR (grant number 20-21339S). The funders had no role in study design, data collection and analysis, decision to publish or preparation of the manuscript.

Author Contributions

RC, FV, MP and JB designed the experiment. RC collected the data. FV provided pre-processing scripts. RC performed the data analysis. JH, PM, AT, NA, PK, EB, MD, LM, LM and SR did the intracerebral investigation and allowed the collection of iEEG data. RC, MP and JB wrote the manuscript. All the authors discussed the results and commented on the manuscript.

Declaration of Interests

The authors declare no competing interests.

6. Supplementary material

Supplementary Table III.S1: Demographical data. M: male; F: female; L: left; R: right; A: ambidextrous; vmPFC: ventromedial prefrontal cortex; daIns: dorsal anterior insula

ID	Sex	Age (years)	Epilepsy onset (age)	Suspected epileptic focus	Hand laterality	Number of electrodes	Number of recording sites	Number of recorded bipoles	Number of bipoles in vmPFC	Number of bipoles in daIns
G1	M	46	23	Right insulo-opercular / Left opercular	L	17	122	85	0	2
G2	M	38	15	Left precentral / Premotor	L	17	122	88	0	1
G3	M	43	7	Right temporal	R	17	122	83	6	3
G4	F	38	3	Bilateral extensive	R	18	122	77	0	2
G5	F	35	4	Several territories	R	16	122	92	6	1
G6	F	45	10	Bi-temporal / Amygdala nucleus	R	17	122	84	6	6
G7	F	46	41	Right temporal	R	13	122	100	4	2
G8	F	43	2	Right insulo-opercular	R	16	122	92	0	3
G9	M	45	41	Left mesio-temporal	R	17	122	90	2	4
L1	F	33	7	Left insulo-opercular / Left amygdala	R	13	137	123	2	4
L2	M	56	36	Left mesio-temporal	R	13	141	127	2	3
L3	F	38	27	Right mesio-temporal	R	9	89	79	2	0
M1	M	56	35	Left temporal	R	14	183	168	0	3
M2	M	34	4	Temporo-frontal bilateral	R	20	253	228	0	13
N1	M	42	6	Left fronto-opercular	R	11	106	93	0	2
P1	M	23	15	Right frontal	R	14	212	86	9	4
P2	M	33	16	Left temporal	R	15	126	93	0	1
P3	F	46	28	Right temporal	R	12	151	136	2	6
R1	M	45	10	Bilateral extensive	R	13	126	112	3	2
R2	F	21	2	Right cingulate gyrus	R	13	166	152	7	3
R3	M	39	30	Right temporal	R	13	183	169	6	4
R4	F	23	20	Right temporo-insulo-perisylvian	A	11	125	113	0	3
R5	F	47	28	Hippocampal sclerosis / Right temporal	R	10	107	96	0	2
R6	M	17	9	Left temporo-insulo-frontal multifocal	R	14	174	159	4	2
R7	F	39	8	Upper posterior frontal gyrus	R	11	126	114	4	2
R8	M	46	33	Orbitofrontal / Right anterior temporal	R	15	195	179	6	1
R9	F	39	26	Right medial temporal	R	11	124	112	4	2
R10	M	21	6	Limbic cingulate	A	13	168	154	6	3
T1	F	49	33	Right anterior temporal	R	13	122	106	5	2
T2	M	58	40	Left fronto-temporal / Left fronto-mesial	R	14	127	104	5	0

Supplementary Table III.S2: ROIs associated with both mood levels and residual error of choice. Areas are ordered according to the maximal absolute t-value obtained by averaging best clusters in the three following regression: BGA against mood ratings, BGA against trial-wise mood estimates from the model (TML) and residual error of choice against BGA. Pos: ROI positively associated with mood levels and residual error of choice; Neg: ROIs negatively associated with mood levels and residual error of choice. P-values were obtained with two-sided, one-sample, Student's t-tests cluster-wise corrected ($p_{corr} < 0.05$). vmPFC: ventromedial prefrontal cortex; Mdm: dorsomedial motor cortex; daIns: dorsal anterior insula; IPCv: ventral inferior parietal cortex; VCrm: rostral medial visual cortex

		Mood ratings			TML			Residual error of choice		
	ROI	Best cluster duration (s)	Sum t-value	p-value	Best cluster duration (s)	Sum t-value	p-value	Best cluster duration (s)	Sum t-value	p-value
Pos.	**PFCvm**	**0,33**	**122,26**	**0,01**	**0,44**	**132,44**	**8.10^{-3}**	**0,33**	**91,2**	**0,02**
Neg.	Mdm	0,58	-153,92	7.10^{-3}	4	-2182,56	$1.7.10^{-5}$	0,46	-114,91	0,013
	daIns	**0,85**	**-325,84**	**$1.7.10^{-5}$**	**0,41**	**-136,38**	**9.10^{-3}**	**0,28**	**-85,17**	**0,029**
	IPCv	0,66	-214,19	3.10^{-4}	0,66	-166,58	4.10^{-3}	0,37	-107,48	0,013
	VCrm	0,37	-115,37	0,022	0,28	-118,65	0,025	0,44	-111,13	0,016

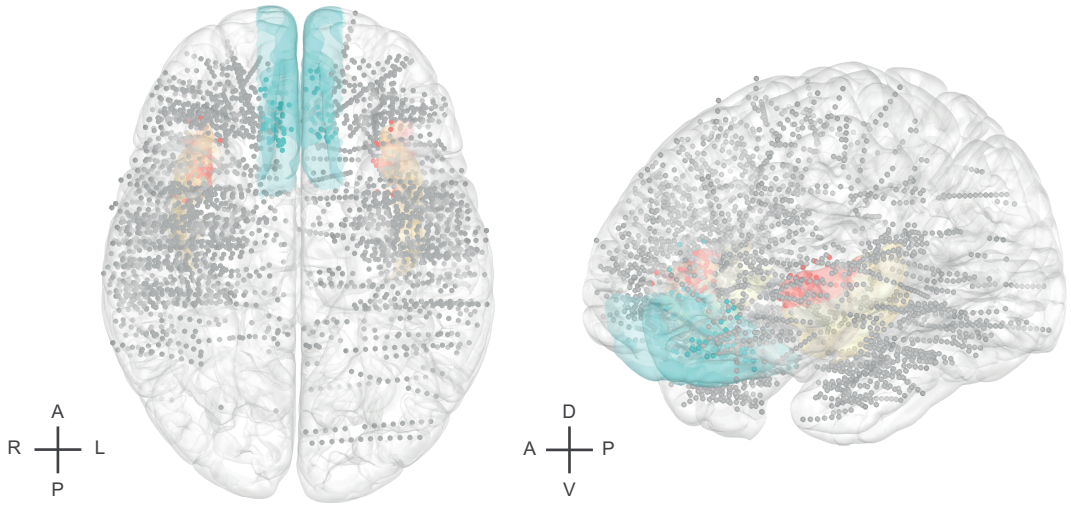

Supplementary Figure III.S1: Anatomical location of all recording sites (n = 3188 sites acquired from 30 epileptic patients) in the standard Montreal Neurological Institute template brain. Colored brain regions represent the vmPFC (blue) and the daINS (red), and colored dots recording sites located in these region. The whole insula is shown in yellow as reference. Each dot (1 x 1 mm^2) represents one recording site (that is, a bipole). Anterior (A), posterior (P), dorsal (D), ventral (V), left (L) and right (R) directions are indicated.

IV

An intracranial study of gaze-dependent value signals predicting multi-attribute choices

Romane Cecchi[1,†], Clarissa Baratin[1,†], Jiri Hammer[2], Petr Marusic[2], Nica Anca[3], Sylvain Rheims[4], Agnès Trebuchon[5], Louis Maillard[6], Lorella Minotti[1,7], Philippe Kahane[1,7], Mathias Pessiglione[8,9,†], Julien Bastin[1,†]

[1] Univ. Grenoble Alpes, Inserm, U1216, CHU Grenoble Alpes, Grenoble Institut Neurosciences, 38000 Grenoble, France
[2] Neurology Department, 2nd Faculty of Medicine, Charles University, Motol University Hos-pital, Prague, Czech Republic
[3] Neurology Department, University Hospital of Rennes, Rennes, France
[4] Functional Neurology and Epileptology Department, Hospices Civils de Lyon and Université de Lyon, Lyon, France
[5] Epileptology Department, Timone Hospital, Public Assistance Hospitals of Marseille, Marseille, France
[6] Neurology Department, University Hospital of Nancy, Nancy, France
[7] Neurology Department, University Hospital of Grenoble, Grenoble, France
[8] Motivation, Brain and Behavior (MBB) team, Paris Brain Institute, Pitié-Salpêtrière Hospi-tal, Paris, France
[9] Université de Paris, Paris, France
[†] These authors contributed equally to this work

In preparation

1. Abstract

Most of our choices rely on the weighting of multiple attribute (e.g., choosing between two meals) which are influenced by attentional processes. Yet, the neuro-anatomical substrates of such processes remain unresolved. Here, we investigated how visual fixations bias human multi-attribute choice behavior. Intracerebral EEG data were collected simultaneously with gaze data in a large group of participants (n = 38), while they were performing an accept/reject multi-attribute choice task. Neural activity (broadband gamma activity, 50-150 Hz) measured during visual fixations on option attributes before the choice onset was confronted to the weighting of option attributes. Results showed that 1) gaze-dependent neural activity correlated positively with a given option attribute value when fixated and negatively with the dimension's value when unfixated in a large brain network, 2) gaze-dependent neural activity in the ventromedial prefrontal cortex (vmPFC) was positively predictive of subject's choices when they looked at gains 3) gaze-dependent neural activity in the anterior insula (aIns) was negatively predictive of subject's choices when they looked at losses. Thus, our findings specify key neuro-anatomical insights into how gaze pattern interferes with neural activity to bias multi-attribute choices.

Keywords

Visual attention, decision-making, risk, electrophysiology, oscillatory activity, broadband gamma, ventromedial prefrontal cortex, anterior insula

2. Introduction

When confronted with a choice involving visible items, such as which pastry to buy in a bakery, shifting our gaze between options is an instinctive precursory step to choosing. Recently, much effort has been dedicated to understanding the role these fixations may have in the decision-making process. An emerging consensus from behavioral studies states that gaze allocation is related to choices made, with the likelihood of choosing a stimulus correlating positively with the amount of time spent looking at it (Armel et al., 2008; Callaway et al., 2021; Fiedler & Glöckner, 2012; Gidlöf et al., 2017; Krajbich & Rangel, 2011; Krajbich et al., 2010; Shimojo et al., 2003; Smith & Krajbich, 2018). This effect, referred to as the gaze time choice bias, would not solely be due to more salient or higher value options attracting visual attention (Shimojo et al., 2003; Stewart et al., 2016; Towal et al., 2013; Vaidya & Fellows, 2015a); instead, information gathered through fixations would bias choices.

Computational models have attempted to provide a mechanistic account of this process, and many of these models are extensions of the drift diffusion model (DDM), which traditionally postulates that making a choice between two options relies on value-based evidence accumulating over time for each option, until a predefined decision threshold is reached for one of them (Ratcliff, 1978; Ratcliff et al., 2016). In contrast, *gaze-driven (attentional)* evidence accumulation models further assume that fixating an option amplifies its value relative to the other, biasing evidence accumulation in its favor (Cavanagh et al., 2014; Krajbich & Rangel, 2011; Krajbich et al., 2010; Smith & Krajbich, 2018; Thomas et al., 2021; Thomas et al., 2019). From a computational behavioral standpoint, the choice bias would therefore rely on a dynamic interaction between fixations and option values.

At the neural level, research has therefore focused on identifying brain regions that would encode both gaze and value signals. In primates, single-cell recording studies have reported attention-modulated representations of values in the orbitofrontal cortex (OFC; Hunt et al., 2018; McGinty, 2019; McGinty et al., 2016; Xie et al., 2018), a brain area priorly found to encode option values during the decision-making process (Padoa-Schioppa & Assad, 2006; Raghuraman & Padoa-Schioppa, 2014; Setogawa et al., 2019; Wallis & Miller, 2003). In humans, an fMRI study using a binary choice task and exogenously-manipulated fixations observed that activity in the ventromedial prefrontal cortex (vmPFC) correlated positively with the value of the fixated item and negatively with the value of the unfixated item (Lim et al., 2011). Considering the key role of the vmPFC in the computation of value reported in a series of fMRI studies (Bartra et al., 2013; Clithero & Rangel, 2014; Lebreton et al., 2009), comparable to that of the

OFC in primates, its identification as a site of gaze interaction is unsurprising. Interestingly though, the authors go on to demonstrate that recorded fixation-dependent values signals are independent from choices made (Lim et al., 2011), thereby raising the question of a causal effect of fixation-modulated value signals on choice behavior. This issue has since been reiterated in a Pavlovian primate study, which observed that neural OFC activity did not statistically mediate the relationship between gaze and conditioned licking responses (McGinty, 2019), and in a human lesion study, which found that damage to the vmPFC did not affect the bias of fixations on choices, while damage to the dmPFC did (Vaidya & Fellows, 2015a).

Thus, despite identifying gaze-modulated value signals in neural activity and providing computational frameworks through which these signals could affect behavior, previous research has left important questions unanswered. First, due to the limited spatial and temporal accuracy of fMRI, the exploration of free-viewing fixations in relation to human neural activity has been severely hindered; therefore, little is known about their encoding in the brain and subsequent effect on choices. Although single-cell recordings have provided suggestions, the technique is limited by its specie-specificity and limited brain coverage which is often limited to a single brain region (but see Hunt et al., 2018). Another limitation is that although humans are regularly confronted with decisions involving the integration of several option attributes, the neuro-computational mechanisms underlying the effect of visual attention on multi-attribute choices is unknown.

Here, we recorded neural activity using intra-electroencephalography (iEEG) along with eye-tracking data, while human subjects performed a multi-attribute accept/reject decision-making task. This combination of techniques allowed us to examine, at a neural level and millisecond timescale, how free-viewing fixations throughout the choice process interact with differential value encoding in the human brain (across many cortical areas) and how choices may in turn be affected.

We hypothesized that visual fixations would interact with gain and loss dimension values analogously to option values in multi-alternative choice tasks such that fixating appetitive attribute (e.g., a monetary gain prospect) would increase the relative decision value signal and thus increase acceptance rates. In contrast, fixating the aversive option attribute (e.g., the monetary loss prospect) would decrease the relative decision value and thus increase rejection rates. Indeed, in contrast to appetitive items, aversive items tend to be chosen less frequently when fixated for a longer period of time (Armel et al., 2008; Fisher, 2017). From a neural standpoint, we hypothesized that dissociable brain regions might encode the appetitive vs. aversive attribute value in a

gaze-dependent frame, with the vmPFC encoding appetitive value signals (Lopez-Persem et al., 2020) and the anterior insula would encode the value of aversive option attributes (Gueguen et al., 2021).

3. Results

Task and choice behavior

Intracerebral electroencephalographic (iEEG) data were collected along with eye-tracking data in thirty-eight patients suffering from refractory epilepsy (35.6 ± 1.8 years old, 18 females) while they performed a choice task (Fig. IV.1a). In this task, participants had to decide whether to accept or reject a given offer before performing a challenge consisting in stopping a moving ball inside a target (Cecchi et al., 2021). The offer comprised of a gain prospect (i.e., the amount of money they would win in case of success), a loss prospect (i.e., the amount of loss in case of failure) and the difficulty of the upcoming challenge (target size). When accepting the offer, subjects played for the proposed amounts of money, otherwise, when declining, they played for minimal stakes (winning or losing 10 cents). All three offer attributes (gain, loss and difficulty) were varied on a trial-by-trial basis. Fixations recorded during the choice task were classified according to their proximity to five regions of interest corresponding to what was displayed on the screen (gains, losses, difficulty, yes and no responses; Fig. IV.1b).

We assessed subject performance by checking that the three attributes of the offer (gain prospect, loss prospect and challenge difficulty) were integrated into choices made (Fig. IV.1c), using a logistic mixed-effects regression model (see Methods). As expected, choice acceptance rate significantly increased with gain ($\beta_{gain} = 0.11 \pm 0.01, t_{6524} = 9.23, p < 1.10^{-15}$), but significantly decreased with loss ($\beta_{loss} = -0.09 \pm 0.01, t_{6524} = -7.19, p = 7.10^{-13}$) and difficulty ($\beta_{diff} = -0.05 \pm 0.01, t_{6524} = -4.68, p = 3.10^{-6}$). Confirmation that participants accounted for all three dimensions in their choices was further demonstrated by fitting a utility-based choice model and computing acceptance probability as a function of subjective utility (Fig. IV.1c). Subjective utility combines all three choice dimensions into a measure of how beneficial the trial is to the subject; it was calculated as the potential gain multiplied by probability of success (p_s, inferred from target size), minus the potential loss multiplied by the probability of failure ($1 - p_s$).

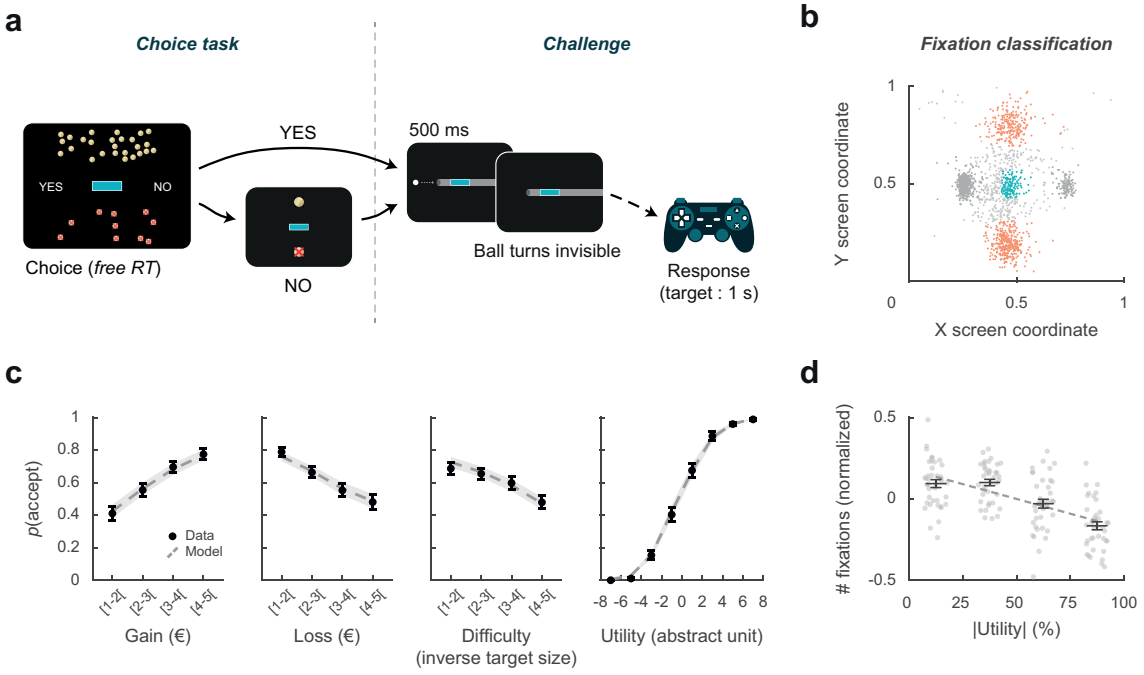

Figure IV.1: Behavioral task and results. (a) Trial structure. Each trial consisted of a choice task followed by a challenge. In the choice task, subjects had to decide whether to accept or reject a given offer by taking into account gain prospects (represented by a bunch of regular 10-cent coins), loss prospects (crossed out 10-cent coins) and difficulty (inversely proportional to the size of the blue bar in the middle of the screen). The challenge consisted in stopping a moving ball, invisible when entering the grey tunnel, inside the blue target. (b) Fixation classification. Sample eye fixation data from a representative individual classified according to five regions of interest: the gain and loss areas (orange, top and bottom of the screen), the difficulty area (blue, center of the screen), and the YES/NO response areas (dark gray, left and right of the screen). The light gray dots indicate fixations classified outside of on-screen ROIs. (c) Choice behavior. Acceptance probability is plotted as a function of the three objective dimensions (gain, loss, difficulty) and modeled subjective utility of the proposed challenge. Circles are binned data averaged across subjects. Dotted lines represent acceptance probability as computed by the choice model. Error bars and shaded areas represent the inter-subject S.E.M of the data and model, respectively. (d) Number of fixations in a trial as a function of the absolute value of expected utility (i.e. how easy the choice is to make). Grey dots represent individual data averaged per percentile group, horizontal lines represent means and error bars ± S.E.M across subjects. The dotted line represents a linear fit through plotted data.

Visual fixations bias multi-attribute choices

We first checked whether the number of fixations towards gain and loss decreased with the absolute value of expected utility (i.e., how easy the choice is to make; Fig. IV.1d), as would be predicted by the attentional drift-diffusion model (aDDM; Krajbich et al., 2010). A negative association was indeed observed (mixed-effects regression: $\beta = -0.12 \pm 0.02, t_{6204} = -7.02, p = 2.10^{-12}$), meaning that an increased number of fixations were made towards gain and loss during harder choices that were also characterized by longer deliberation times (RTs). Next, to explore how visual fixation behavior influenced choices, we focused on the two option attributes which explained choice variance the most (i.e., the monetary prospects), and for which we predicted dissociable neural activities given the results of previous studies using a similar paradigm (Cecchi et al., 2021; Vinckier et al., 2018).

We then tested two core behavioral predictions of visual fixation effects on value-based choices. First, the *gaze time choice bias*, through which additional time spent fixating an option relative to the other correlates with an increased probability of choosing it, was examined using a measure of time advantage towards the gain prospect (i.e, the percentage of trial time spent looking at gain relative to loss prospects; Fig. IV.2a). A mixed-effects regression, revealed that longer overall gaze times towards gain relative to loss did indeed predict a significant increase in acceptance rate ($\beta_{timeAdvG} = 0.01 \pm 0.004, t_{5572} = 2.52, p = 0.02$) on the top of each attribute values which were included in the regression model.

A second bias of particular interest is the *last-fixated option bias*, according to which gazing at an alternative last correlates with an increased probability of choosing it (Callaway et al., 2021; Krajbich & Rangel, 2011; Krajbich et al., 2010). Figure IV.2b illustrates psychometric fits as a function of the value difference between gain and loss for two groups of trials: trials in which, out of all fixations to gain/loss, gain was fixated last, and trials in which, out of all fixations to gain/loss, loss was fixated last. The comparison of individual points of subjective equality (Fig. IV.2b), showed a significant gaze-dependent shift of choice curves ($t_{26} = -3.12, p = 4.10^{-3}$; paired sample t-test; note that point of subjective equality (PSE) could be estimated for n = 27 out of 38 patients, see Methods). Consistent with a last-fixated option bias, this result indicates that, in hard trials (i.e, p(accept) close to 0.5), fixating gain last results in an increased chance of accepting. Both the gaze time and last-fixated option choice biases present in multi-alternative tasks, which are also main predictions of the aDDM (Krajbich et al., 2010), are therefore observable using the gain/loss dimensions of our accept/reject multidimensional task.

Intracerebral recordings

The iEEG dataset included a total of 4381 recording sites (bipolar montage, see Methods) acquired from 38 patients. For each patient, recording sites were localized within the native anatomical brain scan and anatomically labeled according to either MarsAtlas (Auzias et al., 2016), Destrieux (Destrieux et al., 2010) or Fischl (Fischl et al., 2002) parcellation schemes (see Methods). Out of the 4381 recording sites, we finally retained n = 3994 recording sites located within 43 region of interest (ROIs) with at least 10 recording sites recorded across at least five subjects (see Methods). We focused on broadband gamma activity (50-150 Hz, BGA), as converging lines of evidence showed that BGA correlates positively with both fMRI and spiking activity (Lachaux et al., 2007; Manning et al., 2009; Mukamel, 2005; Niessing et al., 2005; Nir et al., 2007; Winawer et al., 2013) and because in three previous studies we demonstrate that neu-

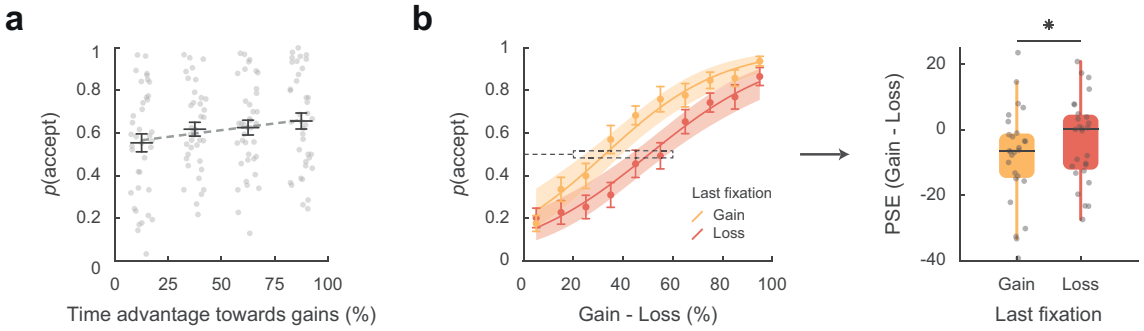

Figure IV.2: Gaze time and last-fixated-option choice biases. (a) Acceptance probability as a function of the amount of time spent looking at gain more than loss per trial. Dots represent individual data binned by percentile, horizontal lines represent means across subjects and error bars represent S.E.M across subjects. (b) Psychometric fits of acceptance probability as a function of value difference between gain and loss, by last fixation location. Filled circles represent data binned per percentile and averaged across subjects, and error bars represent inter-subject S.E.M. The horizontal line denotes the group-level point of subjective equality (PSE). Individual PSEs (grey dots) are compared on the right. Boxplots illustrate PSE distributions and the star indicates significance (paired t-test; $p < 0.05$).

ral activity estimated from lower frequencies was redundant with BGA, at least in the brain network involved during value-based learning and choices (Cecchi et al., 2021; Gueguen et al., 2021; Lopez-Persem et al., 2020).

Intracerebral evidence of gaze-dependent effects on attribute values

In order to analyze BGA in relation to eye fixations and monetary prospect values (i.e., gain vs. loss), we first segmented the BGA time series according to fixations (Fig. IV.3b), then estimated a single measure of BGA power per trial, choice option attribute (and we repeated this procedure for each iEEG-contact within each ROI). Specifically, for each dimension, *fixation-dependent BGA* was computed as a weighted sum of fixation-averaged BGA power by normalized fixation length, such that longer and additional fixations toward a given attribute increased fixation-dependent BGA magnitude. The same procedure was applied to obtain a measure of BGA while not looking at the dimension. We next tested for each ROI and offer attribute, whether gaze-dependent BGA encoded the value of the fixated or unfixated attribute. We used linear mixed-effects regression models, which included subjects and electrodes as random effects (see Methods). Brain regions whose activity was reliably modulated by visual attention were defined as such if their correlations with the value of a given attribute changed sign when fixated and unfixated. Interestingly, all regions corresponding to this criterion correlated positively with a dimension's value when fixated and negatively with the dimension's value when unfixated; no regions demonstrated the opposite pattern (i.e, negatively encoding a fixated value and positively encoding an unfixated one).

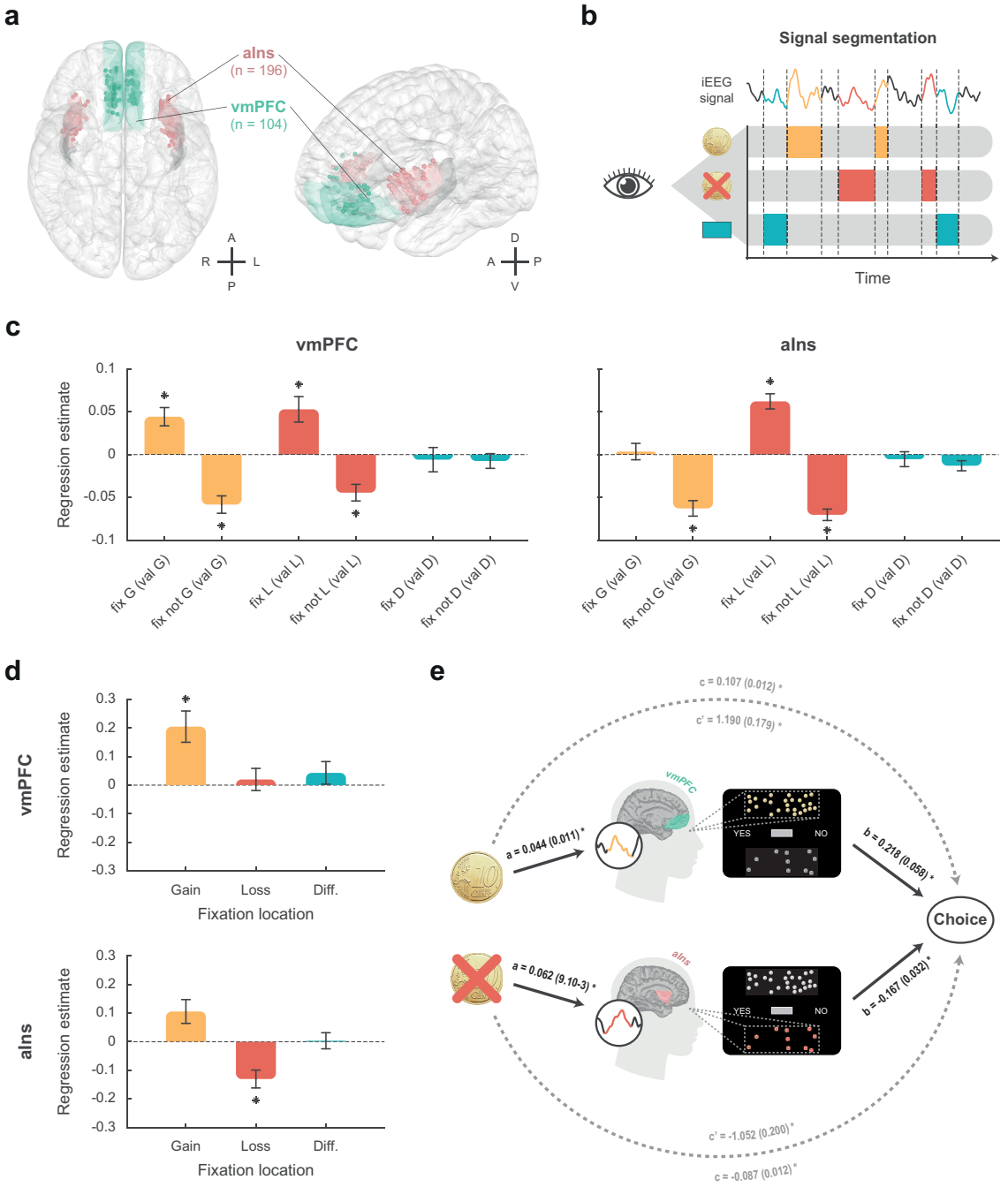

Figure IV.3: Intracerebral activity underpinning the effects of fixation on choices. (a) Anatomical location of the vmPFC (green) and daIns (pink) in the standard Montreal Neurological Institute template brain, along with all recording sites located in these areas (dots) and the entire insula (in dark grey). Anterior (A), posterior (P), dorsal (D), ventral (V), left (L) and right (R) directions are indicated. (b) Segmentation of intracerebral signal according to fixation location. For each trial and dimension, a relative power was computed by summing the activity of all fixations after it was individually averaged and normalized to the choice reaction time. (c) Value encoding according to gaze location. Plots show the estimates obtained from the regression of fixation-dependent BGA against each dimension value in vmPFC (left) and aIns (right). (d) Fixation-dependent activity predicting choices independently of the value of the fixated dimension. Plots show the estimates obtained from the regression of choices against fixation-dependent BGA in vmPFC (top) and aIns (bottom). In panels c-d, bars represent estimated coefficient value and error bars its standard error. (e) Brain-behavior mediation analysis for vmPFC and aIns. The activity of vmPFC during gain fixation mediates the positive effect of gains on acceptance probability, whereas aIns activity during loss fixation mediates the negative effect of losses on willingness to accept. The paths are labeled with path coefficients and standard errors are shown in parentheses. Stars indicate significance ($p_{corr} < 0.05$).

Results showed that the gain value signal was modulated by gaze in a large brain network including most of ROIs within the prefrontal cortex, including the vmPFC ($\beta_{\text{G (fix G)}} = 0.04 \pm 0.01$, $t_{13449} = 4.15, p = 3.10^{-5}$; $\beta_{\text{G (fix not G)}} = -0.06 \pm 0.01, t_{15728} = -5.76, p = 9.10^{-9}$; Fig. IV.3c), as well as the lateral temporal lobe (Supplementary Table IV.S1). The loss value signal was also modulated by visual fixations in the vmPFC ($\beta_{\text{L (fix L)}} = 0.05 \pm 0.01, t_{13449} = 3.55, p = 4.10^{-4}$; $\beta_{\text{L (fix not L)}} = -0.04 \pm 0.01, t_{16040} = -4.58, p = 5.10^{-6}$), as well as several ROIs in the temporal lobe and the insula, encompassing the aIns ($\beta_{\text{L (fix L)}} = 0.06 \pm 0.01, t_{24316} = 7.02, p = 2.10^{-12}$; $\beta_{\text{L (fix not L)}} = -0.07 \pm 0.01, t_{30805} = -10.55, p < 1.10^{-15}$; Fig. IV.3c and Supplementary Table IV.S1). In the case of difficulty, no ROI was found to encode a value signal modulated by visual fixations.

Interestingly, none of the choice dimensions were found to correlate with brain activity in our two a priori ROIs when analyzing BGA across trials without prior segregation by fixations, thereby indicating that monetary prospect value encoding occurred during fixations.

Fixation-dependent neural activity mediates the impact of attribute value on choice

Finally, we investigated the contribution of fixation-dependent activity on choices, using a brain-behavior mediation analysis (see Methods). In brief, the value of each monetary prospect served as a predictor, choices served as the outcome and fixation-dependent BGA was included as a mediator. Path a described change in fixation-dependent BGA based on choice dimension value (Fig. IV.3c) which was estimated using the previously described General Linear Models (GLMs; see Methods). Path b characterized fixation-dependent activity that predicts choices independently of the value of the fixated dimension (Fig. IV.3d). It was estimated by regressing choices against the fixation-dependent BGA of all three dimensions, using a logistic mixed-effects regression model which further included dimension values as fixed effect as well as subjects and electrodes as random effects (see Methods). Paths c' and c correspond to the effect of choice dimension value on acceptance probability with or without taking into account the effect of fixation-dependent BGA, respectively. Statistical testing of mediation was performed using the conjunctive approach (Brochard & Daunizeau, 2020), which relies on the "maximum p-value" (i.e. the mediated effect is significant if both paths a and b are significant). Independent mediation analyses are reported for gain and loss dimensions. For the gain dimension, we found that fixation-dependent activity in the vmPFC (path b: $\beta_{\text{fix G}} = 0.22 \pm 0.06, t_{8400} = 3.74, p = 2.10^{-4}$; Fig. IV.3e) and middle temporal cortex positively mediated the influence of gains value on choices (Supplementary Table IV.S2). Conversely, for losses, the fixation-dependent activ-

ity in the insula, including the anterior (path b: $\beta_{\text{fix L}} = -0.17 \pm 0.03, t_{15257} = -5.21, p = 2.10^{-7}$; Fig. IV.3e) and posterior insula, and the rostral middle temporal cortex were found to negatively mediate the influence of losses on choices (Supplementary Table IV.S2).

4. Discussion

We investigated the role of visual fixations on neural activity and subsequent multi-attribute choices using a combination of eye-tracking and iEEG. Results demonstrate that dissociable intracortical correlates of the effects of visual fixations on specific option attributes which mediate the effect of gaze on behavioral choices, providing the first direct neurophysiological evidence consistent with a mechanisms of value-based accumulation process during multi-attribute choices.

Behavior

Behavioral results replicated two choice biases consistently observed in previous studies, namely the gaze time choice bias and last-fixated option bias. In line with our hypotheses, a longer fixating time towards gain relative to loss was associated with an increased probability of accepting the offer, and vice-versa, even when controlling for dimension value. Additionally, fixating gain last was associated with an increased probability of accepting, while fixating loss last was associated with an increased probability of rejecting. The multi-attribute choice design here used therefore allows us to extend current knowledge of fixations biasing choices towards the fixated item to more complex options, in which potential loss is encoded alongside potential reward and challenge difficulty prior to reaching an accept/reject decision. Our findings provide support for a stable fixation-choice relationship across a wide range of decision-making tasks, as previously argued by (Smith & Krajbich, 2018). It should be noted that fixations during economic risky choices have been studied in the past, but experimental designs either did not include a loss component (Fiedler & Glöckner, 2012; Fisher, 2017; Glickman et al., 2019; Molter et al., 2021; Smith & Krajbich, 2018; Stewart et al., 2016), did not combine gain and loss components in the same trials (Häusler et al., 2016), or did not exploit separate results of fixations towards gain and loss (Purcell et al., 2021).

Intracerebral correlates of visual attention effects on attribute values

Once fixation biases on choices were identified in subjects' behavioral data, our aim shifted towards understanding the neural mechanisms that may mediate such effects. Neural analyses, which capitalized on the high temporal accuracy of intracerebral recordings, revealed differentiated patterns of neural activity across three parameters: gaze location (on/away from a

dimension), dimension (gain/loss), and neuroanatomical region. Throughout regions reliably encoding visual fixations, the influence of gaze location was consistent: when looking at a dimension, an increase in value predicted an increase in BGA, while when looking away from the dimension, an increase in value predicted a decrease in BGA. These results mirror those from a binary-choice fMRI study, which observed that correlations between value and BOLD activity changed sign depending upon fixation location in the vmPFC, ventral striatum, and a number of other regions involved in subjective value representation (Lim et al., 2011). The simultaneous encoding of currently-fixated and stored dimension information we observed, as well as the sign change when gaze switches location, are also consistent with results from a primate study using an accept/reject task (Hunt et al., 2018).

Opponent functions of the vmPFC vs. aIns during multi-attribute choices revealed by gaze-contingent iEEG analyses ?

Although the functional dissociation between aIns and vmPFC was not clear-cut regarding the gaze-dependent encoding of each attribute values (e.g., the vmPFC signaled both gain and loss attributes positively when fixated), the overall results appears consistent with the existence of opponent functional brain networks during value-based choices.

Hence, a growing body of evidence established that the vmPFC is part of the so-called Brain-Valuation System (BVS) which encodes appetitive/pleasant values and reward prediction-errors (e.g., Gueguen et al., 2021; Lebreton et al., 2009; Lopez-Persem et al., 2020) whereas the anterior insula is involved during aversive value encoding during unpleasant value ratings or punishment-prediction error coding (Corradi-Dell'Acqua et al., 2016; Gueguen et al., 2021). Interestingly, we also previously showed that baseline activity in the vmPFC predicted subject's choices positively through a computational increase of how subjects subjectively perceived the monetary gains during the same task whereas in the aIns, baseline activity predicted negatively patients' choices possibly by over-weighting the monetary losses (Cecchi et al., 2021). Here, we addressed more complex choices involving multi-attribute integration. Critically, under such condition, simply averaging the signal over the choice process did not allow us to identify reliable neural correlates of attribute valuation. The picture only became clearer when neural activity was analyzed in association with gaze (and choice data). Whereas the vmPFC appeared to be involved during the processing of both monetary attributes of the offer while subjects were fixating them, only the gaze-dependent iEEG activity when people gazed at the monetary gains was eventually positively associated with risky choices. Conversely, gaze-contingent neural activity in the aIns

was positively associated with losses, and this activity was eventually positively associated with safe choices.

The next step will be to specify the neuro-computational mechanisms underlying these preliminary observations. One plausible possibility is that vmPFC and aINS neural activity would reflect in the model either the attentional modulation of the monetary gain values (for vmPFC) whereas the aIns would have a larger impact on how attention modulates the value of monetary losses. What would also remain to be established is where, when and how the relative value signal is encoded in the brain (i.e., a computational signal combining all three attributes and which ultimately lead to a risky vs. safe decision in a drift diffusion model approach).

Limitations

Our study contains several limitations, some of which may be addressed by further analyses. First, while abstracting over the sequence of fixations allows a relatively straightforward investigation of fixation effects across trials and subjects, it bypasses how intra-trial fixation variability might contribute to the choice processes. Second, neural analyses do not yet control for potential causal effects of values on visual fixations. Indeed, since the computation of fixation-dependent BGA is here partly dependent upon the time spent fixating a dimension and number of fixations towards the dimension, it could be argued that these two factors might drive the observed relationship between value and BGA; the higher a value, the more often and long the eye is drawn to it, and the higher our measure of fixation-dependent BGA would be. Although further analyses are required to revoke this hypothesis, we believe it is unlikely, as it would not explain the sign change observed when a dimension is unfixated. Similarly, the mediation analysis proposed here did not include how gaze impacted choices at the behavioral level so that further work is needed to disentangle the behavioral and neural effects of this study.

5. Material & Methods

Patients and electrode implantation

Intracerebral recordings were obtained from 38 patients suffering from drug-resistant focal epilepsy (35.6 *pm* 1.8 years old, 18 females) in 6 different epilepsy centers (Grenoble University Hospital: n = 18; Rennes University Hospital: n = 11; Lyon Neurological Hospital: n = 5; Prague Motol University Hospital: n = 2; Marseille La Timone Hospital: n = 1; Nancy University Hospital: n = 1). These patients underwent intracerebral recordings by means of stereotactically implanted multilead depth electrodes (iEEG) in order to locate epileptic foci

that could not be identified by non-invasive methods. Electrode implantation was performed according to routine clinical procedures and all target structures for the pre-surgical evaluation were selected strictly according to clinical considerations with no reference to the current study. Nine to twenty semi-rigid electrodes were implanted per patient. Each electrode had a diameter of 0.8 mm and, depending on the target structure, contained 6-18 contact leads of 2 mm wide and 1.5 mm apart (Dixi Medical, Besançon, France). All patients gave written, informed consent before their inclusion in the present study, which received approval from the local ethics committees (CPP 09-CHUG-12, study 0907; CPP18-001b/2017-A03248-45; IRB00003888).

Behavioral tasks

Presentation of visual stimuli and acquisition of behavioral data were performed on a PC (1920 $\times$ 1080 pixels) using custom Matlab scripts implementing the PsychToolBox libraries (Brainard, 1997). All subject responses were recorded with a gamepad (Logitech F310S) using both hands. Data were pooled from the acquisition of two distinct experimental designs sharing the same choice task. For one subset of participants (n = 21), each trial included a quiz task and a rest or mood assessment period before the choice task (previously described in Cecchi et al., 2021). For the other subset of participants (n = 17), the choice task was preceded by a mood rating (on 25% of trials), while each trial included a confidence rating, embedded between the choice and challenge, and a feedback after the challenge. Note that only the choice part of the two tasks was included in the analyses. In both setups, subjects completed two (n = 12) or three (n = 26) sessions of the experiment, each consisting of 64 trials, for a total of 128 or 192 trials.

Choice task. The choice task began with the presentation of an offer consisting of three dimensions: a gain prospect (represented by a bunch of 10-cent coins, range: 1-5€), a loss prospect (represented by crossed out 10-cent coins, range: 1-5€) and the upcoming challenge difficulty (represented by the size of a target window located at screen center, range: 1-5 corresponding to 75-35% theoretical success, from $\sim 0.6° \times 0.8°$ to $\sim 0.6° \times 1.7°$ visual angle; see training section for further details about how difficulty was adjusted for each participant). Subjects were asked to accept or reject this offer, by pressing a left or right button depending on where the choice option ("yes" or "no") was displayed. Subjects' choice determined the amount of money at stake: accepting meant that they would eventually win the gain prospect or lose the loss prospect based on their performance in the upcoming challenge, whereas declining the offer meant playing the challenge for minimal stakes (winning 10 cents or losing 10 cents).

The sequence of trials was pseudo-randomized such that all possible combinations of the three dimensions (gains, losses and challenge difficulty), continuously sampled along four intervals ([1-2],]2-3],]3-4],]4-5]), were displayed for one subject across sessions, with greater sampling of medium difficulty combinations ([2-3] and]3-4]). The positions of gain and loss prospects were randomly determined to be either displayed on top or bottom of the screen (both areas of $\sim 8.9° \times 2.7°$ visual angle) and similarly, the choice options ("yes" or "no") were randomly displayed on the left or right.

Subjects had a free time delay to accept or decline the offer. If they declined the offer, a 500 ms screen displayed the new offer (only gains and loss prospects changed so that subjects performed the challenge for a minimal stake of 10 cents). Thus, the challenge was performed regardless of the choice answer to prevent subjects to eventually reject more offers to decrease experiment duration.

The challenge started with a ball that appeared on the left side of the screen and moved, horizontally and at constant speed, towards the screen center. Subjects were asked to press the confirmation button when they thought the ball was inside the basket displayed at screen center (i.e., the target window which size index the difficulty of the challenge). To facilitate the challenge, the ball always reached the center of the target after 1s. Thus, the size of the target window (i.e. the difficulty of the trial) represented the margin of error tolerated in subject response time (target: 1s after the movement onset of the ball). The larger the basket, the greater the tolerated spatiotemporal error was to consider a trial as successful, and therefore the easier was the trial. Importantly, the moving ball could only be seen during the first 500 ms (half of the trajectory), and subjects had to extrapolate the last 500 ms portion of the ball's trajectory to assess whether the ball was inside the target. To improve subjects' motivation to perform the task as accurately as possible, the total amount of money earned by the participants during a session (calculated by adding gains and losses across all trials) was displayed at the end of a session.

Training. For both experimental designs, the main experiment was preceded by a training – divided into three steps – to familiarize subjects with all sub-parts of the tasks. In the first step, subjects were familiarized with the challenge by completing 28 to 80 trials with a tolerated margin of error from $\pm$ 130 to $\pm$ 80 ms depending on their performance. Each training trial was followed by feedback informing whether the challenge was successful ("ok" in green) or missed ("too slow" or "too fast" in red). In the second step, subjects performed 64 trials of the full choice (i.e., the challenge was always preceded by an offer), and a feedback on the money won/lost in the trial was displayed at the end of each trial. The goal was to train subjects to

properly integrate the three dimensions of the offer (gains, losses and difficulty) when making their choice. To help subjects learning the correspondence between the target size and challenge difficulty, trials were displayed by increasing difficulty level. Finally, the third and last part of the training (10 trials in task 1 and 8 trials in task 2) was totally similar to the main task to allow subjects to familiarize with all remaining parts (e.g. mood ratings).

Another purpose of the training was to tailor the difficulty of the challenge to each patient's ability. To do so, a tolerated margin of error was computed for each difficulty level, ranging from 75% (level 1) to 35% (level 5) of theoretical success which we estimated from each individual subjects by assuming that errors were normally distributed. Note that during training, the difficulty levels were updated after each trial (average and standard deviation of challenge performance were updated), while in the main task, the mean and standard deviation of patient performance (and therefore difficulty levels) were set based on every challenge performed during the training. The range of tolerated margins of error between subjects ranged from [$\pm$ 58 ms (level 1) to $\pm$ 28 ms (level 5)] in the most precise patient to [$\pm$ 198 ms to $\pm$ 123 ms] in the less precise one.

Eye-tracking data

Raw gaze data was recorded at 90 Hz using a laptop-mounted Tobii 4C eye-tracker during both behavioral tasks. An initial calibration was performed prior to each experimental session. Gaze was preprocessed and analyzed during the choice stage only, from offer onset to the choice response.

Fixations were extracted from left-eye on-screen coordinates through a series of preprocessing steps scripted in MATLAB according to suggestions from the Tobii Technology white paper (see Olsen, 2012 for details). First, small gaps in data ($\leq$ 75 ms, which corresponds to an average blink duration) due to trackloss (i.e, data loss due to the eye-tracker not recording) were interpolated linearly using a scaling factor. Data was then smoothed using a moving median window of 5 samples ($\sim$ 56 ms). Next, a velocity-based classification algorithm was applied to differentiate between saccades and fixations; specifically, each sample y was associated with a velocity, based on eye position at sample y and on-screen coordinates at samples $y-1$ and $y+1$. Samples with an associated velocity $\geq$ 50°/s were considered to be part of a saccade, while samples with a velocity under that threshold were deemed part of a fixation. Algorithm performance was assessed visually, and adjacent fixation samples were merged into single fixations.

Once extracted, fixations had to be attributed to on-screen ROIs (SROIs, used to avoid confusion with brain ROIs). First, fixation coordinates were calculated based on the average x, y coordinates of all samples within the fixation. Fixation clusters corresponding to the five SROIs (gains, losses, difficulty, "yes", "no") were observed (see Fig. IV.1b). However, since these clusters were not limited to the borders of SROIs, a k-nearest neighbors' algorithm was applied to avoid unnecessary data removal. The algorithm was trained using x,y coordinates generated randomly within SROI borders, with the addition of a "reject" class between and around SROIs. Predicted fixation classes were adjusted in two cases: if a fixation outside of SROIs ("reject" class) was located between two fixations to the same SROI, it was assumed to be wrongly classified and re-classified as being part of that SROI, and, if two fixations to the same SROI were separated by a period of trackloss, both fixations and trackloss were merged into a single fixation. Finally, fixations lasting less than two samples were unusable and thus eliminated. An example of resulting eye-tracking data classification is visible in Fig. IV.1b.

Choice model

Choices were fitted using a published computational framework, which was shown to best capture choices in this task (Vinckier et al., 2018).

Acceptance probability was calculated as a sigmoid function (softmax) of expected utility:

$$p(accept, t) = \frac{1}{1 + e^{-(utility + k_t \times t)}}$$

where k_t is a free parameter that accounts for a linear drift with time (trial index t) in order to capture fatigue effects. The utility function is based on expected utility theory where potential gains and losses are multiplied by probability of success (p_s) vs. failure ($1 - p_s$):

$$utility = k_0 + p_s \times k_g \times gain - (1 - p_s) \times k_l \times loss$$

However, distinct weights were used for the gain and loss components (k_g and k_l respectively), and a constant k_0 was added in order to capture a possible bias. The subjective probability of success (p_s) was inferred from the target size. The model assumes that subjects have a representation of their precision following a Gaussian assumption, meaning that the subjective distribution of their performance could be defined by its mean (the required 1 second to reach target center) and its width (i.e., standard deviation) captured by a free parameter σ. Thus, the probability of success was the integral of this Gaussian bounded by the target window:

$$p_s = \frac{1}{\sigma\sqrt{2\pi}} \int_{1-Size/2}^{1+Size/2} e^{\frac{-(x-1)^2}{2\sigma^2}} dx$$

This model was inverted for each patient separately with behavioral data, using the ??https://mbb-team.github.io/VBA-toolbox/]Matlab VBA toolbox, which implements Variational Bayesian analysis under the Laplace approximation (Daunizeau et al., 2014).

Statistical analyses

Prior to analyses, trials were excluded based on two criteria: trackloss > 25% of trial length and/or outlier RT (defined as being more than three standard deviations away from the mean). All behavioral analyses including eye-tracking focused on fixations towards gain and loss; fixations to other SROIs were removed beforehand.

Psychometric fits. After having divided trials according to last fixation location (gain or loss), a logistic regression model was fitted to each participants' choice data separately. The regression fit was performed as a function of the difference in value between gain and loss. To quantify the shift between obtained psychometric fits from both fixation groups, the point of subjective equality (PSE) was computed per participant and groups were compared using a paired sample t-test. PSEs represent the value difference between gain and loss when $p_{accept} = 0.5$. Because several participants accepted most of the time or rejected most of the time, we could not obtain reliable measure of PSE for those subjects. Since the range of possible differences between gain and loss being from -400 to 400 cents, subjects with estimated PSE value(s) outside this range were excluded (11 out of 38 patients).

Generalized mixed-effects models. All other statistical analyses were performed with Matlab Statistical Toolbox (Matlab R2018b, The MathWorks, Inc., USA), using generalized linear mixed models (GLMM; estimated with the fitglme function). All reported regression coefficients represent fixed effects from mixed-effects linear (for continuous dependent variables) and logistic (for binary dependent variables) regression models. For each fixed effect, the estimated coefficient value (β) $\pm$ its standard error is reported, as well as the t-statistics (testing that the coefficient is equal to 0) along with its p-value. For behavioral analyses, models included random intercepts for each subject, as well as random subject-slopes for each model coefficient. The mixed models used for electrophysiological analyses are detailed in the corresponding section below, following the Wilkinson-Rogers notation (Wilkinson & Rogers, 1973). All means are reported along with the standard error of the mean.

Intracerebral EEG recordings

Neuronal recordings were performed using video-EEG monitoring systems that allowed for simultaneous recording of 128 to 256 depth-EEG channels sampled at 512, 1024 or 2048 Hz (depending on the epilepsy center). Acquisitions were made with Micromed (Treviso, Italy) system and online band-pass filtering from 0.1 to 200 Hz in all centers, except for Prague (Two Natus systems were used: either a NicoleteOne with a 0.16-134 Hz band-pass filtering or a Quantum NeuroWorks with a 0.01-682 Hz band-pass filtering) and Marseille (Deltamed system, 0.16 Hz high-pass filtering). Data were acquired using a referential montage with the reference electrode located in the white matter. Prior to analyzing, all signals were re-referenced to their nearest neighbor on the same electrode, yielding a bipolar montage.

iEEG pre-processing

Before analysis, bad channels were removed based on a supervised machine-learning model trained on a database of channels pre-classified by experts, and using a set of features quantifying the signal variance, spatiotemporal correlation and non-linear properties (Tuyisenge et al., 2018). The average number of recording sites (one site corresponding to a bipolar contact-pair) recorded per patient was 115 ± 6. Finally, all signals were down sampled to 512 Hz.

Neuroanatomy

The electrode contacts were localized and anatomically labeled using the IntrAnat Electrodes software (Deman et al., 2018), developed as a BrainVisa (Rivière et al., 2009) toolbox. Briefly, the pre-operative anatomical MRI (3D T1 contrast) and the post-operative image with the iEEG electrodes (3D T1 MRI or CT scan), obtained for each patient, were co-registered using a rigid-body transformation computed by the Statistical Parametric Mapping 12 (SPM12; Ashburner, 2009) software. The gray and white matter volumes were segmented from the pre-implantation MRI using Morphologist as included in BrainVisa. The electrode contact positions were computed in the native and MNI referential using the spatial normalization of SPM12 software. Coordinates of recording sites were then computed as the mean of the MNI coordinates of the two contacts composing the bipole. For each patient, cortical parcels were obtained for the MarsAtlas (Auzias et al., 2016) and Destrieux (Destrieux et al., 2010) anatomical atlases, while subcortical structures were generated from Fischl et al. (2002) (as included in Freesurfer). Each electrode contact was assigned to the gray or white matter and to specific anatomical parcels by taking the most frequent voxel label in a sphere of 3 mm radius around each contact center.

The MarsAtlas parcellation scheme was mainly used to label each recording site. This atlas relies on a surface-based method using the identification of sulci and a set of 41 regions of interest (ROIs) per hemisphere. These regions were completed with 7 subcortical regions, obtained from the procedure described by Fischl et al. (2002) (as included in Freesurfer; Deman et al., 2018). However, based on the literature, we applied slight modifications concerning our regions of interest. First, boundaries based on MNI coordinates were set to the ventromedial prefrontal cortex (vmPFC) region so that contacts more lateral than $x = \pm 12$ and more dorsal than $z = 10$ were excluded from the parcel (Lopez-Persem et al., 2019). Second, MarsAtlas parcellation scheme involved the insular cortex as a single region, making it impossible to distinguish sub-insular areas that appear to have distinct functional properties in decision-making (Droutman et al., 2015). We therefore used the Destrieux atlas (performed by Freesurfer; Deman et al., 2018) and MNI coordinates to segment the region corresponding to the insula into 2 sub-regions: (i) the anterior insula (aIns) corresponds to the anterior part ($y < 5$ in MNI space) of parcels 18 (*G_insular_short*), 47 (*S_circular_insula_ant*), 48 (*S_circular_insula_inf*) and 49 (*S_circular_insula_sup*) of the Destrieux atlas, (ii) the posterior insula (pIns) corresponds to the posterior part ($y > 5$ in MNI space) of parcels 17 (*G_Ins_lg_and_S_cent_ins*), 48 and 49 of the Destrieux atlas, leading to a total of 49 ROIs.

For statistical analyses, only the 43 ROIs with at least 10 recording sites recorded across at least five subjects were retained. Among the 4381 initial recorded sites, 3994 recording sites were located within one of these 43 regions and were therefore kept for analysis. Note that data from both hemispheres were collapsed to improve statistical power.

Extraction of frequency envelopes

The time course of broadband gamma activity (BGA) was obtained by band-pass filtering of continuous iEEG signals in multiple successive 10 Hz-wide frequency bands (i.e., 10 bands, beginning from 50-60 Hz up to 140-150 Hz) using a zero-phase shift non-causal finite impulse filter with 0.5 Hz roll-off. The envelope of each band-pass filtered signal was next computed using the standard Hilbert transform. For each frequency band, this envelope signal (i.e., time varying amplitude) was divided by its mean across the entire recording session and multiplied by 100. This yields instantaneous envelope values expressed in percentage (%) of the mean. Finally, the envelope signals computed for each consecutive frequency band were averaged together to provide a single time series (the broadband gamma envelope) across the entire session. By construction, the mean value of that time series across the recording session is equal to 100. Note that computing the Hilbert envelopes in 10 Hz sub-bands and normalizing them individually

before averaging over the broadband interval allows to counteract a bias toward the lower frequencies of the interval induced by the 1/f drop-off in amplitude. Finally, the obtained time series were smoothed using a sliding window of 250 ms, to get rid of potential artifacts, and downsampled at 100 Hz (i.e., one-time sample every 10 ms).

Electrophysiological analyses

The aim was to investigate how fixation patterns influenced neural activity and choices. To account for variability in fixation timing and location (given that subjects were freely viewing), the frequency envelopes of each recording site were epoched at each trial from choice onset (display of the offer) to choice response (YES or NO button press). Then, a relative power was computed separately for all three choice dimensions d = {gain,loss,difficulty} and at each trial as a function of fixation location. Specifically, the power P (normalized envelope) of all fixations from a specific dimension was summed after being individually averaged and normalized to the choice response time (RT = time between choice onset and choice response), thus providing a value for each choice dimension, trial and contact:

$$P_{\text{fix d}} = \sum_{i=1}^{n_d} \overline{P_i} \times \frac{t_i}{RT}$$

With i corresponding to the fixation index, t_i the duration of the ith fixation and n_d corresponding to the number of fixations of dimension d within a trial.

Similarly, another relative power $P_{\text{fix not d}}$ was computed for each choice dimension to track neural activity when all but the considered dimension d were looked at (e.g. $P_{\text{fix not gain}}$ represents the sum of loss and difficulty fixations).

For each ROI, these dimension-specific powers were subsequently analyzed using a series of nested mixed-effects models, including subject and electrode identity as random effects, to account for inter-subject and inter-electrode variability in neural activity.

GLMM 1 & 2: Effect of visual attention on value representation. In a first GLMM, we tested, for each ROI and choice dimension, whether neural activity signaled the value of the fixated dimension:

$$P_{\text{fix d}} \sim 1 + gain + loss + diff + (1 + gain + loss + diff | ELECTRODE : SUBJECT)$$

In the same way, GLMM 2 was designed to investigate whether neural activity signaled the value of the unfixated dimension:

$$P_{\text{fix not d}} \sim 1+gain+loss+diff+(1+gain+loss+diff|ELECTRODE:SUBJECT)$$

With d = {gain,loss,difficulty}. In GLMM 1, the variable of interest was the fixed effect of the fixated dimension (e.g. gain when the dependent variable was $P_{\text{fix gain}}$), while in GLMM 2 the variable of interest was the fixed effect of the unfixated dimension (e.g. gain when the dependent variable was $P_{\text{fix not gain}}$). In both models, the other choice dimensions were included as covariates of non-interest to control for their effect.

Brain-behavior mediation analysis. The focus of this analysis was to investigate brain regions that mediated the impact of the fixated choice dimension (gain, loss or difficulty) on choice. It identifies two statistical paths: (1) path a characterizes the effect of the fixated choice dimension on brain activity and (2) path b reflects the effect of brain activity on choices above and beyond the impact of the fixated choice dimension (path c'). Statistical testing of mediation was performed using the conjunctive approach (Brochard & Daunizeau, 2020) which relies on the "maximum p-value" (i.e. mediated effect is significant if both paths a and b are significant).

For each choice dimension, path a was extracted from GLMM 1 (i.e. the fixed effect of the fixated dimension), while paths b and c' were estimated for each ROI with the following GLMM 3:

$$\begin{aligned} Choice \sim 1 &+ P_{\text{fix gain}} + P_{\text{fix loss}} + P_{\text{fix diff}} + gain + loss + diff \\ &+ (1 + gain + loss + diff|SUBJECT) \\ &+ (1 + P_{\text{fix gain}} + P_{\text{fix loss}} + P_{\text{fix diff}}|ELECTRODE:SUBJECT) \end{aligned}$$

For instance, when exploring brain regions whose activity during gain fixation mediates the effect of gain on choice, path a corresponded to the fixed effect of gain in GLMM 1, path b corresponded to the fixed effect of neural activity during gain fixation ($P_{\text{fix gain}}$ in GLMM 3 and path c' corresponded to the fixed effect of gain in GLMM 3. The other two choice dimensions (loss and difficulty) were analyzed in the same way.

GLMM 1 and 2 were modelled using a Normal response function distribution (linear regression), whereas GLMM 3 was modelled using a binomial response function distribution (logistic regression).

The statistical significance of effects within each ROI was assessed using a Bonferroni adjusted alpha level of 0.001 (p_{corr}; $^{0.05}/_{49}$ ROI).

6. Supplementary material

Supplementary Table IV.S1: Modulation of Broadband Gamma Activity (50-150 Hz) by gaze.

	GAINS					LOSSES			
	fixated (path a)		unfixated			fixated (path a)		unfixated	
ROI	Regression estimate	p-value	Regression estimate	p-value	ROI	Regression estimate	p-value	Regression estimate	p-value
OFCvl	0,061	4,8E-10	-0,079	2,4E-10	**aIns**	0,062	2,2E-12	-0,070	< 1,0E-15
PFcdl	0,053	5,0E-12	-0,091	< 1,0E-15	pIns	0,048	3,0E-09	-0,057	< 1,0E-15
PFCvm	0,044	3,3E-05	-0,058	8,8E-09	**PFCvm**	0,053	3,9E-04	-0,044	4,6E-06
PFrd	0,079	2,9E-09	-0,120	2,2E-16	ITCm	0,066	5,4E-06	-0,067	< 1,0E-15
Pfrdli	0,046	3,8E-08	-0,068	5,0E-10	MTCr	0,051	4,7E-09	-0,076	< 1,0E-15
Pfrdls	0,039	3,4E-06	-0,059	2,5E-06	STCc	0,030	6,3E-04	-0,040	9,6E-12
PFrm	0,082	7,8E-09	-0,145	5,1E-12	STCr	0,047	1,2E-04	-0,069	< 1,0E-15
MTCc	0,032	3,3E-05	-0,049	2,6E-08					
MTCr	0,038	4,0E-08	-0,055	4,4E-16					

Supplementary Table IV.S2: Mediation analysis.

	GAINS					LOSSES			
	path a		path b			path a		path b	
ROI	Regression estimate	p-value	Regression estimate	p-value	ROI	Regression estimate	p-value	Regression estimate	p-value
MTCc	0,032	3,3E-05	0,246	1,2E-10	**aINS**	0,062	2,2E-12	-0,167	1,9E-07
MTCr	0,038	4,0E-08	0,249	1,4E-14	MTCr	0,051	4,7E-09	-0,103	1,8E-05
PFCvm	0,044	3,3E-05	0,218	1,9E-04	pINS	0,048	3,0E-09	-0,211	4,2E-11

V

Dissociable effects of intracranial electrical stimulation in the dorsal and ventral anterior insula on risky-decision making

Romane Cecchi[1], Inès Rachidi[1,2], Lorella Minotti[1,2], Philippe Kahane[1,2], Mathias Pessiglione[3,4,†], Julien Bastin[1,†]

[1] Univ. Grenoble Alpes, Inserm, U1216, CHU Grenoble Alpes, Grenoble Institut Neurosciences, 38000 Grenoble, France
[2] Neurology Department, University Hospital of Grenoble, Grenoble, France
[3] Motivation, Brain and Behavior (MBB) team, Paris Brain Institute, Pitié-Salpêtrière Hospital, Paris, France
[4] Université de Paris, Paris, France
[†] These authors contributed equally to this work

In preparation

1. Abstract

How the human brain decides to take a risky choice in the face of uncertainty depending on subject's performance remains unclear. Here, we investigated the effect of targeted disruption of the anterior insular cortex and the ventromedial prefrontal cortex (vmPFC) on such risky decision-making behavior. The effects of intracranial electrical stimulation delivered directly in the human cortex at 50 Hz in a group of epileptic patients (n = 13) were examined while they were performing a choice task. Results showed a functional dissociation between the dorsal anterior insula (daIns) and the ventral anterior insula (vaIns) which direct electrical stimulation induced respectively a positive vs. a negative bias on the comparison of safe and risky option. Conversely, intracranial electrical stimulation on the vmPFC tended to promote risk taking (as in the daIns). These rare cases highlight the potential causal importance of the anterior insula sub-regions during multi-attribute choices involving uncertainty and provides clues for future mechanistic studies of the anatomy and physiology of choices under uncertainty.

Keywords

Risk, decision-making, reward, direct electrical stimulation, ventromedial prefrontal cortex, anterior insula

2. Introduction

Choices often have to be made in the face of uncertainty. For example, risky decision-making can be viewed as choices that involve some forms of potential threat in comparison with safer options that would involve less negative consequences. In the lab, to study such choices, binary gambling tasks have been widely used to confront the subjects with a binary choice involving a risky option (e.g., having 50% chance to win 10 € vs. 50% of chance to win nothing) and a safe option (e.g., being sure to win 5 €) with both option having identical expected values. Yet, gambling tasks model uncertainty as a decision component that fluctuates independently from the subject's own performance. One of the objective of this study was to clarify how subjects decide to take a risk or not when the source of uncertainty depends on their own performance.

At the neural level, functional magnetic resonance imaging (fMRI) studies in humans have revealed that different parts of the brain may be involved in different behaviors in the face of risk. Specifically, activation of the ventromedial prefrontal cortex (vmPFC) has been shown to promote risk-seeking (Blankenstein et al., 2017; Engelmann & Tamir, 2009; Tobler et al., 2007; Venkatraman et al., 2009; Vinckier et al., 2018; Xue et al., 2009), while activation of the anterior insula (aIns) would precede riskless choices (Kuhnen & Knutson, 2005; Paulus et al., 2003; Rudorf et al., 2012; Venkatraman et al., 2009; Vinckier et al., 2018). Furthermore, the ventromedial versus dorsomedial region and the lateral versus medial region of the prefrontal cortex contribute oppositely to risky decision making (Tobler et al., 2007; Xue et al., 2009), with ventral/medial regions associated with risk seeking and dorsal/lateral regions with risk aversion. Similarly, evidence suggests that the dorsal and ventral parts of the anterior insula may play distinct roles in various domains (Centanni et al., 2021), notably during decision making under risk (Droutman et al., 2015; Preuschoff et al., 2008).

Despite these neuroimaging data, we have relatively little causal information regarding the brain regions involved during risky decision-making. Yet, lesions of the medial prefrontal cortex consistently resulted in increased risk-taking and disadvantageous behaviors (Bechara et al., 1994; Bechara et al., 1999; Clark et al., 2008; Sanfey et al., 2003; Shiv et al., 2005; Weller et al., 2007) or no difference from the control group (Leland & Grafman, 2005; Sanfey et al., 2003), whereas lesions of the insula led to both decreased risky choices (Weller et al., 2009) or increased betting behaviors compared to healthy subjects (Clark et al., 2008; Shiv et al., 2005). These discrepancies between studies and with the fMRI literature may be explained by the scope of the brain lesions, which in some cases extend well beyond the targeted regions, thus reaching adjacent areas that may also contribute to the observed deficits. The current lack of causal evidence is also

partly explained by the deep anatomical location of both vmPFC and aIns which make these territories difficult to target using trans-cranial stimulation methods. In contrast, intracranial electrical stimulation (iES) can be directly applied to assess causality by delivering a volley of electrical discharges in a specific brain area while awake human subjects perform a cognitive task. iES is a common clinical practice used to identify functional boundaries in the brain to guide resection in patients with severe drug-resistant epilepsy or brain tumors (Borchers et al., 2012; Desmurget et al., 2013; Selimbeyoglu & Parvizi, 2010).

Previous studies have reported that electrical stimulation of the insular cortex induced a wide variety of clinical responses, such as visceral, auditory, vestibular, and olfacto-gustatory sensations, somatosensory, emotional, and motor responses, or language disorders (Afif et al., 2010; Feindel & Penfield, 1954; Isnard et al., 2004; Mazzola et al., 2019; Ostrowsky et al., 2000; Stephani et al., 2011). Yet, the vast majority of iES effects in the insular lobe are in the posterior part and relatively little evidence exist regarding the anterior insula. Stimulation of the dorsal part of the anterior insula (daIns) in humans and non-human primates was found to induce ingestive behaviors (e.g., chewing and swallowing; Jezzini et al., 2012) and overwhelming ecstatic sensations (Bartolomei et al., 2019; Picard et al., 2013). Conversely, stimulation of the ventral part of the anterior insula (vaIns) resulted in disgust behavior (Caruana et al., 2011; Jezzini et al., 2012; Krolak-Salmon et al., 2003) and depressed affect (Singh et al., 2021). Furthermore, in a value-based decision-making context, stimulation of the vaIns in macaque monkeys resulted in reduced approaches in appetitive contexts and increased avoidance behaviors in aversive contexts more pronounced than in the daIns (Saga et al., 2019).

In parallel, frontal lobe stimulation studies in humans and non-human primates are also relatively scarce and reported effects are generally limited to single cases that are seldom replicated (K. C. R. Fox et al., 2020; Raccah et al., 2021). While there is some evidence that iES of the lateral orbitofrontal cortex causes conscious changes in affective state (K. C. R. Fox et al., 2018; Rao et al., 2018; Yih et al., 2019) as well as sensory phenomena (K. C. R. Fox et al., 2018; Yih et al., 2019), we are not aware of any previous research reporting significant behavioral effects of vmPFC intracranial stimulation, as the few works that have stimulated this region indicate only null results (K. C. R. Fox et al., 2020; K. C. R. Fox et al., 2018; Selimbeyoglu & Parvizi, 2010).

In the present study, we sought to identify the effects of iES of the aIns and vmPFC on decision-making processes under uncertainty during stereo-electroencephalography (sEEG) recordings of patients with drug-resistant focal epilepsy. We used an accept/reject tasks during which pa-

tients' choice determined the amount of money at stake. Accepting meant that they would eventually win the gain prospect or lose the loss prospect based on their performance during an upcoming challenge, whereas declining the offer meant playing the challenge for minimal stakes (winning 10 cents or losing 10 cents).

3. Results

The aim of this study was to assess whether intracranial electrical stimulation (iES) of key regions involved in decision-making under uncertainty, namely the aIns (ventral and dorsal) and vmPFC, selectively impacted decision-making processes. To do so, 13 subjects with implanted electrodes (33.1 ± 2.5 years old, 7 females, see demographic details in Supplementary Table V.S1) performed an accept/reject choice task involving monetary prospects (gains and losses) while brain stimulation was alternatively applied during 50% of the trials (Fig. V.1). Across subjects, 53 sites were stimulated, of which 26 were in the daIns, 15 in the vaIns and 12 in the vmPFC (note that the individual organization of gyri and sulci within each subject was used to identify the three regions of interest, see Methods).

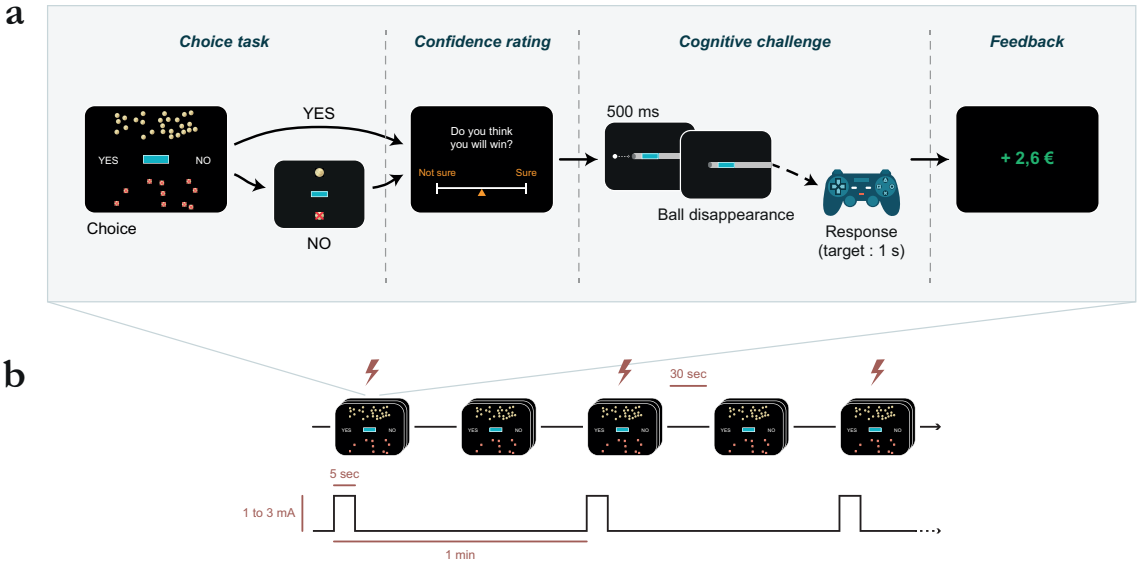

Figure V.1: Experimental design. (a) Trial structure. Each trial included a choice task and a confidence rating followed by a challenge. In the choice task, subjects had to decide whether to accept or reject a given challenge by taking into account gain prospects (represented by a bunch of regular 10-cent coins) and loss prospects (crossed out 10-cent coins). The challenge consisted of stopping a moving ball, invisible when entering the gray tunnel, inside the blue target in the middle of the screen. (b) Overview of stimulation experiments. In each session, 14 trials with intracranial electrical stimulation (iES) alternated with 14 trials without iES. The nature of the first trial (with or without iES) was randomized so that subjects remained blind to experimental conditions. A 30-second interval was observed between each trial, resulting in a 1-minute interval between each stimulation. During iES trials, stimulation was delivered for 5 seconds as pulses of 500 ms width at a frequency of 50 Hz and an amplitude of 1, 2, or 3 mA.

We first assessed whether subjects performed the choice task correctly in order to rule out effects unrelated to the stimulation. We excluded from further analyses experimental sessions during which patients consistently accepted or refused the offer on all trials (independently from the stimulation condition, see Methods for the exact data exclusion criteria). Consequently, of the 53 sessions recorded in 13 patients, 48 sessions were retained for analysis (see Fig. V.2 and Supplementary Fig. V.S1), including 25 sessions in the daIns (17 left and 8 right sessions recorded across 13 patients), 13 sessions in the vaIns (8 left and 5 right sessions recorded across 8 patients) and 10 sessions in the vmPFC (7 left and 4 right sessions recorded across 7 patients).

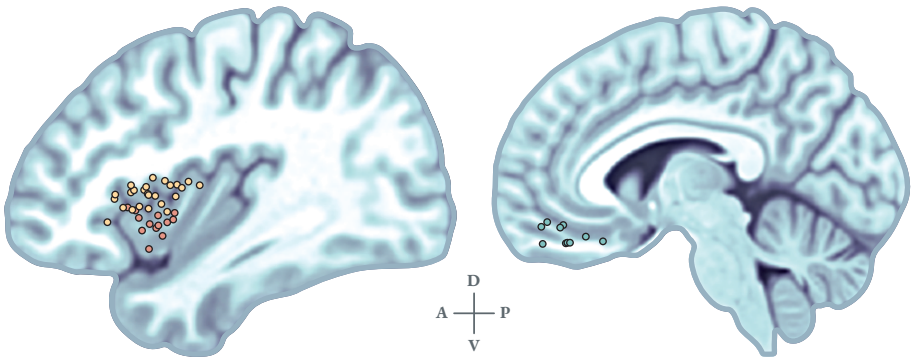

Figure V.2: Location of stimulation sites. Anatomical location of daIns (yellow), vaIns (orange) and vmPFC (green) stimulation sites retained for analysis on the standard Montreal Neurological Institute (MNI) template brain. Anterior (A), posterior (P), dorsal (D) and ventral (V) directions are indicated. Note that stimulation sites have been aggregated on the x-axis for visualization purposes. See Supplementary Fig. V.S1 for a more accurate location of each site.

Next, we checked that the attributes of the offer (monetary prospects and challenge difficulty) were properly integrated into choices made. Using a logistic mixed-effects regression model that included subjects and electrodes as random effects, we confirmed that subjects behaved as expected (Fig. V.3), namely that choice acceptance rate significantly increased with gain ($\beta_{gain} = 0.13 \pm 0.03, t_{689} = 3.82, p = 1.10^{-4}$) while it significantly decreased with loss ($\beta_{loss} = -0.10 \pm 0.03, t_{689} = -3.88, p = 1.10^{-4}$). As expected, challenge difficulty did not significantly modulate choice behavior ($\beta_{diff} = 8.10^{-3} \pm 0.03, t_{689} = -0.33, p = 0.74$), since we restricted the multi-attribute options space to the offers involving challenge difficulty corresponding to "difficult" choices during which the probability to accept the offer was close to 50% (see Methods). This methodological choice was motivated by an attempt to maximize the likelihood of observing an effect of iES on harder choices involving a stronger uncertainty on choices' outcome.

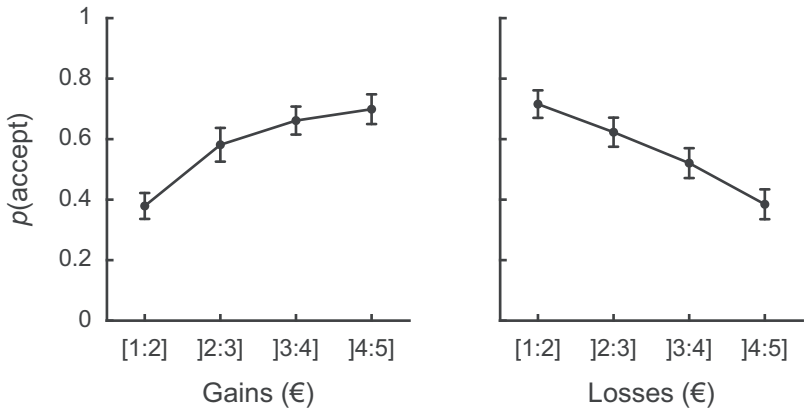

Figure V.3: Choice behavior. Acceptance probability is plotted as a function of the two significant objective dimensions of the task (gain and loss). Circles are binned data averaged across stimulation sites. Error bars represent inter-subject S.E.M.

Finally, we assessed the effect of daIns, vaIns, and vmPFC stimulation on risky decision-making by examining differences in acceptance rates between trials with or without iES (Fig. V.4). We found that stimulation of daIns and vaIns had an opposite effect on choices. Specifically, in daIns, the probability of accepting the offer was significantly higher in trials with iES compared to non-stimulated trials ($0.06 \pm 0.03, t_{24} = 2.15, p = 0.042$; two-tailed paired t-tests). Conversely, in the vaIns, the probability of accepting the offer was significantly lower in stimulated trials compared to non-stimulated trials ($-0.11 \pm 0.04, t_{12} = -2.61, p = 0.023$). In the vmPFC, the probability of accepting the offer tended to be higher in stimulated trials, but the difference with non-stimulated trials did not reach statistical significance ($0.08 \pm 0.04, t_9 = 1.88, p = 0.093$). To reject confounding factors, we also assessed the interaction between stimulation and reaction time or confidence ratings. We found that neither reaction time, nor confidence ratings were significantly modulated by the stimulation conditions in any of the three regions of interest.

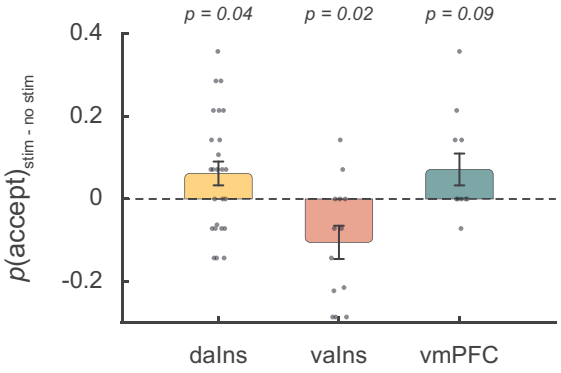

Figure V.4: Stimulation effects on acceptance probability. Difference in the probability of accepting the offer between stimulated and non-stimulated trials for sessions in which daIns (yellow), vaIns (orange), or vmPFC (green) were stimulated. Dots represent individual data for each stimulation site, bars represent means and error bars S.E.M across stimulation sites.

4. Discussion

To understand how the aIns and vmPFC causally contribute to risky decision-making, we applied iES to these two regions while human subjects undergoing an sEEG study for pre-surgical evaluation of drug-resistant focal epilepsy performed an accept/reject task involving monetary prospects that magnitude depended on subjects' decision. We found that stimulation of the dorsal part of the aIns (daIns) induced riskier choices, while in contrast, stimulation of the ventral part of the aIns (vaIns) induced a bias toward more cautious behavior. Stimulation of the vmPFC resulted in a higher acceptance rate, but the difference with non-stimulated sessions failed to reach significance. Our results thus provide causal evidence that intracranial electrical stimulation in distinct sub-regions of the aIns differentially influences approach and avoidance behaviors in the face of uncertain choices. In the following, we successively discuss (1) the effects of iES in the anterior insular lobe and (2) in the vmPFC and (3) the limitations and perspectives of this study.

Opponent role of the dorsal vs. ventral anterior insula

Stimulation of the aIns revealed a striking functional dissociation between the dorsal and ventral aIns; whereas stimulation of the daIns resulted in a higher rate of acceptance of risky options, stimulation of the vaIns increased the probability to choose the safer options. An issue that remains to be resolved is the underlying generative choice mechanism: one possibility is that iES of the vaIns induces rejection of the risky offer in our choice task by increasing of the subjective aversiveness of the offer (i.e., here, the subjective value of the loss prospect). This could be tested by fitting the computational choice model separately for the stimulated vs. non-stimulated trials. Here, we could not formally test this idea due to a low statistical power (the number of trials was too low to obtain reliable model-based effects of iES on the subjective value of the gains vs. losses prospects). Yet, previous fMRI (Vinckier et al., 2018) and iEEG evidence (Cecchi et al., 2021) showed that the anterior insula is preferentially involved during the subjective valuation of the loss prospects (rather than the gain prospect). Thus, we speculate that a possible generative mechanism is that iES applied of the ventral anterior insula might increase the participants' perception of the loss prospect and thus decrease risk-taking.

A more surprising finding was that intracranial stimulation of the daIns induced higher rate of acceptance of the offer, an effect that we initially expected in the vmPFC. This suggests that a possible mechanism would by an over-weighing of monetary gains during the choice process in the dorsal part of aIns. Yet, this hypothesis it not easily concealable with one of our previous re-

sults, obtained using the same task and populations by means of intracerebral recordings, which shows that baseline activity of the daIns tended to decrease in risk-taking (Cecchi et al., 2021). Further studies are therefore needed to determine the origins of these discrepancies. We could also quantify how iES impact remotely broadband gamma activity (BGA) by studying how average BGA measured between offer onset and choice onset is modulated between stimulated and non-stimulated trials in the brain network involved in risky-decision making.

The functional differentiation between the ventral and dorsal aIns could help to explain some of the discrepancies between previous lesion studies. Indeed, because these two sub-regions are extremely close, it seems possible that the distribution of lesions within the group study gives an advantage to one behavior over another. Similarly, although neuroimaging studies tend to implicate the aIns in the processing of negative stimuli and risk-averse behaviors (Kuhnen & Knutson, 2005; Paulus et al., 2003; Rudorf et al., 2012; Venkatraman et al., 2009; Vinckier et al., 2018), there is some evidence for its role in risk-taking (Xue et al., 2010). Nevertheless, few of these studies have considered the different regions of the anterior insula in their analyses. Overall, the present results therefore strongly suggest that a better consideration of the different sub-regions of the insula is crucial for understanding its role in decision making under uncertainty. Interestingly, our results nicely echoes those reported in a recent study in non-human primates showing that stimulation of the vaIns reduced approach behaviors in appetitive contexts and increased escape behaviors in aversive contexts (Saga et al., 2019). In unpublished results, these same authors also found a topographic distribution of neurons within the aIns, with neurons preferring the aversive outcome in the ventral portion, and a mixture of neurons preferring appetitive and aversive outcomes in the dorsal portion (see Discussion of Saga et al., 2019), which would be in keeping with the mechanistic effects of iES on either the loss (vaIns) or gain (daIns) prospects on which we speculated above. Our findings are also consistent with previous studies that have shown opposite effects of stimulation of the ventral and dorsal parts of the aIns; accordingly, stimulation of the vaIns was more associated with negative behaviors such as disgust (Caruana et al., 2011; Jezzini et al., 2012; Krolak-Salmon et al., 2003) or depression (Singh et al., 2021), whereas electrical stimulation of the daIns was more associated with positive behaviors such as ingestion (Jezzini et al., 2012) and ecstatic feelings (Bartolomei et al., 2019; Picard et al., 2013).

Testing the causal role of the vmPFC

Although not significant, vmPFC stimulation increased acceptance rate in the choice task, with only one session showing an opposite effect. Increasing the sample size will hopefully allow us

to reach a conclusion about the effects of stimulating this structure in uncertain decision making. If this trend is confirmed, this study could be the first to show a behavioral effect of vmPFC stimulation. Indeed, to date, stimulation studies that have investigated this brain region have all reported null results (K. C. R. Fox et al., 2020; K. C. R. Fox et al., 2018; Selimbeyoglu & Parvizi, 2010). The lack of significant effects in previous studies could thus be due to the absence of specific tasks that seem to be necessary to evaluate the effects of stimulation on certain cognitive functions such as decision making (the same argument also holds to explain the absence of behavioral effects following aIns stimulation in most of previous studies).

The idea that vmPFC stimulation increases risk-taking would be consistent with a wide range of neuroimaging studies, assuming that vmPFC is a key component of the reward circuit, processing reward prospects and favoring risky options (Bartra et al., 2013; Blankenstein et al., 2017; Engelmann & Tamir, 2009; Haber & Knutson, 2010; Levy & Glimcher, 2012; Tobler et al., 2007; Venkatraman et al., 2009; Vinckier et al., 2018; Xue et al., 2009). Given that vaIns stimulation leads to a decrease in risk taking, such a result would also be consistent with the hypothesis of an opposing involvement of (v)aIns and vmPFC in decision making developed by a substantial body of work (Palminteri & Pessiglione, 2017; Vinckier et al., 2018).

Limitations and perspectives

In this study, we demonstrate the value of iES on brain areas involved in value-based decision making and uncertain choices. To our knowledge, this is the first time that modification of choice behavior has been observed following iES in humans. The strengths of iES is that it has a high spatial specificity which allowed us to highlight sub-regional differences within the aIns between its ventral and dorsal parts. This result is important because it would hardly be obtained with other causal techniques available for human cognitive neuroscience. Indeed, in humans, brain lesions are generally spatially diffuse and only occasionally selective to specific brain areas. Nevertheless, we acknowledge that iES data comes from patients with severe drug-resistant epilepsy so that it remains unclear how our results can generalize to the healthy population. A possible clinical implication of our findings is that demonstrating that iES is effective in modifying choice behavior may therefore provide new tools for neurologists to guide resection and help prevent postsurgical decision-making deficits that need to be further examined in the future (see Von Siebenthal et al., 2016). Another interesting perspective would be to study mood fluctuations induced by intracranial electrical stimulation in epileptic patients. It would also be relevent to examine how broadband gamma activity is modulated in the non-stimulated brain regions during this experiment to clarify the physiological effects of iES and to quantify

network-level effects of intracranial stimulation that likely explain part of the behavioral effects reported in this study.

5. Material & Methods

Patients selection

Subjects were thirteen patients suffering from drug-resistant focal epilepsy and candidates to surgical treatment (33.1 ± 2.5 years old, 7 females, 5 left-handed, see demographic details in Supplementary Table V.S1). As part of their pre-surgical evaluation, they underwent intracerebral recordings by means of stereotactically implanted multilead depth electrodes (sEEG) in the Epilepsy Unit of Grenoble University Hospital (Grenoble, France). Electrode implantation was performed according to routine clinical procedures and all target structures for the pre-surgical evaluation were selected strictly according to clinical considerations with no reference to the current study. Patients were included in the study if they had electrodes implanted in at least one brain regions of interest (i.e., aIns and/or vmPFC), and if they were willing and able to cooperate with study task. All patients were taking anti-epileptic medications (see Supplementary Table V.S1), some of which were reduced or stopped before stimulation sessions on clinical grounds. Anxiety and depression comorbidities were screened via the Hospital Anxiety and Depression Scale when possible (not executed in one patient due to only mild understanding of French language). Exclusion criteria were age under 18 and complete inability to speak French (to prevent improper execution of the behavioral task due to misunderstanding of task instructions). All patients gave oral informed consent before their inclusion in the present study and signed a non-opposition file in the context of the MAPCOG sEEG study (IdRCB: 2017-A03248-45), approved by the Ethics Committee.

Electrodes implantation and location

Depth electrodes were implanted using robot-assisted sEEG electrode implantation technique (ROSA robot). Fifteen to eighteen semi-rigid electrodes were implanted per patient. Each electrode had a diameter of 0.8 mm and, depending on the target structure, contained 10-18 contact leads of 2 mm wide and 1.5 mm apart (Dixi Medical, Besançon, France). Electrodes were localized and anatomically labeled by co-registering a pre-operative anatomical magnetic resonance imaging (MRI, 3D T1 contrast) with a post-operative computed tomography (CT) scan obtained for each patient, using the IntrAnat Electrodes software (Deman et al., 2018).

The ventral anterior insula (vaIns) was defined as the anterior part (y > 5 in MNI space) of parcels 18 (*G_insular_short*), 47 (*S_circular_insula_ant*) and 48 (*S_circular_insula_inf*) of the Destrieux atlas, while the dorsal anterior insula (daIns) was set as the anterior part (y > 5 in MNI space) of parcel 49 (*S_circular_insula_sup*) of the Destrieux atlas (Destrieux et al., 2010). As for the vmPFC, it was specified using the corresponding parcel from the MarsAtlas parcellation scheme (Auzias et al., 2016).

Intracranial electrical stimulation

Intracranial electrical stimulations (iES) were applied between two contiguous contacts located in a region of interest. Bipolar stimuli were delivered on a pair of contacts (defined as a stimulation site) using a constant current rectangular pulse generator designed for a safe diagnostic stimulation of the human brain (Micromed, Treviso, Italy), according to parameters used in clinical procedures and proven to produce no structural damage. High-frequency stimulation at 50 Hz, with a pulse width of 0.5 ms and an intensity of 1, 2, or 3 mA, was applied in a bipolar fashion during a 5 s period on a stimulation site. For a given stimulation site, the stimulation intensity was determined as the highest intensity devoid of clinical symptoms during previous clinical stimulation sessions.

Stimulation sessions

Each session of the experiment corresponded to the stimulation of a specified stimulation site at a given intensity. Thus, the number of sessions performed by each patient was determined by the number of contact pairs available in regions of interest and the number of intensity tested. Each experimental session consisted of 28 trials of a behavioral task alternating between stimulation (n = 14) and non-stimulation (n = 14) trials (Fig. V.1). The first trial of the session was randomly assigned to either stimulation or non-stimulation to maintain patients' blindness on experimental conditions. Stimulations were manually triggered and iEEG activity was monitored in real-time in order to detect stimulation-induced after discharges and electrographic seizures so as to stop session immediately if necessary. The between trials time interval was also kept above 30 seconds, so that two iES remained separated by a minimum interval of one minute. In stimulation trials, the stimulation was initiated about 1 s before the trial onset.

Behavioral task

Presentation of visual stimuli and acquisition of behavioral data were performed on a PC using custom Matlab scripts implementing the PsychToolBox libraries (Brainard, 1997). All patient responses were done with a gamepad (Logitech F310S) using both hands. Before the exper-

iment, participants were informed that various brain regions would be stimulated, but they were blind to experimental conditions, including stimulation parameters, the brain region being tested, and whether stimulation was active. Each trial consisted of a choice task combined with confidence rating and a cognitive challenge (Fig. V.1).

Choice task. The choice task began with the presentation of an offer consisting of three attributes: a gain prospect (represented by a bunch of 10-cent coins, range: 1-5€), a loss prospect (represented by crossed out 10-cent coins, range: 1-5€) and the upcoming challenge difficulty (represented by a target window corresponding to approximately 50% theoretical success). Challenge difficulty was displayed on the center of the screen (see training section for further details about how difficulty was adjusted to each participant). Patients were asked to accept or reject this offer by pressing a left or right button depending on where the choice option ("yes" or "no") was displayed. Patients' choice determined the amount of money at stake: accepting meant that they would eventually win the gain prospect or lose the loss prospect based on their performance in the upcoming challenge, whereas declining the offer meant playing the challenge for minimal stakes (winning 10 cents or losing 10 cents).

The sequence of trials was pseudo-randomized such that all delta values, computed as the difference between gain and loss prospects, continuously sampled along ten intervals ([-40 -30],]-30 -20],]-20 -10],]-10 -5],]-5 0],]0 5],]5 10],]10 20],]20 30],]30 40]), were displayed for one patient during a session, with the four medium intervals (]-10 -5],]-5 0],]0 5] and]5 10]) presented twice (n = 8 out of 14 trials) to maximize the occurrence of difficult choices. The positions of gain and loss prospects were randomly determined to be either displayed on top or bottom of the screen and similarly, the choice options ("yes" or "no") were randomly displayed on the left or right. Stimulation and non-stimulation trials were strictly identical in one session, such that participants served as their own control. Patients had a free time delay to accept or decline the offer. If they declined the offer, a 250 ms screen displayed the new offer (a minimal stake of 10 cents). Thus, the challenge was performed regardless of the choice answer in order to prevent patients from eventually rejecting more offers to decrease experiment duration.

Confidence ratings. Before performing the cognitive challenge, patients were asked to rate their confidence in winning the challenge by answering the following question "Do you think you will win?". Patients had a free time delay to answer by moving a cursor from left (not sure) to right (sure) along a continuous visual analog scale (100 steps) with left and right hand response

buttons. The initial position of the cursor on the scale was randomized to avoid confounding confidence level with movements' quantity.

Cognitive challenge The challenge started right after confidence confirmation: a ball appeared on the left of the screen and moved, horizontally and at constant speed, towards screen center. Patients were asked to press the confirmation button when they thought the ball was inside the basket displayed at screen center (i.e., the target window). The ball always reached the center of the target after 1s. Thus, the size of the target window represented the margin of error tolerated in patient reaction time (target: 1s after the movement onset of the ball). Unbeknownst to the patients, the success rate was maintained at about 50% by decreasing (if the challenge was successful) or increasing (if the challenge was unsuccessful) the tolerated margin of error by 1% theoretical success after each trial. Importantly, the moving ball could only be seen during the first 500ms (half of the trajectory), and patients had to extrapolate the last 500ms portion of the ball's trajectory to assess whether the ball was inside the target. Finally, a feedback of 1 second was given to the patients about their payoff after the challenge. Note also that, to improve patients' motivation to perform the task as accurately as possible, the total amount of money earned by the patients during a session (calculated by adding gains and losses across all trials) was displayed at the end of a session.

Training. Before the main experiment, a training - divided into three steps - familiarized patients with all sub-parts of the task. In the first step, patients were familiarized with the challenge by performing 30 to 80 trials of it. Another aim of this step was to find the target size for which the participant had a 50% success rate. Thus, unbeknownst to the patients, the size of the bar was decreased after each success and increased after each error by 1 pixel, so that their performance converged statistically at 50%. The task was completed when participants' performance stabilized (most often before less than 80 trials). Each training trial was followed by feedback informing whether the challenge was successful ("ok" in green) or missed ("too slow" or "too fast" in red). In the second step, patients performed 64 trials of the full choice (i.e., the challenge was always preceded by an offer), and a feedback on the money won/lost in the trial was displayed at the end of each trial. The goal was to train patients to properly integrate the dimensions of the offer (gains and losses) when making their choice. Finally, the third and last part of the training (8 trials) was totally similar to the main task to allow patients to familiarize with confidence ratings.

Another purpose of the training was to tailor the difficulty of the challenge to each patient's ability. To do so, a tolerated margin of error corresponding to a theoretical success of 55% (i.e. the tolerated margin of error used in the first trial of a session of the main task) was estimated from each individual patient by assuming that errors were normally distributed. Note that during training, this tolerated margin of error was updated after each trial (average and standard deviation of challenge performance were updated). Among patients, the tolerated margins of error corresponding to 55% theoretical success ranged from [± 60 ms] in the most precise patient to [± 206 ms] in the less precise one.

Behavioral analysis

Statistical analyses were performed with Matlab Statistical Toolbox (Matlab R2018a, The MathWorks, Inc., USA).

Choice behavior. Analysis of choice behavior was performed across all sessions (i.e., stimulation sites) using a logistic mixed-effects model (estimated with the *fitglme* function) that included gain and loss magnitude as predictor variables and choice as a dependent variable. The model also comprised a full random-effects structure at the subject and stimulation site levels (intercepts and slopes for all predictor variables). For both fixed effect (gain and loss), the estimated coefficient value (β) $\pm$ its standard error is reported, as well as the t-statistics (testing that the coefficient is equal to 0) along with its p-value.

Stimulation effects. All dependent variables (acceptance probability, reaction time and confidence ratings) were analyzed at the session level and tested for significance at the group level (daIns, vaIns or vmPFC) using two-tailed paired t-tests between stimulation and non-stimulation conditions. All means are reported along with the standard error of the mean (S.E.M).

6. Supplementary material

Supplementary Table V.S1: Demographical data. CAR: carbamazepine; CLO: clobazam; daIns: dorsal anterior insula; F: female; L: left; LAC: lacosamide; LEV: levetiracetam; LOR: lorazepam; M: male; N/A: not available; OXC: oxcarbazepine; PER: perampanel; R: right; vaIns: ventral anterior insula; vmPFC: ventromedial prefrontal cortex; ZON: zonisamide.

ID	Sex	Age (year)	Epilepsy onset (age)	Hand laterality	Anti-epileptic drugs	Stimulation site	Intensity (mA)	ROI
P1	F	38	3	R	LEV, LAC, CLO	Qp1-2	3	daIns
P2	F	31	12	L	CAR, CLO, LEV	X2-3 X3-4 X4-5	1 3 3	vaIns vaIns daIns
P3	F	44	12	R	CAR, LAM, LEV	Op1-2 Qp1-2 Xp4-5	3 2 1	vmPFC daIns daIns
P4	M	41	14	R	CLO, LAC, OXC	O1-2 S1-2 Z1-2 Z5-6	2 1 2 3	vmPFC vmPFC vaIns daIns
P5	F	25	21	L	CLO, LAC, ZON	B1-2 O1-2 Q1-2 Q4-5 R2-3	3 3 3 3 1	daIns vmPFC vaIns daIns daIns
P6	M	41	8	R	CAR, LAC	Op1-2 Qp1-2 Rp1-2	3 2 1	vmPFC daIns daIns
P7	M	37	34	R	CAR, ZON	Xp1-2 Xp4-5	3 2	vaIns daIns
P8	F	48	36	L	CLO, LAC, OXC, ZON	K4-5 Kp7-8 O1-2 R1-2	3 3 3 3	daIns daIns vmPFC daIns
P9	M	31	21	R	CAR, PER, CLO	Op1-2 Qp1-2 Xp3-4 Zp2-3 Zp3-4 Zp4-5 Zp5-6	1 1 3 1 3 3 3	vmPFC daIns vmPFC vaIns daIns daIns daIns
P10	M	25	N/A	R	N/A	Rp1-2	2	daIns
P11	F	18	N/A	L	N/A	Qp1-2 Xp1-2 Xp5-6	3 2 3	daIns vaIns daIns
P12	M	26	N/A	R	N/A	Gp10-11 Kp1-2 Kp3-4 Op1-2 Qp1-2 Xp2-3	3 3 3 3 3 3	daIns vaIns vaIns vmPFC daIns vmPFC
P13	F	25	N/A	L	N/A	Q1-2 X1-2 Xp1-2 Xp4-5 Yp1-2 Yp4-5	3 3 2 3 3 3	daIns vaIns vaIns vaIns vaIns daIns

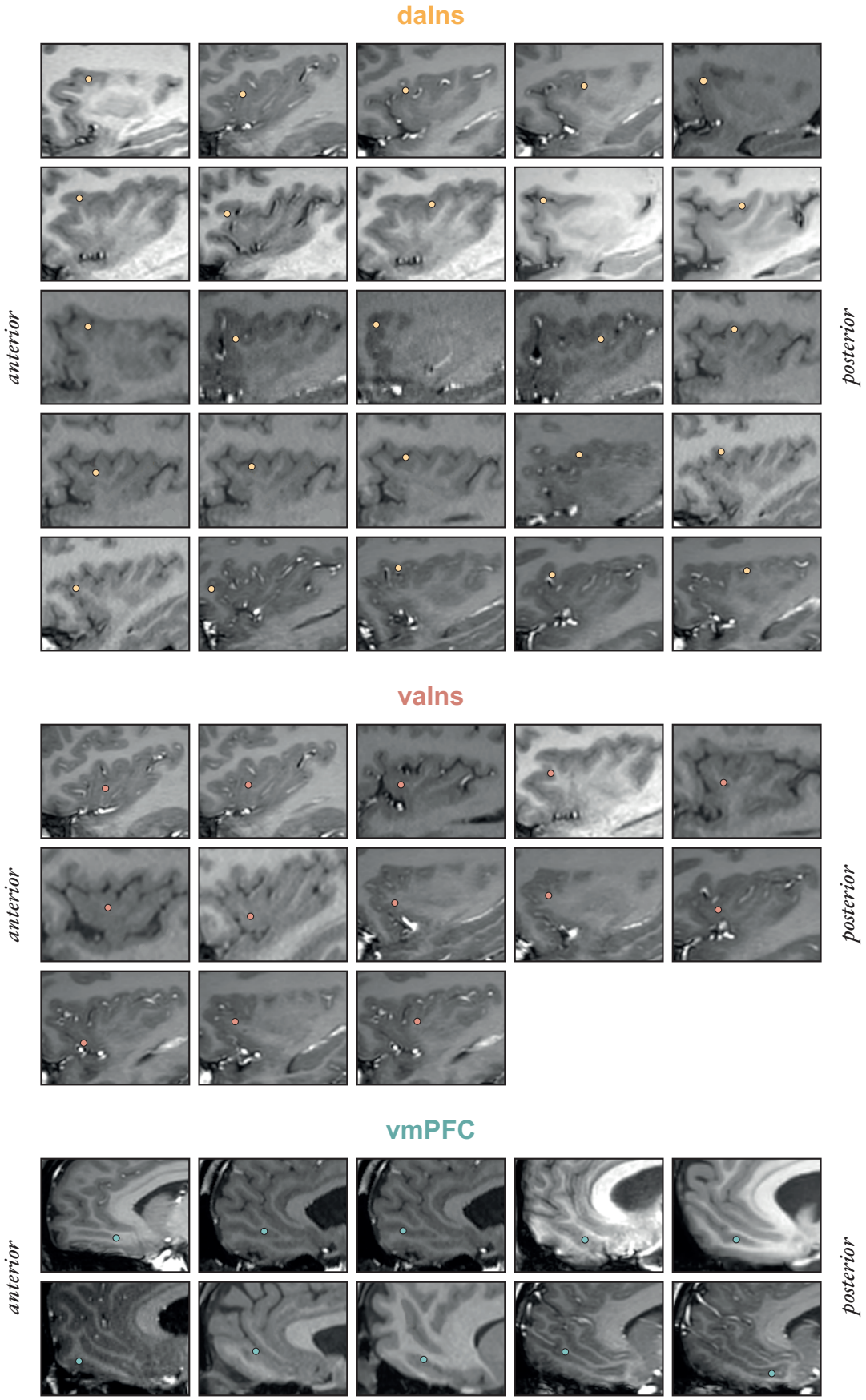

Supplementary Figure V.S1: **Location of stimulation sites on MRI brain slices.** The locations of each stimulation site in the daIns (yellow), vaIns (orange), and vmPFC (green) are displayed on sagittal slices.

VI

General discussion

What have we learned?

The work carried out during this PhD and presented in this manuscript has been articulated around two objectives. First, we sought to elucidate the computational and intracerebral mechanisms underlying the observed variability of choice in particular contexts. To this end, we manipulated mood (Study 1) and monitored visual attention (Study 2) of subjects undergoing invasive electrode monitoring with sEEG for their epilepsy as they performed different versions of the same accept/reject choice task. **We found that mood and visual attention modulated in a valence-specific manner the BGA (50-150 Hz) of two core regions involved in the computation of expected values, namely the ventromedial prefrontal cortex (vmPFC) and anterior insula (aIns), thereby influencing the final decision**. Specifically, in the first study, we showed that high mood levels led to increased baseline broadband gamma activity (BGA) in the vmPFC, which in turn promoted risk taking by selectively increasing the weight of potential gains, whereas low mood levels led to increased baseline BGA in dorsal anterior insula (daIns), which in turn tempered risk taking by selectively increasing the weight of potential losses (Fig. VI.1 top). Similarly, when visual attention was focused on gains, these positively modulated BGA in the vmPFC, thus mediating the positive effect of gains on the likelihood of accepting the offer, whereas when visual attention was focused on losses, these positively

modulated BGA in the aIns, thus mediating the negative effect of losses on the acceptance rate (Fig. VI.1 middle).

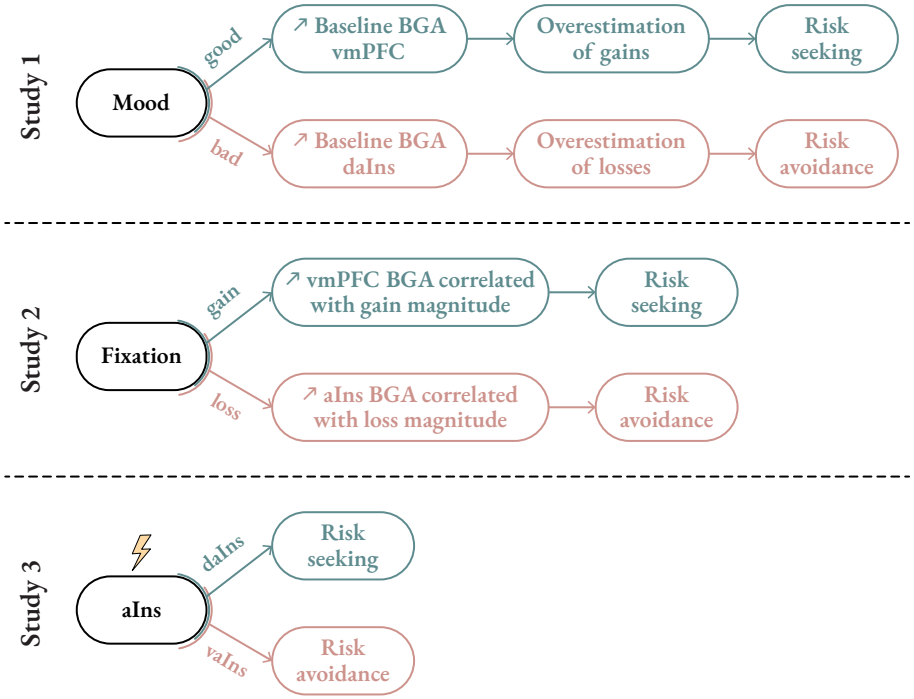

Figure VI.1: Summary of experimental findings. The box-and-arrow diagrams illustrate the main results of the first (top), second (middle), and third (bottom) studies of the PhD work presented in this manuscript. aIns: anterior insula; BGA: broadband gamma activity; daIns: dorsal anterior insula; vaIns: ventral anterior insula; vmPFC: ventromedial prefrontal cortex.

In a second step, we investigated whether the two regions identified in these initial investigations were causally involved in decision making (Study 3). For this purpose, we stimulated the vmPFC and aIns of implanted patients with intracerebral electrodes while they performed the same choice task as in the first two studies. **Our results revealed that stimulation of the aIns was effective in inducing a decision bias and that two sub-regions of this structure were differentially involved in decision making**. Specifically, stimulation of the daIns resulted in a higher acceptance rate of the choice offer, whereas stimulation of the ventral anterior insula (vaIns) decreased this rate (Fig. VI.1 bottom).

Taken together, **these results suggest the existence of opponent brain systems that individually process appetitive and aversive attributes related to choice**. In the following section, I will discuss these findings, starting with the methodological aspect, and then focusing on their theoretical implications. In the course of this discussion, I shall also endeavor to address the limitations and perspectives associated with this experimental work.

1. Methodological considerations

a. Investigating human cognition with intracranial EEG

About the advantages of using intracranial EEG

Traditionally, when studying human cognition, researchers attempting to establish the anatomical location of the neural computations underlying a certain behavior rely on fMRI. This metabolic imaging technique allows precise spatial localization across the brain, but its temporal resolution is limited. If the timing of neural computations is more relevant, electrical imaging techniques, such as EEG or MEG, are therefore preferred. The latter have excellent temporal resolution, but only measure signals from superficial cortical regions, with little spatial certainty about their anatomical origin. To overcome these limitations, an alternative would be to use invasive recording techniques, such as local field potential recording, which allow a more direct measurement of neural processing with high spatial and temporal accuracy, but their use is generally limited to animal studies. In some rare cases, however, such as prior to neurosurgical intervention, intracranial electrophysiological recordings can be performed in humans. During my PhD, I had the unique opportunity to use this approach by performing iEEG recordings in epileptic patients who were implanted with multiple intracranial electrodes as part of presurgical clinical investigations.

Intracranial EEG arguably offers a very interesting compromise between anatomical accuracy, temporal resolution, and simultaneous coverage of multiple nodes of interest for studying the human brain (Parvizi & Kastner, 2018). Yet, meeting these characteristics has proven to be essential to address our experimental questions. Indeed, in the first study, good temporal resolution appeared crucial to distinguish activities related to several temporally close processes such as activity during feedback, baseline activity and activity during decision making. Similarly, in the second study, the temporal resolution of iEEG successfully discriminated brain activity during natural free viewing, which would not have been possible in fMRI. On the other hand, in all three studies, the anatomical accuracy of intra EEG was necessary to explore regions such as vmPFC and aIns that are located deep in the brain, and thus cannot be properly investigated with EEG or MEG. Likewise, this precision allowed us to distinguish two anatomical sub-regions of the aIns that appear to play distinctive roles in decision making (study 1 and 3). Finally, compared to single-unit recordings in non-humans, the concurrent coverage of multiple brain areas allowed us to simultaneously test the involvement of several regions that were potentially related to the processes being tested. For example, in our first study we found

that both vmPFC and aIns were involved in mood encoding, as already identified with fMRI (Vinckier et al., 2018), whereas lOFC, which had previously been negatively correlated with mood (Rao et al., 2018), was not significant. However, it is important to note that, although on average the implantations cover a large portion of the brain, only a very small percentage of it (∼1%) is explored simultaneously in each patient. Furthermore, because the pattern and type of implantation is dictated by clinical need and most epileptic patients have seizures in the limbic and frontal lobes, recordings of the parietal, occipital, and inter-hemispheric areas are relatively scarce (Parvizi & Kastner, 2018). Thus, unlike fMRI, intracranial EEG cannot provide a complete coverage of the brain and null results should be considered with caution.

The processing of intracranial EEG signal

One of the most remarkable features of intracranial EEG is its ability to capture signals in a specific frequency range, such as delta, theta, alpha, beta, and gamma oscillations, as well as the broadband gamma signal (BGA). In our first study, we aimed to investigate whether the amount of activity in each bandwidth (i.e., the amplitude of the filtered signal) contributed to the subjects' mood level. To this end, we compared different generalized linear models (GLM) including the BGA and all possible combinations of the other frequency bands. Our results indicated that for both vmPFC and aIns, BGA was a significant predictor of mood, whereas lower frequency activity provided no additional information and was at best redundant with BGA. Given that these two brain regions have previously been identified as correlated with mood in an fMRI study (Vinckier et al., 2018), these results are consistent with the common understanding that hemodynamic activity corresponds to high-frequency (Logothetis et al., 2001; Manning et al., 2009; Mukamel, 2005; Niessing et al., 2005; Nir et al., 2007). In addition, the finding that the data conveyed by low frequencies does not provide additional information compared with BGA had already been reported in several studies using a similar procedure (Gueguen et al., 2021; Lopez-Persem et al., 2020). Overall, these results prompted us not to pursue the analysis of the low-frequency bands in this first study and to focus exclusively on the BGA in the second study. Nevertheless, we acknowledge that the iEEG signal is very rich, and that examining amplitude changes in specific frequency bands is far from the only way to analyze this signal. In particular, while the BGA appears to reflect the local responses of a population of neurons, the low frequency oscillations (i.e., theta, alpha, and beta) are thought to serve as carrier frequencies used by distant nodes within large-scale networks to communicate (Buzsáki, 2006). Thus, other analyses, such as measuring the coupling between the phase of slow oscillations and the power of higher frequencies (notably the BGA) or measuring the phase coupling between two oscillatory rhythms could also be performed to inform important aspects of the functional dy-

namics of brain activity that we have not addressed in this work, such as the directionality of information flow through a network (Canolty & Knight, 2010).

Towards causal studies of BGA

In our first study, we demonstrated that trial-to-trial variations of baseline activity in the vmPFC and daIns influenced the valuation process at the time of choice, which in turn impacted the behavioral response. As discussed in the introduction of this manuscript, these results are consistent with several previous studies (Kuhnen & Knutson, 2005; Lopez-Persem et al., 2016; Vinckier et al., 2018), reinforcing the idea that spontaneous fluctuations in brain activity play a functional role in the valuation process. However, given their correlative nature, our data cannot elucidate whether baseline activity is causally involved in decision making. In this first study, we predictably manipulated pre-stimulus activity through the use of a mood induction procedure prior to choice. Over the course of this PhD, I also began to implement an alternate method for testing the role of ongoing brain activity in decision making, which involves *analyzing iEEG activity in real time*, triggering the onset of the choice stimulus when target brain regions are in a "up-" or "downstate" (Fig. VI.2).

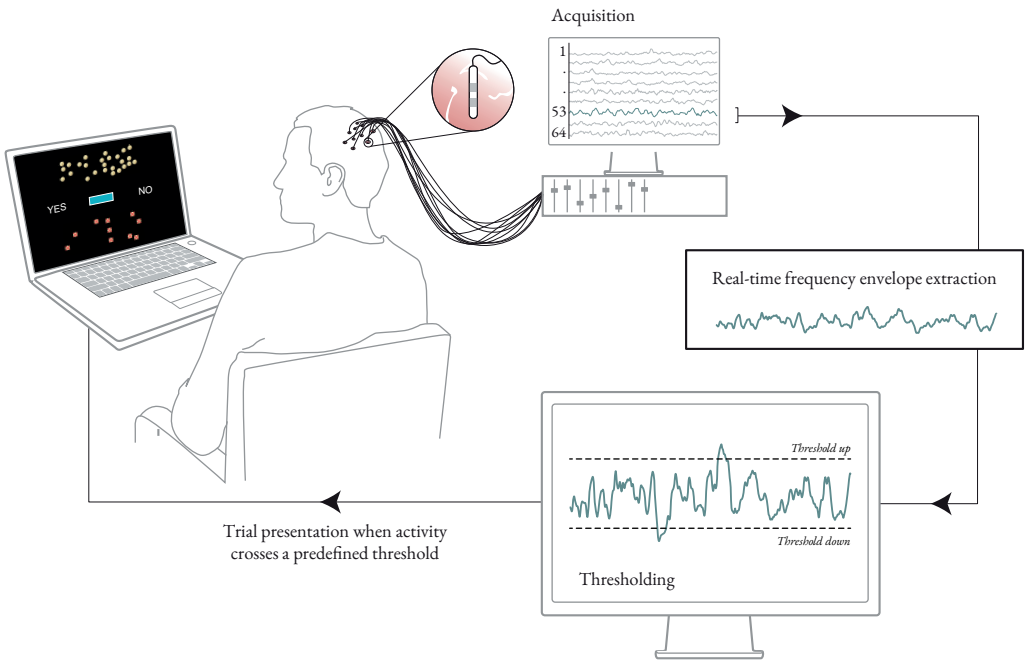

Figure VI.2: Concept of a brain-computer interface for testing the functional role of ongoing oscillatory activity. Incoming sEEG data recorded by intracranial electrodes are retrieved online and the envelope of a specific frequency band is extracted in real-time for a single recording site (i.e., a bipole) located in a region of interest. If the oscillatory activity crosses one of the two predefined thresholds (i.e. in high or low activity states of the chosen frequency band), a stimulus (e.g., choice onset) is displayed on the screen in front of the participant. Adapted from Cerf et al. (2010).

This approach, which has been referred to as contingent trial presentation, has previously been used in work that examined the effects of pre-stimulus memory and learning in rabbit hippocampus (Griffin et al., 2004; Hoffmann & Berry, 2009; Nokia & Wikgren, 2014; Seager et al., 2002). Interestingly, these studies found that trial presentation as a function of theta oscillation quantity had a significant impact on memory encoding and learning. To our knowledge, only two studies have used contingent trial presentation in humans, combined with EEG (Salari & Rose, 2016) or iEEG (Burke et al., 2015). Both studies were able to link the amount of a pre-stimulus electrophysiological signal to a specific behavior, suggesting that this method can, theoretically, allow functional differentiation of the effective role of ongoing oscillatory activity in specific frequency bands.

With respect to this PhD work, the use of a brain-computer interface that monitors the amount of activity in a certain frequency band in real time could help advance several points. First, one possibility would be to trigger the onset of choice based on BGA (and/or lower frequency bands) activity (Fig. VI.2). This setup would allow us to capitalize on the naturally fluctuating neural activities prior to choice onset to test whether the ongoing oscillatory activity in our regions of interest has an influence on value-based decision making. A second possibility would be to trigger a mood rating rather than a choice based on the amount of activity in a certain frequency band. Indeed, in the first study, we found that in addition to BGA, theta, beta and gamma activities were also correlated with mood in daIns. Although we concluded using a model comparison procedure that these frequency bands did not provide any additional information compared to BGA, using such a technique would allow us to further understand whether the information conveyed by distinct frequency bands is truly redundant. Finally, a third possibility could be to use this brain-computer interface to stimulate the brain before a choice while it is in a particular state. Such an approach has already been employed in the field of memory, where it has been shown that stimulation increased memory performance when delivered in poor encoding states, but had the opposite effect when delivered in a high encoding state (Ezzyat et al., 2017). Thus, one might speculate that a similar mechanism is at play when stimulating the vmPFC and aIns during decision making. In particular, this could explain why the effects of stimulation were not stable across sessions. Using this more advanced methodology may help us address this issue. Overall, the advantage of using a brain-computer interface to perform contingent trial/stimulation presentation is that it goes beyond simple correlations between brain and behavior and does not require the use of another task prior to the choice (as in the mood induction procedure used in our first study) or a learning phase (as in neurofeedback experiments).

Toward cellular mechanisms of value-based decision making

As pointed out by Parvizi and Kastner (2018):

> "One advantage of human iEEG studies over those conducted in laboratory animals such as monkeys or rats is that humans can perform tasks based on verbal instructions, and they do so with minimal training and in the absence of ongoing reward or task-cueing. Such an approach allows more ecologically valid and ethologically relevant experiments than are possible in most animal species, also avoiding the potential confound of overtraining."

Added to this is the fact that some specific cognitive functions, such as the concept of mood, are difficult to approach with animal models. Still, single-cell studies in animals retain the advantage of providing access to the activity of individual neurons, which can only be measured indirectly with iEEG. Indeed, as mentioned before, the recorded iEEG signal consists in the sum of local field potentials generated by large populations of cells adjacent to the recording electrode, and is therefore too crude to discern the activity of individual neurons. In a few medical centers, however, it is currently possible to record the activity of single neurons in humans by using specific electrodes provided with microwires into the core of the shaft (Fried et al., 1999) or hybrid electrodes that have high impedance contacts, for the recording of action potentials from single units, interspersed with low impedance contacts for the recording of the electroencephalographic signal (M. A. Howard et al., 1996). Recently, new hybrid electrodes with a smaller diameter and the ability to extend tetrodes with a micrometer screw have also been introduced (Fig. VI.3; Despouy et al., 2020). This specificity is significant in that it improves the search for reactive neurons, which could have been a limiting factor with previous electrodes, and should therefore contribute to make studies using this technique more accessible.

So far, much of the single-neuron research in humans has focused on memory, perception, or navigation (see Mukamel and Fried, 2012; Quiroga, 2019 for reviews). These studies have validated and complemented work done with fMRI or EEG, but have also provided information that could not have been obtained with other techniques, such as the landmark discovery of low-activity neurons known as concept cells (i.e., cells that respond very selectively to specific and well-known concepts). In comparison, very few studies have examined human neural activity in value-based decision making (Jenison et al., 2011; F. Mormann et al., 2019; Unruh-Pinheiro et al., 2020). Thus, we believe that conducting single neuron recordings in the human brain during a decision making task could significantly improve our knowledge of the decision mak-

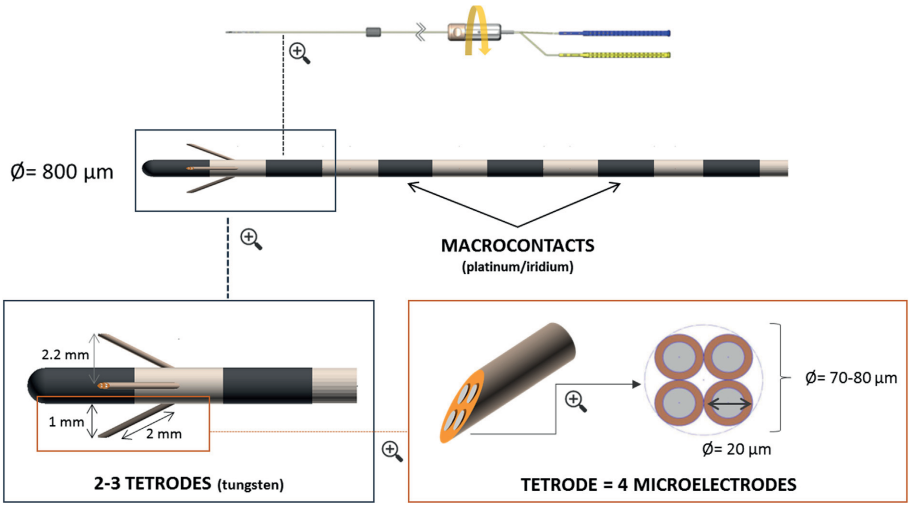

Figure VI.3: New hybrid micro-macroelectrode. The difference with a clinical macroelectrode is the inclusion of three tetrodes that can be extended from the shaft between the most medial macrocontacts by up to 2 mm. Each tetrode is composed of four tungsten microwires with a diameter of 20 mm (overall diameter: 70–80 mm). From Despouy et al. (2019).

ing process. Notably, in this work, we found evidence suggesting that appetitive and aversive processes are encoded in distinct brain regions. In particular, good mood and monetary gains were correlated with the BGA of the vmPFC, whereas bad mood and monetary losses were correlated with the BGA of the aIns. Nevertheless, in the literature, this dissociation is not always observed as some data indicate coding of negative values in the vmPFC (e.g., Plassmann et al., 2010; Tom et al., 2007). Also in our second study, we observed that vmPFC correlated positively with loss value when fixated. Moreover, in our third study, we found a dissociation within the insula itself by showing that stimulation of different sub-regions influenced approach and avoidance behaviors in opposite ways when faced with an uncertain choice. It would therefore be interesting to test whether opposing systems of reward and punishment encoding are also found at the cellular level. For example, one might think that different types of cells would encode aversive and appetitive stimuli, and that these cells might be present in different proportions and/or in different brain structures. At another extreme, there might be neurons that would integrate aversive and appetitive information through opponent signals (e.g., by decreasing their firing rate for aversive stimuli vs. increasing their activity for appetitive stimuli). The exact mechanisms underlying valence encoding at the cellular level remains a debated issue even in non-human primate studies.

Pathological vs. physiological activities

An obvious limitation of iEEG recordings in humans is that these data come from patients with long-standing epilepsy. This fact raises the concern that the results obtained may reflect

different aspects of this pathology rather than normal brain function. Several arguments are, however, opposed to this hypothesis. First, it has been repeatedly observed that the responses obtained with iEEG recordings are remarkably comparable to those obtained in healthy subjects on fMRI, as was the case in our first study (Cecchi et al., 2021) with that of Vinckier et al. (2018). Moreover, similar results are commonly found in patients with different types of epilepsy involving different pathophysiological mechanisms. Despite this, the distinction between pathological and physiological activity had not been explored until recently (S. Liu et al., 2018; S. Liu & Parvizi, 2019; von Ellenrieder et al., 2016). Epileptogenic tissue is thought to be typically characterized by high frequency oscillations (HFOs, 80–500 Hz) that can be recorded with iEEG, and have different temporal characteristics (i.e., bursts of HFOs are of shorter duration than bursts of BGA, see S. Liu and Parvizi, 2019) compared to broadband gamma activity (BGA) that is witnessed under normal conditions. Notably, HFOs are associated with interictal epileptiform discharges and are randomly interspersed with pathological background activity (Jiruska et al., 2017; Schevon et al., 2009), whereas BGA is time-locked to the presentation of specific stimuli or cognitive conditions (Parvizi & Kastner, 2018). In a recent study, S. Liu and Parvizi (2019) explored the extent to which epileptic tissue was able to generate physiological responses to cognitive stimuli. Their results support that non-lesional epileptic tissue still produces functional responses to cognitive stimuli and that the intrinsic HFOs generated by this tissue are different from the BGA activity induced by cognitive stimuli. Notably, this confirms that brains affected by epilepsy are a suitable model to study the normal neural mechanisms underlying various aspects of human cognition and behavior. Strikingly, their study also reveals an inverse functional relationship between pathological and physiological high-frequency activities within the epileptic tissue, which implies that relevant cognitive stimuli fail to activate epileptic tissue if they occur within the time window of HFO epileptic activity. In other words, HFO activity appears to have a transient negative interfering effect on the physiological response profile of brain tissue. In particular, they were able to demonstrate that this effect could explain the subject's impaired performance in recognition memory. In our studies, we always assumed that the pathological activity did not influence the neural or cognitive processes of interest. However, this latest study indicates that HFOs induce a "cognitive refractory state". It would therefore be interesting to re-analyze our dataset with this effect in mind to quantify how pathological HFO interferes with physiological BGA.

b. The use of intracranial electrical stimulation

As previously mentioned, many different analyses can be performed with the iEEG signal, such as processing the amount of activity in each bandwidth or examining the interaction of activity between different frequencies. The richness of this data is a real advantage, but it can also be a burden as it is open to multiple interpretations and can lead to misleading results. Combining passive recordings with active electrical stimulation is regarded as an optimal way to confirm the validity of a hypothesis by providing evidence of causality (Parvizi & Kastner, 2018).

Direct electrical stimulation is an effective tool for disrupting value-based choices and behaviors

In our third study, the use of iES in a structure involved in value-based decision making and uncertain choices resulted in alterations of choice behavior. Specifically, stimulation of the aIns during the display of choice options was effective in inducing a decisional bias. Such results had previously been obtained in an approach/avoidance task in macaque monkeys (Saga et al., 2019), but to our knowledge, this is the first time that modification of choice behavior has been observed following iES in humans. In addition, iES allowed to highlight regional differences within the aIns between its ventral and dorsal parts. This result is of importance because it could probably not have been obtained with a lesion study. Indeed, in humans, brain lesions are generally spatially diffuse and only occasionally selective to specific brain areas. It would therefore be difficult to find patients with non-overlapping lesions in these two spatially very close structures. Finally, iES is originally used in patients with severe drug-resistant epilepsy or brain tumors to precisely delineate the brain area that can be resected without causing neuropsychological deficits (Borchers et al., 2012; Desmurget et al., 2013). Despite these precautions, some surgical procedures remain associated with decisional deficits. Demonstrating that iES is effective in modifying choice behavior may therefore provide new tools for clinicians to guide epilepsy surgery and help prevent postsurgical deficits.

Local vs. network effects of iES

It should be noted that in our third study, we interpreted the results of stimulation as being solely local effects. However, it is widely assumed that electrical stimulation depolarizes a population of neurons around the stimulation site, which will transmit signals along cortico-cortical fibers and remotely depolarize several populations of neurons in other cortical areas (Keller et al., 2014). These responses to stimulation, recorded with intracerebral depth electrodes and averaged over a set of pulses, are called cortico-cortical evoked potentials (CCEP; Fig. VI.4a). Mea-

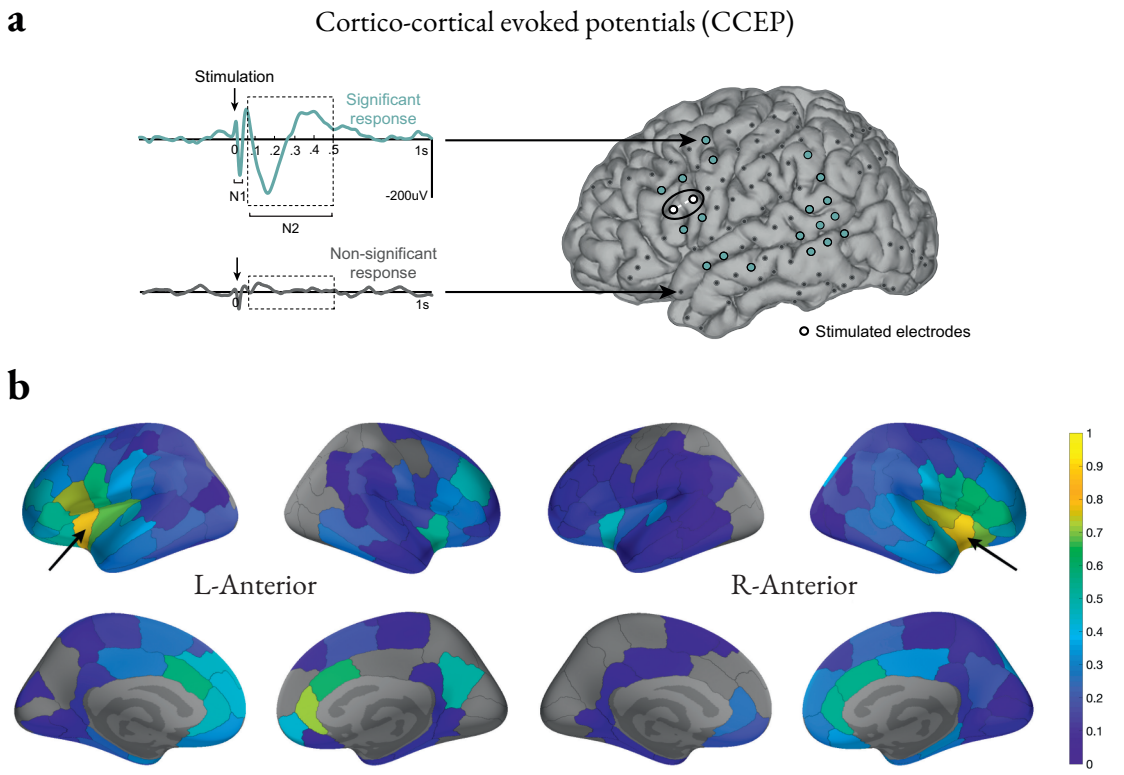

Figure VI.4: Cortico-cortical evoked potentials (CCEP) mapping and connectivity probability. (a) CCEP in response to single-pulse electrical stimulation from an electrode pair (in white) are recorded on all implanted electrodes. The components of the CCEP include an early N1 and late N2. Responses can be classified as significant (green) or non-significant (grey) based on the mean waveform. From Keller et al. (2011). (b) Maps of connectivity probability for the stimulation of the left (L) and right (R) anterior insula. Grey parcel represents no data within that parcel. Black arrow displays the location of stimulation. From Ayoubian et al. (2021).

surement of CCEP to distal cortical stimulation is a well-established technique used in clinical neurophysiology to determine the effective connections between two cortical sites of interest (Gollo et al., 2017). Thus, analyzing the amplitude and latency of CCEPs generated on the three regions of interest of study 3 (daIns, vaIns and vmPFC) would allow us to quantify the cortical circuits that may mediate the reported effects of iES. However, due to time constraints, we were not able to examine intracerebral electrophysiological data in the third study. In any case, connectivity studies from iEEG are not ideal since they suffer from poor spatial sampling available in a single patient and the coverage of recording electrodes is mainly focused on the epileptic network of interest. To circumvent this issue, we could additionally rely on connectivity atlases such as the one constructed from the F-TRACT database (https://f-tract.eu/atlas/), which is based on intra-cortical stimulation and provides a probabilistic quantification of human cortico-cortical connections from a large number of patients (Fig. VI.4b; David et al., 2013; Keller et al., 2014; Trebaul et al., 2018).

2. Theoretical implications

a. Opponent systems vs. alternative hypotheses: how are valence, mood, and attentional bias on choice implemented in the brain?

As discussed in the introduction to this manuscript, the question of the neural basis of appetitive and aversive processes is the subject of much debate. All three experiments conducted in this PhD suggest that two opposing systems coexist in the brain, one used to process rewards and positive stimuli in general and the other that would be used to process punishments and negative stimuli. This result is further discussed in the following section.

The dimensionality of mood

A somewhat related debate in emotion science centers on whether the valence of mood is more accurately conceived of as a bipolar or bivalent construct. According to the bipolar view (Russell, 2003), the valence of mood exists on a continuum ranging from unpleasant affect at one end to pleasant affect at the other end, with neutral mood being a zero point with no valence between these poles. In contrast, according to the bivalent view (Watson et al., 1988; Watson & Tellegen, 1985), the valence of mood varies along two independent dimensions: a positive affect dimension going from neutral to pleasant, and a negative affect dimension going from neutral to unpleasant. In our first study, we found that mood was positively correlated with BGA in the vmPFC and negatively correlated with BGA in the daIns. Furthermore, by analyzing bad, neutral, and good mood levels separately, we found that a higher BGA signaled the two extreme tertiles: good mood in the vmPFC and bad mood in the daIns. Thus, this result is rather consistent with the bivalent view as it suggests that good and bad moods are best conceived as independent components relying on distinct brain systems. However, a limitation of our design was that mood ratings were assigned on a unidimensional scale (from bad mood to good mood), which prevented us from effectively testing for the presence of two underlying dimensions. Furthermore, although our results are in agreement with other previous findings (Eldar & Niv, 2015; Vinckier et al., 2018), there is no consensus regarding how mood is implemented in the brain. Notably, several studies have reported a positive correlation between mood and the insula (Bijanzadeh et al., 2019; Rutledge et al., 2014; Young & Nusslock, 2016). Additional studies using separate rating scales are therefore needed to determine whether mood is indeed supported by two opposite brain systems.

It may also be noted that we found results close to those of Vinckier et al. (2018) using a very similar task, whereas the other studies that found different results did not present the same mood-inducing task structures. Notably, in one of these studies, gains and losses were not present on all trials (Rutledge et al., 2014), while in the other, negative valence was not induced at all (Young & Nusslock, 2016). This raises the question of the extent to which the structure of the mood-inducing task can explain these discrepancies. Similarly, the timescale at which mood fluctuations were assessed could have an impact on the results. In our first study, mood was manipulated through feedback received by patients during a quiz task. Such a procedure had already proved effective in manipulating self-reported mood in laboratory experiments (Eldar & Niv, 2015; Rutledge et al., 2014; Vinckier et al., 2018). Furthermore, we found that our mood measurements reflected the cumulative impact of multiple feedbacks, which distinguished them from emotions related to a single stimulus. Nevertheless, the dynamics of these fluctuations, which last only few minutes, are short-lived compared to more ecological fluctuations collected over several hours in the study by Rao et al. (2018). There is also no evidence that the neural processes underlying mood changes over shorter and longer timescales are identical. Further studies, examining the neural correlates of mood over different timescales, are therefore needed to confirm our findings.

Functional opponency: from baseline iEEG vs. gaze-dependent iEEG

In our first study, we demonstrated that opponent systems existed in the brain even before the choice offer was presented. In particular, baseline activity provided opposing choice predictions in the vmPFC and daIns. Using a computational model, we were able to show that pre-offer activity in the vmPFC and daIns had competing effects on the decision by acting on different attributes of the choice. In particular, baseline activity in the vmPFC positively modulated the weight assigned to gains, while baseline activity in the daIns positively modulated the weight associated with losses. However, this result could not be tested without a model because, although we showed that baseline activity was carried over to choice-related activity, we were unable to find a direct correlation between activity during the decision process and the different attributes of the offer. In conducting the second study, we found that this was actually unattainable without the use of eye fixation data. Indeed, in this study, we showed that the correlation between activity during the decision process and attributes depended on whether the latter were fixated or not, and that simply averaging the signal over the choice process did not allow us to identify reliable neural correlates of attribute valuation. In particular, we showed that the gain value signal was modulated by gaze in the vmPFC and the loss value signal was (notably) modulated by gaze in the aIns. Strikingly, this gain- or loss-fixation-dependent signal positively predicted

choices in the vmPFC and negatively in the aIns, respectively. Although we did not investigate pre-choice activity in this work, it is tempting to relate these results to those of the first study. Notably, it would be consistent with the computational model to assume that the baseline in the vmPFC influences the gain-fixation-dependent signal, which in turn influences choice, whereas the baseline in the aIns would influence the loss-fixation-dependent signal and thus negatively influence choice, but this remains to be demonstrated.

A limitation of the second study is that we did not formulate any computational mechanisms underlying our observations. This is partly because most of the work that has studied attentional bias on value-based decision making has focused on tasks with binary choices containing only a single (usually appetitive) attribute, as is the case for aDDM (Krajbich et al., 2010). However, in our study, we used an accept/reject choice task mixing appetitive and aversive attributes. Sequential sampling models that detail how multi-attribute decisions are made have been developed previously, but these do not incorporate the observed distribution of attention throughout the decision (e.g., Bhatia, 2013; Trueblood et al., 2014; Wollschläger and Diederich, 2012. Recently, however, a study has addressed this decision framework and proposes a modification of the aDDM, called the binary-attribute attentional drift diffusion model (baDDM), to describe the process of choosing between simple binary-attribute options and how it is affected by fluctuations in visual attention (Fig. VI.5).

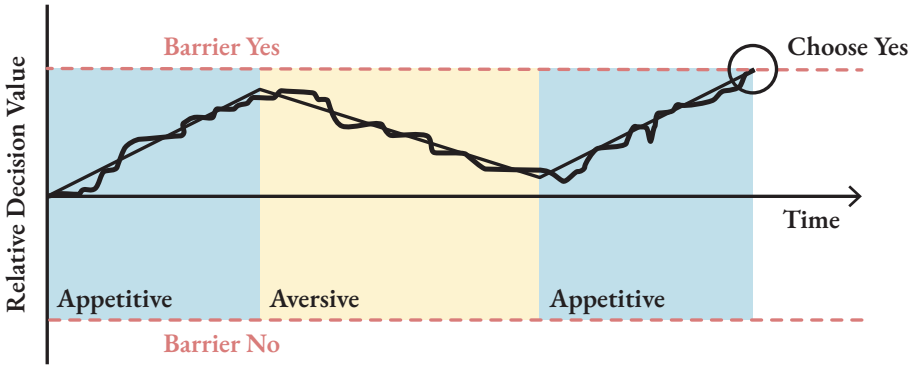

Figure VI.5: Depiction of the binary-attribute attentional drift diffusion model (baDDM). A relative decision value (RDV) signal evolves over time. Its slope is biased towards the fixated item, but random noise is added to the RDV at every millisecond. When the RDV hits a barrier, a decision is made. The shaded vertical regions represent what item is currently fixated. In this example, three fixations are made (appetitive, aversive, appetitive) and the individual chose "yes." The equations below the image describe how the RDV is integrated over time. The parameter δ describes an increase in weight that the attended item receives, while the parameter θ describes a decrease in weight that the unattended item receives. From Fisher (2017).

The aDDM has previously been used to estimate how attention biases the drift rate based on which of several choice options is currently fixated (Krajbich et al., 2010). To do this, a single fixation bias parameter is applied to the unattended option, so that its value is discounted in the evidence accumulation process. The baDDM extends this model by proposing to estimate separately the degree to which the weight of the monitored attribute increases and the degree to which the weight of the unmonitored attribute decreases (Fig. VI.5). Consequently, one could consider using this model to specify the neuro-computational mechanisms in our study. Nevertheless, another difficulty is that baDDM does not account for neuroanatomy. This is in addition to the fact that there are very few studies that show an effect of visual attention on value (see section II.3.c), and to our knowledge we are the first to show a direct effect of attention-modulated brain activity on choice. Thus, it remains to be addressed how distinct regions can be incorporated into the baDDM model.

List of Abbreviations

aDDM attentional drift-diffusion model. 33, 34, 115
aIns anterior insula. 81, 111, 129, 135, 150

baDDM binary-attribute attentional drift diffusion model. 163
BDM Becker-DeGroot-Marschak. 49
BGA broadband gamma activity. 79, 116, 129, 150
BOLD blood-oxygen-level-dependent. 39
BVS Brain-Valuation System. 121

CCEP cortico-cortical evoked potential. 159

daIns dorsal anterior insula. 79, 102, 134, 136, 150
DDM drift diffusion model. 16, 17, 34, 112

EcoG electrocorticography. 37, 38
EEG electroencephalography. 36–38
EU expected utility. 19–21
EV expected value. 19

fMRI functional magnetic resonance imaging. 36, 39, 80, 135

GLM General Linear Model. 88, 103, 119
GLMM generalized linear mixed model. 127, 130

HFO high frequency oscillations. 158

iEEG intra-electroencephalography. 80, 82, 85, 113, 114
iES intracranial electrical stimulation. 136, 137

LFP local field potential. 37
lOFC lateral orbitofrontal cortex. 45

MEG magnetoencephalography. 36
MNI Montreal Neurological Institute. 118, 138
mOFC medial orbitofrontal cortex. 45

OFC orbitofrontal cortex. 45, 112

PFC prefrontal cortex. 45
pIns posterior insula. 129
PPE punishment prediction errors. 11, 59
PSE point of subjective equality. 116, 117, 127

RDV relative decision value. 33
ROI region of interest. 86, 116, 129
RPE reward prediction errors. 11, 47, 59
RRN retrorubral nucleus. 41

SDT signal detection theory. 13, 14, 17
sEEG stereo-electroencephalography. 38, 136
SEU subjective expected utility. 20, 22
SNc substantia nigra pars compacta. 41
STN subthalamic nucleus. 42

TML theoretical mood level. 84, 85, 99

vaIns ventral anterior insula. 86, 102, 134, 136, 151
vmPFC ventromedial prefrontal cortex. 45, 79, 81, 111, 112, 129, 134, 135, 150
VTA ventral tegmental area. 41, 42

List of Figures

List of Tables

References

Abitbol, R., Lebreton, M., Hollard, G., Richmond, B. J., Bouret, S., & Pessiglione, M. (2015). Neural Mechanisms Underlying Contextual Dependency of Subjective Values: Converging Evidence from Monkeys and Humans. *Journal of Neuroscience*, *35*(5), 2308–2320. https://doi.org/10/f6z3hh

Afif, A., Minotti, L., Kahane, P., & Hoffmann, D. (2010). Anatomofunctional organization of the insular cortex: A study using intracerebral electrical stimulation in epileptic patients. *Epilepsia*, *51*(11), 2305–2315. https://doi.org/10/fqmtk7

Allais, M. (1953). Le Comportement de l'Homme Rationnel devant le Risque: Critique des Postulats et Axiomes de l'Ecole Americaine. *Econometrica*, *21*(4), 503–546. https://doi.org/10/dct5zr

Anderson, B. A., Laurent, P. A., & Yantis, S. (2011). Value-driven attentional capture. *Proceedings of the National Academy of Sciences*, *108*(25), 10367–10371. https://doi.org/10/c6pdx8

Arias-Carrión, O., Stamelou, M., Murillo-Rodríguez, E., Menéndez-González, M., & Pöppel, E. (2010). Dopaminergic reward system: A short integrative review. *International Archives of Medicine*, *3*(1), 24. https://doi.org/10/b8js3w

Arieli, A., Sterkin, A., Grinvald, A., & Aertsen, A. (1996). Dynamics of ongoing activity: Explanation of the large variability in evoked cortical responses. *Science (New York, N.Y.)*, *273*(5283), 1868–1871.

Arkes, H. R., Herren, L. T., & Isen, A. M. (1988). The role of potential loss in the influence of affect on risk-taking behavior. *Organizational behavior and human decision processes*, *42*(2), 181–193. https://doi.org/10/d3n77j

Armel, K. C., Beaumel, A., & Rangel, A. (2008). Biasing simple choices by manipulating relative visual attention. *Judgment and Decision Making*, *3*(5), 396–403. http://journal.sjdm.org/8319/jdm8319.pdf

Ashburner, J. (2009). Computational anatomy with the SPM software. *Magnetic Resonance Imaging*, *27*(8), 1163–1174. https://doi.org/10/bvp2mm

Auzias, G., Coulon, O., & Brovelli, A. (2016). MarsAtlas : A cortical parcellation atlas for functional mapping: MarsAtlas. *Human Brain Mapping*, *37*(4), 1573–1592. https://doi.org/10/f9dmmv

Ayoubian, L., Lemaréchal, J.-D., & David, O. (2021). Functional Connectivity of the Insula. https : / / www . researchgate . net / publication / 352648011 _ Functional _ Connectivity _ of _ the _ Insula

Bartolomei, F., Lagarde, S., Scavarda, D., Carron, R., Bénar, C., & Picard, F. (2019). The role of the dorsal anterior insula in ecstatic sensation revealed by direct electrical brain stimulation. *Brain Stimulation*, *12*(5), 1121–1126. https://doi.org/10/gg4b47

Bartra, O., McGuire, J. T., & Kable, J. W. (2013). The valuation system: A coordinate-based meta-analysis of BOLD fMRI experiments examining neural correlates of subjective value. *NeuroImage*, *76*, 412–427. https://doi.org/10/f2dsmq

Bassi, A., Colacito, R., & Fulghieri, P. (2013). 'O Sole Mio: An Experimental Analysis of Weather and Risk Attitudes in Financial Decisions. *Review of Financial Studies*, *26*(7), 1824–1852. https://doi.org/10/gg39jz

Baxter, M. G., Parker, A., Lindner, C. C. C., Izquierdo, A. D., & Murray, E. A. (2000). Control of Response Selection by Reinforcer Value Requires Interaction of Amygdala and Orbital Prefrontal Cortex. *Journal of Neuroscience*, *20*(11), 4311–4319. https://doi.org/10/gmg8zk

Bayer, H. M., & Glimcher, P. W. (2005). Midbrain Dopamine Neurons Encode a Quantitative Reward Prediction Error Signal. *Neuron*, *47*(1), 129–141. https://doi.org/10/cqj4bt

Bechara, A., Tranel, D., Damasio, H., Adolphs, R., Rockland, C., & Damasio, A. R. (1995). Double dissociation of conditioning and declarative knowledge relative to the amygdala and hippocampus in humans. *Science*, *269*(5227), 1115–1118. https://doi.org/10/cj6dr2

Bechara, A., Damasio, A. R., Damasio, H., & Anderson, S. W. (1994). Insensitivity to future consequences following damage to human prefrontal cortex. *Cognition*, *50*(1), 7–15. https://doi.org/10/fkdc56

Bechara, A., Damasio, H., Damasio, A. R., & Lee, G. P. (1999). Different Contributions of the Human Amygdala and Ventromedial Prefrontal Cortex to Decision-Making. *Journal of Neuroscience*, *19*(13), 5473–5481. https://doi.org/10/gfxvqc

Bechara, A., Tranel, D., Damasio, H., & Damasio, A. R. (1996). Failure to Respond Autonomically to Anticipated Future Outcomes Following Damage to Prefrontal Cortex. *Cerebral Cortex*, *6*(2), 215–225. https://doi.org/10/fsn2mw

Becker, G. M., Degroot, M. H., & Marschak, J. (1964). Measuring utility by a single-response sequential method. *Behavioral Science*, *9*(3), 226–232. https://doi.org/10/dkg5gm

Beedie, C. J., Terry, P. C., & Lane, A. M. (2005). Distinctions between emotion and mood. *Cognition and Emotion*, *19*(6), 847–878. https://doi.org/10/cb53sr

Benarroch, E. E. (2019). Insular cortex: Functional complexity and clinical correlations. *Neurology*, *93*(21), 932–938. https : / / doi . org/10/gg4b48

Bennett, D., Davidson, G., & Niv, Y. (2020). A model of mood as integrated advantage [in press]. https://doi.org/10.31234/osf.io/dzsme

Bernoulli, D. (1954). Specimen theoriae novae de mensura sortis [Exposition of a New Theory on the Measurement of Risk]. *Econometrica*, *22*(1), 23–36. https://doi.org/10/cw729v (Original work published 1738)

Berridge, K. C., & Kringelbach, M. L. (2015). Pleasure Systems in the Brain. *Neuron*, *86*(3), 646–664. https://doi.org/10/f7bd4n

Bhatia, S. (2013). Associations and the accumulation of preference. *Psychological Review*, *120*(3), 522–543. https://doi.org/10/f46mpj

Bijanzadeh, M., Desai, M., Wallace, D. L., Mummaneni, N., Kunwar, N., Dawes, H. E., & Chang, E. F. (2019). Decoding Natural Positive Emotional Behaviors from Human Fronto-Temporal Mesolimbic Structures. *2019 9th International IEEE/EMBS Conference on Neural Engineering (NER)*, 1088–1092. https://doi.org/10/gg39kn

Blankenstein, N. E., Peper, J. S., Crone, E. A., & van Duijvenvoorde, A. C. K. (2017). Neural Mechanisms Underlying Risk and Ambiguity Attitudes. *Journal of Cognitive Neuroscience*, *29*(11), 1845–1859. https://doi.org/10/gh5kqq

Bódi, N., Kéri, S., Nagy, H., Moustafa, A., Myers, C. E., Daw, N., Dibó, G., Takáts, A., Bereczki, D., & Gluck, M. A. (2009). Reward-learning and the novelty-seeking personality: A between- and within-subjects study of the effects of dopamine agonists on young Parkinson's patients*. *Brain*, *132*(9), 2385–2395. https://doi.org/10/bg4t76

Borchers, S., Himmelbach, M., Logothetis, N., & Karnath, H.-O. (2012). Direct electrical stimulation of human cortex — the gold standard for mapping brain functions? *Nature Reviews Neuroscience*, *13*(1), 63–70. https://doi.org/10/bwn45h

Bouret, S., & Richmond, B. J. (2010). Ventromedial and Orbital Prefrontal Neurons Differentially Encode Internally and Externally Driven Motivational Values in Monkeys. *Journal of Neuroscience*, *30*(25), 8591–8601. https://doi.org/10/bnw28f

Brainard, D. H. (1997). The Psychophysics Toolbox. *Spatial Vision*, *10*(4), 433–436. https://doi.org/10/c7g6rj

Breiter, H. C., Aharon, I., Kahneman, D., Dale, A., & Shizgal, P. (2001). Functional Imaging of Neural Responses to Expectancy and Experience of Monetary Gains and Losses. *Neuron*, *30*(2), 619–639. https://doi.org/10/dwkw3w

Brochard, J., & Daunizeau, J. (2020). Meet me in the middle: Brain-behavior mediation analysis for fMRI experiments. *bioRxiv*, 2020.10.17.343798. https://doi.org/10/ghsm4v

Brooks, A. M., & Berns, G. S. (2013). Aversive stimuli and loss in the mesocorticolimbic dopamine system. *Trends in Cognitive Sciences*, *17*(6), 281–286. https://doi.org/10/ggnxvw

Buckner, R. L., & DiNicola, L. M. (2019). The brain's default network: Updated anatomy, physiology and evolving insights. *Nature Reviews Neuroscience*, *20*(10), 593–608. https://doi.org/10/ggxg6c

Burke, J. F., Merkow, M. B., Jacobs, J., Kahana, M. J., & Zaghloul, K. A. (2015). Brain computer interface to enhance episodic memory in human participants. *Frontiers in Human Neuroscience*, *8*. https://doi.org/10/gg39j8

Buzsáki, G. (2006). *Rhythms of the brain*. Oxford University Press. https://doi.org/10.1093/acprof:oso/9780195301069.001.0001

Cáceda, R., Nemeroff, C. B., & Harvey, P. D. (2014). Toward an Understanding of Decision Making in Severe Mental Illness. *The Journal of Neuropsychiatry and Clinical Neurosciences*, *26*(3), 196–213. https://doi.org/10/f6dft5

Calder, A. J., Beaver, J. D., Davis, M. H., Ditzhuijzen, J. V., Keane, J., & Lawrence, A. D. (2007). Disgust sensitivity predicts the insula and pallidal response to pictures of disgusting foods. *European Journal of Neuroscience*, *25*(11), 3422–3428. https://doi.org/10/b3n8t8

Callaway, F., Rangel, A., & Griffiths, T. L. (2021). Fixation patterns in simple choice reflect optimal information sampling (S. Palminteri, Ed.). *PLOS Computational Biology*, *17*(3), e1008863. https://doi.org/10/gj3crh

Camille, N., Griffiths, C. A., Vo, K., Fellows, L. K., & Kable, J. W. (2011). Ventromedial Frontal Lobe Damage Disrupts Value Maximization in Humans. *Journal of Neuroscience*, *31*(20), 7527–7532. https://doi.org/10/fqzhc3

Canolty, R. T., & Knight, R. T. (2010). The functional role of cross-frequency coupling. *Trends in Cognitive Sciences*, *14*(11), 506–515. https://doi.org/10/btmc55

Caplin, A., & Glimcher, P. W. (2014). Chapter 1 - Basic Methods from Neoclassical Economics. In P. W. Glimcher & E. Fehr (Eds.), *Neuroeconomics (Second Edition)* (pp. 3–17). Academic Press. https://doi.org/10.1016/B978-0-12-416008-8.00001-2

Caria, A., Sitaram, R., Veit, R., Begliomini, C., & Birbaumer, N. (2010). Volitional Control of Anterior Insula Activity Modulates the Response to Aversive Stimuli. A Real-Time Functional Magnetic Resonance Imaging Study. *Biological Psychiatry*, *68*(5), 425–432. https://doi.org/10/fn8s6t

Carlsson, A. (1959). The Occurrence, Distribution and Physiological Role of Catecholamines in the Nervous System. *Pharmacological Reviews*, *11*(2), 490–493. Retrieved August 9, 2021, from https://pharmrev.aspetjournals.org/content/11/2/490

Caruana, F., Jezzini, A., Sbriscia-Fioretti, B., Rizzolatti, G., & Gallese, V. (2011). Emotional and Social Behaviors Elicited by Electrical Stimulation of the Insula in the Macaque Monkey. *Current Biology*, *21*(3), 195–199. https://doi.org/10/d653xc

Cavanagh, J. F., Wiecki, T. V., Kochar, A., & Frank, M. J. (2014). Eye tracking and pupillometry are indicators of dissociable latent decision processes. *Journal of Experimental Psychology: General*, *143*(4), 1476–1488. https://doi.org/10/f6cpnt

Cavedini, P., Gorini, A., & Bellodi, L. (2006). Understanding Obsessive–Compulsive Disorder: Focus on Decision Making. *Neuropsychology Review*, *16*(1), 3–15. https://doi.org/10/d2f79j

Cecchi, R., Vinckier, F., Hammer, J., Marusic, P., Nica, A., Rheims, S., Trebuchon, A., Barbeau, E., Denuelle, M., Maillard, L.,

Minotti, L., Kahane, P., Pessiglione, M., & Bastin, J. (2021). Intracerebral mechanisms explaining the impact of incidental feedback on mood state and risky choice. *bioRxiv*. https://doi.org/10/gmhdqh

Centanni, S. W., Janes, A. C., Haggerty, D. L., Atwood, B., & Hopf, F. W. (2021). Better living through understanding the insula: Why subregions can make all the difference. *Neuropharmacology*, 108765. https://doi.org/10/gmr3w4

Cerf, M., Thiruvengadam, N., Mormann, F., Kraskov, A., Quiroga, R. Q., Koch, C., & Fried, I. (2010). On-line, voluntary control of human temporal lobe neurons. *Nature*, *467*(7319), 1104–1108. https://doi.org/10/dhjpqg

Chang, L. J., Yarkoni, T., Khaw, M. W., & Sanfey, A. G. (2013). Decoding the Role of the Insula in Human Cognition: Functional Parcellation and Large-Scale Reverse Inference. *Cerebral Cortex*, *23*(3), 739–749. https://doi.org/10/f4kkh9

Chang, S. W. C., Winecoff, A. A., & Platt, M. L. (2011). Vicarious Reinforcement in Rhesus Macaques (Macaca Mulatta). *Frontiers in Neuroscience*, *5*, 27. https://doi.org/10/cr899t

Chew, B., Hauser, T. U., Papoutsi, M., Magerkurth, J., Dolan, R. J., & Rutledge, R. B. (2019). Endogenous fluctuations in the dopaminergic midbrain drive behavioral choice variability. *Proceedings of the National Academy of Sciences*, *116*(37), 18732–18737. https://doi.org/10/gg39kr

Chib, V. S., Rangel, A., Shimojo, S., & O'Doherty, J. P. (2009). Evidence for a Common Representation of Decision Values for Dissimilar Goods in Human Ventromedial Prefrontal Cortex. *Journal of Neuroscience*, *29*(39), 12315–12320. https://doi.org/10/cttnwp

Chou, K.-L., Lee, T. M. C., & Ho, A. H. Y. (2007). Does mood state change risk taking tendency in older adults? *Psychology and Aging*, *22*(2), 310–318. https://doi.org/10/bqzs7c

Chun, M. M., Golomb, J. D., & Turk-Browne, N. B. (2011). A Taxonomy of External and Internal Attention. *Annual Review of Psychology*, *62*(1), 73–101. https://doi.org/10/c9b5jw

Cisek, P. (2012). Making decisions through a distributed consensus. *Current Opinion in Neurobiology*, *22*(6), 927–936. https://doi.org/10/gfvnrs

Clark, L., Bechara, A., Damasio, H., Aitken, M. R. F., Sahakian, B. J., & Robbins, T. W. (2008). Differential effects of insular and ventromedial prefrontal cortex lesions on risky decision-making. *Brain*, *131*(5), 1311–1322. https://doi.org/10/b2995k

Clithero, J. A., & Rangel, A. (2014). Informatic parcellation of the network involved in the computation of subjective value. *Social Cognitive and Affective Neuroscience*, *9*(9), 1289–1302. https://doi.org/10/gmw9bg

Clore, G. L. (1992). Cognitive Phenomenology: Feelings and the Construction of Judgment. In L. L. Martin & A. Tesser (Eds.), *The Construction of Social Judgments* (1st ed., pp. 133–163). Lawrence Erlbaum.

Cohen, J. Y., Amoroso, M. W., & Uchida, N. (2015). Serotonergic neurons signal reward and punishment on multiple timescales (T. Behrens, Ed.). *eLife*, *4*, e06346. https://doi.org/10/ggjxks

Cohen, M. X., Axmacher, N., Lenartz, D., Elger, C. E., Sturm, V., & Schlaepfer, T. E. (2009a). Good Vibrations: Cross-frequency Coupling in the Human Nucleus Accumbens during Reward Processing. *Journal of Cognitive Neuroscience*, *21*(5), 875–889. https://doi.org/10/fnmwvx

Cohen, M. X., Axmacher, N., Lenartz, D., Elger, C. E., Sturm, V., & Schlaepfer, T. E. (2009b). Neuroelectric Signatures of Reward Learning and Decision-Making in the Human Nucleus Accumbens. *Neuropsychopharmacology*, *34*(7), 1649–1658. https://doi.org/10/bdv2xj

Colas, J. T., & Lu, J. (2017). Learning Where to Look for High Value Improves Decision Making Asymmetrically. *Frontiers in Psychology*, *0*. https://doi.org/10/gckx6s

Corradi-Dell'Acqua, C., Tusche, A., Vuilleumier, P., & Singer, T. (2016). Cross-modal representations of first-hand and vicarious pain, disgust and fairness in insular and cingulate cortex. *Nature Communications*, *7*, 10904. https://doi.org/10/f8fwhh

Craig, A. D., & Craig, A. D. (2009). How do you feel–now? The anterior insula and human awareness. *Nature reviews neuroscience*, *10*(1). https://doi.org/10.1038/nrn2555

Crockett, M. J., Clark, L., Smillie, L. D., & Robbins, T. W. (2012). The effects of acute tryptophan depletion on costly information sampling: Impulsivity or aversive processing? *Psychopharmacology*, *219*(2), 587–597. https://doi.org/10/dk6b67

Cromwell, H. C., & Schultz, W. (2003). Effects of Expectations for Different Reward Magnitudes on Neuronal Activity in Primate Striatum. *Journal of Neurophysiology*, *89*(5), 2823–2838. https://doi.org/10/dvkvcq

Damasio, H., Grabowski, T., Frank, R., Galaburda, A. M., & Damasio, A. R. (1994). The return of Phineas Gage: Clues about the brain from the skull of a famous patient. *Science*, *264*(5162), 1102–1105. https://doi.org/10/chc8b4

Daunizeau, J., Adam, V., & Rigoux, L. (2014). VBA: A Probabilistic Treatment of Nonlinear Models for Neurobiological and Behavioural Data (A. Prlic, Ed.). *PLoS Computational Biology*, *10*(1), e1003441. https://doi.org/10/gg39j5

David, O., Job, A.-S., De Palma, L., Hoffmann, D., Minotti, L., & Kahane, P. (2013). Probabilistic functional tractography of the human cortex. *NeuroImage*, *80*, 307–317. https://doi.org/10/f46kmm

Daw, N. D., Kakade, S., & Dayan, P. (2002). Opponent interactions between serotonin and dopamine. *Neural Networks*, *15*(4-6), 603–616. https://doi.org/10/fwr35k

Daw, N. D., Niv, Y., & Dayan, P. (2005). Uncertainty-based competition between prefrontal and dorsolateral striatal systems for behavioral control. *Nature Neuroscience*, *8*(12), 1704–1711. https://doi.org/10/df697s

Daw, N. D., & O'Doherty, J. P. (2014). Chapter 21 - Multiple Systems for Value Learning. In P. W. Glimcher & E. Fehr (Eds.), *Neuroe-*

conomics (Second Edition, pp. 393–410). Academic Press. https://doi.org/10.1016/B978-0-12-416008-8.00021-8

Dayan, P., Niv, Y., Seymour, B., & D. Daw, N. (2006). The misbehavior of value and the discipline of the will. *Neural Networks*, *19*(8), 1153–1160. https://doi.org/10/cs6vm7

Dean, A. F. (1981). The variability of discharge of simple cells in the cat striate cortex. *Experimental Brain Research*, *44*(4), 437–440. https://doi.org/10/chr5vv

Deen, B., Pitskel, N. B., & Pelphrey, K. A. (2011). Three Systems of Insular Functional Connectivity Identified with Cluster Analysis. *Cerebral Cortex*, *21*(7), 1498–1506. https://doi.org/10/fhf9vn

Delgado, M. R., Li, J., Schiller, D., & Phelps, E. A. (2008). The role of the striatum in aversive learning and aversive prediction errors. *Philosophical Transactions of the Royal Society B: Biological Sciences*, *363*(1511), 3787–3800. https://doi.org/10/fd8qdz

Deman, P., Bhattacharjee, M., Tadel, F., Job, A.-S., Rivière, D., Cointepas, Y., Kahane, P., & David, O. (2018). IntrAnat Electrodes: A Free Database and Visualization Software for Intracranial Electroencephalographic Data Processed for Case and Group Studies. *Frontiers in Neuroinformatics*, *12*(40). https://doi.org/10/gdxf7d

de Montmort, P. R. (1713). *Essay d'analyse sur les jeux de hazard* (2nd ed.). Jacques Quillau. Retrieved July 23, 2021, from https://gallica.bnf.fr/ark:/12148/bpt6k110519q

Desmurget, M., Song, Z., Mottolese, C., & Sirigu, A. (2013). Re-establishing the merits of electrical brain stimulation. *Trends in Cognitive Sciences*, *17*(9), 442–449. https://doi.org/10/gdh99p

Despouy, E., Curot, J., Denuelle, M., Deudon, M., Sol, J.-C., Lotterie, J.-A., Reddy, L., Nowak, L. G., Pariente, J., Thorpe, S. J., Valton, L., & Barbeau, E. J. (2019). Neuronal spiking activity highlights a gradient of epileptogenicity in human tuberous sclerosis lesions. *Clinical Neurophysiology*, *130*(4), 537–547. https://doi.org/10/gg58bz

Despouy, E., Curot, J., Reddy, L., Nowak, L. G., Deudon, M., Sol, J.-C., Lotterie, J.-A., Denuelle, M., Maziz, A., Bergaud, C., Thorpe, S. J., Valton, L., & Barbeau, E. J. (2020). Recording local field potential and neuronal activity with tetrodes in epileptic patients. *Journal of Neuroscience Methods*, *341*, 108759. https://doi.org/10/gmtdzv

Destrieux, C., Fischl, B., Dale, A., & Halgren, E. (2010). Automatic parcellation of human cortical gyri and sulci using standard anatomical nomenclature. *NeuroImage*, *53*(1), 1–15. https://doi.org/10/d2d3hp

Deubel, H., & Schneider, W. X. (1996). Saccade target selection and object recognition: Evidence for a common attentional mechanism. *Vision Research*, *36*(12), 1827–1837. https://doi.org/10/bj8xcj

Dolan, R. J., & Dayan, P. (2013). Goals and Habits in the Brain. *Neuron*, *80*(2), 312–325. https://doi.org/10/f5ft22

Dorris, M. C., & Glimcher, P. W. (2004). Activity in Posterior Parietal Cortex Is Correlated with the Relative Subjective Desirability of Action. *Neuron*, *44*(2), 365–378. https://doi.org/10/fc45m4

Droutman, V., Bechara, A., & Read, S. J. (2015). Roles of the Different Sub-Regions of the Insular Cortex in Various Phases of the Decision-Making Process. *Frontiers in Behavioral Neuroscience*, *9*(309). https://doi.org/10/gg39j9

Duann, J.-R., Jung, T.-P., Kuo, W.-J., Yeh, T.-C., Makeig, S., Hsieh, J.-C., & Sejnowski, T. J. (2002). Single-Trial Variability in Event-Related BOLD Signals. *NeuroImage*, *15*(4), 823–835. https://doi.org/10/d522mm

Dunn, J. C., & Kirsner, K. (2003). What can we infer from double dissociations? *Cortex; a Journal Devoted to the Study of the Nervous System and Behavior*, *39*(1), 1–7. https://doi.org/10/dwhbvt

Edgeworth, F. Y. (1881). *Mathematical Psychics: An Essay on the Application of Mathematics to the Moral Sciences*. C. Kegan Paul & Co.

Edmans, A., Garcia, D., & Norli, Ø. (2007). Sports sentiment and stock returns. *The Journal of Finance*, *62*(4), 1967–1998. https://doi.org/10/cb959w

Edwards, A. W. F. (2001). Blaise Pascal. In C. C. Heyde, E. Seneta, P. Crépel, S. E. Fienberg, & J. Gani (Eds.), *Statisticians of the Centuries* (pp. 17–22). Springer. https://doi.org/10.1007/978-1-4613-0179-0_4

Eisenberger, R. (1992). Learned Industriousness. *Psychological Review*, *99*(2), 248–267. https://doi.org/10/frcw7r

Eisenegger, C., Naef, M., Linssen, A., Clark, L., Gandamaneni, P. K., Müller, U., & Robbins, T. W. (2014). Role of Dopamine D2 Receptors in Human Reinforcement Learning. *Neuropsychopharmacology*, *39*(10), 2366–2375. https://doi.org/10/f6c2cq

Eldar, E., & Niv, Y. (2015). Interaction between emotional state and learning underlies mood instability. *Nature Communications*, *6*, 6149. https://doi.org/10/f6xsbn

Eldar, E., Rutledge, R. B., Dolan, R. J., & Niv, Y. (2016). Mood as Representation of Momentum. *Trends in Cognitive Sciences*, *20*(1), 15–24. https://doi.org/10/f76mx3

Elliott, R., Newman, J. L., Longe, O. A., & Deakin, J. F. W. (2003). Differential Response Patterns in the Striatum and Orbitofrontal Cortex to Financial Reward in Humans: A Parametric Functional Magnetic Resonance Imaging Study. *Journal of Neuroscience*, *23*(1), 303–307. https://doi.org/10/gfr932

Ellsberg, D. (1961). Risk, Ambiguity, and the Savage Axioms. *The Quarterly Journal of Economics*, *75*(4), 643–669. https://doi.org/10/d7qb2f

Engelmann, J. B., Meyer, F., Fehr, E., & Ruff, C. C. (2015). Anticipatory Anxiety Disrupts Neural Valuation during Risky Choice. *Journal of Neuroscience*, *35*(7), 3085–3099. https://doi.org/10/gg39kb

Engelmann, J. B., & Tamir, D. (2009). Individual differences in risk preference predict neural responses during financial decision-making. *Brain Research*, *1290*, 28–51. https://doi.org/10/c8cr9c

Erk, S., Spitzer, M., Wunderlich, A. P., Galley, L., & Walter, H. (2002). Cultural objects modulate reward circuitry. *Neuroreport*, *13*(18), 2499–2503. https://doi.org/10/bwwpds

Ezzyat, Y., Kragel, J. E., Burke, J. F., Levy, D. F., Lyalenko, A., Wanda, P., O'Sullivan, L., Hurley, K. B., Busygin, S., Pedisich, I., Sperling, M. R., Worrell, G. A., Kucewicz, M. T., Davis, K. A., Lucas, T. H., Inman, C. S., Lega, B. C., Jobst, B. C., Sheth, S. A., ... Kahana, M. J. (2017). Direct Brain Stimulation Modulates Encoding States and Memory Performance in Humans. *Current Biology*, *27*(9), 1251–1258. https://doi.org/10/b529

Feindel, W., & Penfield, W. (1954). Localization of discharge in temporal lobe automatism. *A.M.A. Archives of Neurology & Psychiatry*, *72*(5), 605–630. https://doi.org/10/gmr4d4

Fellows, L. K. (2012). Group studies in experimental neuropsychology. *APA handbook of research methods in psychology, Vol 2: Research designs: Quantitative, qualitative, neuropsychological, and biological* (pp. 647–659). American Psychological Association. https://doi.org/10.1037/13620-034

Fellows, L. K., & Farah, M. J. (2007). The Role of Ventromedial Prefrontal Cortex in Decision Making: Judgment under Uncertainty or Judgment Per Se? *Cerebral Cortex*, *17*(11), 2669–2674. https://doi.org/10/c78wjb

Fellows, L. K., Heberlein, A. S., Morales, D. A., Shivde, G., Waller, S., & Wu, D. H. (2005). Method Matters: An Empirical Study of Impact in Cognitive Neuroscience. *Journal of Cognitive Neuroscience*, *17*(6), 850–858. https://doi.org/10/fpz7kk

Fiedler, S., & Glöckner, A. (2012). The Dynamics of Decision Making in Risky Choice: An Eye-Tracking Analysis. *Frontiers in Psychology*, *3*, 335. https://doi.org/10/gf5sv5

Fischl, B., Salat, D. H., Busa, E., Albert, M., Dieterich, M., Haselgrove, C., van der Kouwe, A., Killiany, R., Kennedy, D., Klaveness, S., Montillo, A., Makris, N., Rosen, B., & Dale, A. M. (2002). Whole Brain Segmentation. *Neuron*, *33*(3), 341–355. https://doi.org/10/dbx4cf

Fisher, G. (2017). An attentional drift diffusion model over binary-attribute choice. *Cognition*, *168*, 34–45. https://doi.org/10/gbz6b3

Fonseca, M. S., Murakami, M., & Mainen, Z. F. (2015). Activation of Dorsal Raphe Serotonergic Neurons Promotes Waiting but Is Not Reinforcing. *Current Biology*, *25*(3), 306–315. https://doi.org/10/f6zd6p

Forstmann, B., Ratcliff, R., & Wagenmakers, E.-J. (2016). Sequential Sampling Models in Cognitive Neuroscience: Advantages, Applications, and Extensions. *Annual Review of Psychology*, *67*(1), 641–666. https://doi.org/10/gf6bzg

Fouragnan, E., Retzler, C., & Philiastides, M. G. (2018). Separate neural representations of prediction error valence and surprise: Evidence from an fMRI meta-analysis. *Human Brain Mapping*, *39*(7), 2887–2906. https://doi.org/10/gc8hqt

Fox, C. R., & Poldrack, R. A. (2009). Chapter 11 - Prospect Theory and the Brain. In P. W. Glimcher, C. F. Camerer, E. Fehr, & R. A. Poldrack (Eds.), *Neuroeconomics* (pp. 145–173). Academic Press. https://doi.org/10.1016/B978-0-12-374176-9.00011-7

Fox, K. C. R., Shi, L., Baek, S., Raccah, O., Foster, B. L., Saha, S., Margulies, D. S., Kucyi, A., & Parvizi, J. (2020). Intrinsic network architecture predicts the effects elicited by intracranial electrical stimulation of the human brain. *Nature Human Behaviour*, *4*(10), 1039–1052. https://doi.org/10/gmr4qq

Fox, K. C. R., Yih, J., Raccah, O., Pendekanti, S. L., Limbach, L. E., Maydan, D. D., & Parvizi, J. (2018). Changes in subjective experience elicited by direct stimulation of the human orbitofrontal cortex. *Neurology*, *91*(16), e1519–e1527. https://doi.org/10/gmmh5h

Fox, M. D., Snyder, A. Z., Zacks, J. M., & Raichle, M. E. (2006). Coherent spontaneous activity accounts for trial-to-trial variability in human evoked brain responses. *Nature Neuroscience*, *9*(1), 23–25. https://doi.org/10/b4xb64

Frank, M. J., Moustafa, A. A., Haughey, H. M., Curran, T., & Hutchison, K. E. (2007). Genetic triple dissociation reveals multiple roles for dopamine in reinforcement learning. *Proceedings of the National Academy of Sciences*, *104*(41), 16311–16316. https://doi.org/10/b5vrt5

Frank, M. J., Seeberger, L. C., & O'Reilly, R. C. (2004). By Carrot or by Stick: Cognitive Reinforcement Learning in Parkinsonism. *Science*, *306*(5703), 1940–1943. https://doi.org/10/cwmr78

Fried, I., Wilson, C. L., Maidment, N. T., Engel, J., Behnke, E., Fields, T. A., Macdonald, K. A., Morrow, J. W., & Ackerson, L. (1999). Cerebral microdialysis combined with single-neuron and electroencephalographic recording in neurosurgical patients: Technical note. *Journal of Neurosurgery*, *91*(4), 697–705. https://doi.org/10/b2xncc

Fries, P. (2005). A mechanism for cognitive dynamics: Neuronal communication through neuronal coherence. *Trends in Cognitive Sciences*, *9*(10), 474–480. https://doi.org/10/fp6gpp

Gardner, J. L. (n.d.). *Signal detection*. Retrieved September 8, 2021, from http://gru.stanford.edu/doku.php/tutorials/sdt

Garrison, J., Erdeniz, B., & Done, J. (2013). Prediction error in reinforcement learning: A meta-analysis of neuroimaging studies. *Neuroscience & Biobehavioral Reviews*, *37*(7), 1297–1310. https://doi.org/10/f488ss

Ghaziri, J., Tucholka, A., Girard, G., Houde, J.-C., Boucher, O., Gilbert, G., Descoteaux, M., Lippé, S., Rainville, P., & Nguyen, D. K. (2017). The Corticocortical Structural Connectivity of the Human Insula. *Cerebral Cortex*, *27*(2), 1216–1228. https://doi.org/10/f9xjrv

Gidlöf, K., Anikin, A., Lingonblad, M., & Wallin, A. (2017). Looking is buying. How visual attention and choice are affected by consumer preferences and properties of the supermarket shelf. *Appetite*, *116*, 29–38. https://doi.org/10/f97s6c

Glickman, M., Sharoni, O., Levy, D. J., Niebur, E., Stuphorn, V., & Usher, M. (2019). The formation of preference in risky choice. *PLOS Computational Biology*, *15*(8), e1007201. https://doi.org/10/gmw84v

Glimcher, P. W. (2014). Chapter 20 - Value-Based Decision Making. In P. W. Glimcher & E. Fehr (Eds.), *Neuroeconomics (Second Edition)* (pp. 373–391). Academic Press. https://doi.org/10.1016/B978-0-12-416008-8.00020-6

Gloor, P. (1969). Hans Berger and the discovery of the electroencephalogram. In P. Gloor (Ed.), *Hans Berger on the Electroencephalogram of Man. The Fourteen Original Reports on the Human Encephalogram* (pp. 1–36). Elsevier.

Gluth, S., Kern, N., Kortmann, M., & Vitali, C. L. (2020). Value-based attention but not divisive normalization influences decisions with multiple alternatives. *Nature Human Behaviour*, *4*(6), 634–645. https://doi.org/10/ggj7bs

Gluth, S., Sommer, T., Rieskamp, J., & Büchel, C. (2015). Effective Connectivity between Hippocampus and Ventromedial Prefrontal Cortex Controls Preferential Choices from Memory. *Neuron*, *86*(4), 1078–1090. https://doi.org/10/f7cqhk

Gluth, S., Spektor, M. S., & Rieskamp, J. (2018). Value-based attentional capture affects multi-alternative decision making (M. J. Frank, Ed.). *eLife*, *7*, e39659. https://doi.org/10/gf5sxv

Gollo, L. L., Roberts, J. A., & Cocchi, L. (2017). Mapping how local perturbations influence systems-level brain dynamics. *NeuroImage*, *160*, 97–112. https://doi.org/10/gcj6d5

Gottfried, J. A., O'Doherty, J., & Dolan, R. J. (2003). Encoding Predictive Reward Value in Human Amygdala and Orbitofrontal Cortex. *Science*, *301*(5636), 1104–1107. https://doi.org/10/fk43kq

Grande, K. M., Ihnen, S. K. Z., & Arya, R. (2020). Electrical Stimulation Mapping of Brain Function: A Comparison of Subdural Electrodes and Stereo-EEG. *Frontiers in Human Neuroscience*, *14*, 538. https://doi.org/10/gjbxtw

Griffin, A. L., Asaka, Y., Darling, R. D., & Berry, S. D. (2004). Theta-Contingent Trial Presentation Accelerates Learning Rate and Enhances Hippocampal Plasticity During Trace Eyeblink Conditioning. *Behavioral Neuroscience*, *118*(2), 403–411. https://doi.org/10/b5csjq

Gueguen, M. C. M., Lopez-Persem, A., Billeke, P., Lachaux, J.-P., Rheims, S., Kahane, P., Minotti, L., David, O., Pessiglione, M., & Bastin, J. (2021). Anatomical dissociation of intracerebral signals for reward and punishment prediction errors in humans. *Nature Communications*, *12*(1), 3344. https://doi.org/10/gkf49z

Gwinn, R., Leber, A. B., & Krajbich, I. (2019). The spillover effects of attentional learning on value-based choice. *Cognition*, *182*, 294–306. https://doi.org/10/gfgxpq

Haber, S. N., & Knutson, B. (2010). The reward circuit: Linking primate anatomy and human imaging. *Neuropsychopharmacology*, *35*(1), 4–26. https://doi.org/10/bzfzhq

Hacking, I. (1983). *Representing and Intervening: Introductory Topics in the Philosophy of Natural Science*. Cambridge University Press.

Hare, T. A., O'Doherty, J., Camerer, C. F., Schultz, W., & Rangel, A. (2008). Dissociating the Role of the Orbitofrontal Cortex and the Striatum in the Computation of Goal Values and Prediction Errors. *Journal of Neuroscience*, *28*(22), 5623–5630. https://doi.org/10/dx4qj9

Hartikainen, K. M., Ogawa, K. H., & Knight, R. T. (2012). Orbitofrontal cortex biases attention to emotional events. *Journal of Clinical and Experimental Neuropsychology*, *34*(6), 588–597. https://doi.org/10/gmkvnw

Hassani, O. K., Cromwell, H. C., & Schultz, W. (2001). Influence of Expectation of Different Rewards on Behavior-Related Neuronal Activity in the Striatum. *Journal of Neurophysiology*, *85*(6), 2477–2489. https://doi.org/10/gmgzxv

Häusler, A. N., Artigas, S. O., Trautner, P., & Weber, B. (2016). Gain- and Loss-Related Brain Activation Are Associated with Information Search Differences in Risky Gambles: An fMRI and Eye-Tracking Study. *eNeuro*, *3*(5), e.0189-16.2016 1–13. https://doi.org/10/gg39kd

Hayes, D. J., Duncan, N. W., Xu, J., & Northoff, G. (2014). A comparison of neural responses to appetitive and aversive stimuli in humans and other mammals. *Neuroscience & Biobehavioral Reviews*, *45*, 350–368. https://doi.org/10/f6f7kq

Heitz, R. P. (2014). The speed-accuracy tradeoff: History, physiology, methodology, and behavior. *Frontiers in Neuroscience*, *0*. https://doi.org/10/gfw8p2

Henri-Bhargava, A., Simioni, A., & Fellows, L. K. (2012). Ventromedial frontal lobe damage disrupts the accuracy, but not the speed, of value-based preference judgments. *Neuropsychologia*, *50*(7), 1536–1542. https://doi.org/10/f337n7

Hesselmann, G., Kell, C. A., Eger, E., & Kleinschmidt, A. (2008). Spontaneous local variations in ongoing neural activity bias perceptual decisions. *Proceedings of the National Academy of Sciences*, *105*(31), 10984–10989. https://doi.org/10/b4zrzg

Hesselmann, G., Kell, C. A., & Kleinschmidt, A. (2008). Ongoing Activity Fluctuations in hMT+ Bias the Perception of Coherent Visual Motion. *Journal of Neuroscience*, *28*(53), 14481–14485. https://doi.org/10/cmfdh7

Hodges, J. R. (2001). Frontotemporal dementia (Pick's disease): Clinical features and assessment. *Neurology*, *56*, S6–S10. https://doi.org/10/gmg6sv

Hoffman, J. E., & Subramaniam, B. (1995). The role of visual attention in saccadic eye movements. *Perception & Psychophysics*, *57*(6), 787–795. https://doi.org/10/bcwsts

Hoffmann, L. C., & Berry, S. D. (2009). Cerebellar theta oscillations are synchronized during hippocampal theta-contingent trace conditioning. *Proceedings of the National Academy of Sciences*, *106*(50), 21371–21376. https://doi.org/10/c3sjdh

Hollerman, J. R., Tremblay, L., & Schultz, W. (1998). Influence of Reward Expectation on Behavior-Related Neuronal Activity in Primate Striatum. *Journal of Neurophysiology*, *80*(2), 947–963. https://doi.org/10/gmgzx3

Howard, J. D., Gottfried, J. A., Tobler, P. N., & Kahnt, T. (2015). Identity-specific coding of future rewards in the human orbitofrontal cortex. *Proceedings of the National Academy of Sciences*, *112*(16), 5195–5200. https://doi.org/10/f69jkh

Howard, M. A., Volkov, I. O., Granner, M. A., Damasio, H. M., Ollendieck, M. C., & Bakken, H. E. (1996). A hybrid clinical—research depth electrode for acute and chronic in vivo microelec-

trode recording of human brain neurons: Technical note. *Journal of Neurosurgery*, *84*(1), 129–132. https://doi.org/10/d544k8

Huang, Y.-F., Soon, C. S., Mullette-Gillman, O. A., & Hsieh, P.-J. (2014). Pre-existing brain states predict risky choices. *NeuroImage*, *101*, 466–472. https://doi.org/10/f6pz6j

Huettel, S. A., Song, A. W., & McCarthy, G. (2014). *Functional Magnetic Resonance Imaging* (Vol. Third Edition). Sinauer Associates.

Hunt, L. T., Malalasekera, W. M. N., de Berker, A. O., Miranda, B., Farmer, S. F., Behrens, T. E. J., & Kennerley, S. W. (2018). Triple dissociation of attention and decision computations across prefrontal cortex. *Nature Neuroscience*, *21*(10), 1471–1481. https://doi.org/10/gfb67f

Huys, Q. J. M., Cools, R., Gölzer, M., Friedel, E., Heinz, A., Dolan, R. J., & Dayan, P. (2011). Disentangling the Roles of Approach, Activation and Valence in Instrumental and Pavlovian Responding. *PLOS Computational Biology*, *7*(4), e1002028. https://doi.org/10/bjgx56

Isen, A. M., Shalker, T. E., Clark, M., & Karp, L. (1978). Affect, accessibility of material in memory, and behavior: A cognitive loop? *Journal of Personality and Social Psychology*, *36*(1), 1–12. https://doi.org/10/c9r

Isnard, J., Guénot, M., Sindou, M., & Mauguière, F. (2004). Clinical Manifestations of Insular Lobe Seizures: A Stereo-electroencephalographic Study. *Epilepsia*, *45*(9), 1079–1090. https://doi.org/10/bhxjfs

Izquierdo, A., Suda, R. K., & Murray, E. A. (2004). Bilateral Orbital Prefrontal Cortex Lesions in Rhesus Monkeys Disrupt Choices Guided by Both Reward Value and Reward Contingency. *Journal of Neuroscience*, *24*(34), 7540–7548. https://doi.org/10/ftq8cg

Jenison, R. L., Rangel, A., Oya, H., Kawasaki, H., & Howard, M. A. (2011). Value Encoding in Single Neurons in the Human Amygdala during Decision Making. *Journal of Neuroscience*, *31*(1), 331–338. https://doi.org/10/dpjv35

Jezzini, A., Caruana, F., Stoianov, I., Gallese, V., & Rizzolatti, G. (2012). Functional organization of the insula and inner perisylvian regions. *Proceedings of the National Academy of Sciences*, *109*(25), 10077–10082. https://doi.org/10/f337xn

Jiruska, P., Alvarado-Rojas, C., Schevon, C. A., Staba, R., Stacey, W., Wendling, F., & Avoli, M. (2017). Update on the mechanisms and roles of high-frequency oscillations in seizures and epileptic disorders. *Epilepsia*, *58*(8), 1330–1339. https://doi.org/10/gbkqxq

Kable, J. W., & Glimcher, P. W. (2007). The neural correlates of subjective value during intertemporal choice. *Nature Neuroscience*, *10*(12), 1625–1633. https://doi.org/10/cpg6td

Kable, J. W., & Glimcher, P. W. (2009). The Neurobiology of Decision: Consensus and Controversy. *Neuron*, *63*(6), 733–745. https://doi.org/10/dq7vd2

Kahneman, D., Diener, E., & Schwarz, N. (1999). *Well-Being: Foundations of Hedonic Psychology*. Russell Sage Foundation.

Kahneman, D., Knetsch, J. L., & Thaler, R. H. (1990). Experimental Tests of the Endowment Effect and the Coase Theorem. *Journal of Political Economy*, *98*(6), 1325–1348. https://doi.org/10/dktkgn

Kahneman, D., & Tversky, A. (1979). Prospect Theory: An Analysis of Decision Under Risk. *Econometrica*, *47*(2), 263–291. https://doi.org/10/g98

Kahneman, D., Wakker, P. P., & Sarin, R. (1997). Back to Bentham? Explorations of Experienced Utility. *The Quarterly Journal of Economics*, *112*(2), 375–406. https://doi.org/10/fkdkp2

Kandel, E. R., Mack, S., Jessell, T. M., Schwartz, J. H., Siegelbaum, S. A., & Hudspeth, A. J. (2013). *Principles of Neural Science* (Fifth Edition). McGraw Hill Professional.

Kapur, S., & Remington, G. (1996). Serotonin-dopamine interaction and its relevance to schizophrenia. *The American Journal of Psychiatry*, *153*(4), 466–476. https://doi.org/10/gmhmz9

Keller, C. J., Bickel, S., Entz, L., Ulbert, I., Milham, M. P., Kelly, C., & Mehta, A. D. (2011). Intrinsic functional architecture predicts electrically evoked responses in the human brain. *Proceedings of the National Academy of Sciences*, *108*(25), 10308–10313. https://doi.org/10/fc8g52

Keller, C. J., Honey, C. J., Mégevand, P., Entz, L., Ulbert, I., & Mehta, A. D. (2014). Mapping human brain networks with cortico-cortical evoked potentials. *Philosophical Transactions of the Royal Society B: Biological Sciences*, *369*(1653), 20130528. https://doi.org/10/gmh2q5

Kéri, S., Moustafa, A. A., Myers, C. E., Benedek, G., & Gluck, M. A. (2010). A-Synuclein gene duplication impairs reward learning. *Proceedings of the National Academy of Sciences*, *107*(36), 15992–15994. https://doi.org/10/b26j73

Kirkby, L. A., Luongo, F. J., Lee, M. B., Nahum, M., Van Vleet, T. M., Rao, V. R., Dawes, H. E., Chang, E. F., & Sohal, V. S. (2018). An Amygdala-Hippocampus Subnetwork that Encodes Variation in Human Mood. *Cell*, *175*(6), 1688–1700.e14. https://doi.org/10/gfhwnx

Klein, T. A., Ullsperger, M., & Danielmeier, C. (2013). Error awareness and the insula: Links to neurological and psychiatric diseases. *Frontiers in Human Neuroscience*, *7*. https://doi.org/10/gg39j2

Knight, F. H. (1921). *Risk, Uncertainty and Profit*. University of Chicago Press.

Knutson, B., & Cooper, J. C. (2005). Functional magnetic resonance imaging of reward prediction. *Current Opinion in Neurology*, *18*(4), 411–417. https://doi.org/10/bpcfn7

Knutson, B., Fong, G. W., Bennett, S. M., Adams, C. M., & Hommer, D. (2003). A region of mesial prefrontal cortex tracks monetarily rewarding outcomes: Characterization with rapid event-related fMRI. *NeuroImage*, *18*(2), 263–272. https://doi.org/10/fnfpbd

Knutson, B., Rick, S., Wimmer, G. E., Prelec, D., & Loewenstein, G. (2007). Neural Predictors of Purchases. *Neuron*, *53*(1), 147–156. https://doi.org/10/fm2xtw

Knutson, B., Taylor, J., Kaufman, M., Peterson, R., & Glover, G. (2005). Distributed Neural Representation of Expected Value. *Journal of Neuroscience*, *25*(19), 4806–4812. https://doi.org/10/c3ft55

Kobayashi, S., & Schultz, W. (2008). Influence of Reward Delays on Responses of Dopamine Neurons. *Journal of Neuroscience*, *28*(31), 7837–7846. https://doi.org/10/crjj76

Kool, W., McGuire, J. T., Rosen, Z. B., & Botvinick, M. M. (2010). Decision making and the avoidance of cognitive demand. *Journal of Experimental Psychology: General*, *139*(4), 665–682. https://doi.org/10/cwdpp3

Krajbich, I., & Rangel, A. (2011). Multialternative drift-diffusion model predicts the relationship between visual fixations and choice in value-based decisions. *Proceedings of the National Academy of Sciences*, *108*(33), 13852–13857. https://doi.org/10/cd44pd

Krajbich, I. (2019). Accounting for attention in sequential sampling models of decision making. *Current Opinion in Psychology*, *29*, 6–11. https://doi.org/10/gffnhh

Krajbich, I., Armel, C., & Rangel, A. (2010). Visual fixations and the computation and comparison of value in simple choice. *Nature Neuroscience*, *13*(10), 1292–1298. https://doi.org/10/fgkmv7

Krajbich, I., Lu, D., Camerer, C., & Rangel, A. (2012). The Attentional Drift-Diffusion Model Extends to Simple Purchasing Decisions. *Frontiers in Psychology*, *3*(193). https://doi.org/10/gg39jw

Kringelbach, M. L. (2005). The human orbitofrontal cortex: Linking reward to hedonic experience. *Nature Reviews Neuroscience*, *6*(9), 691–702. https://doi.org/10/fj4xfx

Kroemer, N. B., Burrasch, C., & Hellrung, L. (2016). Chapter 6 - To work or not to work: Neural representation of cost and benefit of instrumental action. In B. Studer & S. Knecht (Eds.), *Progress in Brain Research* (pp. 125–157). Elsevier. https://doi.org/10.1016/bs.pbr.2016.06.009

Krolak-Salmon, P., Hénaff, M.-A., Isnard, J., Tallon-Baudry, C., Guénot, M., Vighetto, A., Bertrand, O., & Mauguière, F. (2003). An attention modulated response to disgust in human ventral anterior insula. *Annals of Neurology*, *53*(4), 446–453. https://doi.org/10/brvs93

Kühn, S., & Gallinat, J. (2012). The neural correlates of subjective pleasantness. *NeuroImage*, *61*(1), 289–294. https://doi.org/10/f3xzhr

Kuhnen, C. M., & Knutson, B. (2005). The Neural Basis of Financial Risk Taking. *Neuron*, *47*(5), 763–770. https://doi.org/10/bjmr4w

Kunar, M. A., Watson, D. G., Tsetsos, K., & Chater, N. (2017). The influence of attention on value integration. *Attention, Perception, & Psychophysics*, *79*(6), 1615–1627. https://doi.org/10/gbqmpb

Lachaux, J.-P., Fonlupt, P., Kahane, P., Minotti, L., Hoffmann, D., Bertrand, O., & Baciu, M. (2007). Relationship between task-related gamma oscillations and BOLD signal: New insights from combined fMRI and intracranial EEG. *Human Brain Mapping*, *28*(12), 1368–1375. https://doi.org/10/crn9c3

Larsen, R. J. (2000). Toward a Science of Mood Regulation. *Psychological Inquiry*, *11*(3), 129–141. https://doi.org/10/chcqwd

Laufs, H., Krakow, K., Sterzer, P., Eger, E., Beyerle, A., Salek-Haddadi, A., & Kleinschmidt, A. (2003). Electroencephalographic signatures of attentional and cognitive default modes in spontaneous brain activity fluctuations at rest. *Proceedings of the National Academy of Sciences*, *100*(19), 11053–11058. https://doi.org/10/cwjxjb

Lawson, R. P., Seymour, B., Loh, E., Lutti, A., Dolan, R. J., Dayan, P., Weiskopf, N., & Roiser, J. P. (2014). The habenula encodes negative motivational value associated with primary punishment in humans. *Proceedings of the National Academy of Sciences*, *111*(32), 11858–11863. https://doi.org/10/f6cdsm

Leahy, R. L. (1999). Decision making and mania. *Journal of Cognitive Psychotherapy*, *13*(2), 83–105. https://doi.org/10/gg39k5

Lebreton, M., Jorge, S., Michel, V., Thirion, B., & Pessiglione, M. (2009). An Automatic Valuation System in the Human Brain: Evidence from Functional Neuroimaging. *Neuron*, *64*(3), 431–439. https://doi.org/10/bkxk94

Leland, J. W., & Grafman, J. (2005). Experimental tests of the Somatic Marker hypothesis. *Games and Economic Behavior*, *52*(2), 386–409. https://doi.org/10/bs7hww

Lerner, J. S., & Keltner, D. (2000). Beyond valence: Toward a model of emotion-specific influences on judgement and choice. *Cognition and Emotion*, *14*(4), 473–493. https://doi.org/10/c6gn9p

Lerner, J. S., Li, Y., Valdesolo, P., & Kassam, K. S. (2015). Emotion and Decision Making. *Annual Review of Psychology*, *66*(1), 799–823. https://doi.org/10/gdh74s

Levy, D. J., & Glimcher, P. W. (2011). Comparing Apples and Oranges: Using Reward-Specific and Reward-General Subjective Value Representation in the Brain. *Journal of Neuroscience*, *31*(41), 14693–14707. https://doi.org/10/ccb228

Levy, D. J., & Glimcher, P. W. (2012). The root of all value: A neural common currency for choice. *Current Opinion in Neurobiology*, *22*(6), 1027–1038. https://doi.org/10/f4hknc

Lewandowski, M. (2017). Prospect Theory Versus Expected Utility Theory: Assumptions, Predictions, Intuition and Modelling of Risk Attitudes. *Central European Journal of Economic Modelling and Econometrics*, *9*(4), 275–321. https://doi.org/10/gmbhvt

Li, R., Zhu, X., Zheng, Z., Wang, P., & Li, J. (2020). Subjective well-being is associated with the functional connectivity network of the dorsal anterior insula. *Neuropsychologia*, *141*, 107393. https://doi.org/10/gg39kz

Li, Y., Vanni-Mercier, G., Isnard, J., Mauguière, F., & Dreher, J.-C. (2016). The neural dynamics of reward value and risk coding in the human orbitofrontal cortex. *Brain*, *139*(4), 1295–1309. https://doi.org/10/f8h9hq

Lim, S.-L., O'Doherty, J. P., & Rangel, A. (2011). The Decision Value Computations in the vmPFC and Striatum Use a Relative Value Code That is Guided by Visual Attention. *Journal of Neuroscience*, *31*(37), 13214–13223. https://doi.org/10/cn4tjs

Liu, S., Gurses, C., Sha, Z., Quach, M. M., Sencer, A., Bebek, N., Curry, D. J., Prabhu, S., Tummala, S., Henry, T. R., & Ince, N. F. (2018). Stereotyped high-frequency oscillations discriminate seizure onset zones and critical functional cortex in focal epilepsy. *Brain*, *141*(3), 713–730. https://doi.org/10/gcxw8j

Liu, S., & Parvizi, J. (2019). Cognitive refractory state caused by spontaneous epileptic high-frequency oscillations in the human brain. *Science Translational Medicine*, *11*(514). https://doi.org/10/gjqbpr

Liu, X., Hairston, J., Schrier, M., & Fan, J. (2011). Common and distinct networks underlying reward valence and processing stages: A meta-analysis of functional neuroimaging studies. *Neuroscience & Biobehavioral Reviews*, *35*(5), 1219–1236. https://doi.org/10/d5k842

Loewenstein, G. (1987). Anticipation and the Valuation of Delayed Consumption. *The Economic Journal*, *97*(387), 666–684. https://doi.org/10/dhk9g3

Loewenstein, G., & Lerner, J. S. (2003). The role of affect in decision making. *Handbook of Affective Sciences* (Oxford University Press, pp. 619–642). Davidson RJ, Scherer KR, Goldsmith KR.

Logothetis, N. K., Pauls, J., Augath, M., Trinath, T., & Oeltermann, A. (2001). Neurophysiological investigation of the basis of the fMRI signal. *Nature*, *412*(6843), 150–157. https://doi.org/10/cmrpwx

Lopez-Persem, A., Bastin, J., Petton, M., Abitbol, R., Lehongre, K., Adam, C., Navarro, V., Rheims, S., Kahane, P., Domenech, P., & Pessiglione, M. (2020). Four core properties of the human brain valuation system demonstrated in intracranial signals. *Nature Neuroscience*, *23*, 664–675. https://doi.org/10/ggx5jv

Lopez-Persem, A., Domenech, P., & Pessiglione, M. (2016). How prior preferences determine decision-making frames and biases in the human brain (M. J. Frank, Ed.). *eLife*, *5*, e20317. https://doi.org/10/f9rh9k

Lopez-Persem, A., Verhagen, L., Amiez, C., Petrides, M., & Sallet, J. (2019). The Human Ventromedial Prefrontal Cortex: Sulcal Morphology and Its Influence on Functional Organization. *The Journal of Neuroscience*, *39*(19), 3627–3639. https://doi.org/10/gg39ks

Lorrain, D. S., Riolo, J. V., Matuszewich, L., & Hull, E. M. (1999). Lateral Hypothalamic Serotonin Inhibits Nucleus Accumbens Dopamine: Implications for Sexual Satiety. *Journal of Neuroscience*, *19*(17), 7648–7652. https://doi.org/10/gf4rwh

Lozano, A. M., Lipsman, N., Bergman, H., Brown, P., Chabardes, S., Chang, J. W., Matthews, K., McIntyre, C. C., Schlaepfer, T. E., Schulder, M., Temel, Y., Volkmann, J., & Krauss, J. K. (2019). Deep brain stimulation: Current challenges and future directions. *Nature reviews. Neurology*, *15*(3), 148–160. https://doi.org/10/ggr2f6

Luce, R. D. (1959). On the possible psychophysical laws. *Psychological Review*, *66*(2), 81–95. https://doi.org/10/d5h683

Mackey, S., & Petrides, M. (2010). Quantitative demonstration of comparable architectonic areas within the ventromedial and lateral orbital frontal cortex in the human and the macaque monkey brains. *European Journal of Neuroscience*, *32*(11), 1940–1950. https://doi.org/10/d98dbv

Maia, T. V., & Frank, M. J. (2011). From reinforcement learning models to psychiatric and neurological disorders. *Nature Neuroscience*, *14*(2), 154–162. https://doi.org/10/dtktz5

Manning, J. R., Jacobs, J., Fried, I., & Kahana, M. J. (2009). Broadband Shifts in Local Field Potential Power Spectra Are Correlated with Single-Neuron Spiking in Humans. *Journal of Neuroscience*, *29*(43), 13613–13620. https://doi.org/10/fv2c56

Maoz, U., Rutishauser, U., Kim, S., Cai, X., Lee, D., & Koch, C. (2013). Predeliberation activity in prefrontal cortex and striatum and the prediction of subsequent value judgment. *Frontiers in Neuroscience*, *7*, 225. https://doi.org/10/gmh7gs

Martino, B. D., Camerer, C. F., & Adolphs, R. (2010). Amygdala damage eliminates monetary loss aversion. *Proceedings of the National Academy of Sciences*, *107*(8), 3788–3792. https://doi.org/10/bfk2rz

Matsumoto, M., & Hikosaka, O. (2007). Lateral habenula as a source of negative reward signals in dopamine neurons. *Nature*, *447*(7148), 1111–1115. https://doi.org/10/dsczw5

Matsumoto, M., & Hikosaka, O. (2009). Two types of dopamine neuron distinctly convey positive and negative motivational signals. *Nature*, *459*(7248), 837–841. https://doi.org/10/cm9d9b

Mazzola, L., Mauguière, F., & Isnard, J. (2019). Functional mapping of the human insula: Data from electrical stimulations. *Revue Neurologique*, *175*(3), 150–156. https://doi.org/10/gmmjft

Mazzola, L., Mauguière, F., & Isnard, J. (2017). Electrical Stimulations of the Human Insula: Their Contribution to the Ictal Semiology of Insular Seizures. *Journal of Clinical Neurophysiology*, *34*(4), 307–314. https://doi.org/10/gcwwtx

McClure, S. M., Berns, G. S., & Montague, P. R. (2003). Temporal Prediction Errors in a Passive Learning Task Activate Human Striatum. *Neuron*, *38*(2), 339–346. https://doi.org/10/b54b3g

McGinty, V. B. (2019). Overt Attention toward Appetitive Cues Enhances Their Subjective Value, Independent of Orbitofrontal Cortex Activity. *eNeuro*, *6*(6), ENEURO.0230–19.2019. https://doi.org/10/gmjrs3

McGinty, V. B., Rangel, A., & Newsome, W. T. (2016). Orbitofrontal Cortex Value Signals Depend on Fixation Location during Free Viewing. *Neuron*, *90*(6), 1299–1311. https://doi.org/10/f8r49k

Medvec, V. H., & Savitsky, K. (1997). When doing better means feeling worse: The effects of categorical cutoff points on counterfactual thinking and satisfaction. *Journal of Personality and Social Psychology*, *72*(6), 1284–1296. https://doi.org/10/fq6zd5

Mellers, B. A. (2000). Choice and the relative pleasure of consequences. *Psychological Bulletin*, *126*(6), 910–924. https://doi.org/10/gwf

Mellers, B. A., Schwartz, A., Ho, K., & Ritov, I. (1997). Decision Affect Theory: Emotional Reactions to the Outcomes of Risky Options. *Psychological Science*, *8*(6), 423–429. https://doi.org/10/cmwffx

Mendl, M., Burman, O. H. P., & Paul, E. S. (2010). An integrative and functional framework for the study of animal emotion and mood.

Proceedings of the Royal Society B: Biological Sciences, *277*(1696), 2895–2904. https://doi.org/10/bqggxj

Miller, K. J., Ludvig, E. A., Pezzulo, G., & Shenhav, A. (2018). Chapter 18 - Realigning Models of Habitual and Goal-Directed Decision-Making. In R. Morris, A. Bornstein, & A. Shenhav (Eds.), *Goal-Directed Decision Making* (pp. 407–428). Academic Press. https://doi.org/10.1016/B978-0-12-812098-9.00018-8

Milner, P. M. (1989). The discovery of self-stimulation and other stories. *Neuroscience and Biobehavioral Reviews*, *13*(2-3), 61–67. https://doi.org/10/bjqr32

Molter, F., Thomas, A., Huettel, S. A., Heekeren, H., & Mohr, P. N. C. (2021). Gaze-dependent evidence accumulation predicts multi-alternative risky choice behaviour. https://doi.org/10.31234/osf.io/x6nbf

Montague, P. R., & Berns, G. S. (2002). Neural Economics and the Biological Substrates of Valuation. *Neuron*, *36*(2), 265–284. https://doi.org/10/fnzkmk

Mormann, F., Bausch, M., Knieling, S., & Fried, I. (2019). Neurons in the Human Left Amygdala Automatically Encode Subjective Value Irrespective of Task. *Cerebral Cortex*, *29*(1), 265–272. https://doi.org/10/gcnnr9

Mormann, M. M., Malmaud, J., Huth, A., Koch, C., & Rangel, A. (2010). The Drift Diffusion Model Can Account for the Accuracy and Reaction Time of Value-Based Choices Under High and Low Time Pressure. *Judgment and Decision Making*, *5*(6), 437–449. https://doi.org/10/fxjdhx

Mormann, M. M., Navalpakkam, V., Koch, C., & Rangel, A. (2012). Relative visual saliency differences induce sizable bias in consumer choice. *Journal of Consumer Psychology*, *22*(1), 67–74. https://doi.org/10/c2397z

Mormann, M. M., & Russo, J. E. (2021). Does Attention Increase the Value of Choice Alternatives? *Trends in Cognitive Sciences*, *25*(4), 305–315. https://doi.org/10/gjhp7w

Morris, W. N. (1989). *Mood: The Frame of Mind*. Springer-Verlag. https://doi.org/10.1007/978-1-4612-3648-1

Mrkva, K., & Van Boven, L. (2017). Attentional accounting: Voluntary spatial attention increases budget category prioritization. *Journal of Experimental Psychology: General*, *146*(9), 1296–1306. https://doi.org/10/gcx8q5

Mukamel, R. (2005). Coupling Between Neuronal Firing, Field Potentials, and fMRI in Human Auditory Cortex. *Science*, *309*(5736), 951–954. https://doi.org/10/dhh2v9

Mukamel, R., & Fried, I. (2012). Human intracranial recordings and cognitive neuroscience. *Annual Review of Psychology*, *63*, 511–537. https://doi.org/10/c53gj9

Murphy, F. C., Nimmo-Smith, I., & Lawrence, A. D. (2003). Functional neuroanatomy of emotions: A meta-analysis. *Cognitive, Affective, & Behavioral Neuroscience*, *3*(3), 207–233. https://doi.org/10/bgd8cx

Namburi, P., Al-Hasani, R., Calhoon, G. G., Bruchas, M. R., & Tye, K. M. (2016). Architectural Representation of Valence in the Limbic System. *Neuropsychopharmacology*, *41*(7), 1697–1715. https://doi.org/10/f8m5ts

Napa Scollon, C., Prieto, C.-K., & Diener, E. (2009). Experience Sampling: Promises and Pitfalls, Strength and Weaknesses. In E. Diener (Ed.), *Assessing Well-Being* (pp. 157–180). Springer Netherlands. https://doi.org/10.1007/978-90-481-2354-4_8

Nauta, W. J. H., & Mehler, W. R. (1993). Projections of the Lentiform Nucleus in the Monkey. In W. J. H. Nauta (Ed.), *Neuroanatomy* (pp. 393–431). Birkhäuser. https://doi.org/10.1007/978-1-4684-7920-1_20

Nettle, D., & Bateson, M. (2012). The Evolutionary Origins of Mood and Its Disorders. *Current Biology*, *22*(17), R712–R721. https://doi.org/10/ggd9wk

Niessing, J., Ebisch, B., Schmidt, K. E., Niessing, M., Singer, W., & Galuske, R. A. W. (2005). Hemodynamic signals correlate tightly with synchronized gamma oscillations. *Science (New York, N.Y.)*, *309*(5736), 948–951. https://doi.org/10/bz27m7

Nieuwenhuys, R. (2012). Chapter 7 - The insular cortex: A review. In M. A. Hofman & D. Falk (Eds.), *Progress in Brain Research* (pp. 123–163). Elsevier. https://doi.org/10.1016/B978-0-444-53860-4.00007-6

Nir, Y., Fisch, L., Mukamel, R., Gelbard-Sagiv, H., Arieli, A., Fried, I., & Malach, R. (2007). Coupling between Neuronal Firing Rate, Gamma LFP, and BOLD fMRI Is Related to Interneuronal Correlations. *Current Biology*, *17*(15), 1275–1285. https://doi.org/10/b93t7b

Nokia, M. S., & Wikgren, J. (2014). Effects of Hippocampal State-Contingent Trial Presentation on Hippocampus-Dependent Nonspatial Classical Conditioning and Extinction. *Journal of Neuroscience*, *34*(17), 6003–6010. https://doi.org/10/f5zz2w

Noonan, M. P., Walton, M. E., Behrens, T. E. J., Sallet, J., Buckley, M. J., & Rushworth, M. F. S. (2010). Separate value comparison and learning mechanisms in macaque medial and lateral orbitofrontal cortex. *Proceedings of the National Academy of Sciences*, *107*(47), 20547–20552. https://doi.org/10/bncv3d

Nuwer, M. R., Eliashiv, D., & Stern, J. (2019). Intracranial EEG Monitoring. In M. V. Spanaki & V. S. Wasade (Eds.), *Understanding Epilepsy: A Study Guide for the Boards* (pp. 304–325). Cambridge University Press. https://doi.org/10.1017/9781108754200.017

O'Doherty, J., Kringelbach, M. L., Rolls, E. T., Hornak, J., & Andrews, C. (2001). Abstract reward and punishment representations in the human orbitofrontal cortex. *Nature Neuroscience*, *4*(1), 95–102. https://doi.org/10/cgshnw

O'Doherty, J. P., Dayan, P., Friston, K., Critchley, H., & Dolan, R. J. (2003). Temporal Difference Models and Reward-Related Learning in the Human Brain. *Neuron*, *38*(2), 329–337. https://doi.org/10/bvhv7w

Olds, J., & Milner, P. (1954). Positive reinforcement produced by electrical stimulation of septal area and other regions of rat brain. *Journal of Comparative and Physiological Psychology*, *47*(6), 419–427. https://doi.org/10/bd77b7

Olsen, A. (2012). The Tobii IVT Fixation Filter Algorithm description. Retrieved September 27, 2021, from https://www.semanticscholar.org/paper/The-Tobii-IVT-Fixation-Filter-Algorithm-description-Olsen/66cdac4b380eabb9de3b25c7922c8de92d8d6cae

Öngür, D., & Price, J. (2000). The Organization of Networks within the Orbital and Medial Prefrontal Cortex of Rats, Monkeys and Humans. *Cerebral Cortex*, *10*(3), 206–219. https://doi.org/10/d3t8cp

Öngür, D., Ferry, A. T., & Price, J. L. (2003). Architectonic subdivision of the human orbital and medial prefrontal cortex. *Journal of Comparative Neurology*, *460*(3), 425–449. https://doi.org/10/br4krk

Ostrowsky, K., Isnard, J., Ryvlin, P., Guénot, M., Fischer, C., & Mauguière, F. (2000). Functional Mapping of the Insular Cortex: Clinical Implication in Temporal Lobe Epilepsy. *Epilepsia*, *41*(6), 681–686. https://doi.org/10/d57cw5

Otto, A. R., & Eichstaedt, J. C. (2018). Real-world unexpected outcomes predict city-level mood states and risk-taking behavior. *PLOS ONE*, *13*(11), e0206923. https://doi.org/10/gfscgf

Otto, A. R., Fleming, S. M., & Glimcher, P. W. (2016). Unexpected but Incidental Positive Outcomes Predict Real-World Gambling. *Psychological Science*, *27*(3), 299–311. https://doi.org/10/f8fv5r

Padoa-Schioppa, C. (2009). Range-Adapting Representation of Economic Value in the Orbitofrontal Cortex. *Journal of Neuroscience*, *29*(44), 14004–14014. https://doi.org/10/ccmhdj

Padoa-Schioppa, C. (2013). Neuronal Origins of Choice Variability in Economic Decisions. *Neuron*, *80*(5), 1322–1336. https://doi.org/10/gg39j4

Padoa-Schioppa, C., & Assad, J. A. (2006). Neurons in the orbitofrontal cortex encode economic value. *Nature*, *441*(7090), 223–226. https://doi.org/10/b7xx3b

Padoa-Schioppa, C., & Assad, J. A. (2008). The representation of economic value in the orbitofrontal cortex is invariant for changes of menu. *Nature Neuroscience*, *11*(1), 95–102. https://doi.org/10/dmmf6w

Palminteri, S., & Pessiglione, M. (2017). Opponent Brain Systems for Reward and Punishment Learning. *Decision Neuroscience* (pp. 291–303). Elsevier. https://doi.org/10.1016/B978-0-12-805308-9.00023-3

Palminteri, S., Clair, A.-H., Mallet, L., & Pessiglione, M. (2012). Similar Improvement of Reward and Punishment Learning by Serotonin Reuptake Inhibitors in Obsessive-Compulsive Disorder. *Biological Psychiatry*, *72*(3), 244–250. https://doi.org/10/ggnxsx

Palminteri, S., Justo, D., Jauffret, C., Pavlicek, B., Dauta, A., Delmaire, C., Czernecki, V., Karachi, C., Capelle, L., Durr, A., & Pessiglione, M. (2012). Critical Roles for Anterior Insula and Dorsal Striatum in Punishment-Based Avoidance Learning. *Neuron*, *76*(5), 998–1009. https://doi.org/10/f4gq6b

Palminteri, S., Khamassi, M., Joffily, M., & Coricelli, G. (2015). Contextual modulation of value signals in reward and punishment learning. *Nature Communications*, *6*, 8096. https://doi.org/10/f7pqrn

Palminteri, S., Lebreton, M., Worbe, Y., Grabli, D., Hartmann, A., & Pessiglione, M. (2009). Pharmacological modulation of subliminal learning in Parkinson's and Tourette's syndromes. *Proceedings of the National Academy of Sciences*, *106*(45), 19179–19184. https://doi.org/10/bdxz2k

Parducci, A. (1995). *Happiness, pleasure, and judgment: The contextual theory and its applications*. Lawrence Erlbaum Associates, Inc.

Pärnamets, P., Johansson, P., Hall, L., Balkenius, C., Spivey, M. J., & Richardson, D. C. (2015). Biasing moral decisions by exploiting the dynamics of eye gaze. *Proceedings of the National Academy of Sciences*, *112*(13), 4170–4175. https://doi.org/10/f3ns3f

Parvizi, J., & Kastner, S. (2018). Human Intracranial EEG: Promises and Limitations. *Nature neuroscience*, *21*(4), 474–483. https://doi.org/10/gdcnmz

Pashler, H., Johnston, J. C., & Ruthruff, E. (2001). Attention and Performance. *Annual Review of Psychology*, *52*(1), 629–651. https://doi.org/10/bwbz53

Pauli, W. M., Larsen, T., Collette, S., Tyszka, J. M., Seymour, B., & O'Doherty, J. P. (2015). Distinct Contributions of Ventromedial and Dorsolateral Subregions of the Human Substantia Nigra to Appetitive and Aversive Learning. *Journal of Neuroscience*, *35*(42), 14220–14233. https://doi.org/10/f737bt

Paulus, M. P., Rogalsky, C., Simmons, A., Feinstein, J. S., & Stein, M. B. (2003). Increased activation in the right insula during risk-taking decision making is related to harm avoidance and neuroticism. *NeuroImage*, *19*(4), 1439–1448. https://doi.org/10/fscnx6

Pavlov, I. P. (1927). *Conditioned reflexes: An investigation of the physiological activity of the cerebral cortex*. Oxford Univ. Press.

Payne, J. W., Braunstein, M. L., & Carroll, J. S. (1978). Exploring predecisional behavior: An alternative approach to decision research. *Organizational Behavior and Human Performance*, *22*(1), 17–44. https://doi.org/10/dck9v2

Peck, C. J., Jangraw, D. C., Suzuki, M., Efem, R., & Gottlieb, J. (2009). Reward Modulates Attention Independently of Action Value in Posterior Parietal Cortex. *Journal of Neuroscience*, *29*(36), 11182–11191. https://doi.org/10/cp77vd

Pessiglione, M., & Delgado, M. R. (2015). The good, the bad and the brain: Neural correlates of appetitive and aversive values underlying decision making. *Current Opinion in Behavioral Sciences*, *5*, 78–84. https://doi.org/10/gfpf3g

Pessiglione, M., Seymour, B., Flandin, G., Dolan, R. J., & Frith, C. D. (2006). Dopamine-dependent prediction errors underpin reward-seeking behaviour in humans. *Nature*, *442*(7106), 1042–1045. https://doi.org/10/dczrgr

Pessiglione, M., Vinckier, F., Bouret, S., Daunizeau, J., & Le Bouc, R. (2018). Why not try harder? Computational approach to motivation deficits in neuro-psychiatric diseases. *Brain*, *141*(3), 629–650. https://doi.org/10/gc64fh

Pessoa, L., Gutierrez, E., Bandettini, P. A., & Ungerleider, L. G. (2002). Neural Correlates of Visual Working Memory: fMRI Amplitude Predicts Task Performance. *Neuron*, *35*(5), 975–987. https://doi.org/10/fjf22w

Pessoa, L., & Padmala, S. (2005). Quantitative prediction of perceptual decisions during near-threshold fear detection. *Proceedings of the National Academy of Sciences*, *102*(15), 5612–5617. https://doi.org/10/dm9hcc

Peterson, W., Birdsall, T., & Fox, W. (1954). The theory of signal detectability. *Transactions of the IRE Professional Group on Information Theory*, *4*(4), 171–212. https://doi.org/10/fv7v5j

Picard, F., Scavarda, D., & Bartolomei, F. (2013). Induction of a sense of bliss by electrical stimulation of the anterior insula. *Cortex*, *49*(10), 2935–2937. https://doi.org/10/ggxgfv

Plassmann, H., O'Doherty, J. P., & Rangel, A. (2010). Appetitive and Aversive Goal Values Are Encoded in the Medial Orbitofrontal Cortex at the Time of Decision Making. *Journal of Neuroscience*, *30*(32), 10799–10808. https://doi.org/10/dztntt

Plassmann, H., O'Doherty, J., & Rangel, A. (2007). Orbitofrontal Cortex Encodes Willingness to Pay in Everyday Economic Transactions. *Journal of Neuroscience*, *27*(37), 9984–9988. https://doi.org/10/bgmh66

Platt, M. L., & Plassmann, H. (2014). Chapter 13 - Multistage Valuation Signals and Common Neural Currencies. In P. W. Glimcher & E. Fehr (Eds.), *Neuroeconomics (Second Edition)* (pp. 237–258). Academic Press. https://doi.org/10.1016/B978-0-12-416008-8.00013-9

Preuschoff, K., Quartz, S. R., & Bossaerts, P. (2008). Human Insula Activation Reflects Risk Prediction Errors As Well As Risk. *Journal of Neuroscience*, *28*(11), 2745–2752. https://doi.org/10/fpbf4p

Price, J. L. (2006). Chapter 3: Connections of orbital cortex. In D. H. Zald & S. L. Rauch (Eds.), *The Orbitofrontal Cortex* (pp. 39–55). OUP Oxford.

Price, J. L. (2007). Definition of the Orbital Cortex in Relation to Specific Connections with Limbic and Visceral Structures and Other Cortical Regions. *Annals of the New York Academy of Sciences*, *1121*(1), 54–71. https://doi.org/10/cktn5p

Purcell, J. R., Jahn, A., Fine, J. M., & Brown, J. W. (2021). Neural correlates of visual attention during risky decision evidence integration. *NeuroImage*, *234*, 117979. https://doi.org/10/gjkrst

Quiroga, R. Q. (2019). Plugging in to Human Memory: Advantages, Challenges, and Insights from Human Single-Neuron Recordings. *Cell*, *179*(5), 1015–1032. https://doi.org/10/ghmr7c

Raccah, O., Block, N., & Fox, K. C. R. (2021). Does the Prefrontal Cortex Play an Essential Role in Consciousness? Insights from Intracranial Electrical Stimulation of the Human Brain. *Journal of Neuroscience*, *41*(10), 2076–2087. https://doi.org/10/gjvd99

Raghuraman, A. P., & Padoa-Schioppa, C. (2014). Integration of Multiple Determinants in the Neuronal Computation of Economic Values. *Journal of Neuroscience*, *34*(35), 11583–11603. https://doi.org/10/f6f5rv

Rahman, S., Sahakian, B. J., Hodges, J. R., Rogers, R. D., & Robbins, T. W. (1999). Specific cognitive deficits in mild frontal variant frontotemporal dementia. *Brain*, *122*(8), 1469–1493. https://doi.org/10/bkcz62

Raichle, M. E. (2015). The restless brain: How intrinsic activity organizes brain function. *Philosophical Transactions of the Royal Society B: Biological Sciences*, *370*(1668), 20140172. https://doi.org/10/gfz5g8

Rangel, A., Camerer, C., & Montague, P. R. (2008). A framework for studying the neurobiology of value-based decision making. *Nature Reviews Neuroscience*, *9*(7), 545–556. https://doi.org/10/bx8mxw

Rangel, A., & Clithero, J. A. (2012). Value normalization in decision making: Theory and evidence. *Current Opinion in Neurobiology*, *22*(6), 970–981. https://doi.org/10/gk59wp

Rangel, A., & Clithero, J. A. (2014). Chapter 8 - The Computation of Stimulus Values in Simple Choice. In P. W. Glimcher & E. Fehr (Eds.), *Neuroeconomics (Second Edition)* (pp. 125–148). Academic Press. https://doi.org/10.1016/B978-0-12-416008-8.00008-5

Rangel, A., & Hare, T. (2010). Neural computations associated with goal-directed choice. *Current Opinion in Neurobiology*, *20*(2), 262–270. https://doi.org/10/cmddxw

Rao, V. R., Sellers, K. K., Wallace, D. L., Lee, M. B., Bijanzadeh, M., Sani, O. G., Yang, Y., Shanechi, M. M., Dawes, H. E., & Chang, E. F. (2018). Direct Electrical Stimulation of Lateral Orbitofrontal Cortex Acutely Improves Mood in Individuals with Symptoms of Depression. *Current Biology*, *28*(24), 3893–3902.e4. https://doi.org/10/gfwnt9

Ratcliff, R. (1978). A theory of memory retrieval. *Psychological Review*, *85*(2), 59–108. https://doi.org/10/fjwm2f

Ratcliff, R., & Smith, P. L. (2004). A Comparison of Sequential Sampling Models for Two-Choice Reaction Time. *Psychological review*, *111*(2), 333–367. https://doi.org/10/cwzpgj

Ratcliff, R., Smith, P. L., Brown, S. D., & McKoon, G. (2016). Diffusion Decision Model: Current Issues and History. *Trends in Cognitive Sciences*, *20*(4), 260–281. https://doi.org/10/f8gvmz

Ray, S., Crone, N. E., Niebur, E., Franaszczuk, P. J., & Hsiao, S. S. (2008). Neural Correlates of High-Gamma Oscillations (60-200 Hz) in Macaque Local Field Potentials and Their Potential Implications in Electrocorticography. *Journal of Neuroscience*, *28*(45), 11526–11536. https://doi.org/10/fnnk7j

Redgrave, P., Rodriguez, M., Smith, Y., Rodriguez-Oroz, M. C., Lehericy, S., Bergman, H., Agid, Y., DeLong, M. R., & Obeso, J. A. (2010). Goal-directed and habitual control in the basal ganglia: Implications for Parkinson's disease. *Nature Reviews Neuroscience*, *11*(11), 760–772. https://doi.org/10/c53hd9

Ress, D., & Heeger, D. J. (2003). Neuronal correlates of perception in early visual cortex. *Nature Neuroscience*, *6*(4), 414–420. https://doi.org/10/cgbg6m

Rigoli, F., Pavone, E. F., & Pezzulo, G. (2012). Aversive Pavlovian Responses Affect Human Instrumental Motor Performance. *Frontiers in Neuroscience*, *6*. https://doi.org/10/gk454j

Rigoux, L., Stephan, K., Friston, K., & Daunizeau, J. (2014). Bayesian model selection for group studies — Revisited. *NeuroImage*, *84*, 971–985. https://doi.org/10/f5mnz3

Rivière, D., Geffroy, D., Denghien, I., Souedet, N., & Cointepas, Y. (2009). BrainVISA: An extensible software environment for sharing multimodal neuroimaging data and processing tools. *NeuroImage*, *Supplement 1*(47), S163. https://doi.org/10/bqczdr

Robert, C. P. (2007). *The Bayesian choice: From decision-theoretic foundations to computational implementation* (2nd ed). Springer.

Rolls, E. T., Cheng, W., & Feng, J. (2020). The orbitofrontal cortex: Reward, emotion and depression. *Brain Communications*, *2*. https://doi.org/10/ghp7bp

Rolls, E. T., Sienkiewicz, Z. J., & Yaxley, S. (1989). Hunger Modulates the Responses to Gustatory Stimuli of Single Neurons in the Caudolateral Orbitofrontal Cortex of the Macaque Monkey. *European Journal of Neuroscience*, *1*(1), 53–60. https://doi.org/10/fpp38n

Rossi, M. (2019). A perceptual theory of moods. *Synthese*. https://doi.org/10/gj42rg

Ruckmick, C. A. (1936). *The psychology of feeling and emotion*. McGraw-Hill. https://doi.org/10.1037/10770-000

Rudebeck, P. H., & Murray, E. A. (2011). Dissociable Effects of Subtotal Lesions within the Macaque Orbital Prefrontal Cortex on Reward-Guided Behavior. *Journal of Neuroscience*, *31*(29), 10569–10578. https://doi.org/10/c7g347

Rudorf, S., Preuschoff, K., & Weber, B. (2012). Neural Correlates of Anticipation Risk Reflect Risk Preferences. *Journal of Neuroscience*, *32*(47), 16683–16692. https://doi.org/10/f4hjzf

Ruff, C. C., & Fehr, E. (2014). The neurobiology of rewards and values in social decision making. *Nature Reviews Neuroscience*, *15*(8), 549–562. https://doi.org/10/f59phm

Ruff, C. C., & Huettel, S. A. (2014). Chapter 6 - Experimental Methods in Cognitive Neuroscience. In P. W. Glimcher & E. Fehr (Eds.), *Neuroeconomics (Second Edition)* (pp. 77–108). Academic Press. https://doi.org/10.1016/B978-0-12-416008-8.00006-1

Russell, J. A. (1980). A circumplex model of affect. *Journal of Personality and Social Psychology*, *39*(6), 1161–1178. https://doi.org/10/fc6rg5

Russell, J. A. (2003). Core affect and the psychological construction of emotion. *Psychological Review*, *110*(1), 145–172. https://doi.org/10/cjkdr6

Rutledge, R. B., Skandali, N., Dayan, P., & Dolan, R. J. (2014). A computational and neural model of momentary subjective well-being. *Proceedings of the National Academy of Sciences*, *111*(33), 12252–12257. https://doi.org/10/t3g

Rutledge, R. B., Lazzaro, S. C., Lau, B., Myers, C. E., Gluck, M. A., & Glimcher, P. W. (2009). Dopaminergic Drugs Modulate Learning Rates and Perseveration in Parkinson's Patients in a Dynamic Foraging Task. *Journal of Neuroscience*, *29*(48), 15104–15114. https://doi.org/10/dx88pr

Rutledge, R. B., Skandali, N., Dayan, P., & Dolan, R. J. (2015). Dopaminergic Modulation of Decision Making and Subjective Well-Being. *Journal of Neuroscience*, *35*(27), 9811–9822. https://doi.org/10/f7j7fm

Ryvlin, P., & Picard, F. (2017). Invasive Investigation of Insular Cortex Epilepsy. *Journal of Clinical Neurophysiology*, *34*(4), 328–332. https://doi.org/10/gcv8fk

Sadaghiani, S., Hesselmann, G., Friston, K. J., & Kleinschmidt, A. (2010). The Relation of Ongoing Brain Activity, Evoked Neural Responses, and Cognition. *Frontiers in Systems Neuroscience*, *4*, 20. https://doi.org/10/bfc88q

Sadaghiani, S., Hesselmann, G., & Kleinschmidt, A. (2009). Distributed and Antagonistic Contributions of Ongoing Activity Fluctuations to Auditory Stimulus Detection. *Journal of Neuroscience*, *29*(42), 13410–13417. https://doi.org/10/cqgs7n

Saez, I., Lin, J., Stolk, A., Chang, E., Parvizi, J., Schalk, G., Knight, R. T., & Hsu, M. (2018). Encoding of Multiple Reward-Related Computations in Transient and Sustained High-Frequency Activity in Human OFC. *Current Biology*, *28*(18), 2889–2899.e3. https://doi.org/10/gfcjf5

Saga, Y., Ruff, C. C., & Tremblay, L. (2019). Disturbance of approach-avoidance behaviors in non-human primates by stimulation of the limbic territories of basal ganglia and anterior insula. *European Journal of Neuroscience*, *49*(5), 687–700. https://doi.org/10/gmrwg4

Salari, N., & Rose, M. (2016). Dissociation of the functional relevance of different pre-stimulus oscillatory activity for memory formation. *NeuroImage*, *125*, 1013–1021. https://doi.org/10/f74nsw

Sanfey, A. G., Hastie, R., Colvin, M. K., & Grafman, J. (2003). Phineas gauged: Decision-making and the human prefrontal cortex. *Neuropsychologia*, *41*(9), 1218–1229. https://doi.org/10/frk7pp

Sani, O. G., Yang, Y., Lee, M. B., Dawes, H. E., Chang, E. F., & Shanechi, M. M. (2018). Mood variations decoded from multi-site intracranial human brain activity. *Nature Biotechnology*, *36*(10), 954–961. https://doi.org/10/ctp2

Saunders, E. M. (1993). Stock Prices and Wall Street Weather. *The American Economic Review*, *83*(5), 1337–1345.

Savage, L. J. (1954). *The foundations of statistics*. John Wiley & Sons.

Scherer, K. R. (2000). Psychological models of emotion. *The neuropsychology of emotion* (pp. 137–162). Oxford University Press.

Schevon, C. A., Trevelyan, A. J., Schroeder, C. E., Goodman, R. R., McKhann, G., Jr, & Emerson, R. G. (2009). Spatial characterization of interictal high frequency oscillations in epileptic neocortex. *Brain*, *132*(11), 3047–3059. https://doi.org/10/dbmv5v

Schultz, W., Apicella, P., Scarnati, E., & Ljungberg, T. (1992). Neuronal activity in monkey ventral striatum related to the expectation of reward. *Journal of Neuroscience*, *12*(12), 4595–4610. https://doi.org/10/gmgzx4

Schultz, W. (2007). Multiple Dopamine Functions at Different Time Courses. *Annual Review of Neuroscience*, *30*(1), 259–288. https://doi.org/10/fj4rwh

Schultz, W. (2016). Dopamine reward prediction error coding. *Dialogues in Clinical Neuroscience*, *18*(1), 23–32. Retrieved August 11, 2021, from https://www.ncbi.nlm.nih.gov/pmc/articles/PMC4826767/

Schultz, W., Dayan, P., & Montague, P. R. (1997). A Neural Substrate of Prediction and Reward. *Science*, *275*(5306), 1593–1599. https://doi.org/10/bh8sst

Schultz, W., Tremblay, L., & Hollerman, J. R. (2000). Reward Processing in Primate Orbitofrontal Cortex and Basal Ganglia. *Cerebral Cortex*, *10*(3), 272–283. https://doi.org/10/cc5xb4

Schwarz, N. (2012). Feelings-as-information theory. In P. Van Lange, A. Kruglanski, & E. T. Higgins (Eds.), *Handbook of theories of social psychology* (pp. 289–308). Sage Publications Ltd. Retrieved June 7, 2017, from https://doi.org/10/gjnskm

Schwarz, N., & Clore, G. L. (1983). Mood, misattribution, and judgments of well-being: Informative and directive functions of affective states. *Journal of personality and social psychology*, *45*(3), 513. https://doi.org/10/d9jqnr

Schwarz, N., & Clore, G. L. (2003). Mood as information: 20 years later. *Psychological Inquiry*, *14*(3-4), 296–303. https://doi.org/10.1207/s15327965pli1403&4_20

Schwarz, N., & Clore, G. L. (2007). Feelings and phenomenal experiences. In A. W. Kruglanski & E. T. Higgins (Eds.), *Social psychology: Handbook of basic principles* (pp. 385–407). Guilford.

Schweighofer, N., Bertin, M., Shishida, K., Okamoto, Y., Tanaka, S. C., Yamawaki, S., & Doya, K. (2008). Low-Serotonin Levels Increase Delayed Reward Discounting in Humans. *Journal of Neuroscience*, *28*(17), 4528–4532. https://doi.org/10/d948jb

Seager, M. A., Johnson, L. D., Chabot, E. S., Asaka, Y., & Berry, S. D. (2002). Oscillatory brain states and learning: Impact of hippocampal theta-contingent training. *Proceedings of the National Academy of Sciences*, *99*(3), 1616–1620. https://doi.org/10/ft92hc

Selimbeyoglu, A., & Parvizi, J. (2010). Electrical stimulation of the human brain: Perceptual and behavioral phenomena reported in the old and new literature. *Frontiers in Human Neuroscience*, *4*, 46. https://doi.org/10/d8hrjg

Serences, J. T. (2008). Value-Based Modulations in Human Visual Cortex. *Neuron*, *60*(6), 1169–1181. https://doi.org/10/cq7h6j

Setogawa, T., Mizuhiki, T., Matsumoto, N., Akizawa, F., Kuboki, R., Richmond, B. J., & Shidara, M. (2019). Neurons in the monkey orbitofrontal cortex mediate reward value computation and decision-making. *Communications Biology*, *2*(1), 1–9. https://doi.org/10/gmw86g

Seymour, B., Daw, N., Dayan, P., Singer, T., & Dolan, R. (2007). Differential Encoding of Losses and Gains in the Human Striatum. *Journal of Neuroscience*, *27*(18), 4826–4831. https://doi.org/10/b9wxx7

Seymour, B., & McClure, S. M. (2008). Anchors, scales and the relative coding of value in the brain. *Current Opinion in Neurobiology*, *18*(2), 173–178. https://doi.org/10/bsngrh

Seymour, B., O'Doherty, J. P., Dayan, P., Koltzenburg, M., Jones, A. K., Dolan, R. J., Friston, K. J., & Frackowiak, R. S. (2004). Temporal difference models describe higher-order learning in humans. *Nature*, *429*(6992), 664–667. https://doi.org/10/dqrsq9

Seymour, B., Singer, T., & Dolan, R. (2007). The neurobiology of punishment. *Nature Reviews Neuroscience*, *8*(4), 300–311. https://doi.org/10/cn2zx3

Shadlen, M. N., & Newsome, W. T. (1998). The Variable Discharge of Cortical Neurons: Implications for Connectivity, Computation, and Information Coding. *Journal of Neuroscience*, *18*(10), 3870–3896. https://doi.org/10/gf3zxw

Shadlen, M. N., & Newsome, W. T. (2001). Neural Basis of a Perceptual Decision in the Parietal Cortex (Area LIP) of the Rhesus Monkey. *Journal of Neurophysiology*, *86*(4), 1916–1936. https://doi.org/10/ggfq84

Sheng, F., Ramakrishnan, A., Seok, D., Zhao, W. J., Thelaus, S., Cen, P., & Platt, M. L. (2020). Decomposing loss aversion from gaze allocation and pupil dilation. *Proceedings of the National Academy of Sciences*, *117*(21), 11356–11363. https://doi.org/10/gkztcn

Shepherd, M., Findlay, J. M., & Hockey, R. J. (1986). The relationship between eye movements and spatial attention. *The Quarterly Journal of Experimental Psychology Section A*, *38*(3), 475–491. https://doi.org/10/bfxhgd

Shevchenko, Y. (2018). *The Influence of Mood on Decision-Making* (Doctoral dissertation). University of Mannheim. Mannheim. Retrieved July 30, 2021, from https://madoc.bib.uni-mannheim.de/45647

Shimojo, S., Simion, C., Shimojo, E., & Scheier, C. (2003). Gaze bias both reflects and influences preference. *Nature Neuroscience*, *6*(12), 1317–1322. https://doi.org/10/dgk92m

Shiner, T., Seymour, B., Wunderlich, K., Hill, C., Bhatia, K. P., Dayan, P., & Dolan, R. J. (2012). Dopamine and performance in a reinforcement learning task: Evidence from Parkinson's disease. *Brain*, *135*(6), 1871–1883. https://doi.org/10/f3zzs7

Shiv, B., Loewenstein, G., Bechara, A., Damasio, H., & Damasio, A. R. (2005). Investment Behavior and the Negative Side of Emotion. *Psychological Science*, *16*(6), 435–439. https://doi.org/10.1111/j.0956-7976.2005.01553.x

Shmuel, A., & Leopold, D. A. (2008). Neuronal correlates of spontaneous fluctuations in fMRI signals in monkey visual cortex: Implications for functional connectivity at rest. *Human Brain Mapping*, *29*(7), 751–761. https://doi.org/10/csk373

Singh, T. D., Sabsevitz, D. S., Desai, N. N., Middlebrooks, E. H., Feyissa, A. M., Grewal, S., Wharen, R. E., Tatum, W. O., & Ritaccio, A. L. (2021). Crying with depressed affect induced by electrical stimulation of the anterior insula: A stereo EEG case study. *Epilepsy & Behavior Reports*, *15*, 100421. https://doi.org/10/gmr3zp

Smith, S. M., & Krajbich, I. (2018). Attention and choice across domains. *Journal of Experimental Psychology. General*, *147*(12), 1810–1826. https://doi.org/10/gfr2dt

Smith, S. M., & Krajbich, I. (2019). Gaze Amplifies Value in Decision Making. *Psychological Science*, *30*(1), 116–128. https://doi.org/10/gfpfvs

Softky, W. R., & Koch, C. (1993). The highly irregular firing of cortical cells is inconsistent with temporal integration of random EPSPs. *Journal of Neuroscience*, *13*(1), 334–350. https://doi.org/10/ggzph6

Soubrié, P. (1986). Reconciling the role of central serotonin neurons in human and animal behavior. *Behavioral and Brain Sciences*, *9*(2), 319–335. https://doi.org/10/cm973r

Spies, M., Knudsen, G. M., Lanzenberger, R., & Kasper, S. (2015). The serotonin transporter in psychiatric disorders: Insights from PET imaging. *The Lancet Psychiatry*, *2*(8), 743–755. https://doi.org/10/f7ktgp

Stănişor, L., van der Togt, C., Pennartz, C. M. A., & Roelfsema, P. R. (2013). A unified selection signal for attention and reward in primary visual cortex. *Proceedings of the National Academy of Sciences*, *110*(22), 9136–9141. https://doi.org/10/f44x8z

Stauffer, W. R., Lak, A., & Schultz, W. (2014). Dopamine Reward Prediction Error Responses Reflect Marginal Utility. *Current Biology*, *24*(21), 2491–2500. https://doi.org/10/f6nph7

Stephani, C., Fernandez-Baca Vaca, G., Maciunas, R., Koubeissi, M., & Lüders, H. O. (2011). Functional neuroanatomy of the insular lobe. *Brain Structure & Function*, *216*(2), 137–149. https://doi.org/10/df3dgs

Stewart, N., Hermens, F., & Matthews, W. J. (2016). Eye Movements in Risky Choice. *Journal of Behavioral Decision Making*, *29*(2-3), 116–136. https://doi.org/10/f8f5z7

Strait, C. E., Blanchard, T. C., & Hayden, B. Y. (2014). Reward Value Comparison via Mutual Inhibition in Ventromedial Prefrontal Cortex. *Neuron*, *82*(6), 1357–1366. https://doi.org/10/f56xkp

Strauss, G. P., Waltz, J. A., & Gold, J. M. (2014). A Review of Reward Processing and Motivational Impairment in Schizophrenia. *Schizophrenia Bulletin*, *40*, S107–S116. https://doi.org/10/gf5bfx

Tajima, S., Drugowitsch, J., & Pouget, A. (2016). Optimal policy for value-based decision-making. *Nature Communications*, *7*(1), 12400. https://doi.org/10/gk8xcv

Tanner Jr., W. P., & Swets, J. A. (1954). A decision-making theory of visual detection. *Psychological Review*, *61*(6), 401–409. https://doi.org/10/dvdhcw

Tavares, G., Perona, P., & Rangel, A. (2017). The Attentional Drift Diffusion Model of Simple Perceptual Decision-Making. *Frontiers in Neuroscience*, *11*. https://doi.org/10/gfzjpq

Thomas, A. W., Molter, F., & Krajbich, I. (2021). Uncovering the computational mechanisms underlying many-alternative choice. *eLife*, *10*, e57012. https://doi.org/10/gj35r7

Thomas, A. W., Molter, F., Krajbich, I., Heekeren, H. R., & Mohr, P. N. C. (2019). Gaze bias differences capture individual choice behaviour. *Nature Human Behaviour*, *3*(6), 625–635. https://doi.org/10/ghsxp2

Thorpe, S. J., Rolls, E. T., & Maddison, S. (1983). The orbitofrontal cortex: Neuronal activity in the behaving monkey. *Experimental Brain Research*, *49*(1), 93–115. https://doi.org/10/fvzzmp

Tobler, P. N., O'Doherty, J. P., Dolan, R. J., & Schultz, W. (2007). Reward Value Coding Distinct From Risk Attitude-Related Uncertainty Coding in Human Reward Systems. *Journal of Neurophysiology*, *97*(2), 1621–1632. https://doi.org/10/bvqqbq

Tobler, P. N., & Weber, E. U. (2014). Chapter 9 - Valuation for Risky and Uncertain Choices. In P. W. Glimcher & E. Fehr (Eds.), *Neuroeconomics (Second Edition)* (pp. 149–172). Academic Press. https://doi.org/10.1016/B978-0-12-416008-8.00009-7

Tom, S. M., Fox, C. R., Trepel, C., & Poldrack, R. A. (2007). The Neural Basis of Loss Aversion in Decision-Making Under Risk. *Science*, *315*(5811), 515–518. https://doi.org/10/bhtqgn

Towal, R. B., Mormann, M. M., & Koch, C. (2013). Simultaneous modeling of visual saliency and value computation improves predictions of economic choice. *Proceedings of the National Academy of Sciences*, *110*(40), E3858–E3867. https://doi.org/10/f5cbkw

Trebaul, L., Deman, P., Tuyisenge, V., Jedynak, M., Hugues, E., Rudrauf, D., Bhattacharjee, M., Tadel, F., Chanteloup-Foret, B., Saubat, C., Reyes Mejia, G. C., Adam, C., Nica, A., Pail, M., Dubeau, F., Rheims, S., Trébuchon, A., Wang, H., Liu, S., … David, O. (2018). Probabilistic functional tractography of the human cortex revisited. *NeuroImage*, *181*, 414–429. https://doi.org/10/gfcsvg

Tremblay, L., & Schultz, W. (1999). Relative reward preference in primate orbitofrontal cortex. *Nature*, *398*(6729), 704–708. https://doi.org/10/btbcq8

Trueblood, J. S., Brown, S. D., & Heathcote, A. (2014). The multiattribute linear ballistic accumulator model of context effects in multialternative choice. *Psychological Review*, *121*(2), 179–205. https://doi.org/10/f5zxdk

Tuyisenge, V., Trebaul, L., Bhattacharjee, M., Chanteloup-Forêt, B., Saubat-Guigui, C., Mîndruţă, I., Rheims, S., Maillard, L., Kahane, P., Taussig, D., & David, O. (2018). Automatic bad channel detection in intracranial electroencephalographic recordings using ensemble machine learning. *Clinical Neurophysiology*, *129*(3), 548–554. https://doi.org/10/gc6f3t

Tversky, A., & Kahneman, D. (1981). The framing of decisions and the psychology of choice. *Science*, *211*(4481), 453–458. https://doi.org/10/fj3z3r

Tversky, A. (1969). Intransitivity of preferences. *Psychological Review*, *76*(1), 31–48. https://doi.org/10/d59cww

Tversky, A., & Kahneman, D. (1974). Judgment under Uncertainty: Heuristics and Biases. *Science*, *185*(4157), 1124–1131. https://doi.org/10/gwh

Uddin, L. Q., Kinnison, J., Pessoa, L., & Anderson, M. L. (2014). Beyond the Tripartite Cognition–Emotion–Interoception Model of the Human Insular Cortex. *Journal of Cognitive Neuroscience*, *26*(1), 16–27. https://doi.org/10/gdmwfx

Uddin, L. Q., Nomi, J. S., Hébert-Seropian, B., Ghaziri, J., & Boucher, O. (2017). Structure and Function of the Human Insula. *Journal of Clinical Neurophysiology*, *34*(4), 300–306. https://doi.org/10/gbpr99

Unruh-Pinheiro, A., Hill, M. R., Weber, B., Boström, J., Elger, C. E., & Mormann, F. (2020). Single-Neuron Correlates of Decision Confidence in the Human Medial Temporal Lobe. *Current Biology*, *30*(23), 4722–4732.e5. https://doi.org/10/ghfq33

Vaidya, A. R., & Fellows, L. K. (2015a). Testing necessary regional frontal contributions to value assessment and fixation-based updating. *Nature Communications*, *6*(1), 10120. https://doi.org/10/f76mgv

Vaidya, A. R., & Fellows, L. K. (2015b). Ventromedial Frontal Cortex Is Critical for Guiding Attention to Reward-Predictive Visual Features in Humans. *Journal of Neuroscience*, *35*(37), 12813–12823. https://doi.org/10/f7whhg

Venkatraman, V., Payne, J. W., Bettman, J. R., Luce, M. F., & Huettel, S. A. (2009). Separate Neural Mechanisms Underlie Choices and Strategic Preferences in Risky Decision Making. *Neuron*, *62*(4), 593–602. https://doi.org/10/bbpzgc

Villano, W. J., Otto, A. R., Ezie, C. E. C., Gillis, R., & Heller, A. S. (2020). Temporal dynamics of real-world emotion are more strongly linked to prediction error than outcome. *Journal of Experimental Psychology. General*, *149*(9), 1755–1766. https://doi.org/10/gjgs6k

Vinckier, F., Rigoux, L., Oudiette, D., & Pessiglione, M. (2018). Neuro-computational account of how mood fluctuations arise and affect decision making. *Nature Communications*, *9*(1), 1708. https://doi.org/10/gdh48h

Vinding, M. C., Lindeløv, J. K., Xiao, Y., Chan, R. C. K., & Sørensen, T. A. (2021). Volition in prospective Memory: Evidence against differences between free and fixed target events. *Consciousness and Cognition*, *94*, 103175. https://doi.org/10/gmq2fn

Vlaev, I., Chater, N., Stewart, N., & Brown, G. D. A. (2011). Does the brain calculate value? *Trends in Cognitive Sciences*, *15*(11), 546–554. https://doi.org/10/bbwthf

Volkow, N. D., & Li, T.-K. (2004). Drug addiction: The neurobiology of behaviour gone awry. *Nature Reviews Neuroscience*, *5*(12), 963–970. https://doi.org/10/d34qb6

Von Neumann, J., & Morgenstern, O. (1944). *Theory of games and economic behavior*. Princeton University Press.

Von Siebenthal, Z., Boucher, O., Rouleau, I., Lassonde, M., Lepore, F., & Nguyen, D. K. (2016). Decision-making impairments following insular and medial temporal lobe resection for drug-resistant epilepsy. *Social Cognitive and Affective Neuroscience*, 128–137. https://doi.org/10/gg39kf

von Ellenrieder, N., Frauscher, B., Dubeau, F., & Gotman, J. (2016). Interaction with slow waves during sleep improves discrimination of physiologic and pathologic high-frequency oscillations (80–500 Hz). *Epilepsia*, *57*(6), 869–878. https://doi.org/10/f8zmwg

Wallis, J. D. (2011). Cross-species studies of orbitofrontal cortex and value-based decision-making. *Nature neuroscience*, *15*(1), 13–19. https://doi.org/10/drfnv7

Wallis, J. D., & Miller, E. K. (2003). Neuronal activity in primate dorsolateral and orbital prefrontal cortex during performance of a reward preference task. *European Journal of Neuroscience*, *18*(7), 2069–2081. https://doi.org/10/c55z8b

Wallis, J. D., & Rushworth, M. F. S. (2014). Chapter 22 - Integrating Benefits and Costs in Decision Making. In P. W. Glimcher & E. Fehr (Eds.), *Neuroeconomics (Second Edition)* (pp. 411–433). Academic Press. https://doi.org/10.1016/B978-0-12-416008-8.00022-X

Watson, D., Clark, L. A., & Tellegen, A. (1988). Development and validation of brief measures of positive and negative affect: The PANAS scales. *Journal of Personality and Social Psychology*, *54*(6), 1063–1070. https://doi.org/10/cs7zhv

Watson, D., & Tellegen, A. (1985). Toward a consensual structure of mood. *Psychological Bulletin*, *98*(2), 219–235. https://doi.org/10/dcxmmn

Webb, L. E., Veenhoven, R., Harfeld, J. L., & Jensen, M. B. (2019). What is animal happiness? *Annals of the New York Academy of Sciences*, *1438*(1), 62–76. https://doi.org/10/gfgzrv

Weller, J. A., Levin, I. P., Shiv, B., & Bechara, A. (2007). Neural Correlates of Adaptive Decision Making for Risky Gains and Losses. *Psychological Science*, *18*(11), 958–964. https://doi.org/10/dg5wtt

Weller, J. A., Levin, I. P., Shiv, B., & Bechara, A. (2009). The effects of insula damage on decision-making for risky gains and losses. *Social Neuroscience*, *4*(4), 347–358. https://doi.org/10/bh6c35

West, E. A., DesJardin, J. T., Gale, K., & Malkova, L. (2011). Transient Inactivation of Orbitofrontal Cortex Blocks Reinforcer Devaluation in Macaques. *Journal of Neuroscience*, *31*(42), 15128–15135. https://doi.org/10/b9zgb7

Westbrook, A., Kester, D., & Braver, T. S. (2013). What Is the Subjective Cost of Cognitive Effort? Load, Trait, and Aging Effects Revealed by Economic Preference. *PLOS ONE*, *8*(7), e68210. https://doi.org/10/f5bxc6

Westermann, R., Spies, K., Stahl, G., & Hesse, F. W. (1996). Relative effectiveness and validity of mood induction procedures: A meta-analysis. *European Journal of Social Psychology*, *26*(4), 557–580. https://doi.org/10/df9vkv

Wiech, K., Lin, C.-s., Brodersen, K. H., Bingel, U., Ploner, M., & Tracey, I. (2010). Anterior Insula Integrates Information about Salience into Perceptual Decisions about Pain. *Journal of Neuroscience*, *30*(48), 16324–16331. https://doi.org/10/c3cn2h

Wilkinson, G. N., & Rogers, C. E. (1973). Symbolic Description of Factorial Models for Analysis of Variance. *Journal of the Royal Statistical Society: Series C (Applied Statistics)*, *22*(3), 392–399. https://doi.org/10/d66r47

Williams, Z. M., Elfar, J. C., Eskandar, E. N., Toth, L. J., & Assad, J. A. (2003). Parietal activity and the perceived direction of ambiguous

apparent motion. *Nature Neuroscience*, *6*(6), 616–623. https://doi.org/10/fkm6st

Wilson, T. D., & Gilbert, D. T. (2005). Affective Forecasting: Knowing What to Want. *Current Directions in Psychological Science*, *14*(3), 131–134. https://doi.org/10/d6nz6w

Winawer, J., Kay, K. N., Foster, B. L., Rauschecker, A. M., Parvizi, J., & Wandell, B. A. (2013). Asynchronous Broadband Signals Are the Principal Source of the BOLD Response in Human Visual Cortex. *Current Biology*, *23*(13), 1145–1153. https://doi.org/10/f456nj

Wise, R. A. (1982). Neuroleptics and operant behavior: The anhedonia hypothesis. *Behavioral and Brain Sciences*, *5*(1), 39–53. https://doi.org/10/djc6n6

Wise, R. A. (1996). Neurobiology of addiction. *Current Opinion in Neurobiology*, *6*(2), 243–251. https://doi.org/10/cb34b8

Wollschläger, L., & Diederich, A. (2012). The 2N-ary Choice Tree Model for N-Alternative Preferential Choice. *Frontiers in Psychology*, *3*, 189. https://doi.org/10/gmw5ch

Wyart, V., & Tallon-Baudry, C. (2009). How Ongoing Fluctuations in Human Visual Cortex Predict Perceptual Awareness: Baseline Shift versus Decision Bias. *Journal of Neuroscience*, *29*(27), 8715–8725. https://doi.org/10/dwmnqk

Wysiadecki, G., Małkiewicz, A., Rożniecki, J., Polguj, M., Haładaj, R., Żytkowski, A., & Topol, M. (2018). Anatomical variations of the insular gyri: A morphological study and proposal of unified classification. *Clinical Anatomy*, *31*(3), 347–356. https://doi.org/10/gmmdfn

Xie, Y., Nie, C., & Yang, T. (2018). Covert shift of attention modulates the value encoding in the orbitofrontal cortex (J. Wallis, Ed.). *eLife*, *7*, e31507. https://doi.org/10/gc5797

Xue, G., Lu, Z., Levin, I. P., & Bechara, A. (2010). The impact of prior risk experiences on subsequent risky decision-making: The role of the insula. *NeuroImage*, *50*(2), 709–716. https://doi.org/10/dwrzbh

Xue, G., Lu, Z., Levin, I. P., Weller, J. A., Li, X., & Bechara, A. (2009). Functional Dissociations of Risk and Reward Processing in the Medial Prefrontal Cortex. *Cerebral Cortex*, *19*(5), 1019–1027. https://doi.org/10/bd6s65

Yacubian, J., Gläscher, J., Schroeder, K., Sommer, T., Braus, D. F., & Büchel, C. (2006). Dissociable Systems for Gain- and Loss-Related Value Predictions and Errors of Prediction in the Human Brain. *Journal of Neuroscience*, *26*(37), 9530–9537. https://doi.org/10/d64k67

Yarkoni, T., Poldrack, R. A., Nichols, T. E., Van Essen, D. C., & Wager, T. D. (2011). Large-scale automated synthesis of human functional neuroimaging data. *Nature Methods*, *8*(8), 665–670. https://doi.org/10/btqbtq

Yih, J., Beam, D. E., Fox, K. C. R., & Parvizi, J. (2019). Intensity of affective experience is modulated by magnitude of intracranial electrical stimulation in human orbitofrontal, cingulate and insular cortices. *Social Cognitive and Affective Neuroscience*, *14*(4), 339–351. https://doi.org/10/gmqzjm

Young, C. B., & Nusslock, R. (2016). Positive mood enhances reward-related neural activity. *Social Cognitive and Affective Neuroscience*, *11*(6), 934–944. https://doi.org/10/f8z9nm

Yuen, K. S., & Lee, T. M. (2003). Could mood state affect risk-taking decisions? *Journal of Affective Disorders*, *75*(1), 11–18. https://doi.org/10/dhq99k

Zaghloul, K. A., Blanco, J. A., Weidemann, C. T., McGill, K., Jaggi, J. L., Baltuch, G. H., & Kahana, M. J. (2009). Human Substantia Nigra Neurons Encode Unexpected Financial Rewards. *Science*, *323*(5920), 1496–1499. https://doi.org/10/c2wzv5

Zhang, C., Li, D., Jin, H., Zeljic, K., & Sun, B. (2017). Target-specific deep brain stimulation of the ventral capsule/ventral striatum for the treatment of neuropsychiatric disease. *Annals of Translational Medicine*, *5*(20), 402. https://doi.org/10/gck2vh

Zhang, Y., Pan, X., Wang, R., & Sakagami, M. (2016). Functional connectivity between prefrontal cortex and striatum estimated by phase locking value. *Cognitive Neurodynamics*, *10*(3), 245–254. https://doi.org/10/gdh9kt

Résumé

L'identification des facteurs dont les fluctuations sont associées à des choix incohérents est un enjeu majeur pour la théorie de la décision rationnelle. Dans cette thèse, nous avons étudié comment l'activité cérébrale explique en partie la variabilité des choix lors d'une tâche de choix multi-attributs en profitant de la possibilité rare d'enregistrer directement l'activité intracorticale du cerveau humain ou de réaliser des stimulations intracorticales pour sonder l'implication causale de régions corticales clés.

Dans la première étude, nous avons examiné les mécanismes neuro-computationnels par lesquels les fluctuations de l'humeur peuvent influencer le comportement de choix humain. Des données EEG intracérébrales ont été recueillies chez un grand groupe de participants (n = 30), alors qu'ils effectuaient des tâches de quiz et de choix entremêlées. L'activité neuronale basale précédant le début du choix a, dans un premier temps, été confrontée au niveau d'humeur (estimé par un modèle computationnel intégrant les feedbacks reçus dans la tâche de quiz), puis aux poids des attributs des options, à l'aide d'un modèle computationnel prédisant l'attitude à l'égard du risque dans la tâche de choix. Les résultats ont montré que 1) une activité gamma large bande (BGA) élevée dans le cortex préfrontal ventromédian (vmPFC) et l'insula antérieure dorsale (daIns) signalait respectivement les périodes d'humeur élevée et faible, et 2) qu'une activité BGA élevée dans le vmPFC et le daIns favorisait et tempérait respectivement la prise de risque en surpondérant les perspectives de gain et de perte monétaires. Ainsi, ces résultats montrent que les feedbacks induisent des états cérébraux qui correspondent à différentes humeurs et biaisent la comparaison des options sûres et risquées. Plus généralement, cette première étude pourrait expliquer pourquoi les personnes qui expérimentent des événements positifs (ou négatifs) dans une partie de leur vie ont tendance à s'attendre à un succès (ou un échec) dans une autre. Dans la deuxième étude, nous nous sommes concentrés sur les corrélats neuroanatomiques qui sous-tendent les effets des fixations visuelles sur le choix. Des données d'EEG intracérébral ont été collectées simultanément avec des données de fixations oculaires chez un grand groupe de participants (n = 38) alors qu'ils effectuaient une tâche de choix multi-attributs dans laquelle ils devaient accepter ou refuser une offre risquée. L'activité neuronale (BGA) mesurée pendant les fixations visuelles sur les attributs de l'option a alors été corrélée avec la valeur de l'attribut (gains monétaires vs. pertes). Les résultats de cette deuxième étude ont montré que 1) l'activité neuronale dépendant du regard est corrélée positivement avec la valeur d'un attribut donné lorsqu'il est fixé et négativement avec la valeur de celui-ci lorsqu'il n'est pas fixé et ce, dans un large réseau cérébral, 2) l'activité neuronale dépendant du regard dans le vmPFC permet de prédire les choix risqués des sujets lorsqu'ils regardent les gains et 3) l'activité neuronale dépendant du regard dans l'aIns permet de prédire les choix vers l'option sûre lorsque les sujets regardent les pertes. Ainsi, nos résultats permettent de clarifier des éléments neuroanatomiques clés sur la façon dont l'attention visuelle interfère avec l'activité neuronale pour moduler nos choix. Dans la troisième étude de cette thèse, nous avons étudié l'effet de la perturbation ciblée du cortex insulaire antérieur et du vmPFC sur les choix risqués. L'effet de la stimulation électrique intracrânienne (iES) délivrée directement dans le cortex humain à 50 Hz chez un groupe de patients épileptiques (n = 13) a été examiné pendant que les sujets effectuaient une tâche de choix similaire à celle utilisée dans les deux études précédentes. Les résultats ont montré une dissociation fonctionnelle au sein de l'insula antérieure : la stimulation de l'insula antérieure dorsale (daIns) augmentait les choix risqués tandis que la stimulation de l'insula antérieure ventrale (vaIns) favorisait les choix plus sûrs. À l'inverse, la stimulation électrique intracrânienne du vmPFC a eu tendance à favoriser la prise de risque (comme dans daIns). Ces données exceptionnelles soulignent l'importance causale de ces zones cérébrales lors de choix multi-attributs impliquant une incertitude et fournissent des indices pour de futures études mécanistiques de l'anatomie et de la physiologie des choix.

Dans l'ensemble, cette thèse a permis de mieux comprendre les mécanismes neurocomputationnels qui sous-tendent les choix multi-attributs en suggérant que des systèmes cérébraux dissociés pourraient être impliqués dans la représentation de la valeur des attributs appétitifs ou aversifs avant et pendant le processus de choix.

Summary

Identifying factors whose fluctuations are associated with choice inconsistency is a major issue for rational decision theory. In this thesis, we investigated how brain activity partly explain choice variability during a multi-attribute choice task by taking advantage of the rare opportunity to either directly record intracortical activity in the human brain or to perform intracortical stimulation to probe the causal involvement of key cortical regions.

In the first study, we investigated the neuro-computational mechanisms through which mood fluctuations may bias human choice behavior. Intracerebral EEG data were collected in a large group of participants (n = 30), while they were performing interleaved quiz and choice tasks. Neural baseline activity preceding choice onset was confronted first to mood level, estimated by a computational model integrating the feedbacks received in the quiz task, and then to the weighting of option attributes, in a computational model predicting risk attitude in the choice task. Results showed that 1) elevated broadband gamma activity (BGA) in the ventromedial prefrontal cortex (vmPFC) and dorsal anterior insula (daIns) was respectively signaling periods of high and low mood, 2) increased vmPFC and daIns BGA respectively promoted and tempered risk taking by overweighting gain versus loss prospects. Thus, incidental feedbacks induce brain states that correspond to different moods and bias the comparison of safe and risky options. More generally, this first study might explain why people experiencing positive (or negative) outcome in some part of their life tend to expect success (or failure) in any other. In the second study, we focus on the neuro-anatomical correlates underlying the effects of visual fixations on multi-attribute choices. Intracerebral EEG data were collected simultaneously with gaze data in a large group of participants (n = 38), while they were performing an accept/reject multi-attribute choice task. Neural activity (BGA) measured during visual fixations on option attributes before the choice onset was confronted to the weighting of option attributes. Results from study 2 showed that 1) gaze-dependent neural activity correlated positively with a given option attribute value when fixated and negatively with the dimension's value when unfixated in a large brain network, 2) gaze-dependent neural activity in the vmPFC was positively predictive of subject's choices when they looked at gains 3) gaze-dependent neural activity in the aINS was negatively predictive of subject's choices when they looked at losses. Thus, our findings specify key neuro-anatomical insights into how gaze pattern interferes with neural activity to bias multi-attribute choices. In the third empirical study of this thesis, we investigated the effect of targeted disruption of the anterior insular cortex and the ventromedial prefrontal cortex on risky choices. The effects of intracranial electrical stimulation (iES) delivered directly in the human cortex at 50 Hz in a group of epileptic patients (n = 13) were examined while they were performing a multi-attribute choice task during which they had to choose between risky vs. safe monetary prospects. Results showed a functional dissociation within the anterior insula: iES on the dorsal anterior insula (daIns) increased risky choices whereas iES on the ventral anterior insula (vaIns) promoted safer choices. Conversely, intracranial electrical stimulation on the vmPFC tended to promote risk taking (as in the daIns). These rare cases highlight the potential causal importance of these brain areas during multi-attribute choices involving uncertainty and provides clues for future mechanistic studies of the anatomy and physiology of choices under uncertainty.

Overall, this PhD extended the knowledge about the neuro-computational mechanisms underlying multi-attribute choices by suggesting that dissociable brain system might mediate appetitive vs. aversive attribute value representation both prior and during the choice process.